ANALYTICAL TECHNIQUES IN POLYMER CHEMISTRY WITH SPECIAL REFERENCE TO UREA-FORMALDEHYDE RESINS

BY

ERNST EDUARD FERG

A thesis submitted to the Faculty of Science,
University of the Witwatersrand, Johannesburg,
in fulfilment of the requirements
for the degree of

MASTER OF SCIENCE
(CHEMISTRY)

"Degree awarded with distinction 6 May 1993

Promoters: Prof. A. Pizzi - Polymer Chemistry
Dr. D. Levendis - Structural Chemistry

Abstract

One of the greatest environmental drives in the synthetic resins field has been to decrease the formaldehyde emission from cured urea formaldehyde (UF) resins, without adversely affecting their excellent technical performance. The effect of modifying a UF resin was investigated by producing two series of resin (A and B) where the addition of urea to a existing resin was done in one single step (A) and in multiple steps (B). Particleboards made from the resins were tested for I.B. (Internal Bond) strength and formaldehyde emission. The cured and liquid resins were investigated by I.R. and ^{13}C NMR spectroscopy and X-ray diffraction. A relationship between the analysis of liquid resin by ^{13}C NMR and the physical properties of the particleboard was obtained. Predictions can therefore be made about I.B. strength and the formaldehyde emission from a board for a specific homologous series of resins by considering the ^{13}C NMR peak ratio of certain species in the liquid resin. The UF resins performance can be improved by increasing the number of urea additions during the resins synthesis. Also, the performance can improve by adding a small amount of formaldehyde to the resin during the last step of resin synthesis.

Acknowledgment

I would like to extend my sincere thanks to:
- My supervisors Prof. A. Pizzi for his enthusiastic input and motivation and Dr. D. Lenvendis for his interest and encouragement throughout the project.
- Dr. H. Marques for the use of the fluorescence spectrometer.
- The Structural Chemistry group of Wits Chemistry for the use of their computer facilities.
- The Polymer Chemistry group of Wits Chemistry for the use of their equipment and chemicals.

Related Publications by the Author

- This work was presented at the Fifth International Chemistry Conference in Africa (ICCA); Gaborone; Botswana; 27-31 July 1992.
- D. Levendis, A. Pizzi and E.Ferg; The Correlation of Strength and Formaldehyde Emission with the Crystalline/Amorphous Structure of UF Resins; Holz-Forschung; 46; 263 (1992).

Declaration

I declare that this dissertation is my own, unaided work. It is being submitted for the degree of Master of Science at the University of the Witwatersrand, Johannesburg. It has not been submitted before for any degree or examination in any other University.

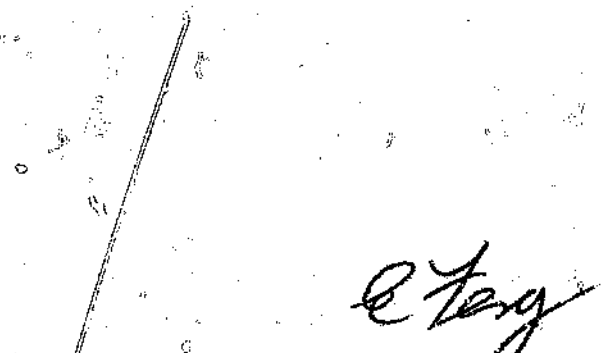

E. E. Feng

Table of Contents **Page**

List of Tables

List of Figures

List of Abbreviations

UF- Urea-Formaldehyde
HCHO- Formaldehyde
F- Formaldehyde
Hr- Hour
rel- relative
ppm- parts per million
X_{cr}- Crystallinity of a polymer
I_f- Fluorescence Intensity
M_{cr}- Mass of crystalline region
M_{ar}- Mass of amorphous region
M- Total mass
I_{cr}- Intensity from crystalline region
I_{ar}- Intensity from amorphous region
I.R.- Infra-Red
NMR- Nuclear Magnetic Resonance
I.B.- Internal Bond
DDL- 3,5-diacetyl-1,4-dihydrolutidine
D.P.- Degree of Polymerization

Chapter 1.

1.1. Introduction

The formation of large synthetic molecular units by the combination of smaller units has revolutionized material science at the turn of the century. With the introduction of these new materials, a need developed for specialized analytical techniques to study their properties and structures. Through changing structural characteristics, specialized mechanical and chemical properties can be obtained.

The analytical techniques in polymer studies are limited to nondestructive techniques because the structural information required is often of the bulk material. In analysis, it is important to make distinction between homopolymers, copolymers, linear, branched and cross-linked polymers, and limitations pertaining to thermoset and thermoplastic polymers.

The developments of analytical techniques in polymer science are discussed by various authors[1]. Meyers [1] discussed many analytical techniques in studying urea formaldehyde systems. IR, NMR and X-ray diffraction were some of the analytical techniques used to investigate the properties and structures of urea-formaldehyde resins.

---

[1] Various authors and their books covering the subject in greater detail are shown in the bibliography.

1.2. Background and theory of urea-formaldehyde resins.

Urea-formaldehyde (UF) resins are widely used in the field of wood binders, especially in the production of particleboards. Particleboards were commercialized in the 1950s, 25 years after the chemical formulation and manufacturing of UF resins started. Today, UF resins constitute about 5% of the worlds total resins. Formaldehyde emission from UF bonded wood products has been recognized as a source for indoor air pollution.

1.2.1. Resin

UF resins are relatively inexpensive and versatile in their application, making them one of the most common synthetic binders. They are difficult to understand and to analyze the complex reaction mechanism and structures involved.

The advantages of amino resins are:
Their initial water solubility making them suitable for bulk and relative inexpensive production; a hard thermoset plastic after curing; nonflammability; good thermal properties; colourless; and adaptable for a variety of curing conditions. The greatest disadvantage of the resin is its chemical bond deterioration caused by water after curing.

UF resin chemistry consists of a step-wise addition of urea and formaldehyde. The reaction between urea and formaldehyde can be divided into two stages.
a) The formation of mono-, di-, and trimethylolureas during alkaline condensation.
b) Formation of soluble and insoluble linear and cross-linked compounds during the acid condensation of the methylolureas formed during the first stage.

The formation of mono- and dimethylolureas in the presence of an alkaline catalyst can be schematically represented as follows.

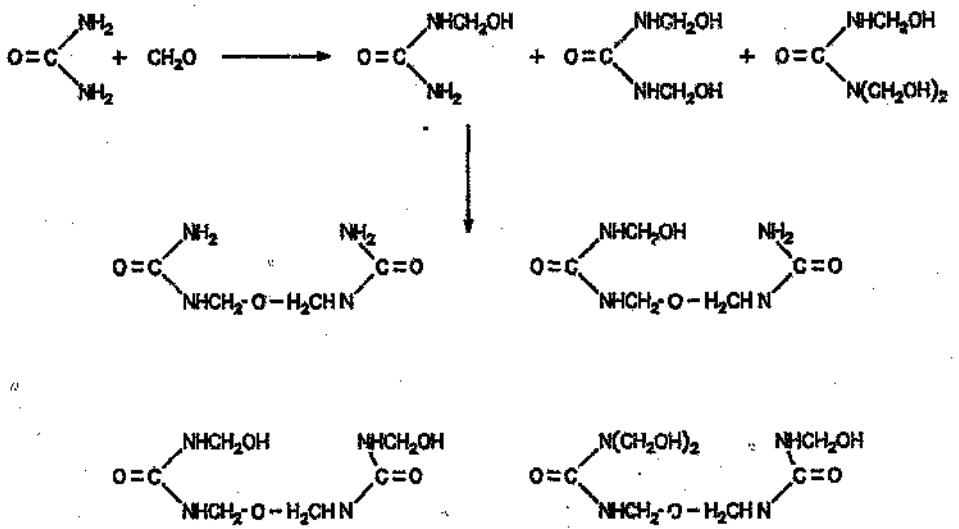

The following scheme shows how the higher branched methylene-ureas are formed by the methylolureas copolymerizing under acidic conditions.

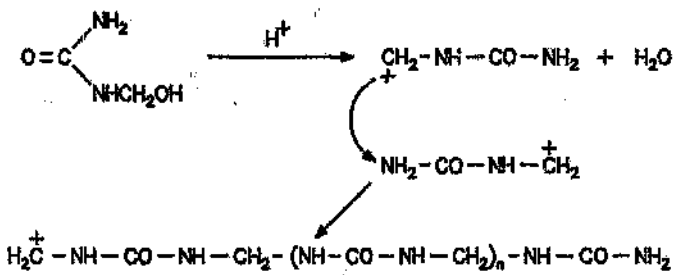

A number of other products are formed at lower concentrations. These include cyclic products such as uron, monomethyloluron, dimethyloluron. In the presence of excess formaldehyde, methylurea could dimerize to form diureamethyl ethers.

A number of important factors control the properties and performance of the final resin. Factors relating to the gluing properties of individual species to wood will be discussed later.

Properties such as resin viscosity and the amount of certain species depends on several factors including: i) The purity and ii) the molar proportions of the reactants, iii) the pH control, and iv) the temperature and time of the reactions. These properties are discussed in more detail below.

i) The purity of the reactants.
Commercial urea is almost 99% pure, and can be used. Formalin solutions contain up to 12% methanol for stabilization and 30-40% total formaldehyde. UF resins are more stable with less methanol. Methylated UF resins, on curing remain unchanged, and are water soluble. This problem is usually avoided by distilling off the methanol from the commercial formaldehyde solutions before use. The aqueous solution is made up of methylene glycol, polyoxymethylene glycol, formaldehyde hemiformal, polyoxymethylene hemiformal, trioxane and paraformaldehyde. Investigation of the available formalin solutions with ^{13}C NMR showed the various species present (see spectrum 18). On the other hand, commercial paraformaldehyde is relatively pure if used quickly before decomposition (see spectrum 19). Para-formaldehyde proved to be more sensitive to reaction conditions than formalin solution.

ii) The molar proportions of the reactants.
The degree of condensation and the hydrogen bonding ability of the finished resin are important factors relating to the durability of the resin. Higher formaldehyde content resins have been shown to have excellent gluing capabilities [2]. Resins of a molar

ratio 1:1.8 to 1:2 exhibit slower bond deterioration under accelerated aging conditions than resins in the range 1:1.4 to 1:1.6 [3]. An example of the variation of properties between particleboard manufactured with different molar ratio resins is shown in table 1 [4].

Table 1. A comparison between particleboards prepared with different UF molar ratios.

U/F molar ratio	Approx. Density ($g.cm^{-3}$)	Internal bond (MPa)	% water swelling (2Hr)	% HCHO released*
1:1.4-1.5	0.680	0.7-0.8	4	0.08-0.10
1:1.3-1.35	0.680	0.6-0.7	4-5	0.04-0.05
1:1.2-1.25	0.680	0.45-0.55	5	0.025-0.035

* Perforator method

iii) pH control.

The pH level during and after the resin synthesis plays an important role. The commercial formalin often contains formic acid that acts as a catalyst in the irreversible curing of the resin. If warm formaldehyde solutions are exposed to air, the formaldehyde slowly oxidizes to formic acid by the Cannizzaro reaction:

$$2CH_2O + O_2 \longrightarrow 2HCOOH$$

The Cannizzaro reaction could also occur in alkaline solutions:

$$2CH_2O + NaOH \longrightarrow HCOONa + CH_3OH$$

The reaction of urea and formaldehyde occurs in two steps:

a) Addition $U + F \longrightarrow U\text{-}CH_2OH$

b) Condensation $U + U\text{-}CH_2OH \longrightarrow U\text{-}CH_2\text{-}U + H_2O$

The first reaction is often called methylolation and is

catalysed by both acid and base. The condensation is only catalysed by acid. The reaction rate is shown in figure 1 [5].

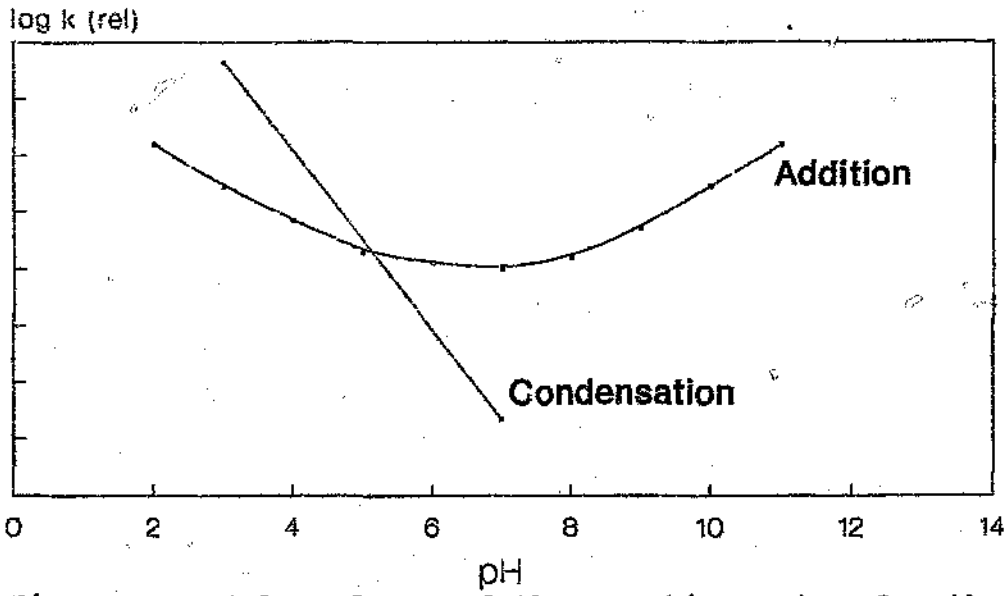

Figure 1. pH dependence of the reaction rates for the initial UF steps.

The pH has to be carefully controlled during the reaction, to produce the desired amounts of condensation and methylolation products.

iv) The temperature and time of reactions.

When we look at the temperature and time required for the formation of the resin, we must consider the formation (reaction) rates of individual species. For example: The initial formation of monomethylolureas in a weak alkaline aqueous solution is very fast followed by a slower bi-molecular reaction. The reaction rates of individual species is discussed in more detail by G. Grove and C. Lynch [6]. Temperature and duration of synthesis change for different manufactures. Resins are usually cooked at 95°C to allow rapid formation of the products.

Controlling factors such as the turbidity point and the water tolerance point of the resin are used to determine the limits of certain size species to be formed during synthesis.

UF resins are usually manufactured in two forms. The spray-dried resin and aqueous resin containing between 35 to 80% resin solid. The dry resin has the advantage of lower shipping cost and better storage stability. But with a disadvantage in the price. UF-resins are not water soluble they are colloidal dispersions. Water toleration depends on their composition, age, temperature and many other factors.

UF resins are almost always modified before their final use to improve the performance and decrease the expense. The unmodified resins are often brittle and crack due to some trapped water during board manufacture. The addition of alcohols increases the formation of ethers and esters thereby reducing crosslinking. This has the advantage that there are more longer chain polymer groups increasing its plasticity. Scheiber [7] gave an excellent summary of results obtained by final resin modifications.

Horioka et al [8] demonstrated that the addition of a second amount of urea during the preparation reaction improves adhesion strength. Urea is also often added before application and acts as a formaldehyde scavenger by reacting with the resin. In some cases solid formaldehyde is added to secure the curing of the resin. The addition of multiple steps of urea to a commercial resin was reported by D. Levendis, A. Pizzi and E. Ferg [9].

Some applications for UF resins are listed below.
Japan uses UF foams in soundproofing and heat insulating panels [10]. UF foams are also used as insulation in

ships [11], electrical insulators [12], oil absorbers [13], medical applications [14] and in agricultural uses [15]. Beat Meyer [16] covers a wide range of application which include coatings, paper, construction materials, binders for metal casting and waste treatment only. The application of UF resins as a wood binder for particle boards will be considered.

1.2.2. Particleboards

UF make up 6-10% wt of the particleboard. The main advantage of particleboards over solid wood boards are their production versatility, the ability of using waste raw materials and the more pronounced isomorphism of the final product. The board can be made according to the users specifications. Other advantages include the production of large size boards which are relatively lighter than solid wood planks. Solid wood planks are often susceptible to brittle failure at the higher stress points due to natural defects such as knots and cracks. The boards are usually manufactured from planer shavings, sawdust, or plywood trimmings. Solid logs are sometimes chipped exclusively for the use in particle board manufacture. The most common wood types used in South Africa are pine and eucalyptus.

Certain parameters and properties in particle board manufacturing have to be taken into consideration. Chemical bonding in wood chemistry could be defined as the process for joining two or more pieces of wood via a direct chain of covalent bonds between adjacent surfaces. The different types of bonding included are mechanical entanglement, adsorption (specific adhesion), electrostatic (donor-acceptor interactions) direct chemical bonding and cohesion. Adhesion involves chemical, physical and mechanical principles. The bond formation

and bond performance are two factors that are vital in considering adhesion. An adhesive must perform equally well at all points between the pure, bulk glue line and the surface contact between wood and glue. The links in the adhesive bond between wood surfaces is shown in the diagram below [17].

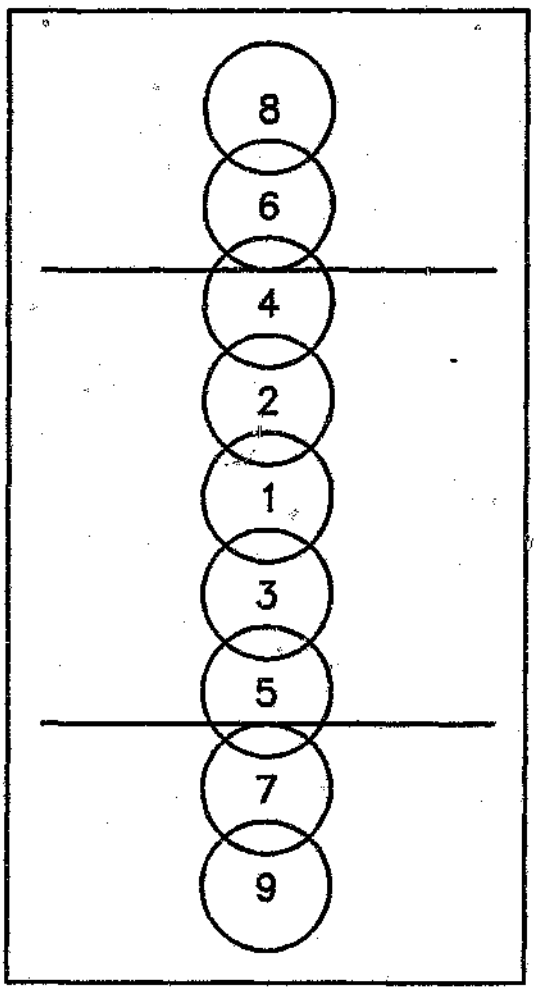

1) the Adhesive film,
2) and 3) Intra-adhesive Boundary Layer,
4) and 5) Adhesive-Adherent Interface (site of adhesion forces),
6) and 7) Adherent Surface, partially fractured during preparation for bonding,
8) and 9) Adherent Bulk.

Figure 2. Links in the Adhesive Bond between Wood Surfaces

UF resins have several intrinsic properties that are

essential for matching the multitudes of demands in wood bonding. The UF resin contains a mixture of chemical fractions with different molecular weights that provides an almost ideal spectrum of bonds. Each of which reacts and performs differently. The higher molecular fractions coalesce and form the main bulk of the glue line. The lower weight methylol functional group fractions readily diffuse through the wood and establish surface contact with the hydroxyl groups in H-bonded cellulose. Intermediate species (such as ethers and esters) establish other less important links. If any of the conditions are slightly wrong the resin would almost fail completely with a very small margin for error.

Wood adhesives must also be flexible and soft to allow for swelling of the wood and shrinking during drying. The following factors have been shown to play important roles in the final properties of the resin in relation to the wood glue strength [18, 19].

1. The bond strength increases with the degree of condensation.
2. The adhesion strength appears to be at its highest at a relatively low average molecular weight. Dimethylolureas are the main components governing the adhesive forces between the glue and wood.
3. The higher molecular weight (higher resin viscosities) result in a more durable glue-wood bond. Higher molecular weight species govern the cohesive forces.

The final boards physical strength such as bending, tensile and compressive strengths, the rate of water absorption and equilibrium moisture content depend on the final boards density. The standard density of particleboards is about 0.7 gcm^{-1}. The pressing cycle of the board (the sequence of temperature and pressure applied) produces a gradient of density through the thickness of

the board causing nonuniform properties to exist.

The alignment of the particles should be completely random, giving the board its isomorphous properties. But in the manufacturing, a slight preferred alignment is usually achieved. This is due to the type of spreading and size of the particles. Formation of particle alignment causes the board to increase its physical properties in the particular direction but to the expense of the other directions.

During the pressing of the particle boards, the moisture content becomes important. High moisture content causes delays in adhesive curing, and excessive flow causes the resin to be soaked into the wood causing glue line starvation. A too low moisture content could cause poor adhesive flow and moisture absorption stresses in the final board. The amount of moisture depends largely on the size of the wood particles used. The final moisture content of the boards should be between 7 and 8% for the core, and 10 to 12% for the surface. Most manufactures add water to the resin to decrease the viscosity to facilitate spraying.

Other components are added to the resin before application, to increase the physical strength and durability of the final board. Insecticides, wax emulsions and fire retarding agents (ammonium phosphates) are often added. Several tests are performed on the particleboards for durability and quality determinations. Cold and boiling water swelling, water absorption, strength test, bending tests, torsion tests, nail and screw holding tests, surface abrasiveness, formaldehyde emission and others. Standards for the manufacturing of particleboards have been introduced, and some of them are summarized in table 2.

Table 2. Classification and properties of particleboards, based on data compiled by Forest Products Laboratory-United States Department of Agriculture [20].

Particleboard	Thickness (cm)	Density ($g.cm^{-1}$)	Modulus of Rapture (MPa)
Low Density	0.64-1.91	0.40-0.80	2.76-27.58
High Density	0.25-0.95	0.80-1.12	20.69-51.71

Particle-board	Tensile Strength parallel to surface (MPa)	Tensile Strength perpendicular to surface (MPa)	Water Abs. 24hr immersion %/weight
Low Density	0.69-9.31	0.62-2.76	5-50
High Density	2.07-17.24	1.90-2.76	15-40

1.2.3 Formaldehyde release

Over the last 15 years, resin chemists have attempted to decrease the formaldehyde content of the final resin due to environmental concerns. Formaldehyde has a pungent odour and could cause irritation of the eyes and the mucous membranes of the respiratory tracts. Detailed information on the subject can be found in the original literature published by various authors such as Wittmann [21], Roffael [22] and Meyer [23]. This formaldehyde release can occur for years. This is especially evident in humid climatic regions of North America and Europe

since the combination of humidity and temperature directly affects the emission rate. Formaldehyde release is especially evident in closed furniture cabinets that are built from particleboards.

Normal cured UF resin products are almost odour free. Chronic odour is a sign of incomplete cured resin, bad formulated, or resin decay. Cured resin that is exposed to water leads to hydrolysis. The susceptibility to moisture differs for the different components found in UF resins. Table 3 shows the stability of the various resin components. The weakest link being the cellulose-resin link, the hemiacetals, ethers, and methylo s. The oxygen free methylene linkages are most resistant [24].

Table 3. The relative stability of bonds in cured UF-resins (in order of increasing stability).

Bond Type	Structure
C-O in cellulose to resin	R-O-CH_2NHCONH-
C-O in methylene ether	-NHCONHCH_2-OCH_2NHCONH-
N-C in amido methylol	-NHCONH-CH_2OH
C-O in polyformal	-NHCONHCH_2O- CH_2OCH_2NHCONH-
C-N in primary amide	-NHCONHCH_2NHC-NH_2
C-N in secondary amide	-NHCONHCH_2NH-CNH-
C-N in tertiary amide	-NHCONHCH_2NCONH-;-CH_2- ;-NHCH_2NCONH-

In 1977 the West German Federal Health Board introduced regulations for the emission of formaldehyde from particleboards (see table 4). The Hazardous Compounds Act of Germany recommended a value of 0.1 ppm for all

Dwellings [25]. Emission classes and techniques for detecting formaldehyde emission were introduced and are used for standardizing the production of particleboards.

Table 4. West German Regulation for Formaldehyde emission from particleboards used in buildings.

Emission Class	Formaldehyde concentration (ppm)*	Perforator value EN 120 (mg/100g board)
E3	>1.0-2.2	>30-60
E2	>0.1-0.9	>10-30
E1	<0.1	<10

* Determined in a 40 m^3 test chamber.

Numerous methods are available for the determination of formaldehyde emission from particleboards. The sampling of formaldehyde from particleboards could be categorized as follows. a) Ambient air concentration of formaldehyde above the source, b) total free formaldehyde in the source, or c) the release of formaldehyde into the air space per time and surface area. Roffael [26] presented a careful comparison of several sampling methods and some of them are discussed below.

The perforator method determines the amount of free formaldehyde present in the particleboard. The value is usually slightly low, because it does not consider the formaldehyde emitted due to hydrolysis. The method relies on large and complicated equipment and the use of toluene could create a potential health and fire hazard [48].

The chamber test is a more accurate representation of the formaldehyde released by particleboards. The method

relies on a room with a volume of 34 m^3, containing 40 m^2 of board at 20°C and 45% humidity [49]. But requires large amount of sample and cumbersome equipment.

A technique similar to the Japanese desiccator method [50] was used by the author. The method was modified to allow the use of smaller amounts of particleboard samples. The technique determines the release of formaldehyde into the air space per time and surface area. Fuji [51] showed that there is a linear relationship between the formaldehyde released from the sample surface and that collected in the water for the 24 hour Japanese desiccator test. The technique is discussed in more detail in chapter 4 (Experimental).

Numerous methods for the determination of formaldehyde in water was discussed in detail by Marutzky [52]. The one found most suited was the fluorometric acetylacetone method based on the Hantzsch reaction developed by S. Belman and Bisbaard et al respectively [53, 54]. The sampling medium was water and therefore most suitable for stationary sampling.

3,5-diacetyl-1,4-dihydrolutidine (DDL) which flouresces is formed from formaldehyde, ammonia and acetylacetone.

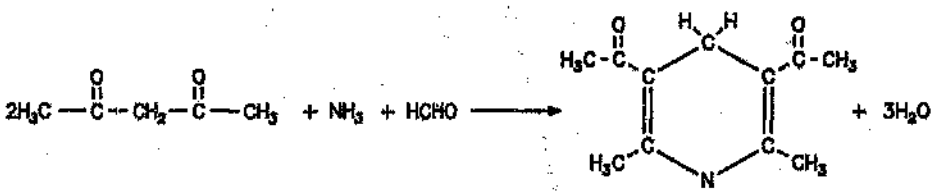

Standards with different formaldehyde concentrations were prepared by dissolving a known amount of paraformaldehyde in water. A standard curve was determined by the linear

regression using the relationship

$$I_f \propto [HCHO]$$

The results were plotted on a graph and used as a standard for the determination of the formaldehyde absorbed by the water in the desiccator method.

The above desiccator method was standardized to the WKI method described by E. Roffael and L. Mehlhorn [55].

The following reasons are why the desiccator method was used instead of the WKI method for the analysis.

1. In the WKI method, the particle boards are suspended directly above the water. Pieces of the board could fall into the water and introduce error.
2. The final concentration of the formaldehyde solution from the WKI method was very high, and had to be diluted to be used for the acetylacetone method of analysis. Thus increasing the error of the final results.
3. The bottle and sample had to be moved in and out of the oven. Whereas the desiccator would remain stationary throughout the analysis period, decreasing possible error.
4. The high temperature of the WKI method could cause unnecessary hydrolysis of the sample boards and result in higher formaldehyde emission.
5. Due to the higher release of formaldehyde by the particleboard at elevated temperature, equilibrium between formaldehyde absorbed by the water and emitted by the board could be reached sooner.
6. There was a higher temperature fluctuation during the 24 hour testing period for the WKI method than for the desiccator method.

1.3. Techniques available for analysis

1.3.1 Infra-red Spectroscopy

The most common analytical techniques used in polymer science are spectroscopic techniques. Techniques such as mass spectroscopy have been used on a limited scale due to its destructiveness. In general, spectroscopic techniques are applicable only for short range phenomena, whereas crystallographic techniques deal with long range order.

IR spectroscopy is one of the most commonly used analytical techniques in polymer studies. It is used to provide information about chemical structures, crystallinity and tacticity. The technique is relatively cheap, and can be used to analyze solid or liquid samples with ease. Infra-red spectroscopy does not indicate all vibrations theoretically possible in polymers. Each molecule has 3n-6 fundamental vibrations where n is the number of atoms forming the molecule. Polymers should have a nearly infinite number of vibrational bands and no useful information could then be obtained from the spectra. This is often true for amorphous polymers whose vibrational spectra cannot be distinguished from corresponding spectra of monomeric model compounds. Various carbonyl and amine functional groups in UF samples were identified by various authors [27, 28, 29]. IR assignments cited in the literature are summarised in table 13.

1.3.2. NMR Spectroscopy

NMR spectroscopy is based on the spin resonance of selected atoms. In Spin Resonance Spectroscopy the absorption is of low energy (microwave and radio frequency). Effects such as magnetic dipole interaction,

chemical shift and the nuclear spin-spin coupling of molecules are important when considering chemical applications.

NMR is a useful analytical tool to study and identify functional groups in liquid UF resins. Proton NMR spectroscopy was used by a number of authors [30, 31] to study UF resins. Measurements of UF resins in DMSO-d_6 solution has made the determination of $-NH_2$ and =NH groups possible. This method seemed ineffective for the determination of methylol groups because of the interference from hydrogen bonding and water. Chemical treatment of the sample would be required before analysis.

Water does not play an interfering role in the analysis of UF resins by ^{13}C NMR spectroscopy. It was found that liquid ^{13}C NMR provided more useful results, especially in investigating various synthesis parameters of the resin where small variations within individual species occur. The signals due to various carbonyl groups of UF resins could be easily isolated and identified. Various authors [32, 33] have isolated the signals by comparing the chemical shifts to those of synthesized standard derivatives. Table 16 summarizes the signals assigned by some authors. Solid State ^{13}C NMR was used to study cured UF resins samples [34]. The authors used cross-polarization and magic-angle spinning to obtain reasonable spectra. The scanning times are usually very long, and peak deconvelution would be required to interpret the broad spectra obtained.

1.3.3. X-ray diffraction

X-ray diffraction techniques looks at long range phenomenon. Polymer type materials exhibit structures that cover the entire range from total amorphous to crystalline. Data obtained from X-ray diffraction analysis of crystalline polymers can give information about:
1) The identification of the material, 2) its crystallinity, 3) the geometry of the crystallites and 4) the possible relative positions of the atoms in the crystallites.

The crystallite sizes contained in an amorphous matrix of a polymer could be determined from the broadening of the diffraction pattern. The broadening of the diffraction pattern could be influenced by other factors such as:
a) Broadening due to imperfect or very small crystals.
b) Broadening contributed by the apparatus (instrumental broadening).

If one assumes that the broadening of the observed diffraction peak is not due to any of the above phenomenon, and that the crystallite is a cube of edge length t=Na, then the following Scherrer formula could be used. Scherrer and Bragg [35] gave the following approximation based on the Laue diffraction function for the broadening of diffraction.

$$\beta = K\lambda / t\cos\theta$$

where λ=the wavelength, θ=the Bragg angle, K=the Scherrer constant and β=the half width of the diffraction.
For the half-breadth $\beta_{1/2}$ K=0.9
For the integral breadth β (general) K=1.05
The above equation is for an ideal situation. Often,

there is a distribution of crystallite sizes in a specimen. The broadening of the diffraction profile results from the contributions of the profiles due to the various crystallite sizes and the analysis becomes more difficult.

The crystallinity of a polymer can be determined from the analysis of the diffraction profile obtained from X-ray analysis. Assuming a constant X-ray intensity, then the total intensity of the coherent scattering from a scattering body of fixed mass should be constant. The crystallinity of a polymer X_{cr} is defined as the ratio of the respective masses of the crystalline (M_{cr}) and amorphous (M_{ar}) regions to the total mass.

$$X_{cr} = M_{cr}/M \text{ where } M_{cr} + M_{am} = M$$

The ratio of the scattering intensities due to the crystalline and amorphous regions is nearly equal to the density of the two types of regions. If one assumes that the masses of the two regions are approximately equal to their respective densities, then the following relation could be considered.

$$I_{cr}/I_{am} \propto M_{cr}/M_{am}$$

This is the basis of the crystallinity measurements in general use.

There are two types of cases:
1) Where completely amorphous or completely crystalline specimens cannot be obtained, and 2) where completely amorphous or completely crystalline specimens can be obtained.

1) A smooth curve is drawn to connect the minima between

the crystalline peaks (fig 3) and the assumption is made that the intensity above is the contribution by the crystalline region and below by the amorphous region.

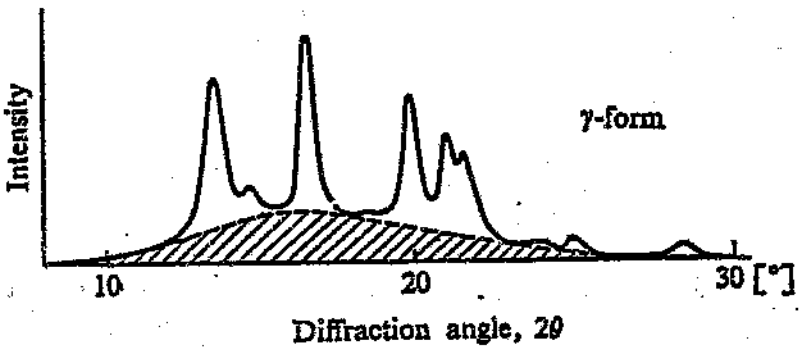

Figure 3. X-ray diffraction trace of a polymer showing the contribution due to amorphous and crystalline regions respectively [36].

This method gives a high value for the amorphous region. The reasons for error being:

i) The fitted smooth curve could incorporate weak crystalline diffractions and transfer their contribution to the amorphous scattering.

ii) The strong crystalline peaks are usually superimposed on the maxima of the amorphous halos, and the base of the crystalline peak is included in I_{am}.

iii) Diffuse scattering due to crystal lattice imperfections and background scattering due to lattice distortions cannot be properly distinguished from the amorphous halo.

2) It is possible to determine the amorphous fraction of a semi-crystalline polymer by comparing the intensity of the diffraction halo for a completely amorphous sample to that of the unknown specimen under identical conditions. The problem being that there are few so-called pure crystalline or pure amorphous polymers obtainable. It is customary to use specimens that are nearly amorphous as possible. The amorphous halo could change in shape with

temperature and is dependant on the method of synthesis for the polymer.

Koutsky [37] suggested that UF resins with low F:U ratio have a degree of crystallinity present within its structure. In the higher F:U ratio resins, there is a high degree of crosslinking, making it amorphous. Suggestions made for the crystallinity was that a high amount of methylene linkages are present [37]. Koutsky also showed that crystals are formed in the incipient stages of cure and that the crystallinity is considerably reduced in the presence of water.

There is however no guarantee that the crystallinity observed by the resin cured by itself will be evident when cured with wood chips. Previous studies [9] suggested that the crystallinity of the resin breaks down when reacted with wood chips.

X-ray diffraction patterns of various UF standard derivatives have been studied [38, 39, 40] and are also available from the international ASTM data base [41]. Traces of some of the most common derivatives are shown in Traces 1 to 8.

Aim

There are a variety of controlling factors in the synthesis of UF resins. It would be impossible to consider all possible variations in the synthesis, and how the resultant resins influence the final particleboards properties. The aim of the project would consider only one variable in the synthesis of the resin, and see how it influences the final particleboards properties. The analytical techniques available would aid in relating the resins structural and physical properties to the use in its final application.

Chapter 2. Discussion

2.1. Resin

A low formaldehyde emission UF resin with good glueing properties is known [9]. The formulation relied on subsequent additions of urea to a high F to U ratio resin. The results produced a resin with good gluing properties and low formaldehyde emission. The effect of the subsequent additions were not fully understood.

O'Neill and Steiger [43] described a 4 stage UF resin synthesis, with the third stage being a formaldehyde increase and the fourth stage an addition of 10% urea. Brunnmüller et al [44] described a continuous process for making UF resins with backmixing.

The effect of an extra addition of urea to a resin was investigated as follows. A starting commercial resin synthesized according to a commercial UF resin (see experimental for the formulation). The percent solid was calculated to be 61.3%. The U:F molar ratio was 1:1.8.

The percent solid was determined by heating a known amount of resin for 1 hour at 140°C. This is not a true reflection of the active solid content of the resin, since about 14% of the active resin is converted to water during heating. For the above resin, a 75% active content was considered, and the subsequent additions of urea was calculated according to the active content.

The approach used would demonstrate to what extent extra urea addition has on the final resin properties. Thus, two sets of resin were prepared with similar U:F molar ratios, but with different synthesis approaches.

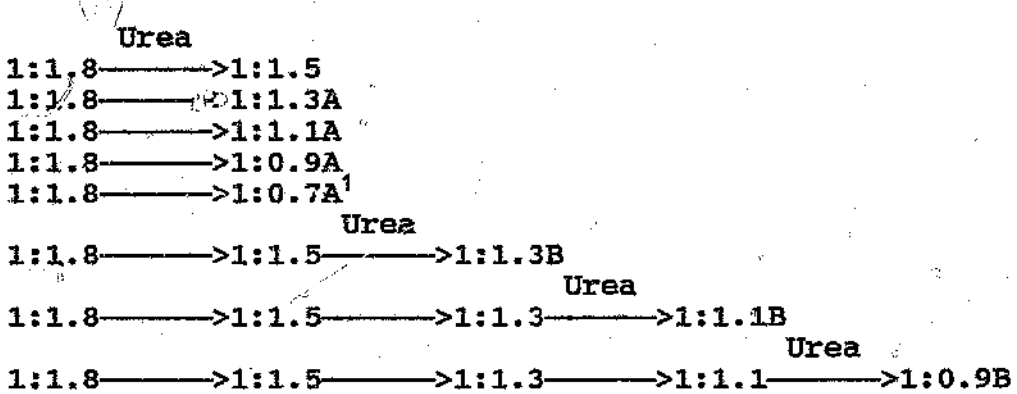

The effect of back addition of formaldehyde was investigated by preparing the following resin.

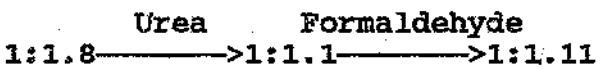

The results for the different resins viscosity and % solid determinations are presented in table 5.

As the amount of urea added to the resin increased, so a general increase in the % solid content and a decrease in the final viscosity was noted. Reasons for the phenomena was that the solid urea added increased the solid content of the resin. The decrease of viscosity could be ascribed to the fact that the urea reacted with the free formaldehyde to form low molecular weight species. Hence, a shift downwards in the degree of polymerization (D.P.) of the resin. The viscosity for the step addition of urea (1:1.3B, 1:1.1B and 1:0.9B) were slightly higher than for the single step addition of urea (1:1.3A, 1:1.1A and 1:0.9A) for the same UF ratios. The difference could be due to the fact that the multiple step urea addition resins had undergone longer periods of cooking than the

---

[1] 1:0.7 ratio resin was synthesised but solidified after one day. The resin proved to be unsuitable for application and analysis, and was only considered for X-ray diffraction analysis in the cured solid form.

single step urea addition resins. Hence, the possibility of forming larger molecular species during the multiple step urea addition. The increase in low molecular weight species is greater for the single-step urea addition than for the multiple step urea addition, resulting in a greater downward shift in the D.P. distribution, hence a lower viscosity. The lower viscosity for the single step urea addition could also be ascribed partly to the fact that the % solid content for the multiple step urea addition is slightly higher for the 1:1.1 and 1:0.9 respective ratio resins (table 5.).

2.2. Particleboards

The results for the tensile strength tests perpendicular to the surface of the boards (made from the above resins) are shown in figure 4. The tabulated results are shown in table 6. The average densities are in $g.cm^{-3}$ and the preparation conditions for the boards are described in more detail in chapter 4 (experimental). The preparation conditions for the different boards were kept the same.

The strength test results of a board with the same resin differ with change in the boards density. There was no significant decrease in the boards average strength for the boards prepared with the different resins from 1:1.8 to 1:1.3B. The strength then started to decrease slightly until the boards prepared with the 1:0.9 (A and B) resins were considerably weaker. The results compared favourably with the United States Department of Agriculture (table 2) standards for the manufacturing of particleboards. The standards suggested a tensile strength perpendicular to the surface for a low density board (density between 0.40 to 0.80 $g.cm^{-1}$) to be between 0.62 to 2.76 MPa.

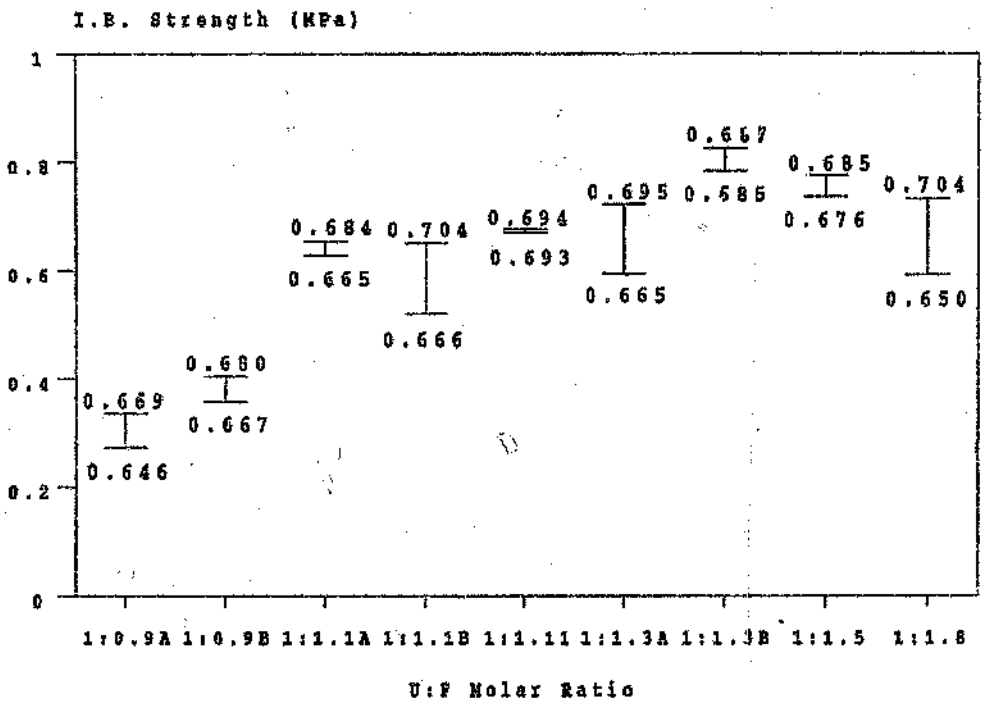

Figure 4. Internal Bond (I. B.)Strength test results for board strengths with the ranges of board densities in g/cm^3, prepared with the different modified resins.

The I.B. strength results of the boards in figure 4 can be interpreted by fitting an approximate non-linear multi-variable regression equat on, linking I.B. strength, density and U:F molar ratio of the resin used.

A multivariable equation was obtained by using the Levenberg-Marquardt modelling. The equation that fitted the experimental data the best for the A and B series resins, is shown below.

For the A series (single urea addition step).

$$I=-2.810+2.897U-0.9626U^2+2.456D^{1.495}$$

The estimated standard deviation =0.058 for an I.B. range between 0.274 and 0.825 MPa (see table 6)

For the B series (multiple urea addition).

$$I=-3.428+3.611U-1.217U^2+2.483D^{1.228}$$

The estimated standard deviation =0.052 for an I.B. range as above.

Where I=I.B. Strength (Mpa)
U=U:F molar ratio
D=Density (g/cm^3)

The surface representing the equation for the A series is shown in figure 4a. Figure 4b shows a different viewpoint of the same surface, with the closeness of fit to the experimental points. Figure 4 c and d show the respective surfaces for the B series boards.

For simplicity, the I.B. strength results of the above boards could also be interpreted by fitting an approximate non-linear regression equation, linking only the I.B. strength of a board to the U:F molar ratio of the resin used. The I.B. strengths corresponding to an approximate density of $0.680 g/cm^3$ for each board was considered.

For the A series resins

$$\ln I=-0.738+0.932\ln U \qquad r=0.689$$

For the B series resins

$$\ln I=-0.711+0.781\ln U \qquad r=0.687$$

Where
I=I.B. Strength (Mpa)
U=U:F molar ratio
and r =the correlation coefficient defined in chapter 5.4.

Figure 4e and f show the fit of the equations to the experimental data for A and B series boards respectively. It can be seen from the above that the phenomena can at best be explained to about 70% accuracy by a power regression equation. On the other hand, the phenomena could be better explained by a polynomial equation, as shown below.

For the A series resins

$$I=-1.823+3.482U-1.166U^2 \qquad r=0.972$$

For the B series resins

$$I=-1.692+3.273U-1.084U^2 \qquad r=0.942$$

Where

I=I.B. Strength (MPa)
U=U:F molar ratio

A correlation factor greater than 0.9 is considered to be acceptable. But the polynomial fit is often not a true reflection of the phenomena, since fitting polynomial equations, the tendency is to adjust, to include all the experimental points and does not consider deviations that could be due to experimental error.

An increase in the final tensile strength of the 1:1.5 and 1:1.3B boards when compared to the 1:1.8 board was observed. B. Tomita and S. Hatono [32] described an equation that used ^{13}C NMR results to give some indication of the possible degree of cross-linking present in the resin after curing (see later for detailed discussion of the equation). The results showed that there was only a small decrease in the amount of possible cross-linking between the 1:1.8 and the 1:1.5 and 1:1.3A resins (fig 16). The ^{13}C NMR results comparing the methylene to

methylol species ratios (see later for more detailed discussion) showed that the 1:1.5 and 1:1.3A resins had considerably more methylol species present than the 1:1.8 resin (fig 17). An increase in methylol species would increase the adhesion properties of the resin. Considerable amounts of free urea and free formaldehyde was observed by ^{13}C NMR to be present in the 1:1.5 and 1:1.3A resins (see figs 14 and 21 respectively and are discussed in more detail later). On curing, the free formaldehyde could react with the urea to form low molecular mass fractions that contribute to the adhesion to the adherent surface and adherent bulk at the resin-wood interface (fig 2). The I.B. strength tests for the boards made from the 1:0.9 (A and B) resins were considerably weaker and thus could be explained as follows. The ^{13}C NMR results for the respective liquid resins showed that the methylene to methylol ratio was very high (fig 17) indicating that proportionately much fewer reactive groups exist in this resin, mostly on lower molecular mass fractions. Hence, decreasing the adhesive strength of the wood-resin interface. The degree of possible cross-linking for the resins was very low (fig 16) causing a lower cohesion of the resin as well as lower glue-line bonds. The above resins had a very high concentration of free urea in the resin, which on curing could have remained unreacted.

The increase in the I.B. strength for the boards made with the 1:1.3B resin (multiple-step urea addition) compared to the 1:1.3A (single-step urea addition) showed that the multiple addition of urea to the resin increases the adhesive properties of the resin. This could also be seen by comparing the strength test results for 1:1.1A to 1:1.1B and 1:0.9A to 1:0.9B respectively. The 1:1.1B board did not perform as well as expected. The reasons for this could be seen from the ^{13}C NMR results. That

showed that the resin had a large amount of free unreacted urea present (fig 14) affecting the number of methylol groups present, and finally contributing adversely to the cross-linking. On curing, not all of the free urea would react, hence, decreasing the final boards strength.

There was no significant change in the strength for the board prepared with the 1:1.11 UF resin (back addition with formaldehyde) when compared to the boards of 1:1.1 (A and B) respectively. The back addition of formaldehyde to a 1:1.1 UF resin does not influence the final tensile strength of the board to a great extent. However, the ^{13}C NMR results showed that there are considerable differences in the species content of the final resins of 1:1.11 and 1:1.1 (A and B) respectively. The following differences were observed (the NMR results will be discussed in more detail later). An increase in the possible cross-linking capabilities (fig 14c) and an increase in methylene species for the 1:1.11 resin (fig 17c). The resin showed to have good cross-linking capabilities, but factors such the presence of free urea (fig 14c) and a high methylene to methylol species ratio, could have adversely influenced the wood-glue line properties, resulting in a board with lower internal bond strength. The lower methylol content and the higher free urea, means that there are proportionately fewer reactive sites, adversely affecting the adhesion properties of the resin.

2.3. Formaldehyde emission

A comparison between the different techniques for determining formaldehyde emission and relating them to the emission classes defined previously [25] is discussed below. The results are summarized in table 7.

1) The comparison between the perforator and air chamber method.
The data were obtained from Barghoorn [49], and are shown in figure 5. See table 8 for the tabulated results.

The equation for the straight line graph of Barghoorn's data was determined by the author to be as follows:

$$P=23.86A+8.12 \qquad r=0.998$$

where

P= Perforator (mg F/100g Board)
A= Air Chamber (ppm F)

If extrapolating the above straight line to the air chamber method of a value of 0 ppm formaldehyde, the perforator method should theoretically show a value of 8.12 mg F/100g of board. The discrepancy could be explained by considering the fact that the perforator method determines a higher formaldehyde content, since it considered all free formaldehyde and the break down of ethers to formaldehyde present in the board. The air chamber method on the other hand is time dependent whereas the perforator method is not, and would only measure the slow formaldehyde release due to free formaldehyde and resin decomposition. Though, the contribution to the formaldehyde emission due to resin

decomposition is very little. The value of 8.12 mg F/100g of board may be to high due to extrapolation. But, considering the fact that no values in the E1 range were determined, increasing the possibility of error in the small range.

2) The comparison between the perforator and WKI method. The results were obtained from Roffael [55] and independent studies and are shown in figure 6. (See table 9 for tabulated results).

The equation for the above straight line graph is:

$$W=0.92P+2.79 \qquad r= 0.978$$

where
W= WKI (mg F/100g board)
P= Perforator (mg F/100g board)

The WKI method determines the formaldehyde in the air above the sample and is time dependant. Hence, it would consider the formaldehyde due to free formaldehyde and formaldehyde due to hydrolysis from the board released over a certain period of time. Greater possibility of resin decomposition could occur in using the WKI method because the samples are kept in a high humidity container at elevated temperature. The perforator method would consider all the free formaldehyde and due to the ethers decomposing to formaldehyde in the board. If extrapolating the above equation of the perforator method to a value of 0 mg F/100g of board, the WKI method would have a value of 2.7 mg F/100g of board. This discrepancy could be due to the fact that a lot more species in the cured resin decomposes due to hydrolysis at elevated temperatures, resulting in a slightly higher formaldehyde. emission when compared to the perforator method.

3) The comparison between the WKI method and the desiccator method.
The desiccator method is similar to the Japanese Standard desiccator method [50], with a slight modification to allow for smaller board samples.

The results were obtained from independent studies and are shown in figure 7 (See table 10 for the tabulated results.)

The equation for the above straight line graph is as follows.

$$D=0.24W-0.65 \quad r=0.998$$

where
D= Desiccator (mg F/100g of board)
W= WKI (mg F/100g of board)

The formaldehyde emission measured by the WKI method is higher than those for the desiccator method. The reasons being:
a) The experimental temperature for the WKI was higher than for the desiccator method. Hence, higher emission of formaldehyde is expected.
b) The volume of air in the sample chamber for the WKI method was smaller than that for the desiccator method. Hence, for the same period of time, the formaldehyde concentration in a smaller space of air is higher.
c) The water sample used to absorb the formaldehyde was less for the WKI method than for the desiccator method. A water sample with higher formaldehyde concentration for the WKI method could be expected.

4) A comparison between the desiccator and air chamber method. A graphical representation between these two techniques was done for comparison purposes. It was of

interest to relate the desiccator method to a well known internationally acceptable technique for formaldehyde emission determination such as the air chamber method. The graph is shown in figure 8 and the values were obtained from table 7.

The equation for the above straight line graph is:

$$D=5.22A+1.77 \qquad r=0.999$$

where

D=Desiccator (mg F/100g of board)

A=Air Chamber (mg F)

A summary of the above results are shown in table 7, and could be used as a standard for comparing formaldehyde emission techniques in particleboards.

Table 7. Comparison between different formaldehyde emission determination techniques.

Emission Class [25]	Perforator mg F/100g of board	WKI mg F/100g of board	Air Chamber ppm	Desiccator mg F/100g of board
E1	0↔10	0↔11.8	0↔0.1	0↔2.21
E2	10↔30	11.8↔30	0.1↔0.9	2.21↔6.61
E3	30↔60	30↔57.3	0.9↔2.2	6.61↔13.2

For the analysis of the boards prepared with the different modified resins, and the standardising of the desiccator method variant, standard solutions were prepared using paraformaldehyde dissolved in distilled water. The fluorescence of the standards were determined and their results were plotted on a graph with a best curve fit (see figure 9 and table 11 for the tabulated results). The graph obeyed Beers law at low formaldehyde

concentrations, but deviated from linearity at higher concentrations. This was due to self absorption of the sample in the high concentrated solutions. In determining the formaldehyde concentration of the solutions obtained from the desiccator and WKI method with high formaldehyde concentrations, the solutions were first diluted to decrease the error due to the deviation from Beers law.

A best fit polynomial equation for the graph for figure 9 was obtained and is shown below.

$Y=111.385+303.696X-44.430X^2+2.878X^3-0.0707X^4$ $r=0.989$

Where

Y= Fluorescence Int.

X= Formaldehyde conc. (mg/l)

The boards prepared with the modified resins were cured with NH_4Cl only. No accelerators or formaldehyde catchers were used. The boards prepared were "core only" boards. The formaldehyde emission from "core only" boards are usually much higher than the normal three layer commercial boards.

The formaldehyde emission of the boards prepared with the different resins were determined by using the desiccator method. The boards were tested two weeks after manufacturing. Selected boards were tested three months after manufacturing, and their results compared to the previous ones. Figure 10 shows the results of the emission tests and the tabulated results are shown in table 12.

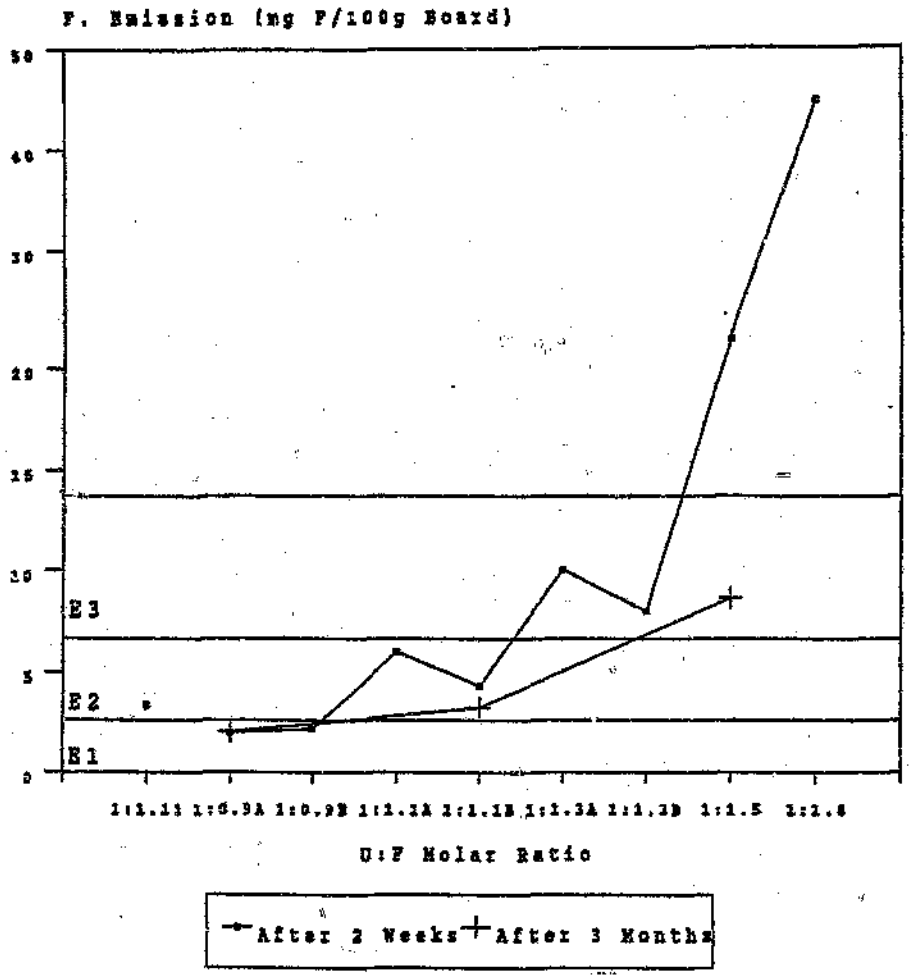

Figure 10. Formaldehyde emission from particleboards prepared with the different modified resins.

The dependence of formaldehyde emission to the U:F molar ratio, for the A-type resins (modified resins with a single addition of urea), appears to follow an exponential regression curve, of equation.

$$\ln F = -2.126 + 3.378U \quad r = 0.956$$

while the B-type resins (modified resins with multiple urea additions) follow an almost similar mathematical relationship.

$$\ln F = -2.223 + 3.340U \quad r = 0.950$$

where

U= U.F. molar ratio

F= formaldehyde emission (mg F/100g of board)

As it can be seen, the equation explain the phenomena well. The graph and experimental data point are shown in figure 10a and 10b respectively.

The boards with free formaldehyde in the resin have very high emission even after two weeks (1:1.8 and 1:1.5). ^{13}C NMR results showed free formaldehyde present in the liquid resin of 1:1.8 and 1:1.5 (see spectrum 20 and 21 respectively in which the free formaldehyde peak is at 84.7 ppm). The ^{13}C NMR also showed that these two resins had relatively high concentrations of amido methylol species (see spectrum 4 and 5 respectively in which the amido methylol species peak is at 88.7 ppm). Amido methylol species are known to exist in the following equilibrium

$$-CH_2OH \rightleftharpoons \text{Urea} + \text{Formaldehyde},$$

and could contribute to the high formaldehyde emission of the boards. The presence of these species are not evident from the NMR studies of the other U:F modified resins, therefore can be assumed to be of very low concentrations.

The 1:1.5 board showed a considerable decrease in formaldehyde emission after three months. The 1:1.1B and 1:0.9A boards with little free formaldehyde in the resin (see spectrum 10 and 11 respectively in which no free formaldehyde peak could be seen at 84.7 ppm) showed little difference between the two weeks and three months tests. Marutzky [47] suggested that the formaldehyde emission straight after pressing is high, drops off and levels to a constant rate after about two weeks. This is only true if the free formaldehyde content of the final resin is very low. Hence, the free formaldehyde and species that hydrolyse easily play an important role in the final formaldehyde emission of the boards, and decreases considerably with time. Thus, for the 1:1.5 resin, one could relate the difference observed between the 2 weeks and 3 months emission purely to the free formaldehyde present in the resin. Hence, from the results of the formaldehyde tests between the 2 week test and 3 month test, the rate of formaldehyde emission due to free formaldehyde could be about 1.07 mg F/ week (4.29 mg F/ month). This rate decreases significantly with time as the free formaldehyde content of the board decreases, and emission is then primary due to hydrolysis or decomposition of some species present in the board.

A lower formaldehyde emission was obtained for the boards prepared with the multiple-step urea addition to the single-step urea addition (compare 1:1.3A to 1:1.3B and 1:1.1A to 1:1.1B respectively). The reason for this could be that there was initially less free formaldehyde in the resins prepared by the multiple step urea addition than the single step urea addition (see figure 21 for the NMR results of free Formaldehyde to methylene species ratio). The modification by multiple step addition of urea to the resin could also decrease the species that hydrolyse easily.

The addition of formaldehyde in the final step (see results for 1:1.11) increases the formaldehyde emission of the board. The ^{13}C NMR showed free formaldehyde in the resin (see spectrum 13 in where the free formaldehyde peak is at 84.7 ppm). But the increase in the final formaldehyde emission for the board (1:1.11) was not as high as when compared to the boards that also had free formaldehyde in the resin (1:1.8 and 1:1.5). This suggests that the free formaldehyde in the 1:1.11 resin had almost all reacted with either the free urea or other species present during cure. The 1:1.11 resin has slightly higher formaldehyde content when compared to the 1:1.1A type resin. But their respective final emission were almost the same. This is significant when considering the fact that the final internal strength of the 1:1.11 board was slightly higher than the 1:1.1A. Hence, a board with reasonable internal bond strength can be made with a class E2 formaldehyde emission by simple back addition of a very small amount of formaldehyde in the last step of the synthesis. The species composition in the liquid resin before cure and a possible relation to the above phenomena, will be discussed later.

Various manufactures of particleboards include catchers or accelerators in the resin before use. A common catcher comprises of a low condensation with about 1:0.4 U:F molar ratio mix. This acts as an formaldehyde scavenger during cure. Accelerators are usually UF mixture with a U:F molar ratio of 1:2. Good E2 boards were made with the 1:1.1 molar ratio resins. If formaldehyde catchers and accelerators were used in the production of the boards, the boards would have been quite likely in an E1 emission class. The 1:0.9 resins are clearly in an E1 emission class, but their final internal bond strengths were a lot weaker.

2.4. IR spectroscopy

S. Jada [27] suggested freeze-drying of the samples prior to analysis. He showed that a more defined spectra could be obtained, especially in the region of 3600-2600 cm^{-1}. The freeze-dried technique was not used for the resin samples in question because the IR spectrometer did not allow the use of a holder for freeze-dried samples, and a change in the resins composition was suspected when the sample dehydrates.

Due to the complexity of the resin structures polymeric state, and the presence of byproducts such as water and formaldehyde, the transmittance frequencies are generally very broad and overlap. The table of band wavelengths and the spectra for the different liquid and UF modified resins cured with 3% NH_4Cl are shown in table 14 respectively.

The IR computer software used did not provide the opportunity of determining the peak areas of bands in a spectrum. Therefore the % transmittance of certain bands was used for quantification. By considering the change in the intensity ratios of certain bands, a change in the concentration of the respective species present in the resin could be done. A detailed analysis of each IR band assignments is described in chapter 5. The change in some of the band heights were compared to a band height that remained relatively constant over the range of samples analyzed. The band at 1653 cm^{-1} for Amide I remained relatively constant. The ratio of certain bands to the amide I band was obtained and are summarised in table 15.

Figure 11 shows the ratio % transmittance of the amide II band (1558-1548 cm^{-1}) to the amide I band for the liquid and cured resins. The ratio does not change significantly

for the different modified resins.

The bands at 1470-1452 cm^{-1} and 1155-1131 cm^{-1} show the amount of $-CH_2-$ groups (methylene bridges) present in a UF resin (fig 12a and 12b respectively). These groups are important as regards to the degree of polymerisation (DP) of the resin and when considering the strength of the glue-line and the possible cross-linking in the final board. Hence, a possible measure of the cohesion in the glue-line of the particleboards. The 1470-1452 cm^{-1} bands were ascribed to the $-CH_2-$ bending mode of the $-CH_2-N$ groups. The bands at 1155-1131 cm^{-1} was ascribed to the asymmetric stretching of $=N-CH_2-N=$ groups by S. Jada [27]. Meyers [28] ascribed the band to the C-O stretch of aliphatic methylene ethers. The ratios of both bands in relation to the amide I band behaved in a very similar way (see fig 12a and 12b respectively). An initial increase in $-CH_2-$ groups, followed by a large decrease at the 1:1.3B resin. The resins prepared with the multiple-step urea addition had a lower ratio than those resins synthesised with a single step urea addition. Hence, an overall lower amount of $-CH_2-$ groups present in the liquid resins. From the results and behaviour of the graph, the band at 1155-1131 cm^{-1} would be ascribed to that suggested by S. Jada [27]. The error involved in considering only band heights is large, and therefore no clear conclusions about the relative behaviour between the different modified resins can be done. Also, no clear values for the 1470-1452 cm^{-1} region from the cured resins of lower U:F ratio resins could be obtained.

Other important bands are the 1385-1351 cm^{-1} describing the CH_2OH groups. A general trend could be seen showing the decrease in the CH_2OH groups as the amount of urea added increased. But no significant trend could be seen when compared to the amide I band (fig 13). The graphs

behaved very similarly to those graphs assigned to the $-CH_2-$ groups.

The technique is not effective in studying small changes in modified resins, and will not be used further for quantitative analysis of the modified resins. The advantage of the technique is that one can analyze liquid and cured resins.

2.5. NMR spectroscopy

The ^{13}C NMR spectra of UF resins can be split up into four main areas.

1) The substituted and unsubstituted urea carbonyl groups with signals from 160-170 ppm,
2) Methylene groups with signals from 45-60 ppm,
3) Methylol groups with signals from 65-72 ppm and
4) Methylene-Ether groups with signals from 69-90 ppm.

There are also less important species present at much lower concentrations such as the methylene glycols, but these will not be considered.

No quantitative results can be obtained directly from the raw spectra. By considering peak ratios of certain chemical species and groupings, differences between the various synthesis parameters and the final resin's properties could however be deduced and some quantitative considerations derived. See table 18 for the tabulated results of peak ratios discussed below.

Urea/(C1+C2)

The peak arising at 165 ppm is due to the carbonyl group of free urea. This peak was not evident in the unmodified commercial resin (1:1.8) (see spectrum 20). Increases in free urea was noted in the modified resins as more urea

was added during the synthesis steps. This can be seen when considering the intensity ratios of free urea to the sum of the total intensities of the other carbonyl groups (urea/(C1+C2)) (fig 14). The peak at 163.6 ppm was assigned to the methylol carbonyl group $NH_2\underline{C}ONHCH_2OH$ (C1). The peak at 162.0 ppm was assigned to general carbonyl groups where the -NH groups next to the -C=O groups has more than one substitution and are present in larger molecular species, ie. =N$\underline{C}$ON= groups (C2). B.Tomita and S. Hatono [32] suggested that the peak at 162.0 ppm is an overlap of various carbonyl groups that have very small differences in chemical shifts.

Figure 14 shows that the multiple step addition of urea from 1:1.8 to 1:1.3B and 1:0.9B respectively produces resins with lower free urea that resins with the same UF ratio but with the urea added in one step (compare 1:1.3A to 1:1.3B and 1:0.9A and 1:0.9B respectively). A discontinuity was observed with the 1:1.1A and 1:1.1B resins. The free urea for 1:1.1B was higher than for 1:1.1A. The difference could be due to the lower concentration of the other carbonyl groups (C1+C2) in the 1:1.1B resin than in the 1:1.1A resin. Figure 14a and 14b show that a relationship can be obtained between the amount of urea added to a prepared resin under the same synthesis conditions to the urea/(C1+C2) ratio present in the final resin. Predictions about the urea/(C1+C2) ratio in the final resin could be done by considering the amount of urea to be added, and keeping the synthesis conditions the same. A decrease in formaldehyde content due to the addition of urea to a resin would almost double the increase in the urea/(C1+C2) ratio of the final resin. For the single-step urea addition type resins (A series), an exponential relationship would be represented by the regression equation (fig 14a)

$$\ln Y = 3.596 - 3.962U \qquad r = 0.940$$

A reasonable relationship can be observed for the step-wise urea addition resins (B series). Thus, an exponential regression equation could also describe the phenomena for the multiple-urea addition resins (fig 14b)

$$\ln Y = 3.213 - 3.666U \qquad r = 0.937$$

Where

Y= Peak ratio (urea/(C1+C2))

U= U:F molar ratio

The increase in urea/(C1+C2) ratio to a decrease in the formaldehyde content due to addition of urea is lower for the multiple step addition than for the single-step urea addition. Hence, more urea reacted during the multiple-step urea addition than the single step addition.

A high urea/(C1+C2) ratio for the 1:1.11 resin was observed (fig 14c). Formaldehyde was added to the resin during the last step of the resins modifications. This could have caused the formaldehyde to react preferably with the carbonyl species than with urea. Hence, decreasing the final (C1+C2) concentration.

C1/C2

The ratio C1/C2 for the different resins is shown in figure 15.

A large drop in the methylol carbonyl group (C1) concentration from the initial 1:1.8 UF resin was observed. No significant change in the ratio (C1/C2) was seen for the subsequent modified resins. The urea reacted with the free formaldehyde and other components to increase the carbonyl groups that do not have a terminating methylol group. The free urea could have also

reacted with the methylol carbonyl groups, and decreasing its concentration. But this is not as evident, since the NMR spectra do not show a large decrease in the amount of C1 species after the urea was added (see spectra 11 and 12 for the 1:0.9 A and B resins respectively).

Regression equations explaining the phenomena relating the NMR peak ratios for the C1/C2 to the urea content are as follows:
For the A-type resins (single urea addition) the curve could be interpreted by an exponential fit (fig 15a)

$$\ln Y = -1.790 + 1.779U \qquad r = 0.831$$

Similar, the B-type resins (multiple-urea addition) could also be explained using an exponential fit (fig 15b)

$$\ln Y = -2.629 + 2.3\ldots \qquad r = 0.937$$

Where

Y= Peak Ratio (C1/C2)
U= U:F molar ratio

No significant change was observed in the C1/C2 ratio for the modified resin where formaldehyde was added in the final step (see 1:1.11 in figure 15c). Hence, the addition of formaldehyde in the final step does not seem to influence the C1/C2 ratio.

Cross-linking

B. Tomita and S. Hatono [32] formulated an equation that considered the peak intensities of the methylene species in the liquid resin. The equation would give some indication to the degree of cross-linking present after curing.

Degree of cross-linking = (C+2E)/(A+C+E) where
A=-NHCH$_2$NH-, C=-N(CH$_2$-)CH$_2$NH- and E=-N(CH$_2$-)CH$_2$N(CH$_2$-)-.

Methylene species are important contributors to the final cross-linking capabilities of the resin in the cured state and to the final internal bond strength of the board. The comparison between the possible cross-linking for the different modified resins to the U:F ratio is shown in figure 16.

An overall decrease of possible crosslinking as predicted by the equation, was observed from the unmodified (1:1.8) resin to the 1:0.9 ratio resins. The subsequent addition of urea to UF resins decreases the cross-linking capacity of the resins. A higher proportion of cross-linking was observed for the modified resins with the multiple-step urea addition than for the single step urea addition (compare 1:1.3A to 1:1.3B and 1:1.1A to 1:1.1B). There is a relationship between the possible cross-linking in a resin to the amount of urea added to the resin. This can be expressed by the following power regression equations for the A and B series resins respectively (fig 16a and 16b)

For the A-type resins

$$\ln Y = -0.621 + 0.466 \ln U \qquad r = 0.832$$

For the B-type resins

$$\ln Y = -0.595 + 0.543 \ln U \qquad r = 0.889$$

where

Y= Peak Ratio (possible cross-linking)

U= U:F molar ratio

An increase of about 12% in the cross-linking capabilities for a resin modified by a multiple-step urea addition to that by direct urea addition was observed. The addition of urea increases the -NHCH$_2$NH- groups, and

seem to react with the branched groups $-N(CH_2-)\underline{C}H_2NH-$ and $-N(CH_2-)\underline{C}H_2N(CH_2-)-$ preferentially.

Comparison between the predicted cross-linking from NMR studies and I.B. strength tests results could be done[2]. For the B-type resins, a good linear relationship could be obtained as follows (fig 16d).

$$IB=1.492Y-0.335 \qquad r=0.919$$

Where

IB= I.B. Strength (MPa)

Y= Peak Ratio (possible cross-linking)

The A type resins did not follow the same trend as the B type resins. Note, that the last point (1:0.9A) was omitted due to the large error.

But a tentative equation could be formulated as follows

$$I=0.157Y+0.602 \qquad r=0.449$$

An interesting point to note is that the slope for the two curves are very different. Hence, the B series resins are far more influenced by the possible cross-linking factors than the A-series resins. Thus, at least for a homologous series of resins, such as the B-series resins, a direct mathematical relationship between the predicted board strength and molar standardised conditions can be derived. This relationship would of course differ for other types of homologous resins. The relationship will also be different for instance if more resin is used and other standard conditions of application are varied. Nonetheless the important principle remains that there is

[2]The I.B. strength values used had an average density of 0.680 $g.cm^{-3}$.

an excellent relationship between cross-linking measured by NMR and actual I.B. strength of boards manufactured under the same conditions. As a consequence, one can substitute the equation obtained by B. Tomita and S. Hatono [32] as follows

$$\text{I.B. Strength} = a\{(C+2E)/(A+C+E)\} + b$$

Where the coefficients a and b can vary according to the homologous series of boards and resins with the standardised conditions chosen. The equation relating I.B. strength to the NMR measurements can be taken further by considering the ratios of other species. This will be done at a later stage.

A significant increase in cross-linking is observed for the 1:1.11 UF modified resin when compared to the 1:1.1A and 1:1.1B UF resins respectively (fig 16c). The extra addition of formaldehyde in the final step seems to increase the cross-linking capabilities of the resin considerably. Hence, an increase in the branched species $-N(CH_2-)\underline{C}H_2NH-$ and $-N(CH_2-)\underline{C}H_2N(CH_2-)-$.

Me/Mo

The ratio of total methylene (Me) to total methylol (Mo) groups in UF resins is also an important factor to consider. Figure 17 shows the relationship between the calculated ratios for the different modified resins. There was an initial decrease in the ratio for the first two modified resins (1:1.5 and 1:1.3A), followed by an increase for the remaining resins (1:1.3B to 1:0.9B). The addition of urea increases the methylene content of the resin whereas the first two modified resins showed an increase in methylol species. This can be an indication that the urea initially reacted with the free formaldehyde that was present in the initial resin to

form methylol species. Considering the resins that were modified by a single addition of urea (1:1.5, 1:1.3A, 1:1.1A and 1:0.9A) respectively, a polynomial curve could be obtained that shows the change in UF ratio of a resin by addition of urea to the Me/Mo ratios content of the resin (fig 17a).

$$Y=0.229U^2-0.631U+0.615 \qquad r=0.996$$

A similar relationship could be obtained when considering only the modified resins with the multiple-step urea addition (1:1.3B, 1:1.1B and 1:0.9B respectively) (fig 17b).

$$Y=0.222U^2-0.632U+0.640 \qquad r=0.808$$

Where

Y= Peak ratio (Me/Mo)

U= U:F molar ratio

The significance is that a minimum in the Me/Mo ratio can be obtained by a higher U:F ratio resin with modification by multiple-step urea addition than with a single urea addition. This is important when considering the adhesive properties of a resin in relation to the components present. ie. Methylene species play an important part in the cohesive performance of the glue-line. Whereas, methylol species on the other hand might play an important part in the adhesion at the wood-adhesive boundary and also contribute to the cohesion properties in the cured state. Properties such as water uptake and hydrolysis are influenced by the amount of these species present in the resin. An optimized ratio between these two species should be obtained to produce a resin whose total adhesive properties are being used.

Figure 17c shows the ME/MO ratio obtained by back-

addition with formaldehyde. The back-addition with formaldehyde produces a considerable higher ME/MO species ratio, than with the simple urea modification (compare values for 1:1.11 to 1:1.1A and 1:1.1B respectively). The higher methylene content improves the glue-line strength considerably. But a decrease in the overall lower molecular weight methylol species can adversely affect the adhesion properties of the wood-adhesive boundary. A good balance between these two species would be required to optimise the resins performance.

E1/E2

The contribution of ether species to the final properties of the resin are less significant, but can be considered. The ratios of the branched and unbranched methyl methylene ethers for the different modified resins are shown in figure 18 (E1/E2)
where E1=-$NHCH_2OCH_3$ and E2=-$N(CH_2-)CH_2OCH_3$.

A large decrease of the unbranched methyl methylene ether (E1) was observed in the addition of urea to the 1:1.8 commercial resin. An increase in branched methyl methylene ethers (E2) was observed for the multiple-step urea addition when compared to the single-step urea addition resin synthesis (compare 1:1.3A to 1:1.3B, 1:1.1A to 1:1.1B and 1:0.9A to 1:0.9B). The modified resins with the single urea addition (1:1.5, 1:1.3A, 1:1.1A and 1:0.9A) has about 10% higher E1 content than those modified with the step wise urea addition (1:1.3B, 1:1.1B and 1:0.9B). The higher concentrations for branched methyl methylene ethers bridges (E2) content for the multiple-step urea addition might be ascribed to the longer synthesis time that has to be used and might be an important characteristic to the performance of the final resin. The following non-linear regression equations can be fitted to the two series of resins to describe the

phenomena. For the A series resins (fig 18a)

$$\ln Y = 0.414 + 0.784U \qquad r = 0.784$$

Similar for the B series resins (fig 18b)

$$\ln Y = -0.756 + 1.494U \qquad r = 0.922$$

Where

Y= Peak Ratio (E1/E2)

U= U:F molar ratio

On the other hand, the above phenomena could be better explained by a polynomial equation, as shown below.

For the A-series resins

$$Y = 19.350 - 27.716U + 11.815U^2 \qquad r = 0.996$$

and for the B-series resins

$$Y = 12.494 - 20.1\_\_U + 9.765U^2 \qquad r = 0.974$$

A considerable increase in the E1/E2 ratio was observed for the 1:1.11 UF resin when compared to the 1:1.1 (A and B) resins (fig 18c). An extra addition of formaldehyde in the final step increases the unbranched methyl methylene ethers content. Hence, the addition of formaldehyde in the last step could break up the branching ethers. The extent of the contribution of the branched and unbranched methyl methylene ethers to the final performance of the resin is not well known. But the following speculations about the influence of unbranched species has on the D.P. can be done. Less branching of a species would infer that there are less sites for branching and forming cross-linked species on curing. This would influence the D.P. distribution, even slightly. Ether can decompose in the liquid and after curing, to emit formaldehyde. For

example.

$$Urea\text{-}CH_2\text{-}O\text{-}CH_2\text{-}Urea \longrightarrow Urea\text{-}CH_2\text{-}Urea + Formaldehyde$$

Hence, the ethers could play a role in the overall formaldehyde emission of a particleboard.

(E1+E4)/(E2+E5)

Other ether ratios were also considered (fig 19). The ratios of methyl methylene ethers to the methylene ether bridges ((E1+E2)/(E4+E5)) and the ratios of (E1+E4)/(E2+E5) respectively. Where E4=-NH$\underline{CH_2}O\underline{CH_2}$NH- and E5= -N(-$CH_2$-)$\underline{CH_2}OCH_2$NH-.

A rapid decrease for both ratios from the unmodified resin (1:1.8) to the 1:0.9 UF resins was observed. The addition of urea decreases the methyl methylene ether content of the resins considerably from the unmodified resin. Hence, the urea could react with the end methylol end groups forming longer ether chains. Regression equations can be obtained for the two resins types (A and B). Although, the correlation coefficient is low.
For the A type resins (fig 19a)

$$\ln Y = -0.1955 + 0.746U \qquad r = 0.811$$

Similar for the B type resins (fig 19b)

$$\ln Y = -0.949 + 1.196U \qquad r = 0.913$$

where

Y= Peak Ratio ((E1+E4/(E2+E5))
U= U:F molar ratio

The modified resins with formaldehyde back addition 1:1.11 is shown fig 19c. A slight increase in the ratio is noted for this resin when compared to the other 1:1.1 resins. Hence, the extra addition of formaldehyde in the

last step causes an increase in the methyl methylene ether species in the resin.

(E1+E2)/(E4+E5)

The ratio of unbranched ether species to the branched ether species ((E1+E2)/(E4+E5)) has the same trend as observed for the above (fig 20). The addition of urea increases the total amount of branched ether species. Regression equations can be obtained to express the above phenomena for the two types of resin.

For the A type resin (fig 20a)

$$\ln Y = -0.437 + 0.8892U \qquad r = 0.752$$

Similar for the B type resins (fig 20b)

$$\ln Y = -1.143 + 1.343U \qquad r = 0.886$$

where

Y= Peak Ratio ((E1+E2)/(E4+E5))

U= U:F molar ratio

An increase in the ratios was observed for the 1:1.11 UF ratio resin. The addition of formaldehyde in the last step influences the ratios considerably. Hence, the addition of formaldehyde produces more unbranched ether species and methyl methylene ethers (fig 20c).

The above phenomena could be explained with a better correlation factor by a polynomial type of equation as follows. For the A-series resins

$$Y = 12.482 - 18.578U + 7.784U^2 \qquad r = 1.000$$

Similar for the B-series resins

$$Y = 8.339 - 13.126U + 6.021U^2 \qquad r = 0.950$$

The ratio of free formaldehyde to the total methylene content of the modified resins could give some indication to what extent the influence of the extra urea addition has on the free formaldehyde content of the resins. The ratio is not a true representation since the methylene content is not constant for all the resins. The free formaldehyde could not be observed by ^{13}C NMR for the resins that are below 1:1.1A UF ratio. The resin where formaldehyde was added in the final step showed a small increase in free formaldehyde (fig 21c). Figure 21 shows how the free formaldehyde content decreases rapidly with the addition of urea to the resin. Regression equations for the A series (fig 21a)

$$\ln Y = -5.956 + 3.376U \qquad r = 0.932$$

Similar for the B series resins (fig 21b)

$$\ln Y = -6.894 + 3.908U \qquad r = 0.948$$

where

Y= Peak Ratio (free F/Me)

U= U:F molar ratio

It is of importance to relate the ratios and equations obtained by ^{13}C NMR studies to the physical properties of the final boards. The species ratio are related to the UF molar ratio. Hence, being able to speculate about the physical properties of a UF particle board by considering only the ^{13}C NMR studies of the particular resin before use.

Firstly, one would have to consider which species and to what extent does each species influence the respective physical property. There are a number of physical properties of a particle board that could be related to the species ratio in the initial resin. For example, I.B.

strength, formaldehyde emission, water solubility, thermal conductivity, aging and related bond deterioration with time and others.

The I.B. strength and formaldehyde emission of the boards will be considered in relation to NMR species ratio. The approach taken to investigate the NMR ratio studies of species present in the liquid resin to that of, say I.B. strength was done as follows.

The results of each one of the above eight ratios studied were taken in turn and compared to the I.B. strength results for the particular series (A and B) respectively. If the species ratio correlated reasonably well with the I.B. strength results, the species could be considered. Also, the literature mentioned that certain species play more of an important role than other in the final strength of a board. Hence, taking the above mentioned factors into consideration, the following deductions and equations were obtained.

Table 19 shows the NMR species ratio correlation to I.B. strength for the respective series of resins. As can be seen from the results of the table, only certain species ratio correlate with I.B. strength. It can also further be deduced from literature studies that ratios such as Me/Mo are likely to play an important role in the final I.B. strength of a board. As discussed previously, the equation by B. Tomita and S. Hatono for possible cross-linking can also be considered. From the correlation studies, the urea/(C1+C2) ratio could also play a role in the strength. This makes sense, since an increase in free urea content of a resin should adversely affect the boards performance. The other species (ethers) do not correlate as well, and there final contribution to the I.B. strength of a board would be low, and from the

literature, their importance is not clear. But since ethers decompose, and emit formaldehyde, they play an important role in the final formaldehyde emission from particleboards, and will be considered later.

Therefore the three discussed species ratio can be related to the I.B. strength by taking the respective experimental data and obtain the following equation for the A series resins.

$$IB=0.4275Y_4-0.3623Y_1+2.389Y_5$$

with an estimated standard deviation = 0.204

Similarly for the B-series resins

$$IB=1.077Y_4-0.1130Y_1-0.1424Y_5$$

with an estimated standard deviation = 0.115
where

IB= I.B. Strength (MPa)
Y_1= urea/(C1+C2) peak ratio
Y_4= possible cross-linking peak ratio from the Tomita equation [32]
Y_5= Me/Mo peak ratio

It must however be remembered that the equation coefficients are unique for each specific homologous resin. The equation would change for resins synthesized and boards made under different conditions, and this can be seen by the following example.

Consider the ^{13}C NMR species ratio results (table 18) and I.B. strength (table 6) for the 1:1.11 ratio resin. A resin synthesised by a single addition of urea to obtain

a 1:1.1 UF resin, followed by a addition of formaldehyde to obtain a final U:F resin 1:1.11 (see the experimental chapter for more detail on the synthesis). The resins synthesis and respective particleboard manufacture were very similar to the A-series resins. Therefore the equation obtained for the A-series resins can be used to predict the I.B. strength of the board by simply considering NMR species ratio. The following table show the results obtained from predictions and experiment.

Table 21. Comparing the predicted and experimental I.B. strength for the 1:1.11 UF ratio resin.

Predicted I.B. Strength (MPa)*	Experimental density ($g.cm^{-3}$)	Measured I.B. strength (MPa)
A-Series equ: 0.634 B-Series equ: 0.575	0.694	0.676

I.B. strength at an average density of 0.680 $g.cm^{-3}$

Considering the fact that the density of the board was higher, and the synthesis scheme slightly different, the predicted I.B. strength, using the A series equation, correlates closely with the measured I.B. strength of the particleboard. The predicted I.B. strength using the B series equation does differ considerably to the experimental results. Hence, this does show that the equations are unique for a homologous set of resins, and variations in synthesis schemes does play an important role.

But an important fact can be deduced from the above, that the physical property (I.B. strength) can be related to the species ratio present in the resin before cure. There are also other species ratios that could be considered, but their significance would be low. Species such as the

ethers contribute very little to the I.B. strength. They tend to decompose under humidic conditions, and emit free formaldehyde. Species such the free F/Me ratio seem to correlate, but only due to the type of experimental setup, where the formaldehyde content was decreased sequentially by the addition of urea. This is true in most industrial applications, but for resins synthesised by simple first urea addition, the relationship would not hold.

Hence, a general equation can be obtained relating I.B. strength to the NMR peak ratio studies of certain species.

Thus: Strength={(C+2E)/(A+C+E)}+{urea/(C1+C2)}+{Me/Mo}
and therefore for the I.B. strength

IB=a{(C+2E)/(A+C+E)}+b{urea/(C1+C2)}+c{Me/Mo}

where
a, b, and c are independent variables for the unique homologous UF resin series.

A= $-NH\underline{C}H_2NH-$ (peak at 48.8 ppm)
C= $-N(CH_2-)\underline{C}H_2NH-$ (peak at 55.5 ppm)
E= $-N(CH_2-)\underline{C}H_2N(CH_2-)-$ (peak at 61.6 ppm)
C1= $NH_2\underline{C}ONHCH_2OH$ (peak at 162.0 ppm)
C2= larger molecular species ie. $=N\underline{C}ON=$ groups (peak at 162.0 ppm)
urea= free urea (peak at 165 ppm)
Me= A+C+E, total methylene species (peak from 45-60 ppm)
Mo= total methylol species (peak from 65-72 ppm)

A similar approach can be taken for relating NMR peak ratio species to the formaldehyde emission. Table 20 shows the NMR species ratio correlation to formaldehyde emission for the respective series of resins.

A lot of the species ratio seem to correlate with the formaldehyde emission. Logically and clearly, the free F/Me ratio correlates excellently with the formaldehyde emission from particle boards. The effect of the other species such as the C1/C2 have on the final emission of formaldehyde from the board is not clear. An equation relating only the free F/Me ratio to the formaldehyde emission can be obtained for the A series resins (fig 22).

$$F=2.927+37.11Y_8 \qquad r=0.996$$

Similar for the B series resins (fig 23)

$$F=2.847+36.35Y_8 \qquad r=0.997$$

where

F= formaldehyde emission (mg F/ 100 g of board)

Y_8= free F/Me

The above correlation could only be applicable for shorter periods of time. Since, it was shown that the formaldehyde emission from boards made with a resin that initially contained high amounts of free formaldehyde in the liquid resin (1:1.5), showed a considerable decrease in emission when tested again after three months.

The correlations of formaldehyde to the other species NMR peak ratios were reasonably good, and the following species ratio could also be considered to play a role in the formaldehyde emission of particleboards and be included in a final equation that expresses the formaldehyde emission of a board to the species ratio present in the liquid resin.

Urea/(C1+C2) (Y1) ratio should logically belong to the equation. Since, the presence of free urea in the system would affect the final formaldehyde emission by possibly

"capturing" free formaldehyde during the curing stages of the resin.

The correla[illegible] of the C1/C2 ratio seems to be very good. But there contribution to the final formaldehyde emission of a board is not clear. Since, the carbonyl ratios have been indirectly considered by the Urea/(C1+C2) ratio, the ratio could be redundant.

It is clear that the cross-linking ratio (Y4) should have some influence on the formaldehyde emission of a particleboard. This is especially true for boards that are used for long periods of time and are exposed to high humidity conditions. Since, with time, most of the other species (free formaldehyde) that influence the emission considerably have almost all disappeared, the presence of $-CH_2-$ groups then play a role. Hence, an increase in cross-linking of a resin means that there is a higher concentration of $-CH_2-$ groups present, that with time can hydrolyse and emit formaldehyde.
The following species ratio to consider are the ethers. The correlation of all three species ratio (Y3, Y6 and Y7) are respectively good. But only one of the ratios was considered and the reasons for rejecting the others is as follows.
One has to look at the chemistry of each of the ethers present, and consider which of them would contribute to the formaldehyde emission. The E1/E2 ratio where
E1=$-NH\underline{C}H_2OCH_3$ and E2=$-N(CH_2-)\underline{C}H_2OCH_3$ would not influence the emission. Since, the species would only decompose and emit a methylol rather than formaldehyde. The (E1+E2)/(E4+E5) species ratio was considered to contribute to the formaldehyde emission over the (E1+E4)/(E2+E5) species ratio. Even though that the correlation of the second ratio was slightly better. Where E4=$-NH\underline{C}H_2O\underline{C}H_2NH-$ and E5= $-N(CH_2-)\underline{C}H_2OCH_2NH-$. The E4

and E5 species can decompose and emit formaldehyde as follows

$$-NHCH_2OCH_2NH- \longrightarrow -NHCH_2NH- + \text{formaldehyde}$$

The E5 species would decompose similarly, since the presence of the extra (CH_2-) group would not influence the emission. Hence, a decrease in the (E4+E5) species would decrease the emission of formaldehyde.

From the literature, species such as the decomposition of amido methylol play a minor role in the formaldehyde emission. Table 3 shows that the amido methylol (E3) species also contribute to the formaldehyde emission of particle-boards. Unfortunately the NMR technique used was not sensitive enough to detect the low traces of the particular species in most of the resins analyzed (table 17 where the amido methylol species is at 88.7 ppm), and was only observed in the 1:1.8 and 1:1.5 UF liquid resins. Hence, their contribution to these specific set of resins would be low, and will only be considered in the general equation and not the specific equations for the A and B series resins respectively.

An equation can be obtained that is unique for the specific set of homologous resins. Also unique for the particular formaldehyde emission determination method (desiccator). A general equation linking the species ratio of free F/Me, (amido methylol)/Me, Urea/(C1+C2), Possible cross-linking, (E1+E2)/(E4+E5) and E3/Me to the formaldehyde emission of a board can be expressed as follows.

$$F=a\{\text{free F/Me}\}+b\{(C+2E)/(A+C+E)\}+c\{\text{urea}/(C1+C2)\}+d\{(E1+E2)/(E4+E5)\}+e\{E3/Me\}$$

where

a, b, c, d, and e are independent variables for the unique homologous UF resin series.

free F= Free formaldehyde (peak at 84.7 ppm)
Me= Sum of all Methylene groups
A= $-NH\underline{C}H_2NH-$ (peak at 48.8 ppm)
C= $-N(CH_2-)\underline{C}H_2NH-$ (peak at 55.5 ppm)
E= $-N(CH_2-)\underline{C}H_2N(CH_2-)-$ (peak at 61.6 ppm)
C1= $NH_2\underline{C}ONHCH_2OH$ (peak at 162.0 ppm)
C2= larger molecular species ie. $=N\underline{C}ON=$ groups (peak at 162.0 ppm)
urea= free urea (peak at 165 ppm)
E1=$-NH\underline{C}H_2OCH_3$ (peak at 73.4 ppm)
E2=$-N(CH_2-)\underline{C}H_2OCH_3$ (peak at 88.7 ppm)
E4=$-NH\underline{C}H_2O\underline{C}H_2NH-$ (peak at 70.3 ppm)
E5= $-N(CH_2-)\underline{C}H_2OCH_2NH-$ (peak at 75.0)
E3= $-NHCH_2OCH_2OH$ (peak at 88.7 ppm)

Therefore the discussed species ratio can be related to the formaldehyde emission for the specific series of resins by taking the respective experimental data and obtain the following equation for the A series resins.

$$F=19.18Y_8-11.66Y_1+7.166Y_4+4.126Y_7$$

with an estimated standard deviation= 0.389

Similarly for the B-series resins

$$F=21.71Y_8-6.086Y_1+2.389Y_4+4.346Y_7$$

with an estimated standard deviation= 2.013

where

F= Formaldehyde emission (mg F/100g of Board)
Y_1= urea/(C1+C2) peak ratio
Y_4= possible cross-linking peak ratio from the Tomita equation [32]
Y_8= Free F/Me peak ratio
Y_7= (E1+E2)/(E4+E5) peak ratio

Similarly one can use the ^{13}C NMR species ratio and formaldehyde emission results for the 1:1.11 ratio resin and apply the above equations. Hence, the resin synthesis and formaldehyde emission method are very similar to the A series resins. The following table show the results obtained from the comparison.

Table 22. Comparing the predicted and experimental formaldehyde emission for the 1:1.11 UF ratio resin.

Predicted F. emission (mg F/100g board)	Measured F. emission (mg F/100g board)
A-Series equ: 9.15 B-Series equ: 11.90	3.38

The measured formaldehyde emission is considerably lower than the predicted values. The formaldehyde emission equations seem to be a lot more sensitive to the specific series of resins. Formaldehyde was added in the last step during the above resins synthesis, and free formaldehyde is a crucial contributing factor to the formaldehyde emission from the boards. Error in the prediction could be expected. But still, it can be seen that the predictions with the A series equation was slightly lower than the prediction with the B series equations. Since the synthesis of the A series resins were slightly similar to the 1:1.11 U:F resin.

Hence, the above sets of equations can be used in predicting some of the physical properties by studying the ^{13}C NMR peak ratio of certain species.

2.6. X-ray diffraction

Samples of the series of modified resins (1:1.8 to 1:0.7A) were cured with 3 and 9% NH_4Cl at 140 °C for 1 hour respectively. Traces 14 and 15 show how the crystallinity changes from an almost amorphous material (1:1.8) to a semi-crystalline (1:0.7A). The two methods of synthesis had no apparent effect on the final cured resins crystallinity (see trace 15 and compare the different resins synthesised by a multiple-step urea addition (B) and the single urea addition step (A)). Resins 1:1.8, 1:1.5, 1:1.3A, 1:1.1A, 1:0.9A and 1:0.7A will only be considered for crystallite size and % crystallinity calculations.

Trace 16 shows the respective resins cured with 9% NH_4Cl. A number of sharp peaks appear for the higher UF resins. These peaks arise due to crystalline NH_4Cl salt which did not dissolve completely during cure. The samples cured with 3% NH_4Cl were only considered for further analysis.

Previous studies [9], showed that the crystallinity of UF resins breaks down when cured with wood chips as well as some previous theoretical considerations for this have been reported [42]. Wood comprises of about 30-35% native crystalline cellulose. The X-ray diffraction pattern of native cellulose and the reference ASTM pattern are shown in trace 9. It was of interest to see how the crystallinity of the UF resins change when reacted with pure native cellulose. Mixtures of native cellulose with the high crystalline resin (1:0.9A) were prepared by curing the resin with 3% NH_4Cl and 9:1 and 1:1 cellulose respectively at 120°C for 45 minutes.

Traces 10 and 11 show the X-ray diffraction traces of a resin:cellulose mixture of 9:1 superimposed with the

traces of native cellulose and pure cured resin 1:0.9A respectively. The crystallinity of the mixture did not change much with respect to the pure cured resin. The crystalline cellulose concentration was to low to have any significant affect on the crystallinity of the cured resin.

Traces 12 and 13 show the diffraction traces of a 1:1 resin:cellulose mixture superimposed with the traces of native cellulose and pure cured resin 1:0.9A respectively. The crystallinity of the resin has virtually disappeared. The dominant peak of the pure resin at 21.7° (2θ) was superimposed by the strong cellulose peak in the same region. A slight shoulder could be seen at 24.5° (2θ) for the cellulose/resin mixture trace. This shoulder could be from the broad crystalline peak of the pure resin in the region. From the above results, it can be seen that the crystallinity of the resin decreased considerably when reacted with pure cellulose of higher concentration. Also, the overall crystallinity of the cellulose decreased considerably. Hence, it can not be assumed that the crystallinity of the resin observed in a pure cured state, would exist when cured with wood.

Nabiev [38] studied the X-ray diffraction traces of various standard derivatives (see traces 6, 7, and 8 respectively). Trace 17 and 18 show the trace of 1:0.9A cured resin superimposed with that of trimethylene-tetraurea and urea respectively. The most intense 2θ peak for both trimethylenetetraurea (trace 8) and urea (trace 1) almost coincide with the most intense peak of the resin. The slight shift in the peaks could be ascribed to the amorphous matrix influencing the crystalline regions of the resins. Hence, the resin had similar d-spacing to that of the urea and trimethylenetetraurea. The other

standard derivatives do not show any clear resemblance to that of the resin (traces 2-7). Since urea and trimethylenetetraurea comprise largely of methylene species, from the literature [37] and the above results, it could be assumed that the crystalline regions in cured UF samples are also largely due to methylene species. This could be an indication that the species that are present in the high U:F ratio resins comprise largely of linear molecules in an amorphous matrix. Hence, tri-dimensional branching occurring between the resin species decreases as the U:F ratio increases. This makes sense, since studies and predictions from ^{13}C NMR studies using the .B. Tomita and S. Hatono [32] equation for possible cross-linking in the liquid resin decreased as the U:F ratio increased.

The X-ray diffraction pattern of some of the cured 1:0.9A resin was done at 170°C. No apparent change in the diffraction trace was observed from its room temperature trace. This suggests that the crystallite regions of the resin are not separate from the bulk amorphous region but rather consists of small regions were crystalline order is formed by sections of the molecules (see figure 22).

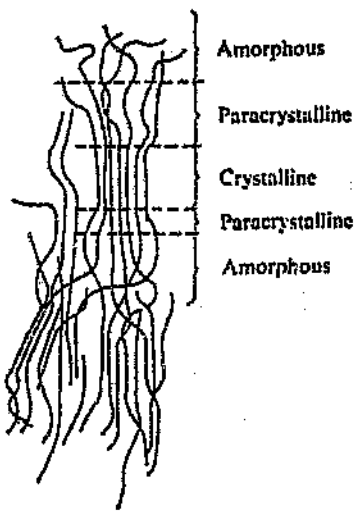

Figure 22. Semi-crystalline region part of the amorphous bulk.

The Philips Diffractometer Software was used to calculate a best peak fit for the different diffraction traces obtained from the resins. No unique peak fits could be obtained for the 1:1.8, 1:1.5 and 1:1.3A cured resin traces (see traces 19, 20, and 21 respectively). Best peak fits were obtained for the 1:1.1A, 1:0.9A and 1:0.7A cured resin traces (see traces 22, 23 and 24 respectively) (The results from the peak fitting are summarized in table 24). Assuming an average crystallite size distribution, the crystallite sizes for these three samples was determined by considering the peak width and using the Scherrer formula (see introduction).

The crystallite sizes were determined from the peak widths of the most intense peak ($2\theta=21.6°$). The average crystallite sizes for the 1:1.1A, 1:0.9A and 1:0.7A cured resins was 60.2Å, 72.6Å and 115.2Å respectively (see chapter 4 for the calculations) (table 25).

The above set of points could be explained by a power regression equation, but considering the fact that there are to few point to make any meaningful contribution (fig 23).

$$\ln Cr = 5.382 - 0.950 \ln U \qquad r = 0.953$$

where

Cr= crystallite size

U= U:F molar ratio

Previous studies [9] suggested that the UF commercial 1:1.8 resin was amorphous, and comprised of large random tridimentional molecular networks.

Rammon [33] suggested that the organization present in the liquid was carried over to the solid state. He stated that the ordered structure is present in the resin

solution as a liquid crystal and is maintained into the cured state. It was therefore of interest to investigate this phenomenon further. Some of the 1:0.7 synthesised resin was placed in a Lindemann tube. The sample was analyzed by the Debye-Scherrer method for 6 hours. No diffraction pattern of the proposed liquid crystalline state was observed. This suggested that there was no ordered structure in the liquid form.

The % crystallinity for the different cured resins was determined by considering the best smooth curve drawn to connect the minima between the crystalline peaks. The assumption is made that the intensity above is the contribution by the crystalline region and below by the amorphous region [38] (see introduction for more detail) (see traces 25-28). The traces were smoothed by a factor of 5 to allow for simpler area determination of the respective regions. The crystallinity was determined by considering the area of the peaks due to the crystalline region to that of the total area. The proportion of crystallinity of the respective resins alone is summarized as follows.

	Increase in Urea →					
	1:1.8;	1:1.5;	1:1.3A;	1:1.1A;	1:0.9A	1:0.7A%
Crystallinity	17%	21%	24%	43%	47%	74%

See figure 23 for the graphic representation of the results.

The following regression equation represents the above phenomena

$$\ln C\% = 5.183 - 1.188 \ln U \qquad r = 0.946$$

Where

C%= % crystallinity

U= U:F molar ratio

Taking the fact into consideration that there are only three experimental points for the crystallite size determination. Similarities between the change in crystallite size and change in crystallinity can be seen from there respective graphs. This is to be expected. If the % crystallinity of a material increases, then the region of crystallites should increase proportionately.

The % crystallinity can also be related to the species ratios obtained from NMR studies. This is of interest to see which species influence the crystallinity of the cured resin. The approach was similar to that done for the correlation between the physical properties of the particle board and NMR species ratio. Table 23 shows the NMR species ratio with its respective correlation to % crystallinity.

Only certain species seem to influence the % crystallinity. The possible cross-linking ratio plays an important role because, it can be understood that if the tridimentional cross-linking in the cured resin decreases, so the % crystallinity increases. Hence, the concentration of linear species increases, allowing for a higher degree of ordered packing to take place. Similar, the urea/(C1+C2) ratio. As the urea content of a resin increases, so does the % crystallinity. The following equation can be obtained relating the % crystallinity of the cured resin to the NMR ratio of species present before cure.

$$C=25.75Y_1+40.64Y_4$$

with an estimated standard deviation= 6.85

where

C= % crystallinity of cured resin

Y_1= urea/(C1+C2) peak ratio

Y_4= possible cross-linking peak ratio according to the Tomita equation [32]

The error in the above equation appears to be on the high side. This could be explained by the fact that not all possible factors that could contribute to the crystallinity has been considered, due to the limited amount of experimental data.

Possible correlation between the I.B. strength and % crystallinity was done. But since not all the terms considered in the I.B. strength equation are present in the % crystallinity equation, no good correlation was obtained. So, the two terms (I.B. strength and % crystallinity) seem to influence one another, but are not really correlated [9].

Chapter 3. Conclusion

It was possible to investigate two series of resins with similar U:F ratios that were modified by changing the subsequent additions of urea to a known starting commercial resin. The first series of resins were prepared by adding a single addition of urea to a commercial 1:1.8 resin (series A) to obtain the required series. The second series of resins were prepared by multiple additions of urea to a commercial 1:1.8 resin (series B) to obtain the required series. An overall increase in the % solid content and a decrease in the modified resins viscosity was observed. Further investigations of resins modification was done by considering the effect of back addition of formaldehyde to a high U:F ratio resin. The liquid resins were analyzed by I.R. and ^{13}C NMR spectroscopy respectively, where NMR proved to be the most informative of the two methods. The respective modified resins were cured with NH_4Cl and analyzed again by I.R. spectroscopy and X-ray diffraction that considered any long range phenomena. Again, the I.R. spectroscopic technique proved to be ineffective when considering only small changes from one modified resin to another.

The % crystallinity of the cured resin was determined, and depended on the respective U:F ratio of a resin and not on the method of synthesis. Crystallite sizes of some of the modified cured resins were determined, and the trend showed to behave in a very similar way to the respective % crystallinity of the cured resin. This showed that the % crystallinity of a cured resin increased proportionately to the crystallite sizes.

Investigation on the possible structural properties between the cured resin and pure cellulose was done and

showed that the crystalline phenomena found in pure cured resin breaks down when cured with native cellulose. This is consistent with the theoretical results obtained by A. Pizzi [42] which indicated that when on wood in a covered glue line, UF resins cannot exist in a crystalline form. ie. A resin with possible low cross-linking, could still be amorphous on wood.

X-ray diffraction traces of various standard UF derivatives were compared to the crystalline UF cured resins. The traces of urea and trimethylenetetraurea compared favourably, suggesting that the crystalline regions in UF resins comprise largely of linear methylene species arranged in an amorphous matrix.

Particleboards were made from the modified resins, followed by respective I.B. strength tests and formaldehyde emission test. It was clearly shown that boards manufactured from the B-series resins (multiple addition resins) performed better than boards made with the A-series resins (single urea addition). ie. The I.B. strength and formaldehyde emission of the respective B-series boards were better. The board made with the resin that was modified with the back addition of formaldehyde in the last step (1:1.11), performed reasonably well when compared to the other 1:1.1 U:F molar ratio boards. Hence, a good E2 formaldehyde emission board can be made with a U:F ratio resin of 1:1.11 by simple back addition with some formaldehyde.

A technique similar to the Japanese Desiccator method [50] was developed for determining the formaldehyde emission from particleboards. A number of methods used for emission testing were compared, and standardized to known emission classes [25] (table 7).

^{13}C NMR spectroscopy proved to be a useful technique in the study of liquid U:F resins. It was possible to correlate species ratio from the respective NMR spectra to the I.B. strengths and formaldehyde emission for the specific series of resins. Hence, predictions about the respective I.B. strength and formaldehyde emission for a specific homologous series of resins can be done by just considering the ^{13}C NMR peak ratio of certain species.

The specific equations for the homologous series of resins studied are as follows:
I.B. strength for the A series resins.

$$IB=0.4275Y_4-0.3623Y_1+2.389Y_5$$

with an estimated standard deviation= 0.204

Similarly for the B-series resins

$$IB=1.077Y_4-0.1130Y_1-0.1424Y_5$$

with an estimated standard deviation= 0.115

Formaldehyde emission for the A-series of resins.

$$F=19.18Y_8-11.66Y_1+7.166Y_4+4.126Y_7$$

with an estimated standard deviation= 0.389

Similarly for the B-series resins

$$F=21.71Y_8-6.086Y_1+2.389Y_4+4.346Y_7$$

with an estimated standard deviation= 2.013

where

IB= I.B. Strength (MPa)
F= Formaldehyde emission (mg F/100g of Board)
Y_1= urea/(C1+C2) peak ratio

Y_4= possible cross-linking peak ratio from the Tomita equation [32]

Y_8= Free F/Me peak ratio

Y_7= (E1+E2)/(E4+E5) peak ratio

Y_5= Me/Mo peak ratio

These equations were successfully used to predict the performance of a resin (1:1.11) that was synthesised similarly to that of the A-series resin. Showing that the equations are unique for the homologous series of resins and that they could be used for resins that are similar in synthesis and application.

General equations relating the physical properties (I.B. strength and formaldehyde emission) to the NMR peak ratio studies of certain species was obtained.

For I.B. strength of particleboards

IB=a{(C+2E)/(A+C+E)}+b{urea/(C1+C2)}+c{Me/Mo}

where

a, b and c are independent variables for the unique homologous UF resin series.

For formaldehyde emission from particleboards

F=a{free F/Me}+b{(C+2E)/(A+C+E)}+c{urea/(C1+C2)}
+d{(E1+E2)/(E4+E5)}+e{E3/Me}

where

a, b, c, d and e are independent variables for the unique homologous UF resin series.

and where

free F= Free formaldehyde (peak at 84.7 ppm)

Me= A+C+E, total methylene species (peak from 45-60 ppm)

Mo= total methylol species (peak from 65-72 ppm)

A= $-NH\underline{C}H_2NH-$ (peak at 48.8 ppm)

C= $-N(CH_2-)\underline{C}H_2NH-$ (peak at 55.5 ppm)

E= $-N(CH_2-)\underline{C}H_2N(CH_2-)-$ (peak at 61.6 ppm)

C1= $NH_2\underline{C}ONHCH_2OH$ (peak at 162.0 ppm)

C2= larger molecular species ie. =N<u>C</u>ON= groups (peak at 162.0 ppm)

urea= free urea (peak at 165 ppm)

E1=$-NH\underline{C}H_2OCH_3$ (peak at 73.4 ppm)

E2=$-N(CH_2-)\underline{C}H_2OCH_3$ (peak at 88.7 ppm)

E4=$-NH\underline{C}H_2O\underline{C}H_2NH-$ (peak at 70.3 ppm)

E5= $-N(CH_2-)\underline{C}H_2OCH_2NH-$ (peak at 75.0)

E3= $-NHCH_2OCH_2OH$ (peak at 88.7 ppm)

A similar approach was taken in relating the % crystallinity obtained from the cured U:F resins to the NMR species ratio.

Hence, for the specific set of resins:

$$C=25.75Y_1+40.64Y_4$$

with an estimated standard deviation= 6.85

where

C= % crystallinity of cured resin

Y_1= urea/(C1+C2) peak ratio

Y_4= possible cross-linking peak ratio according to the Tomita equation [32]

Therefore it is possible to correlate physical properties and the application of cured UF resins to liquid ^{13}C NMR studies. The study of species present in the liquid resin before cure and application by NMR techniques can give some tentative information about the performance of the final particleboard made wit UF resins.

Further, UF resins performance can be improved by increasing the number of urea additions during a resin synthesis. Hence, using UF resins that have more than

extra addition of urea during the synthesis. It was also shown that an addition of a small amount of formaldehyde in the last step of the synthesis improves the resins performance during application.

Chapter 4. Experimental

4.1. Resin

The formulation for the commercial resin is as follows: 2.2 moles of formaldehyde is dissolved in water and heated to 50°C. The pH is increased to 8.5 using NaOH solution. Addition of the first urea. 1 mole urea is added obtain a U:F ratio of 1:2.2 molar. The temperature is increased to 95°C, and kept there for 15 minutes. Formic acid is added to decrease the pH to 5.2. The solution is cooked for a further 15-20 minutes at 95°C before NaOH is added to increase the pH to 6.5. The solution is cooled to 60°C and the second urea is added to have a final U:F ratio of 1:1.8. The final product is kept at 60°C for 20 minutes, before being cooled to room temperature.

The effect of an extra addition of urea to a resin was investigated by starting with the commercial resin. The percent solid was calculated to be 61.3%. The U:F molar ratio was 1:1.8.

The percent solid was determined by heating a known amount of resin for 1 hour at 140°C. This is not a true reflection of the active solid content of the resin, since about 14% of the active resin is converted to water during heating. For the above resin, a 75% active content was considered, and the subsequent additions of urea was calculated according to the active content.

The required amount of urea was added to the 1:1.8 commercial resin active content at 60°C to make up the modified resins. The resin was kept at that temperature for 45 minutes, then cooled and left for 24 hours to mature before analysis and application. A waiting period

of 24 hours was allowed during the synthesis of the multiple-step addition resins before the next addition of urea.

Two sets of resin were prepared with similar U:F molar ratios, but with different synthesis steps.

Xg of urea was added to 200g of resin and stirred continually at 60°C for 45 minutes. The mixture was cooled and left for 24 hours to mature before application and analysis.

Where X= 15.78g for the 1:1.8———>1:1.5 UF resin
X= 30.28g 1:1.8———>1:1.3A
X= 50.18g 1:1.8———>1:1.1A
X= 78.90g 1:1.8———>1:0.9A
X= 124.10g 1:1.8———>1:0.7A[1]

The multiple-step urea addition resins were prepared in a similar way as above. A waiting period of 24 hours was allowed before the next step of urea addition was done.

For example:
1:1.8———>1:1.5———>1:1.3B
15.78g of urea was added to 200g of resin and stirred continually at 60°C for 45 minutes. The mixture was cooled and left for 24 hours to mature before the 14.50g of urea was added again at 60°C, stirred continually for 45 minutes, cooled and left standing for another 24 hours before application and analysis.

The following two resins were done with a similar approach.

---

[1] 1:0.7 ratio resin was synthesised but solidified after one day. The resin proved to be unsuitable for application and analysis, and was only considered for X-ray diffraction analysis of the solid cured form.

	24 hours	24 hours	24 hours
1:1.8	——>1:1.5	——>1:1.3	——>1:1.1B
15.78g U	14.50g U	19.90g U	

	24 hours	24 hours	24 hours	24 hours
1:1.8	——>1:1.5	——>1:1.3	——>1:1.1	——>1:0.9B
15.78g U	14.50g U	19.90g U	28.72g U	

The back addition of formaldehyde was investigated by preparing the following resin:

Urea		Formaldehyde
1:1.8	——>1:1.1	——>1:1.11

50.18g urea was added to 200g of resin at 60°C, stirred continually for 15 minutes before 0.2g of formaldehyde was added. The paraformaldehyde was dissolved in water before use. The mixture was stirred continually at 60°C for a further 30 minutes. The mixture was cooled and left standing to mature for 24 hours before application and analysis.

A small scale reactor vessel was built to simulate the synthesis conditions for the industrial manufacture of UF resins. This allowed a uniform heating of the resin during synthesis and better control over the reaction temperature and pH. A schematic representation of the reactor setup is shown in figures 26 and 27.

The solid content of the modified resins was determined by heating a known amount of sample at 140°C for 1 hour. The viscosity of the resins in centipoise (mPa.s) was determined by using a Brookfield viscometer.

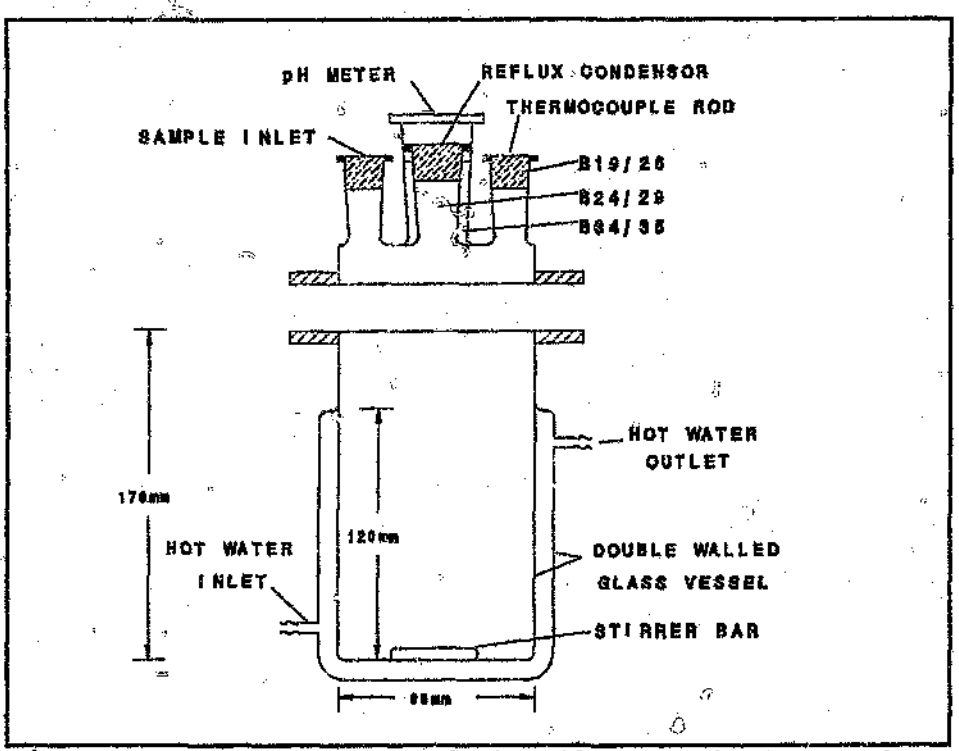

Figure 26. Reactor vessel for the manufacture of UF resins.

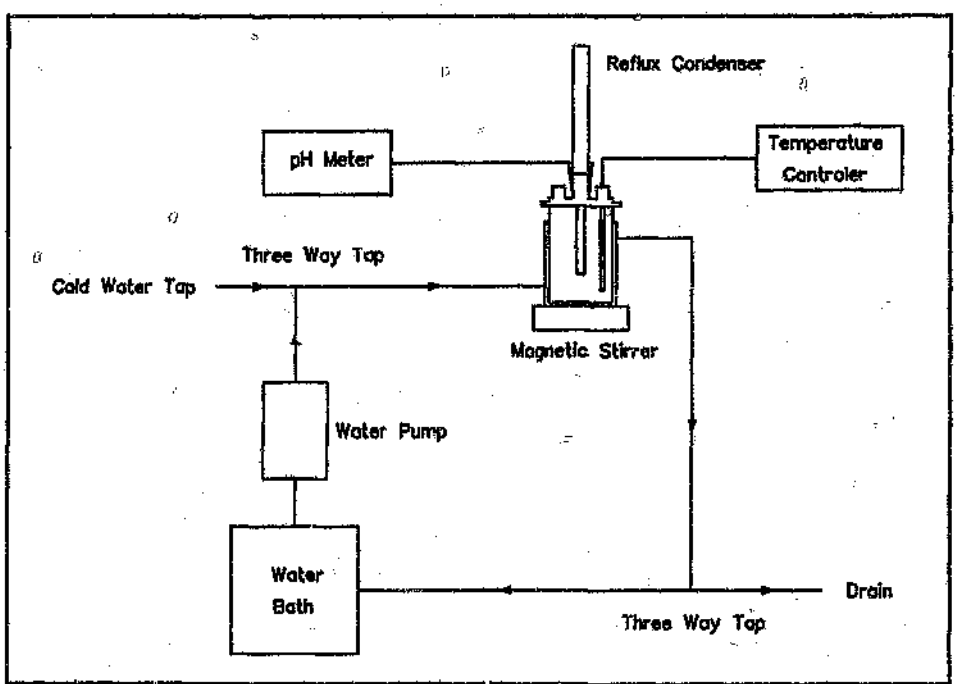

Figure 27. Schematic representation of the reactor setup.

4.2. Particle boards

Particleboards were made from the modified resins. The following set of conditions were kept the same for each of the boards prepared.

Wood used: Pine chips ranging in size from 1mm to 25mm.
Glue used: 7% of the solid content.
Hardener used: 2% NH_4Cl of solid glue.
A moisture content of 12-15% was obtained by adding the required amount of water to the liquid resin before application. The wood chips were spread evenly in a wooden frame giving a particleboard size of
26 × 21 × 1 cm.

A particleboard hot press was used.
Pressure time for each board was 4.5 minutes:
1 minute at 23.5 kg/cm^2
1.5 minutes at 11.7 kg/cm^2
2 minutes at 3 kg/cm^2
The temperature during pressing was 190°C.

The boards were left standing in a well vented room for two weeks before analysis.

Strength tests of the particle boards were done by subjecting small blocks of the boards (50mm × 50mm × thickness) to an Internal Bond (I.B.) tensile strength test using a Hounsfield tensiometer. The tension was subjected perpendicular to the boars surface, giving a reading in Newtons. The results in MPa were compared to the American standard specifications for interior grade particleboard.

4.3. Formaldehyde Release.

Results from independent studies and from the literature for different techniques in measuring formaldehyde releases from particleboards were compared and quantified according to the emission classes [25].

The desiccator method was used to determine the formaldehyde emission of the particleboards prepared with the modified resins.

The desiccator method used a 2 litre desiccator (see figure 28), in which a 200 ml glass dish filled with 100ml of distilled water was placed. The particle board specimens were cut (25mm × 25mm × thickness), weighed and suspended over the water by a porcelain desiccator plate. The desiccators were kept at 25 ± 1°C for 24 hours. An average of 6 samples per board were analyzed.

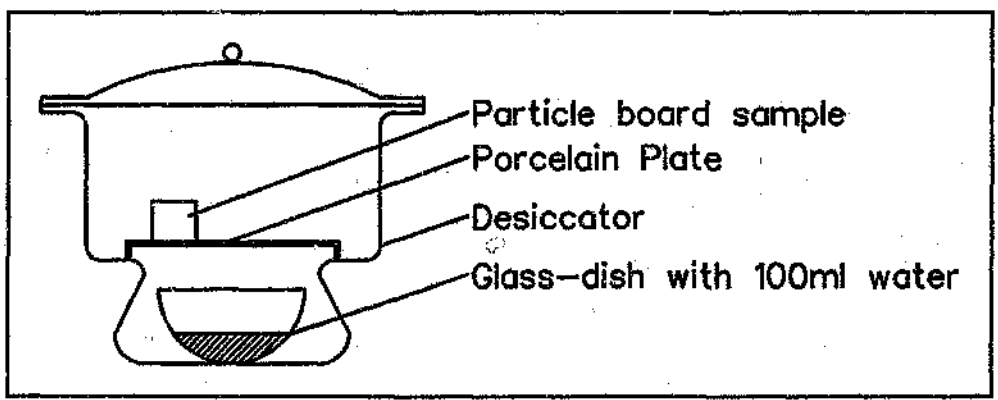

Figure 28. Desiccator Method.

The method most suited for the determination of formaldehyde in water was found to be the fluorometric acetylacetone method based on the Hantzsch reaction developed by S. Belman and Bisbaard et al respectively [53, 54]. The sampling medium was water and therefore

most suitable for stationary sampling.

The Hantzsch reagent consisted of:
0.4ml acetylacetone (BDH),
0.6ml acetic acid (Merck) and
30.8g ammonium acetate (Analar).

The components were dissolved in distilled water and diluted to 200ml. This reagent was prepared daily as required. Prior to analysis, 10 ml of the standard or sample solutions were mixed with 10 ml of the Hantzsch reagent respectively. These solutions were heated to 60°C for 15 minutes. The reaction is complete in the pH-range of 5.5 to 6.5. After cooling, the fluorescence (I_f) of the solutions was measured using a Perkin Elmer LS-5 Luminescence Spectrophotometer. The fluorescence of DDL was measured in aqueous solution at λ_{em}=510nm. The molecular extinction has its maximum at λ_{ex}=410nm.

The standards with different formaldehyde concentrations were prepared by dissolving a known amount of para-formaldehyde in water and diluted to the required concentrations (see table 11 for the concentrations and respective fluorescence).

The above desiccator method was standardized to the WKI method described by E. Roffael and L. Mehlhorn [55]. A number of boards with different formaldehyde concentrations were used. Some board samples were sent to J. Valenzuela, Conception, Chile for independent formaldehyde emission studies using the WKI method. Some low formaldehyde emission boards were analyzed by the author using the WKI method.

The WKI method relied on two pieces of particle board (25mm × 25mm × thickness each) being suspended over 50ml

distilled water in a 500ml bottle. The samples were supported by elastic bands and string. The bottles were then kept at 40 ±3°C for 24 hours. The samples were cooled in ice water for half an hour before analysis by the acetylacetone method. A schematic representation of the WKI method is shown in figure 29.

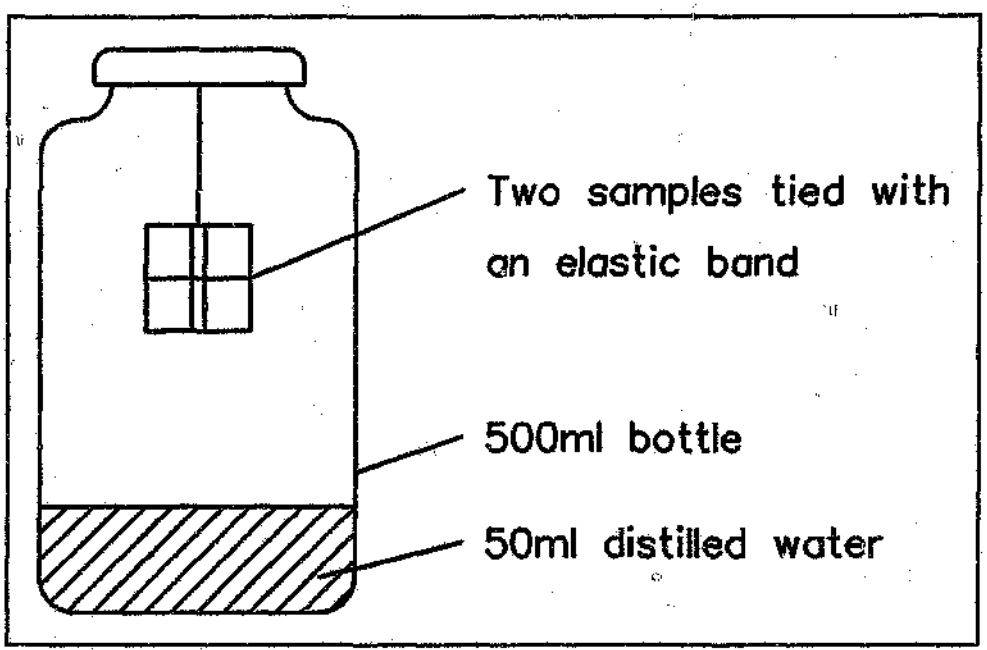

Figure 29. WKI method according to Roffael [55]

4.4. Infra Red Spectroscopy.

The analysis of the spectra were done between 700 and 3500cm^{-1}. The bands above and below this region were very weak and the literature assigned bands pertaining to this region only (see table 13) [28, 27].

Emission spectra were obtained between 400 and 4000 cm^{-1} on a Bruker FT-IR CS-03 spectrometer with OPUS Ver1.2 Spectroscopic Software using 20 sample and reference beam scans. Analysis of the liquid resin was done by spreading

a thin film of the resin between two NaCl plates. KBr pellets were prepared for the analysis of the cured resins. For accurate quantitative analysis, peak area determination would have been ideal. But unfortunately the software did not provide such a facility. Relative peak transmittance heights were considered. Tables of the band spectra and wavelengths are in table 14.

4.5. ^{13}C NMR spectroscopy.

Proton NMR was not considered due to the time required for collecting the spectra, and the large interference that would be present due to water. ^{13}C NMR spectra were obtained on a Bruker AC 200 spectrometer. Chemical shift was calculated relative to deuterium oxide for NMR control. About 0.1ml of liquid resin sample was placed in a NMR tube and diluted with water. About 0.4ml Deuterium oxide was added directly to sample. A knowledge of the spin-lattice relaxation time of ^{13}C is an important factor in setting the pulse intervals. B. Tomita and S. Hatono [32] suggested a pulse interval of 5 seconds was needed to obtain a reliable spectrum. No direct quantitative results could be obtained from the spectra. But by considering certain peak ratios, some information was obtained about the behaviour of certain species. ^{13}C solid state NMR was done on the cured resins with 3% NH_4Cl, but the results proved to be uninformative for qualitative or quantitative analysis of the different resins. ^{13}C solid state NMR was not considered for further studies.

4.6. X-ray Crystallography.

X-ray diffraction patterns of the cured resins were collected on an Automated Philips Powder Diffractometer PW1830/00 that recorded the intensity of the X-rays diffracted by the sample as a function of the Bragg angle

using the Phillips computer software. Cu radiation (λ=1.5405Å) was used with a nickel filter and a graphite monochromator. The scan speed was 0.02 (°2θ/s) with a 0.02 (°2θ) step. The different cured resins were ground to a particle size of about 2-10μm using a mortal and pestle and packed tightly on an aluminium sample holder. A best possible curve fitting was done with the computer software provided. No unique curve fit could be obtained for the cured UF resins of molar ratio 1:1.8, 1:1.5 and 1:1.3A (see traces 19, 20 and 21 respectively). Assuming an overall broad amorphous peak to be present in all the samples, peak assignments for the 1:1.3A (not unique), 1:1.1A, 1:0.9A and 1:0.7A was done and the results are shown in table 24 (see traces 21, 22, 23 and 24 respectively).

The crystallite sizes were determined for the 1:1.1A, 1:0.9A and 1:0.7A UF ratio resins. The Scherrer formula was used for the first most intense 2θ peak only. The results are summarized in table 25.

The percentage crystallinity for the different cured resins was determined by considering the areas for the crystalline region to that of the total area. A best curve was drawn under the crystalline region to represent the amorphous regions. The results are shown in traces 25 to 30. Figure 25 shows the graphical representation of the % crystallinity and crystallite size determination for the different modified resins.

Chapter 5. Results

5.1. Resin

The percent solid content and viscosity was determined for each of the modified commercial resins and the results are tabulated in table 5.

5.2. Particleboards

5.2.1. Strength Test

Two sets of boards with slightly different densities were made with each of the modified resins. The strength test in MPa of 6 samples for each of the boards were determined and averaged. The averaged results are tabulated in table 6. Figure 4 shows a graphical representation of the results with the respective boards densities.

5.2.2. Formaldehyde Release

The fluorescence and concentration results for the standard solutions are tabulated in table 11 and a graphical representation is shown in figure 9.

Six samples from each of the first boards (I) prepared were analyzed by the desiccator method after two weeks of preparing the boards. Some selected boards were again analyzed for formaldehyde emission after three months of preparation. The average results are tabulated in table 12 and the graphical representation in figure 10.

5.3. Infra Red Spectroscopy

The band wavelengths and spectra for the different liquid and cured with 3% NH_4Cl UF modified resins are shown in table 14 (spectra 1-15).

A detailed analysis of the bands obtained by IR spectroscopy for the different resins is as follows:

3500-2500 cm^{-1} Region

Very little information was obtained in this region due to the strong band of OH stretching of water. S. S. Jada [27] reported that freeze-dried UF polymers showed distinct bands at 3340 cm^{-1} indicating the NH stretching modes of free NH_2.

The slight shoulder bands between 3238-3223 cm^{-1} and 3122-3097 cm^{-1} could be assigned to -NH stretching of the bonded -NH group. As the urea content of the modified resins increases from the 1:1.8 UF to the 1:0.9 UF modified resin, the relative intensity of the shoulders increased. The cured resins showed a slight but not significant change in this area of the spectrum.

The respective peaks between 2962-2958 cm^{-1} were assigned to the sy CH mode of CH_2 of ether, CH_2OH and NCH_2. There was no significant change in the relative intensity for the different liquid UF resin samples. An initial decrease in peak intensity was observed in this region for the lower cured UF ratio resins. Hence, lower amount of CH_2 of ethers, CH_2OH and NCH_2 in cured resin.

Peaks between 2912-2892 cm^{-1} were assigned to the asy-CH mode of $-CH_2OH$. Peaks between 2848-2811 cm^{-1} were not assigned in the literature. Considering the IR spectra of

some of the prepolymers, the bands were assigned to the $N-CH_3$ stretching. There are no significant changes in their relative intensities for the different resins.

1664-1620 cm^{-1} Region

The strong bands between 1664-1653 cm^{-1} were largely ascribed to the C=O stretching mode generally termed as Amide I. A single absorption band at the wavelength indicated a high conversion of the NH_2 group. For the liquid UF samples 1:0.9, a doublet was observed in the 1624 cm^{-1} region. This could be ascribed to contribution of the NH mode of the free NH_2 groups. This shows that there is a considerable amount of free urea in the resins. The doublet in this region become more evident for the cured resins. This showed that there were more NH_2 terminating groups in the cured 1:0.9 (A and B) resins than for the lower UF resins.

1558-1548 cm^{-1} Region

The strong bands between 1558-1548 cm^{-1} were ascribed to the amide II band. This band was usually strong in uncured UF polymers that contained secondary amides. The amide II band observed was estimated to arise from 61% (C-N) and 30% (N-H) [45]. The ratio of amide I to Amide II does not change significantly for the different liquid and cured resins.

Two bands occurred in this region for the cured resins with lower UF ratio (1:1.8; 1:1.5 and 1:1.3). Myers [28] suggested a shift in the secondary amide band for cured samples, because the secondary amide is in an environment where H bonding is repressed due to steric constraints, and the secondary amides were converted to tertiary amides. The two bands could therefore be ascribed to the

conversion of secondary and primary amides respectively.

1470-1452 cm^{-1} Region

The relative weak bands in this region for all UF samples were ascribed due to the CH_2 bending mode of the $-CH_2-N$ group. The intensity for this peak increases from the 1:1.8 to the 1:0.7 modified liquid resins, showing an increase of the $=N-CH_2-N=$ groups. There was a decrease in band intensity for the respective cured resins when compared to the liquid (almost no CH_2 in the cured 1:1.8, 1:1.5 and 1:1.3 resins).

1389-1351 cm^{-1} Region

All UF samples showed a medium band in the region of 1389-1385 cm^{-1} with a shoulder band between 1365-1351 cm^{-1}, becoming stronger for the lower UF ratio resins. The band 1389-1385 cm^{-1} was assigned to the CH stretching of the CH_2OH group. The band at 1365-1351 cm^{-1} was attributed to the C-N stretching. The relative intensities were an indication of the amount of $-CH_2OH$ and the C-N present in the resins. There was a small change in band (CH_2OH) intensity for the lower UF ratio resins. No significant difference between the cured and liquid samples.

1255-1253 cm^{-1} Region

A strong broad band was observed at 1255-1253 cm^{-1} with a slight shoulder at about 1300 cm^{-1} for all UF resin samples. The shoulder band were ascribed to the -OH deformation of CH_2OH. The other band were ascribed to the secondary amide III band. The potential energy distribution of amide III in dimethylol urea showed that it consisted of 52% (N-H) and 24% (C-N) [46]. No significant changes between the cured and liquid samples

was observed.

1195-1131 cm^{-1} Region

Medium Bands at 1191-1195 cm^{-1} are only observed for the low UF (1:1.8) ratio resins. This band becomes a weak shoulder in the latter resins. A possible assignment of the band according to Myers [28] was to the methyl group. The band at 1155-1131 cm^{-1} was ascribed to the asymmetric stretching of $=N-CH_2-N=$ by S. Jada [27]. But Myers [28] ascribes it to the C-O stretch of aliphatic ether.

1016-1014 cm^{-1} Region

No clear assignment for the band can be obtained from the literature. Pshenitsyna et al [45] ascribed it to CH_2OH in UF prepolymers. Others authors observed two bands in the region 1060 and 1020 cm^{-1}, assigning them to ether and methylol groups respectively.

908-778 cm^{-1} Region

The band at 902-908 cm^{-1} have not been assigned in the literature. The band at 849-841 cm^{-1} were ascribed to symmetric -C-O-C- stretch for cyclic model compounds. S. Jada [27] assigned the 720-700 cm^{-1} band to C-N of $NH-CH_2-NH$ group. The band 778-781 cm^{-1} of the UF samples are higher in wavenumber, therefore no clear assignment could be made.

From the above assignments and the change in relative intensities from sample to sample, it can be seen that only certain bands could be used for qualitative analysis of the resins.

5.4. NMR spectroscopy

The peak assignment for the different modified liquid resins are shown in table 17. Tabulated results for the peak ratio analysis are in table 18.

The correlation between the NMR species ratio and the physical properties (I.B. strength, formaldehyde emission and % crystallinity) are summarised in table 19, 20 and 23 respectively.

The correlation was done by considering a linear regression of the species ratio to the physical properties in question: $Y=MX+B$, and obtaining a correlation coefficient r where

$$r=(n\Sigma XY-\Sigma X\Sigma Y)/\sqrt{\{n\Sigma X^2-(\Sigma X)^2\}\{n\Sigma Y^2-(\Sigma Y)^2\}}$$

5.5. X-ray diffraction

The X-ray diffraction traces for the different modified resins cured with 3% and 9% NH_4Cl are shown in traces 14, 15 and 16 respectively.

The crystallite sizes were determined for 1:1.1A, 1:0.9A and 1:0.7A cured UF resins using the Scherrer and Bragg formula [35].

$$\beta=K\lambda/t\cos\theta$$

Hence, t (crystallite size in Å) can be determined

$$t=K\lambda/\beta\cos\theta$$

where θ= half of 2θ (angle of the first most intense diffracted peak)

λ= 1.541nm for Cu radiation

K= 0.9 for the determination at 0.5 β

β= peak width at half height, and has to be in radians.

The results are summarised in table 25.

References

1) B. Meyer; Urea-Fromaldehyde Resins; Addison-Wesley Publishing Company Inc.; Massachusetts; (1979).

2) R. Marutzky and L. Ranta; The properties of urea-formaldehyde resins with low formaldehyde content and particle boards bonded with these resins. 1. Effect of the molar ratio on the properties of raw sizing resins; Holz Roh-Werkst.; **37(10)**; 389 (1979).

3) P. R. Steiner; Durability of Urea-Formaldehyde Adhesives, Effects of Molar Ratio, Second Urea and Filler; For. Prod. J.; **23(12)**; 32 (1973).

4) A. Pizzi; Wood Adhesives Chemistry and Technology; Marcel Dekker Inc.; p95; (1983).

5) L. Bettelheim and J. Cedwall; Sven. Kem. Tidskr.; **60**; 208 (1948).

6) G. Grove and C. Lynch; J. Am. Chem. Soc.; **70**; 3795 (1948).

7) J. Scheiber; Chemie und Technologie der Künstlichen Harze; Wissenschaftliche Verlagsges, m. b. H.; Stuttgart; (1943).

8) K. Horioka et al.; Bul. Gov. For. Exp. Sta. Tokyo; **113**; 20 (1959).

9) D. Levendis, A. Pizzi and E. Ferg; The Correlation of Strength and Formaldehyde Emission with the Crystalline/Amorphous Structure of UF Resins; Holz-Forschung; **46**; 263 (1992).

10) K. Oshima, Y. Ito and S. Suzuki; Foaming Fibrous Fleece; USP 3764428; Oct 9 (1973).

11) H. Baumann; Isolierung von Schiffen mit Spritzbarem Schaumkunstoff; Hansa; **1**; 2 (1959).

12) Brown Boveri und Cie; Stiff Foam with Open Cells; Fr. Demande 2193699; Feb. 22 (1974).

13) S. Gruben and S. Persson; Preparing Urea Resin Foams Intended as Absorbents for Oil; Swed. P. 336470; July 5 (1971).

14) H. Baumann and G. Schmidt; Überprüfung der Reizlosigkeit eines Puders und einer neuen Wundauflage aus Kunstharzschaumstoff; Fortschritte der Medizin; **76(2)**;59 (1958).
15) H. Baumann; Die Ausnutzung der Sonnenenergie; Chemiker Zeitung-Chemische Apparatur; **87(8)**; 267 (1963).
16) B. Meyer; Urea Formaldehyde Resins; Addison-Wesley Publishing Company, Inc; Massachusetts; p 199-214 (1979).
17) A. Mara; Kolthoff's Treatise on Analytical Chemistry Part III vol 4 section D; Interscience; New York; (1977).
18) A. Pizzi; Wood Adhesives Chemistry and Technology; Maecel Dekker Inc.; (1983).
19) B. Meyer; Urea Formaldehyde Resins; Addison-Wesley Publishing Company, Inc; Massachusetts; (1979).
20) H. Deppe and K. Ernst; Taschenbuch der Spanplatten Technik; DRW-Verlag; Stuttgart; (1977).
21) O. Wittmann; Holz Roh-Werkst.; **20**;221 (1962).
22) E. Roffael and L. Mehlhorn; Holz-Zentralbl.; **102**;2202 (1976).
23) B. Meyer and K. Hermanns; Formaldehyde indoor air problems; Proc. APCA Annu. Meet.; **77(2)**; 84 (1984).
24) B. Meyer, Urea Formaldehyde Resin; Addison-Wesley Publishing Company, Inc.; Massachusetts; p 232 (1979).
25) ETB-Richtlinie über die Verwendung von Spanplatten hinsichtlich der Vermeidung unzumutbarer Formaldehyd-konzentrationen in der Raumluft-Fassung; Ausschuss für Einheitliche Technische Baubestimmungen (ETB); Beuth. Verlag; Berlin; (1980).
26) E. Roffael; Comparison of Several Methods for Determination of Formaldehyde Release; Holz-Zentralblatt; **103(27)**; 400 (1977).
27) S. Jada; The Structure of Urea-Formaldehyde Resins; J. Appl. Polym. Sci.; **35**; 1573 (1988).
28) G. Myers; Investigation of Urea-Fromaldehyde Polymer Cure by Infrared; J. Appl. Polm. Sci.; **26**; 747 (1981).
29) R. Schmoke, K. Dietrich, R. Nastke, D. Kunath and W.

Teige; Infrarot-spektroskopiesche Untersuchungen an Harnstoff-Formaldehyd-Festoffen; Acta Polymerica; 38(10); 574 (1987).
30) S. Kambanis and R. Vasishth; NMR Studies of Urea-Fromaldehyde Resins; J. Appl. Polym. Sci.; 15; 1911 (1971).
31) M. Chiavarini, R. Bigatto and N. Conti; Synthesis of Urea-Formaldehyde Resins: NMR Studies on Reaction Mechanisms; Angew. Makromol. Chem.; 70(1020); 49 (1978).
32) B. Tomita and S. Hatono; Urea-Formaldehyde Resins III. Constitutional Characterization by ^{13}C Fourier Transform NMR Spectroscopy; J. Polym. Sci.; 16; 2509 (1978).
33) R. Rammon; The Chemical Structure of UF Resins; J. Adhesion; 19; 115 (1986).
34) G. Maciel, N. Szeverenyi, T. Carly and G. Myers; ^{13}C NMR Studies of Solid Urea-Formaldehyde Resins Using Cross Polarization and Magic-Angle Spinning; Macromolecules; 16; 598 (1983).
35) M. Kakudo and N. Kasai; X-ray Diffraction by Polymers; Kodansha Ltd, and Elsevier Publishing Company; Tokyo and Amsterdam; p329 (1972).
36) A. Turner Jones, J. Aizlewood and D. Beckett; Makromol. Chem.; 75; 134 (1964).
37) J. Koutsky; Structural Studies on Thermosetting Resins-Implications for Urea-Fromaldehyde and Phenol-Formaldehyde systems; Wood Adhesives in 1985. Status and Needs. Proceedings of a Conference sponsored by the Forest Products Laboratory; p102.
38) M. Nabiev et al; X-ray Diffraction Studies of Urea-Formaldehyde Compounds; Deposited Doc. VIN1T1; 1885-84 (Russian).
39) C. Aravindakskan and B. Banerjiee; Crystallographic Data for Dimethylene Triurea; Technology; 5(1); 50 (1968).

40) C. Aravindakskan and B. Banerjiee; Unit Cell and Space Group for Methylene Diurea; Technology; 5(3); 237 (1968).
41) ASTM Powder Diffraction File JCPDS; International Centre for Diffraction Data; USA (1989).
42) A. Pizzi; A molecular mechanics approach to the Adhesion of Urea-Formaldehyde resins to cellulose Part I Crystalline Cellulose I; J. Adhesion Sci. Technol.; 4(7); 573 (1990).
43) O'Neil and Steiger USP 3996190; 1976
44) F. Brunnmüller, H. Schatz, J. Mayer and O. Grabowsky; Continuous Manufacture of Amino Resin Solutions; USP 3816376; June (1974).
45) V. P. Pshenitsyna, N. N. Molotkova, M. P. Novoskova and B. Ya. Akselrod; Appearance of absorbtion bands of amide II in spectra of products of the reaction of urea with formaldehyde; Zh. Prikl. Spektrosk.; 29(3); 486 (1978).
46) Y. Mido; Infrared spectra and configurations of dialkylureas; Spectrochim. Acta; 28A; 1503 (1972).
47) R. Marutzky; Release of Formaldehyde by Wood Products; Wood Adhesives Chemistry and Technology Vol 2, (A. Pizzi Editor); Marcel Dekker Inc.; New York; (1989).
48) L. Mehlhorn, E. Roffael and H. Miertzsch; Erfahrungen mit den von FIHH-Karlsruhe vorgeschlagenen Prüfmethoden zur Bestimmung des Formaldehyds; Holz-Zentralblatt; 104; 345 (1978).
49) A. Barghoorn; Spanplatten und Formaldehyd; Holz-Zentralblatt; 104; 994 (1978).
50) T. Matsumoto; Concentration of Formaldehyde Released from Plywood in an Environmental Test Room; Rinsyo Shikenjo Kenkya Hokoku; 262; 41 (1974).
51) S. Fujii, T. Suzuki and S. Koyagashiro; Kenzai Shiken Joho Transl.; 9(3); 10 (1973).
52) R. Marutzky; Release of Formaldehyde by Wood Products; Wood Adhesives Chemistry and Technology Vol 2,

(A. Pizzi Editor); Marcel Dekker Inc.; New York; p327 (1989).
53) S. Belman; The Fluorometric Determination of Formaldehyde; Anal Chim. Acta; 29; 120 (1963).
54) P. Bisgaard, L. Molhave, B. Rietz and P. Wilhardt; Quantitative Determination of Formaldehyde in Air using the Acetylacetone Method; Analytical Letters; 16(A1/&18); 1457 (1983).
55) E. Roffael and L. Mehlhorn; Erfahrungen mit einer einfachen Methode zur Bestimmung der Formaldehydabgabe von Spanplatten; Holz-Zentralblatt; 102; 2202 (1976).

Bibliography

- Polymers Structure and Bulk Properties; P. Meanes; van Nostrand Reinhold Company; London; (1965).
- Techniques of Polymer Characterization; P.W. Allen; Butterworths Scientific Publications; London; (1959).
- The NMR of Polymers; I. Ya. Shonim and A.N. Lyubimov; Plenum Press; New York; (1970).
- Applied Polymer Analysis and Characterization vol II; J. Mitchell, Jr; Hanser, Oxford University Press; New York; (1991).
- B. Meyer; Urea-Fromaldehyde Resins; Addison-Wesley Publishing Company Inc.; Massachusetts; (1979).
- A. Pizzi; Wood Adhesives Chemistry and Technology; Marcel Dekker Inc.; p95; (1983).
- A. Pizzi; Wood Adhesives Chemistry and Technology Vol 2; Marcel Dekker Inc.; New York; (1989).
- M. Kakudo and N. Kasai; X-ray Diffraction by Polymers; Kodansha Ltd, and Elsevier Publishing Company; Tokyo and Amsterdam; p329 (1972).
- H. Peiser and H. Rookspy; X-ray diffraction by polycrystalline materials; Institute of Physics; London; (1955).
- B. Meyer, B.A. Kottes Andrews and R.M. Reinhardt; Formaldehyde Release from Wood Products; ACS Symposium Series 316; American Chemical Society; Washington DC (1986).

Tables

Table 1. A comparison between particleboards prepared with different UF molar ratios.

U/F molar ratio	Approx. Density ($g.cm^{-3}$)	Internal bond (MPa)	% water swelling (2Hr)	% HCHO released*
1:1.4-1.5	0.680	0.7-0.8	4	0.08-0.10
1:1.3-1.35	0.680	0.6-0.7	4-5	0.04-0.05
1:1.2-1.25	0.680	0.45-0.55	5	0.025-0.035

* Perforator method

Table 2. Classification and properties of particleboards, based on data compiled by Forest Products Laboratory-United States Department of Agriculture [20].

Particleboard	Thickness (cm)	Density ($g.cm^{-1}$)	Modulus of Rapture (MPa)
Low Density	0.64-1.91	0.40-0.80	2.76-27.58
High Density	0.25-0.95	0.80-1.12	20.69-51.71

Particle-board	Tensile Strength parallel to surface (MPa)	Tensile Strength perpendicular to surface (MPa)	Water Abs. 24hr immersion %/weight
Low Density	0.69-9.31	0.62-2.76	5-50
High Density	2.07-17.24	1.90-2.76	15-40

Table 3. The relative stability of bonds in cured UF-resins (in order of increasing stability).

Bond Type	Structure
C-O in cellulose to resin	R-O-CH_2NHCONH-
C-O in methylene ether	-NHCONHCH_2-OCH_2NHCONH-
N-C in amido methylol	-NHCONH-CH_2OH
C-O in polyformal	-NHCONHCH_2O- CH_2OCH_2NHCONH-
C-N in primary amide	-NHCONHCH_2NHC-NH_2
C-N in secondary amide	-NHCONHCH_2NH-CNH-
C-N in tertiary amide	-NHCONHCH_2NCONH-;-CH_2- ;-NHCH_2NCONH-

Table 4. West German Regulation for Formaldehyde emission from particleboards used in buildings.

Emission Class	Formaldehyde concentration (ppm)*	Perforator value EN 120 (mg/100g board)
E3	>1.0-2.2	>30-60
E2	>0.1-0.9	>10-30
E1	<0.1	<10

* Determined in a 40 m^3 test chamber.

Table 5. % Solid content and viscosity determinations for the different modified resins.

Modified Commercial Resin	1:1.8	1:1.5	1:1.3A	1:1.3B
% Solid Content	61.3	63.5	66.3	66.2
Viscosity at 23°C in cps	2460	1000	880	1330

Modified Commercial Resin	1:1.1A	1:1.1B	1:0.9A	1:0.9B
% Solid Content	67.9	70.7	68.5	72.0
Viscosity at 23°C in cps	610	800	358	660

Resin	Modified commercial resin 1:1.11
% Solid Content	59.7
Viscosity at 23°C in cps	200

Table 6. The averaged results for the strength test of particleboards prepared with the modified resins.

Resin Sample	Surface Area (cm^2)	Density ($g.cm^{-3}$)	Force (kN)	Pressure (MPa)
1:1.8 (I)	27.6	0.650	1.63	0.592
1:1.8 (II)	26.3	0.704	1.93	0.733
1:1.5 (I)	27.6	0.685	2.14	0.776
1:1.5 (II)	26.3	0.676	1.94	0.737
1:1.3A (I)	27.4	0.695	1.63	0.594
1:1.3A (II)	26.5	0.665	1.92	0.724
1:1.3B (I)	27.4	0.687	2.27	0.825
1:1.3B (II)	26.5	0.685	2.08	0.784
1:1.1A (I)	27.6	0.665	1.74	0.629
1:1.1A (II)	26.5	0.684	1.77	0.655
1:1.1B (I)	27.6	0.666	1.43	0.520
1:1.1B (II)	26.7	0.704	1.74	0.651
1:0.9A (I)	27.6	0.646	0.76	0.274
1:0.9A (II)	26.5	0.669	0.89	0.336
1:0.9B (I)	27.6	0.680	1.12	0.405
1:0.9B (II)	26.5	0.667	0.95	0.358
1:1.11 (I)	25.4	0.694	1.72	0.676
1:1.11 (II)	26.2	0.693	1.76	0.671

Table 7. Comparison between different formaldehyde emission determination techniques.

Emission Class [25]	Perforator mg F/100g of board	WKI mg F/100g of board	Air Chamber ppm	Desiccator mg F/100g of board
E1	0↔10	0↔11.8	0↔0.1	0↔2.21
E2	10↔30	11.8↔30	0.1↔0.9	2.21↔6.61
E3	30↔60	30↔57.3	0.9↔2.2	6.61↔13.2

Table 8. Comparison between the perforator and air chamber techniques for formaldehyde emission according to Barghoorn [49]

Air Chamber Technique ppm formaldehyde	Perforator Technique mg formaldehyde/100g board
0.1	10
0.5	20
0.6	23
0.9	30
1.3	40
1.8	50
2.2	60
2.6	70
3.0	80
3.2	84
3.4	90

Table 9. Comparison between the perforator and WKI method for formaldehyde emission.

Perforator mg F/100g board	WKI[1] mg F/100g board	WKI[2] mg F/100g board	WKI[3] mg F/100g board
5	8.25		
13			13.6
14			18.5
16			18.9
17			19.6
18			20.1
19			21.5
20			16.7
22			24.5
23		19.3	
29		28.9	
31			29.3
35			33.7
40			42.5
41			42.3
47			45.9

[1] Unpublished results by A. Pizzi and J. Valenzuela, Conception, Chile (1992).
[2] Roffael [55]
[3] Unpublished results by J. Valenzuela and Quimicos Coronel, Conception, Chile (1992).

Table 10. Comparison between the WKI and Desiccator method for formaldehyde emission.

Desiccator mgF/ 100g board	WKI[1] mgF/ 100g board	WKI[2] mgF/ 100g board
0.33	4.0	
1.50	8.2	
2.11		11.0
3.01		14.6
8.67		38.2

[1] Studies done by the author
[2] Independent studies done by J. Valenzuela, Conception, Chile.

Table 11. Formaldehyde concentration and fluorescence intensity for the standard solutions.

Formaldehyde Concentration ($mg.l^{-1}$)	Fluorescence Intensity
0.00	107
0.32	187
0.64	300
1.28	457
3.12	692
6.24	862
9.36	894
12.48	852
15.60	779

Table 12. Average results for the formaldehyde emission from the particleboards using the desiccator method.

Board Sample	Mass (g)	Fluorescence	Concentration ($mg.l^{-1}$)	mg formaldehyde per 100g board
1:1.8	4.86	652[1]	21.75	44.75
1:1.5	5.41	676[2]	11.65	20.53
1:1.5*	4.53	695[3]	6.32	8.67
1:1.3A	5.15	640[3]	5.18	10.06
1:1.3B	5.80	612[3]	4.66	8.03
1:1.1A	5.50	525[3]	3.32	6.04
1:1.1B	5.36	613	2.33	4.35
1:1.1B*	4.73	510	1.54	3.26
1:0.9A	5.29	405	1.05	1.98
1:0.9A*	4.78	375	0.97	2.03
1:0.9B	5.59	445	1.23	2.20
1:1.11	4.81	513	1.63	3.38

* Sample tested after three months
[1]Diluted by 1/8 [2]Diluted by 1/4 [3]Diluted by 1/2

Table 13. Table of band assignments cited in the Literature.

Assignment of IR Bands cited in literature				
Frequency (cm^{-1})	Comments	Assignment [28]	Comments	Assignment [27]
3440-3445			Medium	NH mode in free NH_2
3340-3345			Strong	NH mode of bonded NH_2
3015-3020			Medium to weak	asy CH mode of the $-CH_2-O-CH_2-$
2960-2970			Strong	asy CH mode of CH_2 of ether, CH_2OH, and $N-CH_2$
2900-2910			Weak	asy CH mode of $-CH_2OH$
1670-1650	very weak	Amide I, primarily C=O stretch and NH deformation		
1660-1630			Very strong in all prepolymers	Amide I mainly due to C=O stretching
1610-1600	Very weak or absent from most polymer spectra, probably masked by other bands	amide II, NH_2 deformation for primary amide		
1600-1550			Strong in all polymers	Amide II, mixture of C-N and NH def; the contribution of NH def. is higher

Assignment of IR Bands cited in literature				
Frequency (cm^{-1})	Comments	Assignment [28]	Comments	Assignment [27]
1560-1550	Strong in uncured polymer spectra	Amide II, combined C-N stretch and NH deformation		
1520-1510	Usually absent from uncured polymer spectra, appears during cure and can become strong on extended cure	amide II, due to linear or cyclic tertiary amide and possibly secondary amide in a constrained, nonhydrogen bonded environment		
1470-1460	Very Weak to Weak	most likely CH bending in NCH_2N, CH_2O and OCH_3.	Weak	Most likely due to CH bending in CH_2 of NCH_2N
1400-1390	Weak	CH mode in CH_2 and CH_3	Weak	CH of CH_2OH
1370-1360			Medium	C-N mode
1305-1300			Strong	OH def of CH_2OH
1300-1290	Weak in most UF polymers, becomes more distinct upon cure.	OH deformation in CH_2OH plus contribution from cyclic amide III		
1260-1265	Medium	Amide III bond for secondary amide, combined CN and NH	Medium	Amide III

Assignment of IR Bands cited in literature				
Frequency (cm^{-1})	Comments	Assignment [28]	Comments	Assignment [27]
1200-1180	Varies from absent to medium	Unknown		
1150-1130	absent to medium	aliphatic ether (C-O stretch) plus C-N stretch in secondary amide	Medium	asy =N-CH_2-N=
1060-1065			Very strong	C-O of ether
1000-1005		C-O stretch in methylol	Very strong	OH def of CH_2OH
800-780			Medium	Sym cyclic C-O of -C-O-C-

Table 14. I.R. Spectra of modified U.F. liquid resin in wavenumber cm^{-1}.

VS=Very Strong; S=Strong; M=Medium; W=weak; VW=Very Weak; VVW=Very Very Weak

1:1.8	Comment	1:1.5	Comment	1:1.3A	Comment	1:1.3B	Comment
3325	VS,broad	3333	VS, Broad	3339	VS,broad	3339	VS,broad
3106	VW,	3097	VVW,	3120	VVW,	3122	VVW,
2960	M,sharp	2958	W,	2961	W,	2960	W,
2908	VW,	2912	VVW	2904	VVW,	2907	VVW
2844	VVW,			2848	VVW,		
1653	VS,sharp	1653	VS,sharp	1653	VS,sharp	1653	VS,sharp
1558	VS,sharp	1552	VS,sharp	1554	VS,sharp	1558	VS,sharp
1464	VW,	1461	VW,	1454	W,	1457	W,
1387	W,Sharp	1386	W,	1386	W,	1387	W,

		1365	VVW,	1358	VVW,	1362	VVW,
1253	M,sharp	1253	M,	1255	M,	1253	M,
1181	VW,	1195	VVW,				
1131	VVW,	1133	VW,	1137	W,	1135	W,
1015	S,sharp	1011	M,sharp	1016	S,	1014	S,
905	VVW,	903	VW,	902	VW,	901	VW,
841	W,sharp	839	VW,	841	VW	842	VW,
778	M,sharp	779	W,sharp	779	W,	778	W,

1:1.1A	Comment	1:1.1B	Comment	1:0.9A	Comment	1:0.9B	Comment
3336	VS,broad	3339	VS,broad	3336	VS,broad	3341	VS,broad
3225	VVW,	3238	VVW,	3223	VVW,	3234	VVW,
2958	W,	2960	W,	2962	W,	2961	W,
2900	VVW,	2897	VW,	2895	VW,	2892	VW,
2836	VVW,	2816	VVW,	2820	VVW,	2811	VW,
1660	VS,	1653	VS,	1664	VS,broad	1653	VS,
				1624	VW,	1623	VVW,
1548	VS,	1558	VS,	1550	VS,broad	1550	VS,
1453	W,	1456	W,	1452	M,	1453	M,
1385	VW,	1387	W,	1386	W,	1389	W,
1357	VVW,	1354	W,	1355	W,	1351	W,
1255	W,	1253	M,	1255	M,	1253	M,
1138	W,	1136	M,	1155	M,	1137	M,
1015	S,	1014	S,	1014	S,	1014	S,
900	VW,	902	VW,	903	VW,	902	VW,
842	VW,	841	VW,	841	VW,	841	VW,
779	W,	779	W,	781	W,	780	W,

I.R. Spectra of modified U.F. resins cured with 3% NH_4Cl

1:1.8	Comment	1:1.5	Comment	1:1.3A	Comment	1:1.3B	Comment
3338	VS,broad	3349	VS,broad	3350	VS,broad	3349	VS,broad
3106	VVW,			3095	VVW,		
2964	VVW,	2960	VVW,	2961	VVW,	2958	VW,
1653	VS,sharp	1653	VS,	1656	VS,	1653	VS,
1539	S,sharp	1558	S,	1547	VS,	1558	S,
1505	S,sharp	1505	S,	1503	S,	1507	VW,
1384	W,	1384	M,	1385	M,	1387	W,
1297	M,	1294	M,	1300	VW,	1298	VVW,
		1253	M,	1241	M,	1244	M,
1175	W,	1178	W,	1180	VW,	1174	VVW,
1136	VW,	1130	W,	1134	W,	1136	M,
1003	M,broad	1036	M,	1036	M,	1037	M,
802	M,	802	W,	803	VVW,		
				775	W,	777	W,
753	M,	756	M,	756	W,	755	VVW,

1:1.1A	Comment	1:1.1B	Comment	1:0.9A	Comment	1:0.9B	Comment
3349	VS,	3350	VS,	3346	VS,	3345	VS,
						3200	VVW,
3040		3034	W,	3034	W,	3035	W,
2965		2964	W,	2965	W,	2964	W,
		2844	VVW,	2854	VVW,	2849	VW,
1653	VS,	1653	S,	1653	S,	1653	S,
1603	VW,			1602	VVW,	1603	VW,
1558	S,	1558	S,	1558	S,	1560	S,
1438	W,	1438	W,	1438	W,	1438	W,
1389	M,	1388	M,	1389	M,	1389	M,
				1357	W,	1357	VW,
1242	S,	1240	S,	1246	M,	1245	M,

1:1.1A	Comment	1:1.1B	Comment	1:0.9A	Comment	1:0.9B	Comment
1137	M,	1136	M,	1137	M,	1137	M,
1037	M,	1036	M,	1036	M,	1036	M,
		1002	VW,	1003	W,	1002	W,
780	W,	779	W,	779	W,	779	W,

Table 15. Tabulated results of certain band ratios

Liquid

1:1.8		1:1.5		1:1.3A		1:1.3B	
1558	0.988	1552	0.955	1554	0.969	1558	0.945
1464	0.506	1461	0.591	1454	0.750	1457	0.587
1387	0.612	1386	0.621	1386	0.729	1387	0.565
1131		1133	0.530	1137	0.656	1135	0.500

Cured

1:1.8		1:1.5		1:1.3A		1:1.3B	
1539	0.965	1558	0.965	1547	0.988	1558	0.951
1384	0.907	1384	0.906	1385	0.917	1387	0.802
1136	0.884	1130	0.882	1134	0.905	1136	0.778

Liquid

1:1.1A		1:1.1B		1:0.9A		1:0.9B	
1548	0.916	1558	0.933	1550	0.863	1550	0.890
1453	0.675	1456	0.573	1452	0.674	1453	0.626
1385	0.602	1387	0.494	1386	0.705	1389	0.473
1138	0.553	1136	0.483	1155	0.653	1137	0.484

Cured

1:1.1A		1:1.1B		1:0.9A		1:0.9B	
1558	0.978	1558	0.975	1558	0.968	1560	0.980
1438	0.811	1438	0.800	1438	0.753	1438	0.786
1389	0.867	1388	0.850	1389	0.860	1389	0.867
1137	0.833	1136	0.800	1137	0.796	1137	0.857

Table 16. Table of Band Assignments cited in the Literature for ^{13}C NMR.

Functional Group	NMR Signal (ppm) [32]	NMR Signal (ppm) [33]
Carbonyl group		
$NH_2\underline{C}ONHCH_2OH$	161.9	
$=N\underline{C}ON=$	160.2	
Methylene group		
$-NH\underline{C}H_2NH-$	47.7	47.2
$-N(CH_2-)\underline{C}H_2NH-$	53.8	53.5
$-N(CH_2-)\underline{C}H_2N(CH_2-)-$	60.0	
Methylol group		
$-NH\underline{C}H_2OH$	65.1	64.8
$-N(CH_2OH)_2$		71.6
$-N(CH_2-)\underline{C}H_2OH$	71.7	
Ether		
$-NH\underline{C}H_2OCH_3$	73.2	
$-N(CH_2-)\underline{C}H_2OCH_3$	79.7	
$-NHCH_2O\underline{C}H_2OH$	87.1	
$-NH\underline{C}H_2O\underline{C}H_2NH-$	69.4	69.6
$-N(CH_2-)\underline{C}H_2O\underline{C}H_2NH-$	76.0	76.2
Methoxy group		
$-NHCH_2O\underline{C}H_3$	55.6	
Methylene glycol species		

Functional Group	NMR Signal (ppm) [32]	NMR Signal (ppm) [33]
$HO\underline{C}H_2OH$	83.1	82.9
$HO\underline{C}H_2O\underline{C}H_2OH$	86.6	86.3
$HO\underline{C}H_2OCH_3$	90.7	90.5
$HOCH_2O\underline{C}H_2OCH_2OH$		86.8
$H(OCH_2)_nO\underline{C}H_2OCH_3$	95.0	
Methanol $\underline{C}H_3OH$	50.0	
Urea $NH_2\underline{C}ONH_2$	163.6	

Table 17. Table of ^{13}C NMR Peak Assignment for the different UF Resins.

Functional Group (ppm)	1:1.8	1:1.5	1:1.3A	1:1.3B	1:1.11
Carbonyl group {C}					
$NH_2\underline{C}ONHCH_2OH$ (163.6) {C1}	23.7	52.5	42.1	58.8	10.7
$=N\underline{C}ON=$ (162.0) {C2}	4.0	27.7	37.3	14.0	18.5
Methylene group {Me}					
$-NH\underline{C}H_2NH-$ (48.8)	2.4	9.0	7.1	3.7	4.1
$-N(CH_2-)\underline{C}H_2NH-$ (55.5)	3.5	9.6	6.2	3.1	4.9
$-N(CH_2-)\underline{C}H_2N(CH_2-)-$ (61.6)	1.0	2.7	1.0	1.2	0.9
Methylol group {Mo}					
$-NH\underline{C}H_2OH$ (66.6) {Mo1}	26.3	101.5	68.0	31.0	28.2
$-N(CH_2-)\underline{C}H_2OH$ (71.0) {Mo2}	5.3	18.4	12.2	6.9	7.4
Ether {E}					
$-NH\underline{C}H_2OCH_3$ (73.4) {E1}	10.2	12.9	6.5	2.8	7.5
$-N(CH_2-)\underline{C}H_2OCH_3$ (77.7) {E2}	1.3	3.2	1.9	1.2	1.4

Functional Group (ppm)	1:1.8	1:1.5	1:1.3A	1:1.3B	1:1.11
$-NHCH_2O\underline{C}H_2OH$ (88.7) {E3}	2.0	2.2	-	-	-
$-NH\underline{C}H_2O\underline{C}H_2NH-$ (70.3) {E4}	-	3.7	2.5	1.5	1.0
$-N(CH_2-)\underline{C}H_2OCH_2NH-$ (75.0) {E5}	1.7	3.9	3.1	2.0	2.0
Methanol $\underline{C}H_3OH$ (51.7)	1.3	3.5	1.8	-	-
Free Formaldehdye (84.7)	7.9	9.4	2.4	1.3	1.3
Urea $NH_2\underline{C}ONH_2$ (165.4)	-	6.6	21.3	5.5	26.4

Functional Group (ppm)	1:1.1A	1:1.1B	1:0.9A	1:0.9B
Carbonyl group {C}				
$NH_2\underline{C}ONHCH_2OH$ (163.6) {C1}	58.8	18.0	28.9	11.4
$=N\underline{C}ON=$ (162.0) {C2}	54.2	20.5	25.1	15.0
Methylene group {Me}				
$-NH\underline{C}H_2NH-$ (48.8)	14.0	2.9	8.9	4.7
$-N(CH_2-)\underline{C}H_2NH-$ (55.5)	12.2	2.3	8.0	3.1
$-N(CH_2-)\underline{C}H_2N(CH_2)-$ (61.6)	1.3	1.0	1.2	0.5
Methylol group {Mo}				
$-NH\underline{C}H_2OH$ (66.6) {Mo1}	115.9	28.7	67.1	25.3
$-N(CH_2-)\underline{C}H_2OH$ (71.0) {Mo2}	21.3	4.7	11.9	6.1
Ether {E}				
$-NH\underline{C}H_2OCH_3$ (73.4) {E1}	9.5	1.9	9.2	1.8
$-N(CH_2-)\underline{C}H_2OCH_3$ (77.7) {E2}	2.8	0.7	2.4	0.9
$-NHCH_2O\underline{C}H_2OH$ (88.7) {E3}	-	-	-	-
$-NH\underline{C}H_2O\underline{C}H_2NH-$ (70.3) {E4}	3.3	0.7	2.4	0.9

Functional Group (ppm)	1:1.1A	1:1.1B	1:0.9A	1:0.9B
$-N(CH_2-)\underline{C}H_2OCH_2NH-$ (75.0) {E5}	5.2	0.9	3.2	1.3
Methanol $\underline{C}H_3OH$ (51.7)	-	-	-	-
Free Formaldehdye (84.7)	3.3	-	-	-
Urea $NH_2\underline{C}ONH_2$ (165.4)	55.5	23.5	49.7	20.7

Table 18. Certain NMR peak ratios

	urea/ (C1+C2)	C1/C2	E1/E2	Cross-Linking	ME/MO	free F/Me	E1+E4/ E2+E5	E1+E2/ E4+E5
1:1.8	0	5.9	7.85	0.72	0.22	1.15	3.73	4.26
1:1.5	0.08	1.9	4.03	0.70	0.18	0.44	2.34	2.12
1:1.3A	0.27	1.1	3.42	0.57	0.18	0.17	1.80	2.50
1:1.3B	0.18	1.25	2.33	0.69	0.21	0.16	1.34	1.14
1:1.1A	0.49	1.1	3.39	0.49	0.20	0.12	1.60	1.45
1:1.1B	0.62	0.88	2.71	0.60	0.19	0	1.53	1.63
1:0.9A	0.92	1.2	3.83	0.57	0.23	0	2.07	2.07
1:0.9B	0.78	0.76	2.00	0.49	0.26	0	2.23	1.23
1:1.11	0.90	0.578	5.36	0.68	0.28	0.13	2.50	2.97

Table 19. Table correlating the NMR species ratio to the I.B. strength

	NMR Species Ratio	Correlation for A series resins	Correlation for B series resins
Y1	Urea/(C1+C2)	0.888	0.895
Y2	C1/C2	0.228	0.412
Y3	E1/E2	0.145	0.357
Y4	Cross-linking	0.410	0.919
Y5	Me/Mo	0.780	0.482
Y6	(E1+E4)/(E2+E5)	0.139	0.336
Y7	(E1+E2)/(E4+E5)	0.063	0.277
Y8	Free F/Mo	0.424	0.456

Table 20. Table correlating the NMR species ratio to the formaldehyde emission

	NMR Species Ratio	Correlation for A series resins	Correlation for B series resins
Y1	Urea/(C1+C2)	0.805	0.786
Y2	C1/C2	0.954	0.973
Y3	E1/E2	0.927	0.986
Y4	Cross-linking	0.844	0.705
Y5	Me/Mo	0.099	0.153
Y6	(E1+E4)/(E2+E5)	0.939	0.985
Y7	(E1+E2)/(E4+E5)	0.909	0.966
Y8	Free F/Mo	0.996	0.997

Table 21. Comparing the predicted and experimental I.B. strength for the 1:1 [illegible] UF ratio resin.

Predicted I.B. Strength (MPa)*	Experimental density ($g.cm^{-3}$)	Measured I.B. strength (MPa)
A-Series equ: 0.634 B-Series equ: 0.575	0.694	0.676

* I.B. strength at an average density of 0.680 $g.cm^{-3}$

Table 22. Comparing the predicted and experimental formaldehyde emission for the 1:1.11 UF ratio resin.

Predicted F. emission (mg F/100g board)	Measured F. emission (mg F/100g board)
A-Series equ: 9.15 B-Series equ: 11.90	3.38

Table 23. Table correlating the NMR species ratio to the % crystallinity

	NMR Species Ratio	Correlation for A series resins
Y1	Urea/(C1+C2)	0.941
Y2	C1/C2	0.621
Y3	E1/E2	0.569
Y4	Cross-linking	0.800
Y5	Me/Mo	0.439
Y6	(E1+E4)/(E2+E5)	0.631
Y7	(E1+E2)/(E4+E5)	0.542
Y8	Free F/Me	0.759

Table 24. Peak Assignments for three Samples of the Modified cured UF Resins.

Sample 1:1.3A	2°θ Position	2θ Width	Height (Counts)	Total Area (Counts)
1	21.1	2.39	67.2	277.2
2	22.8	11.51	191.8	3412.3
3	23.8	1.60	36.6	101.1
4	31.4	6.48	39.3	435.9
5	40.0	13.24	68.6	1395.3
6	50.7	7.18	12.4	113.7

Sample 1:1.1A	2°θ Position	2θ Width	Height (Counts)	Total Area (Counts)
1	21.6	2.69	334.0	1554.9
2	24.5	2.26	211.8	827.5
3	28.4	17.89	79.3	2056.7
4	31.2	2.10	112.4	407.9
5	40.4	3.63	95.0	593.6
6	44.9	4.10	34.8	242.6
7	50.6	5.10	19.4	150.7

Sample 1:0.9A	2°θ Position	2θ Width	Height (Counts)	Total Area (Counts)
1	21.7	2.23	382.5	1476.1
2	24.5	2.14	216.2	802.9
3	25.8	13.85	87.0	1851.7
4	31.4	2.80	106.2	513.2
5	40.4	5.07	103.0	893.7
6	45.3	3.14	30.6	165.0
7	50.4	8.27	23.1	227.5

Sample 1:0.7A	2°θ Position	2θ Width	Height (Counts)	Total Area (Counts)
1	21.9	1.38	533.4	1276.0
2	24.6	1.24	264.7	569.5
3	25.1	8.79	121.3	1773.1
4	31.2	2.09	171.9	620.4
5	37.5	6.20	65.5	695.3
6	41.0	2.81	72.7	353.1
7	44.9	2.97	59.1	302.1
8	50.9	3.43	24.5	138.8

Table 25. Crystallite Size determinations for the UF cured Resins 1:1.1A, 1:0.9A and 1:0.7A respectively.

Sample	1:1.1A	1:0.9A	1:0.7A
θ (°)	10.80	10.85	10.95
λ (nm)	1.541	1.541	1.541
K	0.9	0.9	0.9
ß (2θ)	2.69	2.23	1.38
ß (Rad)	0.02347	0.01946	0.01304
t (Å)	60.2	72.6	115.2

Figures

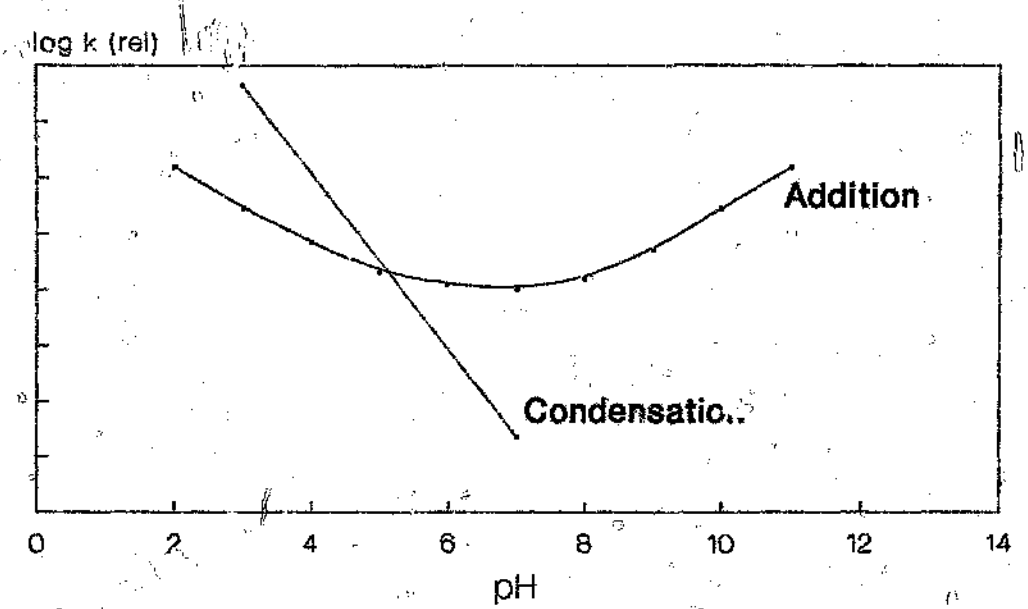

Figure 1. pH dependence of the reaction rates for the initial UF steps.

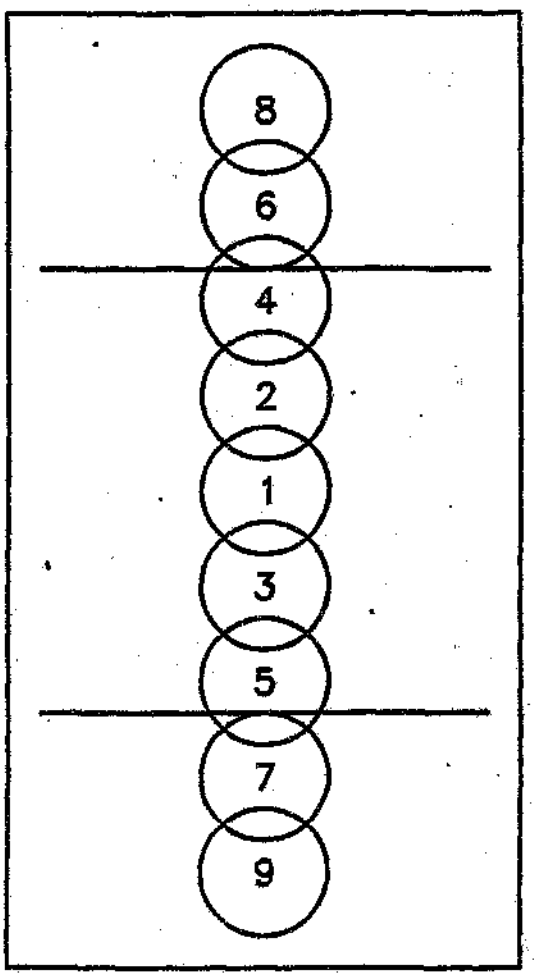

Figure 2. Links in the Adhesive Bond between Wood Surfaces

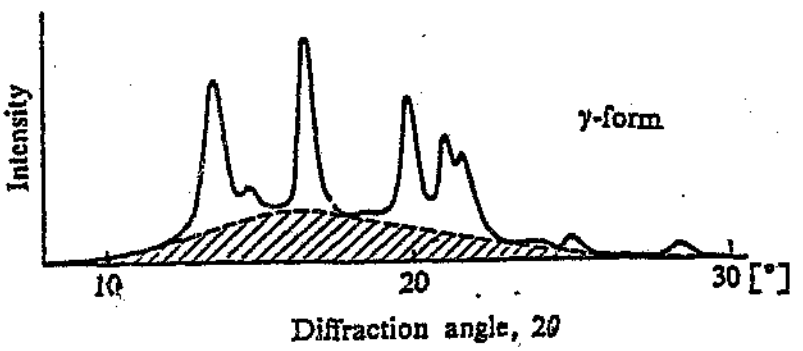

Figure 3. X-ray diffraction trace of a polymer showing the contribution due to amorphous and crystalline regions respectively [36].

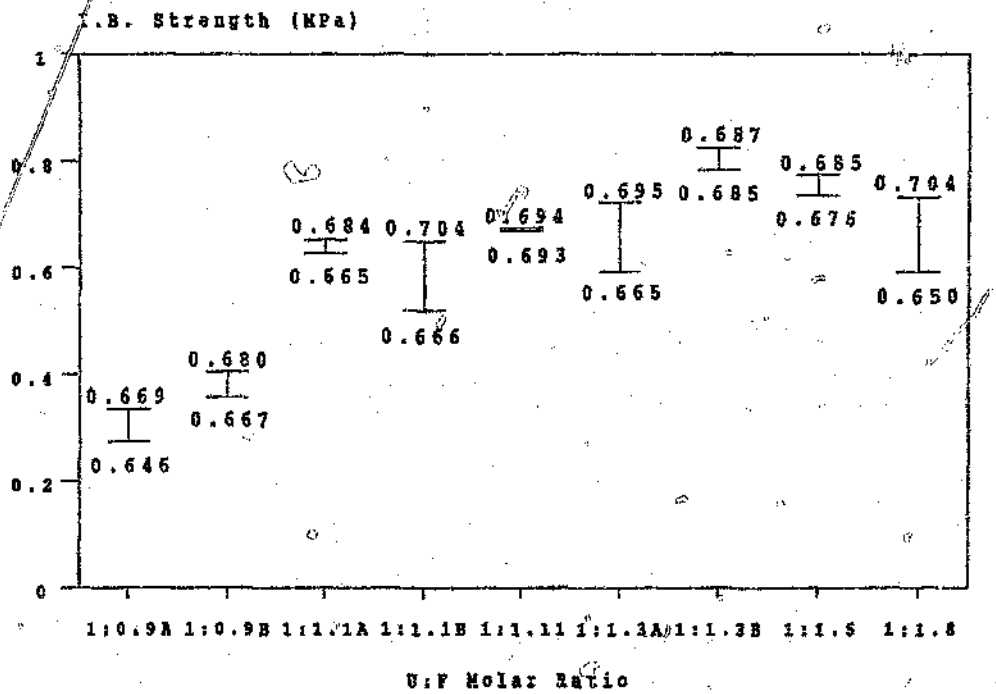

Figure 4. Internal Bond (I.B.) Strength test results for board strengths with the ranges of board densities in g/cm^3, prepared with the different modified resins.

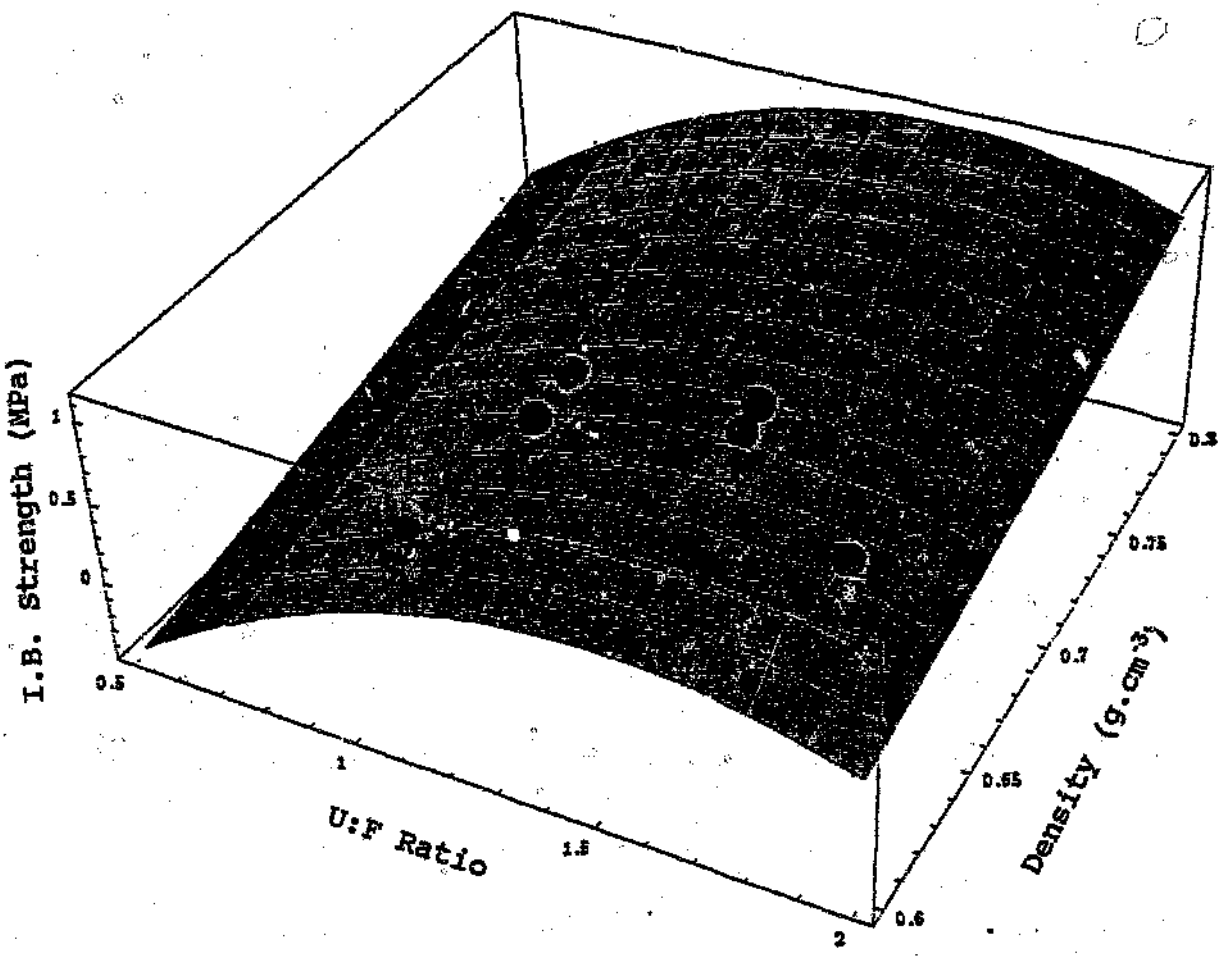

Figure 4a. Surface representing the 3 variables I.B. Strength, density and U:F molar ratio for the boards modified with the A series resins. The points representing the experimental values.

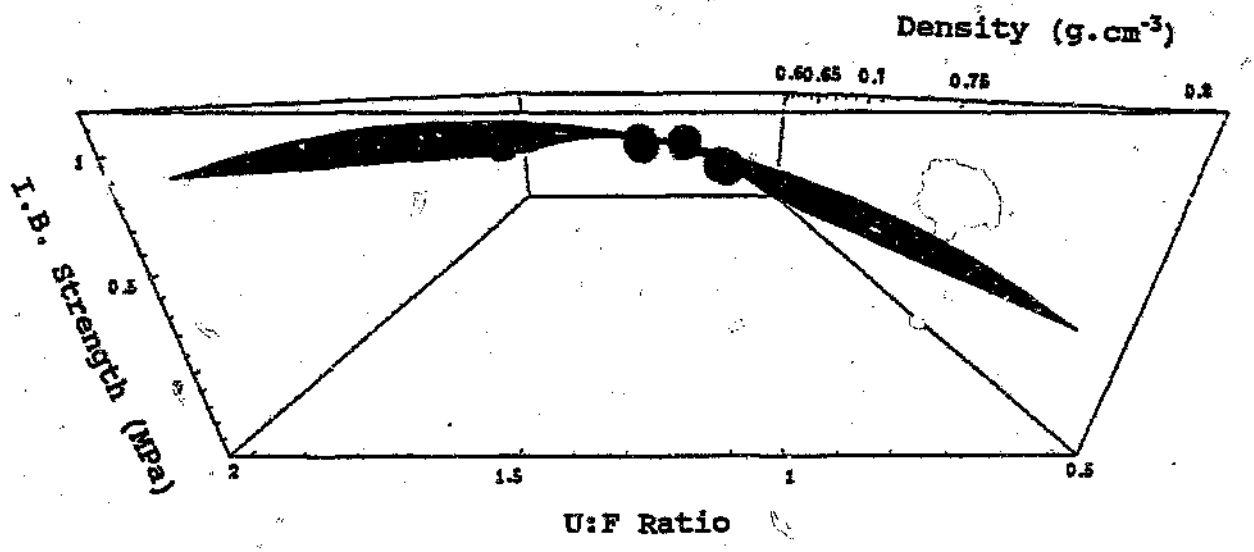

Figure 4b. Surface representing the 3 variables I.B. Strength, density and U:F molar ratio for the boards modified with the A series resins. Viewed along one of the axis and the points representing the experimental values.

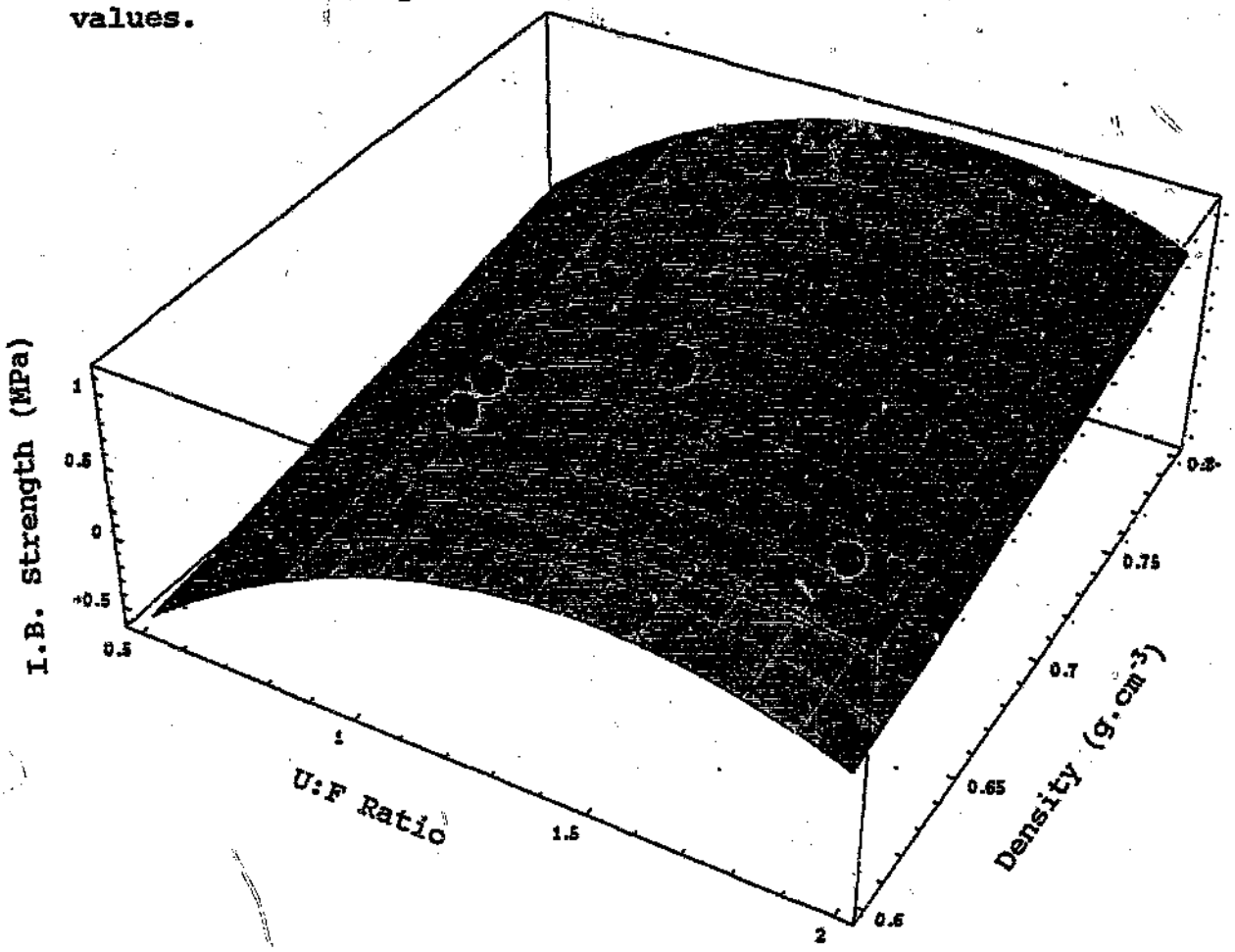

Figure 4c. Surface representing the 3 variables I.B. Strength, density and U:F molar ratio for the boards modified with the B series resins. The points representing the experimental values.

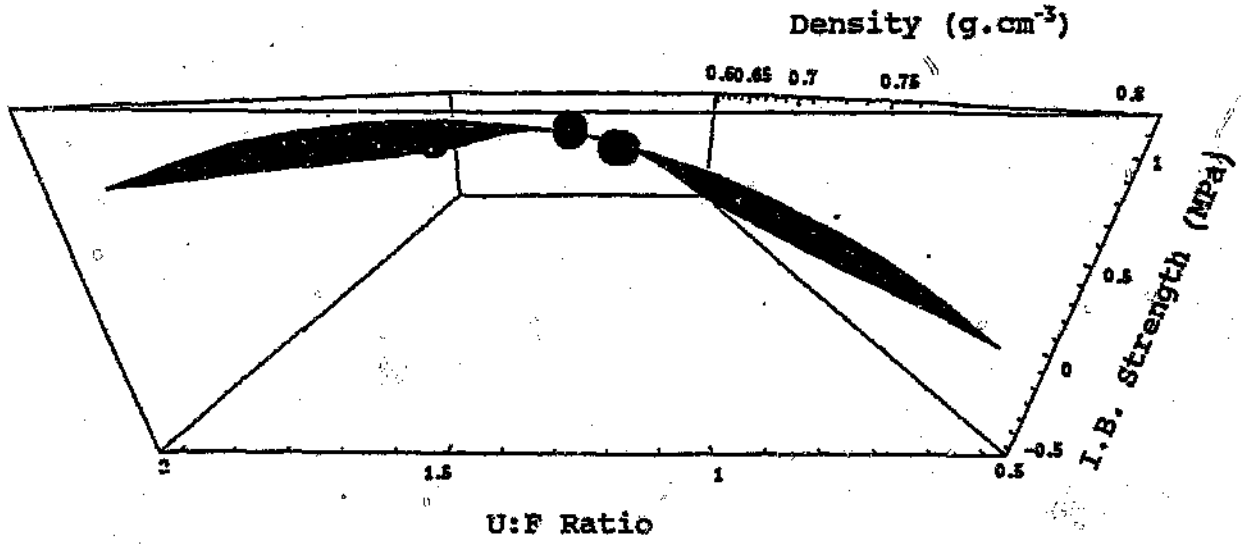

Figure 4d. Surface representing the 3 variables I.B. Strength, density and U:F molar ratio for the boards modified with the B series resins. Viewed along one of the axis and the points representing the experimental values.

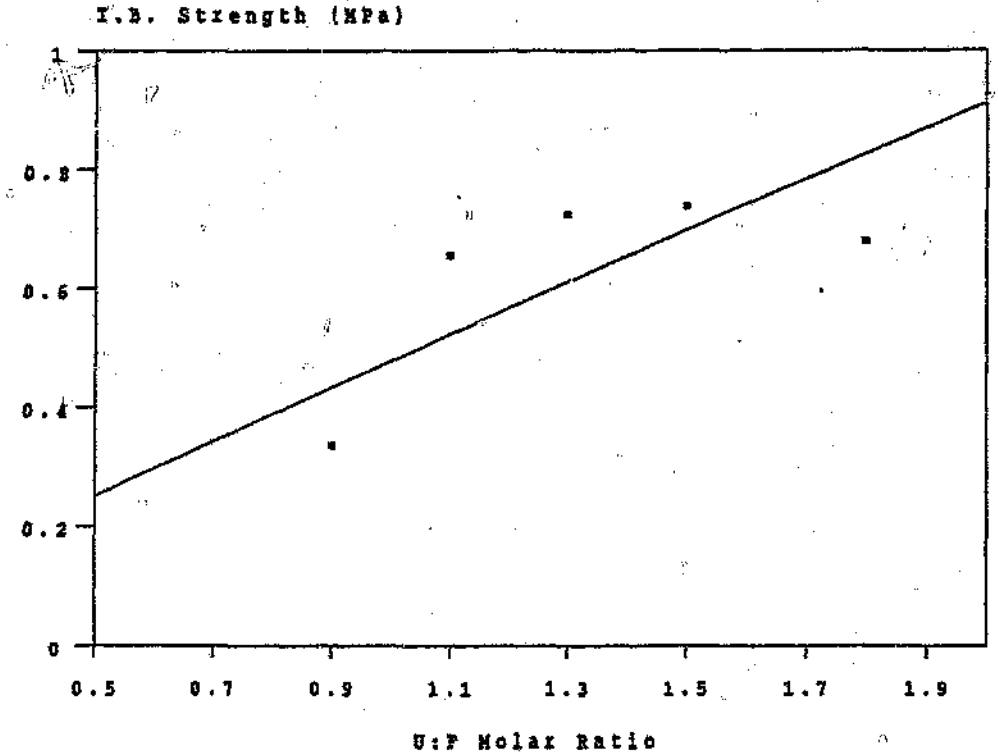

Figure 4e. I.B. strength test results for boards made with the A series resins.

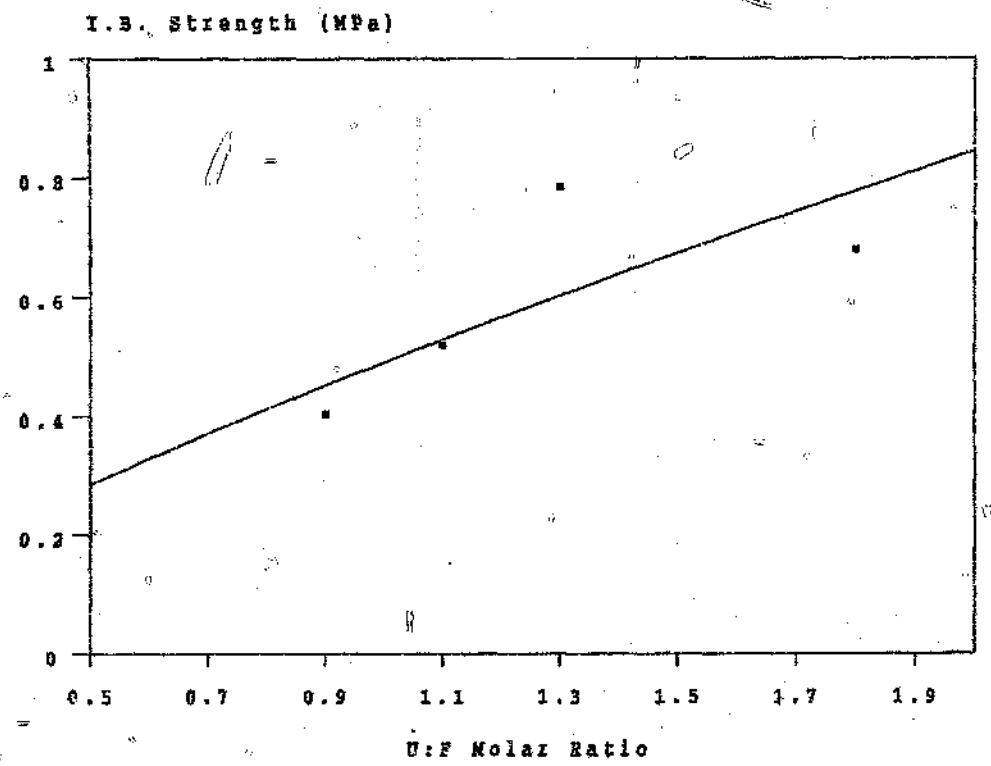

Figure 4f. I.B. strength test results for boards made with the B series resins.

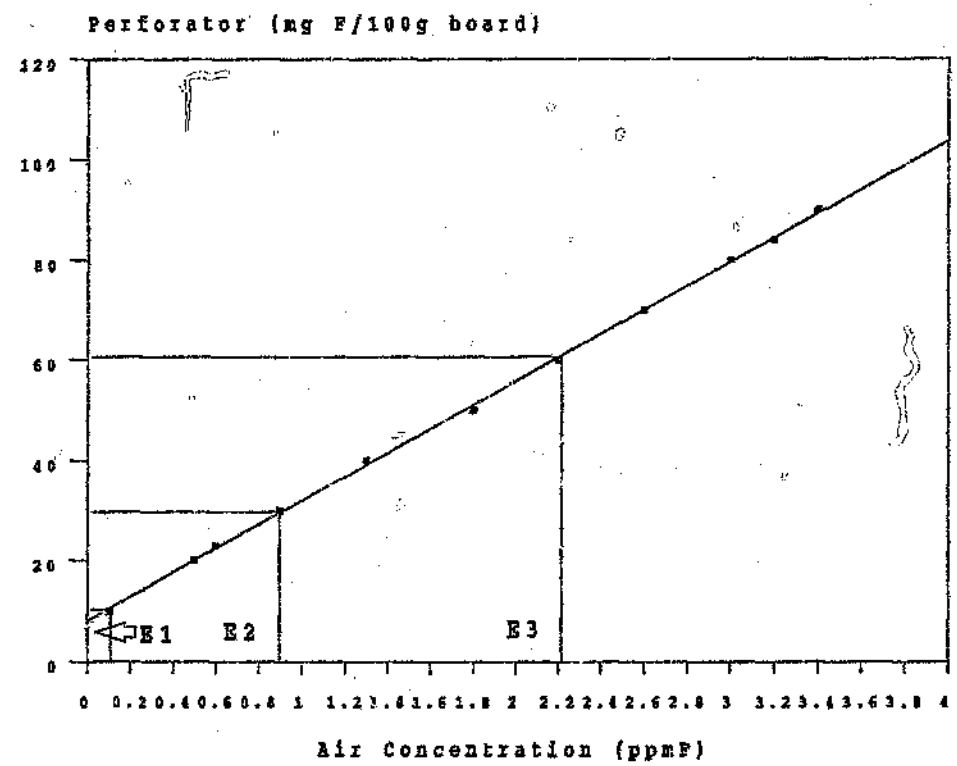

Figure 5. Comparison between the perforator and air chamber methods for formaldehyde emission.

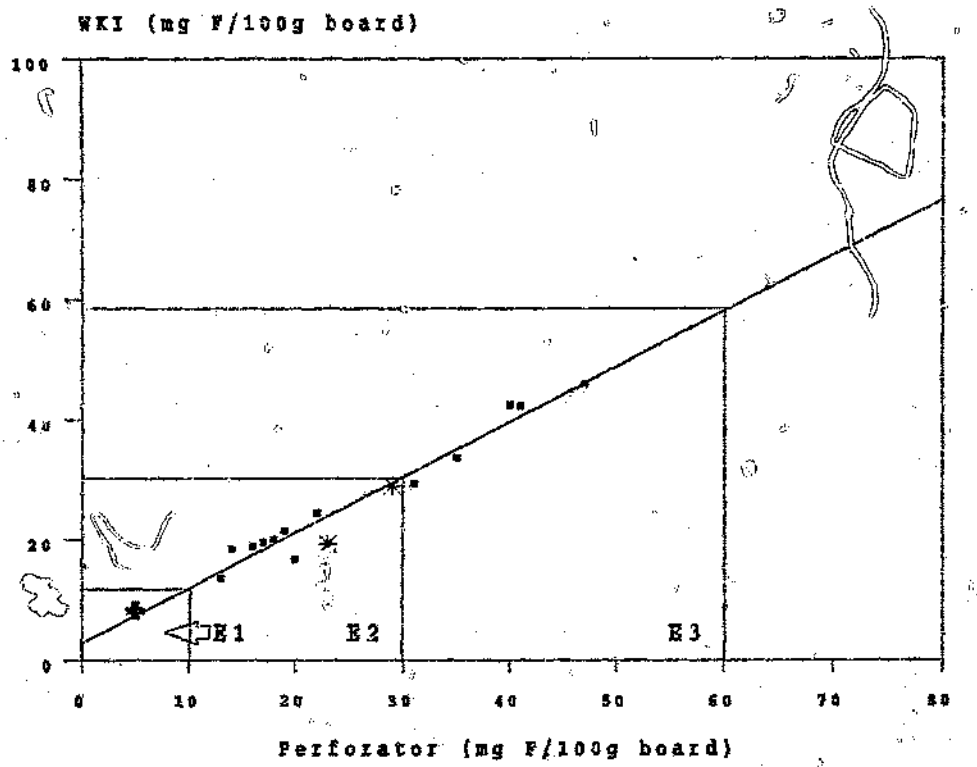

Figure 6. Comparison between the perforator and WKI method for formaldehyde emission.

+ Unpublished results by A. Pizzi and J. Valenzuela, Conception, Chile (1992).
* Roffael [55]
▪ Unpublished results by J. Valenzuela, Quimicos Coronel, Conception, Chile (1992).

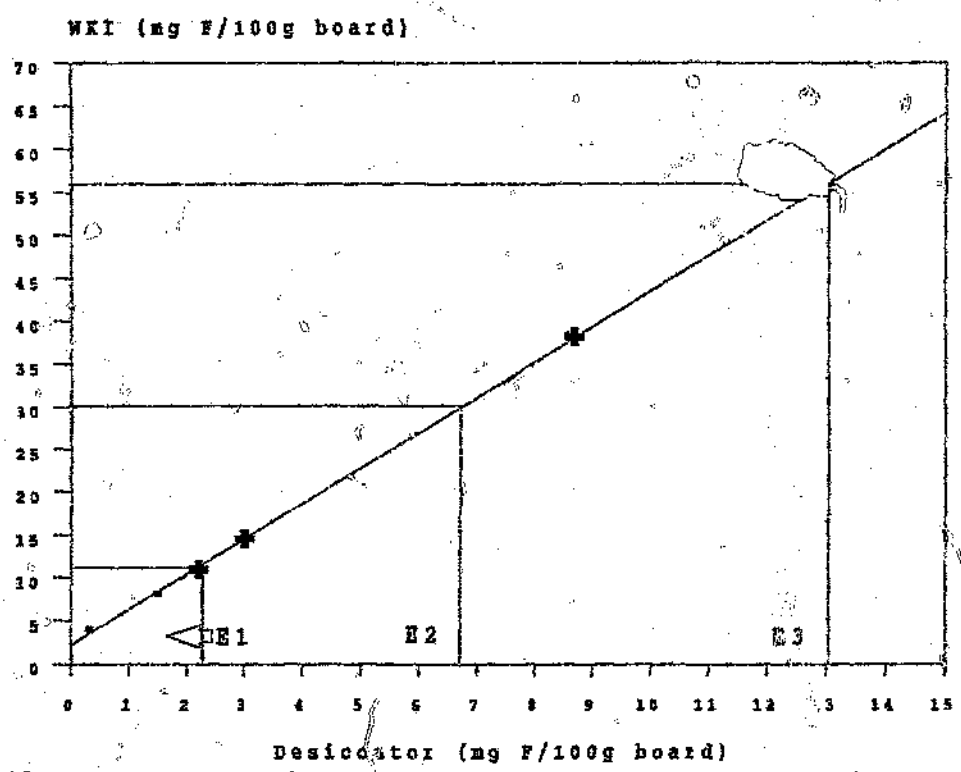

Figure 7. Comparison between the WKI and the desiccator method for formaldehyde emission.

+ Studies done by the Author.
▪ Independent studies done by J. Valenzuela, Conception Chile.

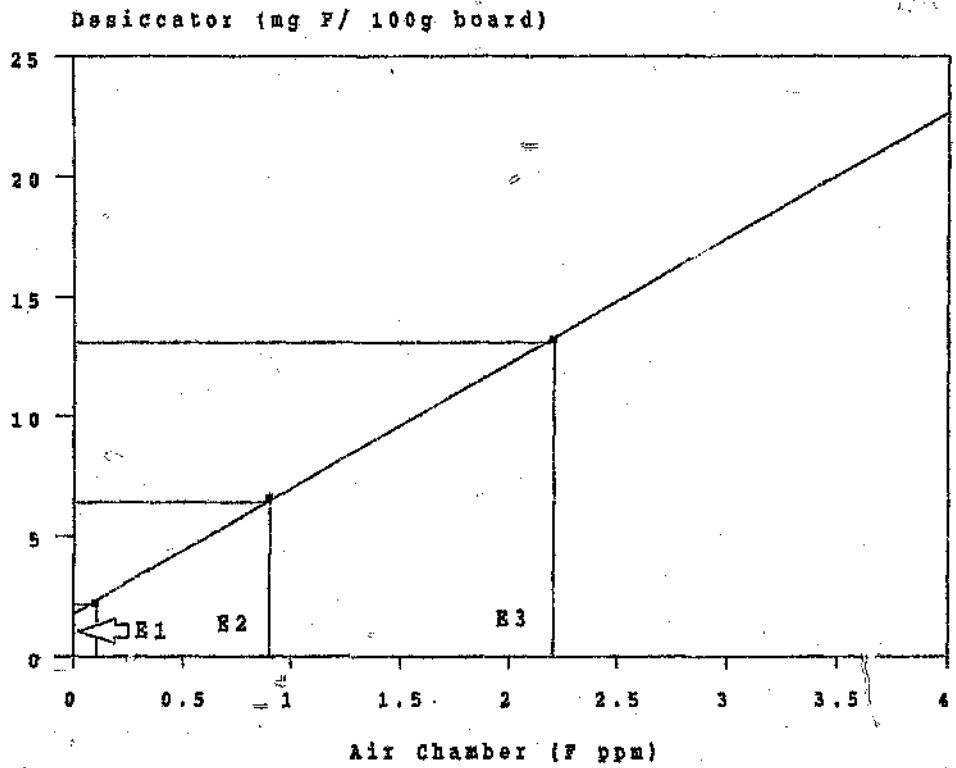

Figure 8. Comparison between the desiccator and air chamber method for formaldehyde emission.

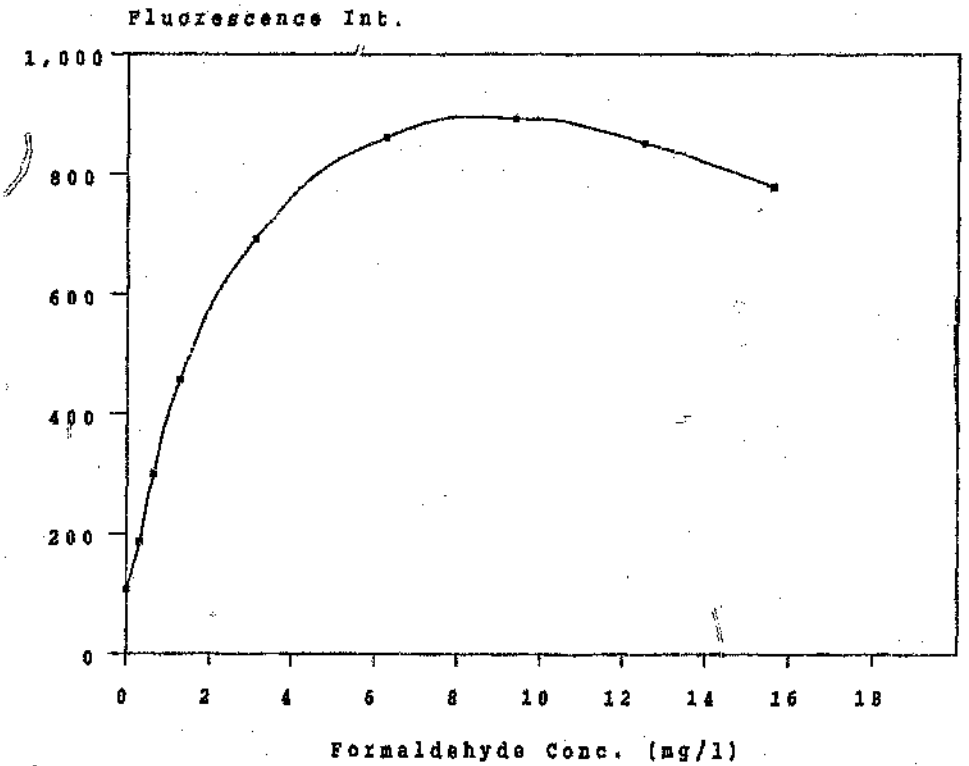

Figure 9. Graph relating the fluorescence and the formaldehyde concentration for the standard solutions.

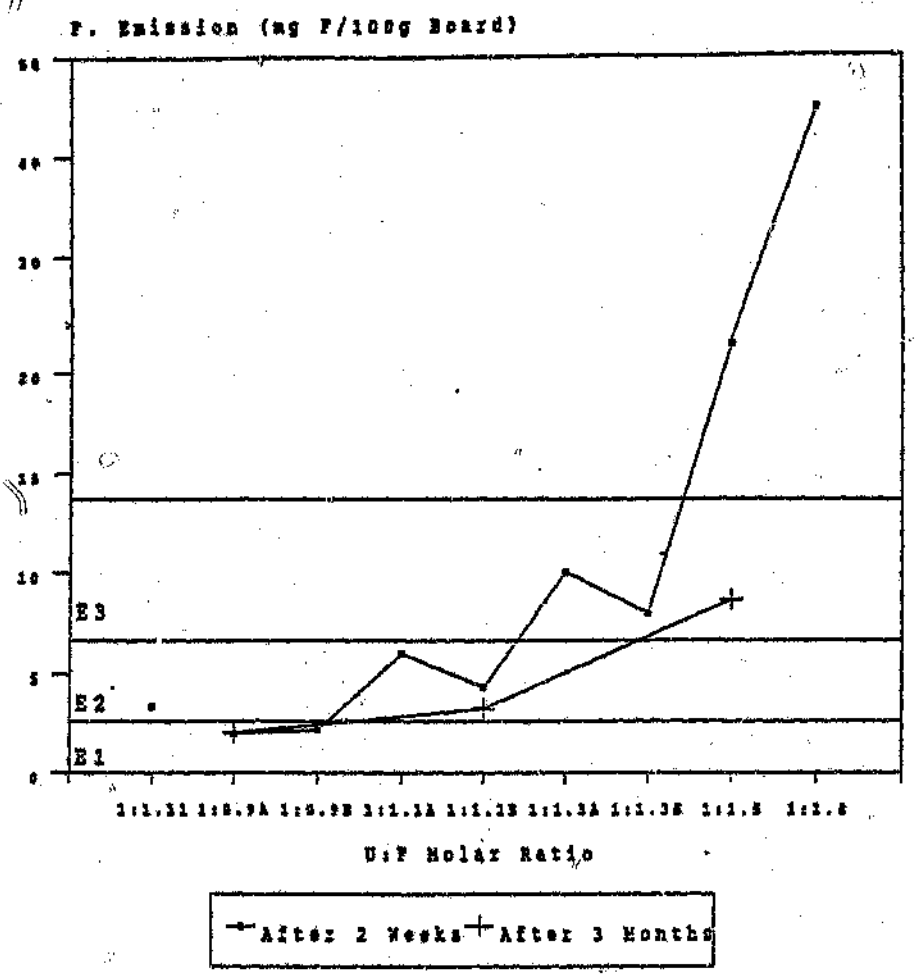

Figure 10. Formaldehyde emission for particleboards prepared with different modified resins.

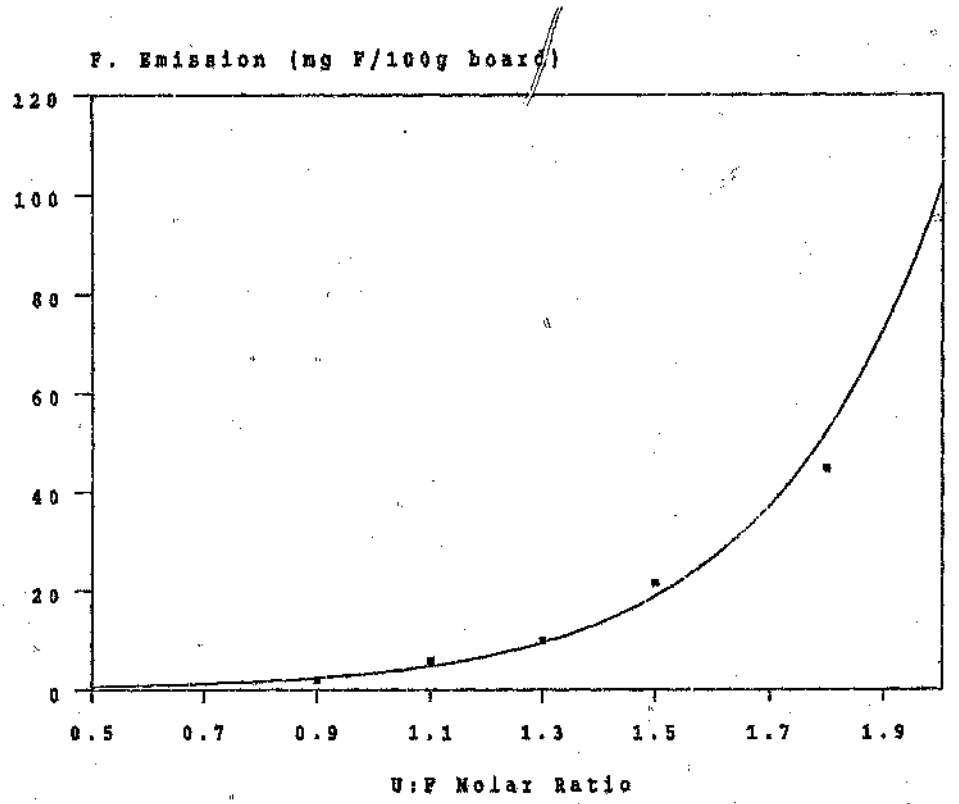

Figure 10a. Formaldehyde emission for series A resins.

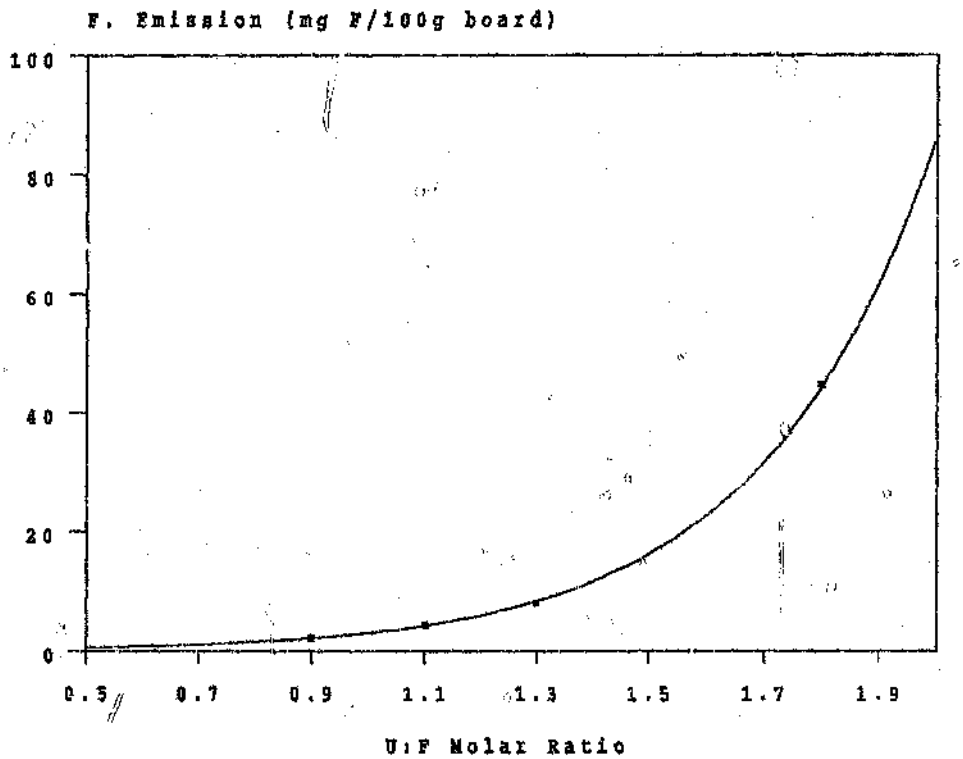

Figure 10b. Formaldehyde emission for B series resins.

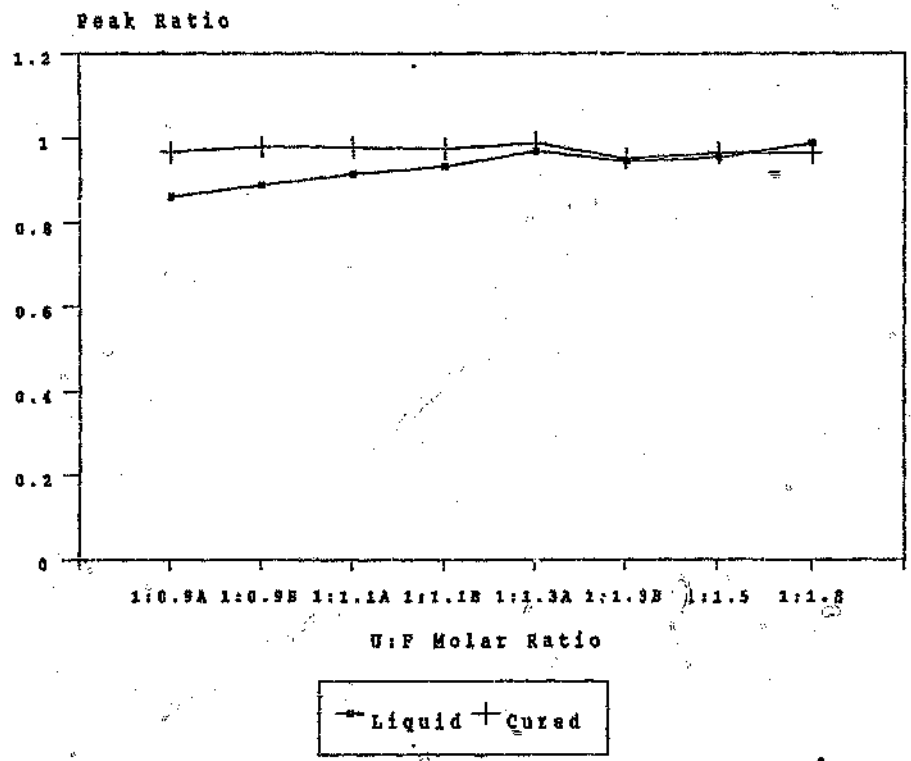

Figure 11. IR peak ratio for the bands 1558 cm^{-1} (amide II) and the constant amide I of liquid and cured UF resins.

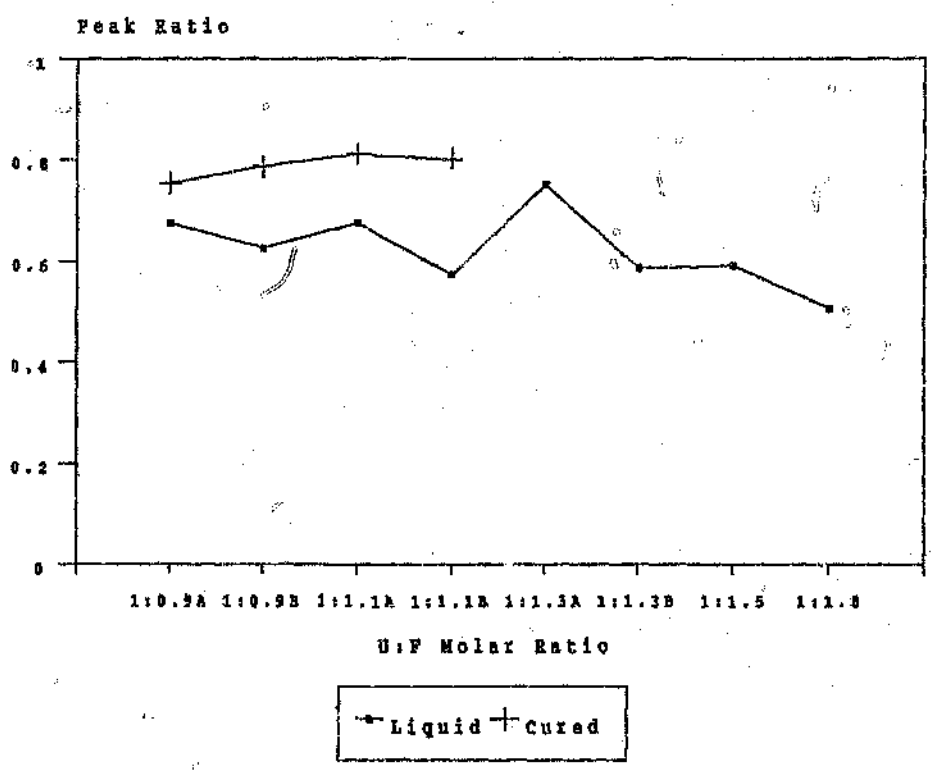

Figure 12a. IR peak ratio of band 1461 cm^{-1} ($-CH_2-$) to the constant amide I band for liquid and cured UF resins.

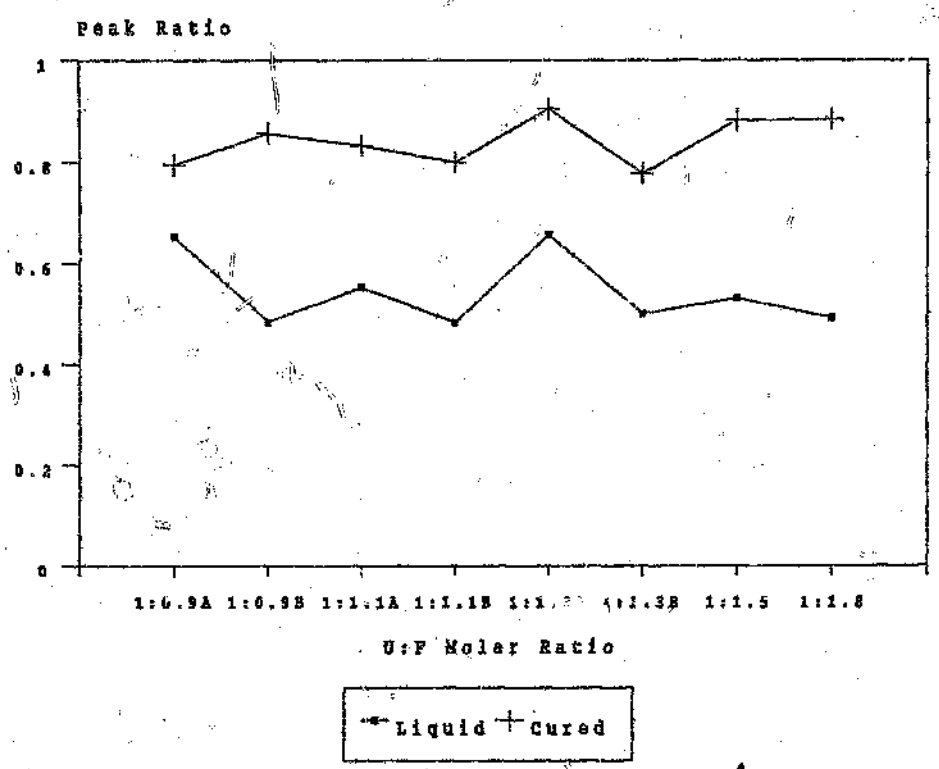

Figure 12b. IR peak ratio of the 1131 cm^{-1} ($-CH_2-$) band to the amide I band for liquid and cured UF resins.

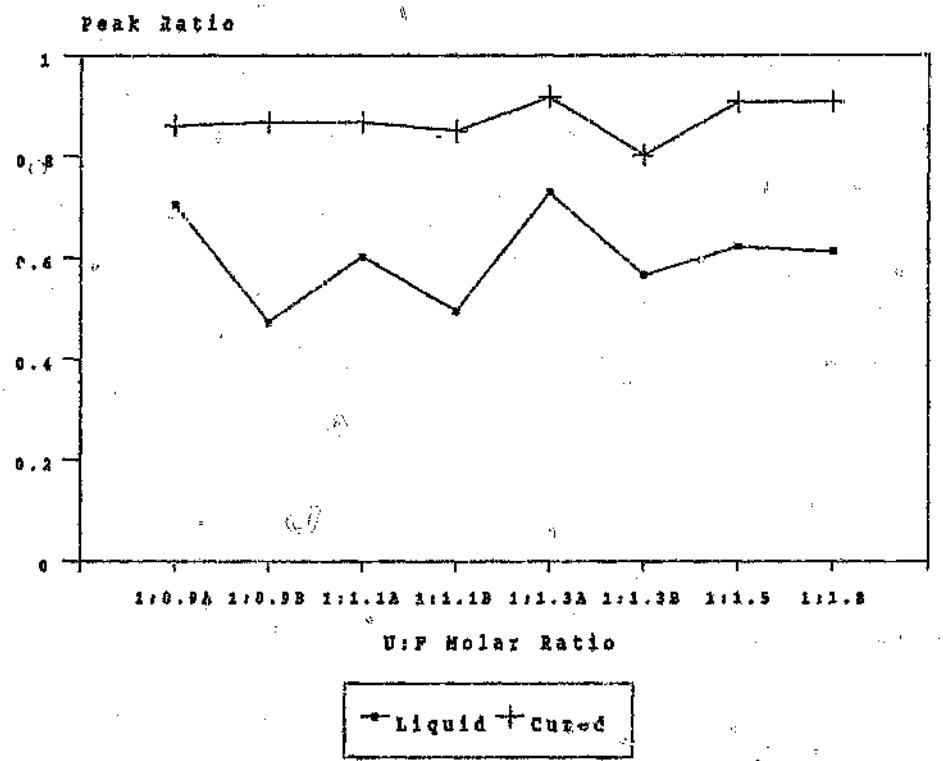

Figure 13. IR band ratio of band 1385 cm^{-1} ($-CH_2OH$) to the constant amide I band for liquid and cured UF resins.

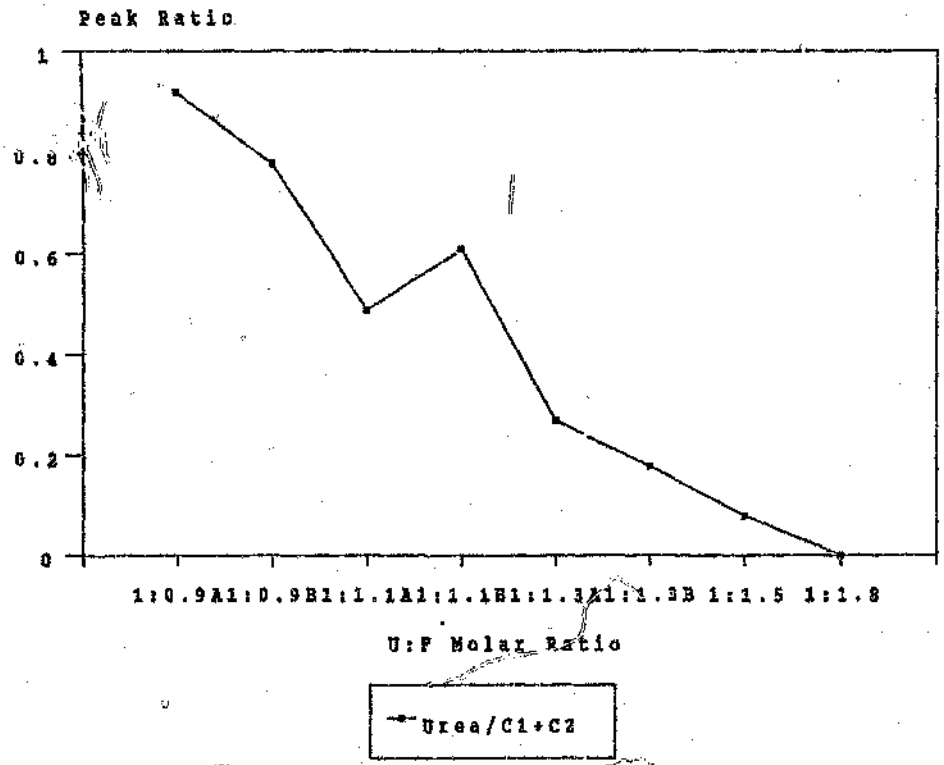

Figure 14. ^{13}C NMR peak ratios fo[illegible]ee urea (165 ppm) to the sum of the other carbonyl [illegible]oups.

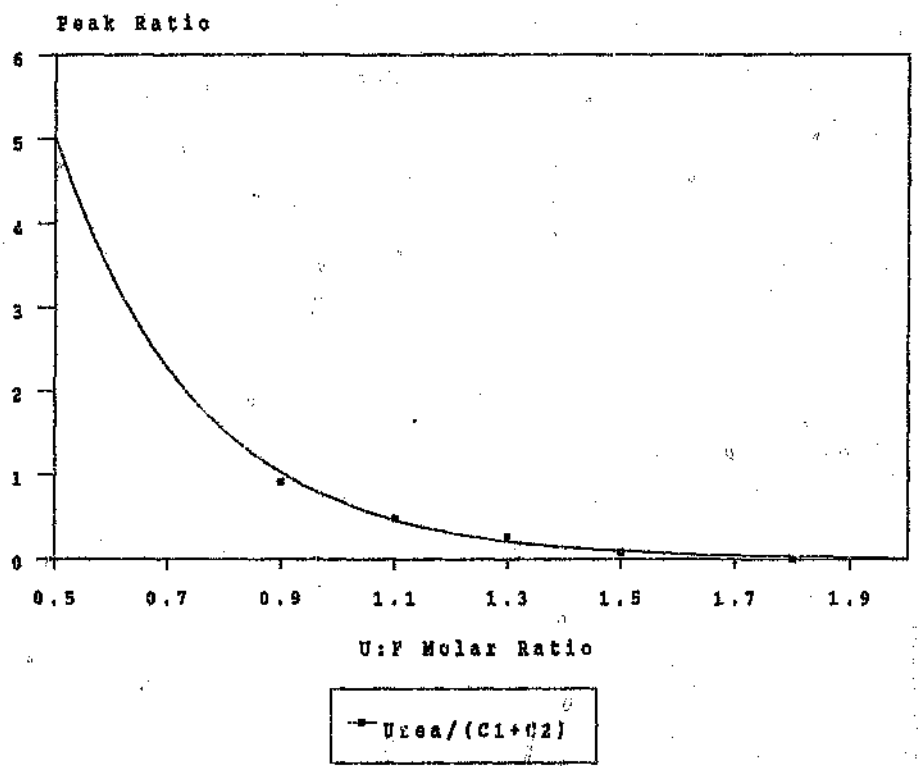

Figure 14a. ^{13}C NMR peak ratio for free urea (165 ppm) to the sum of the other carbonyl groups for the A series resins.

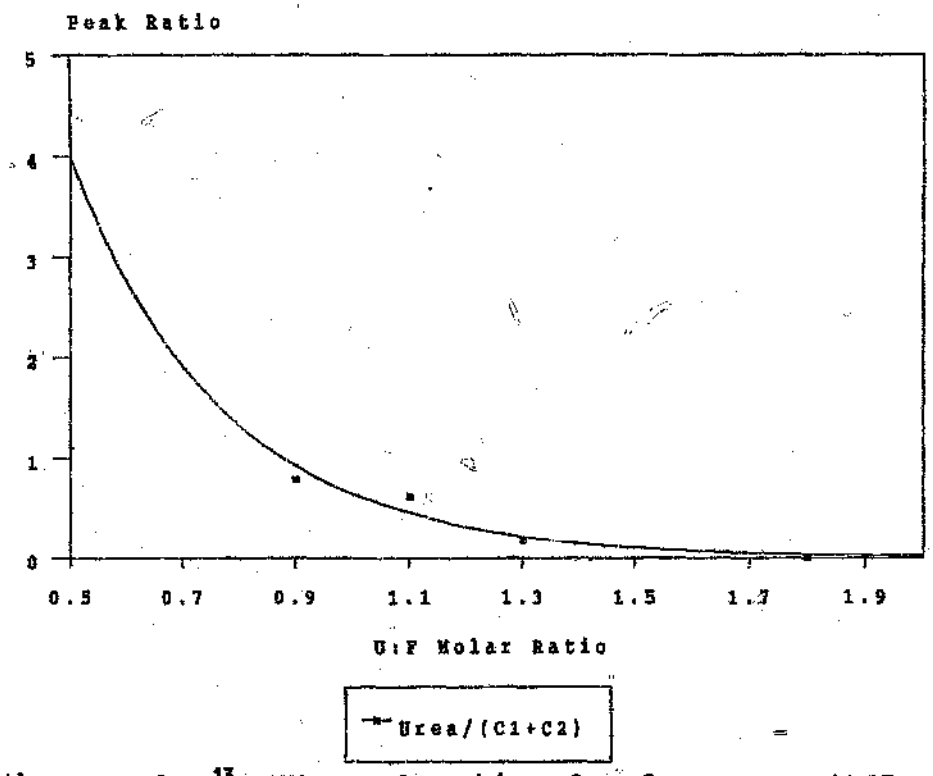

Figure 14b. ^{13}C NMR peak ratios for free urea (165ppm) to the sum of the other carbonyl groups for the B series resins.

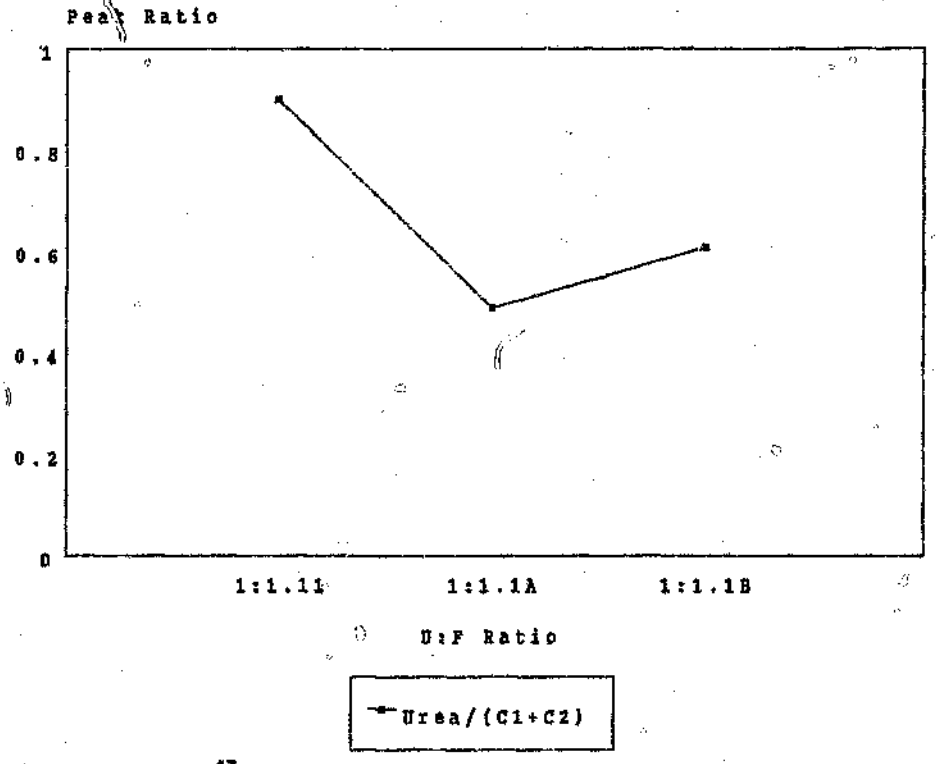

Figure 14c. ^{13}C NMR peak ratio for free urea (165 ppm) to the sum of the other carbonyl groups.

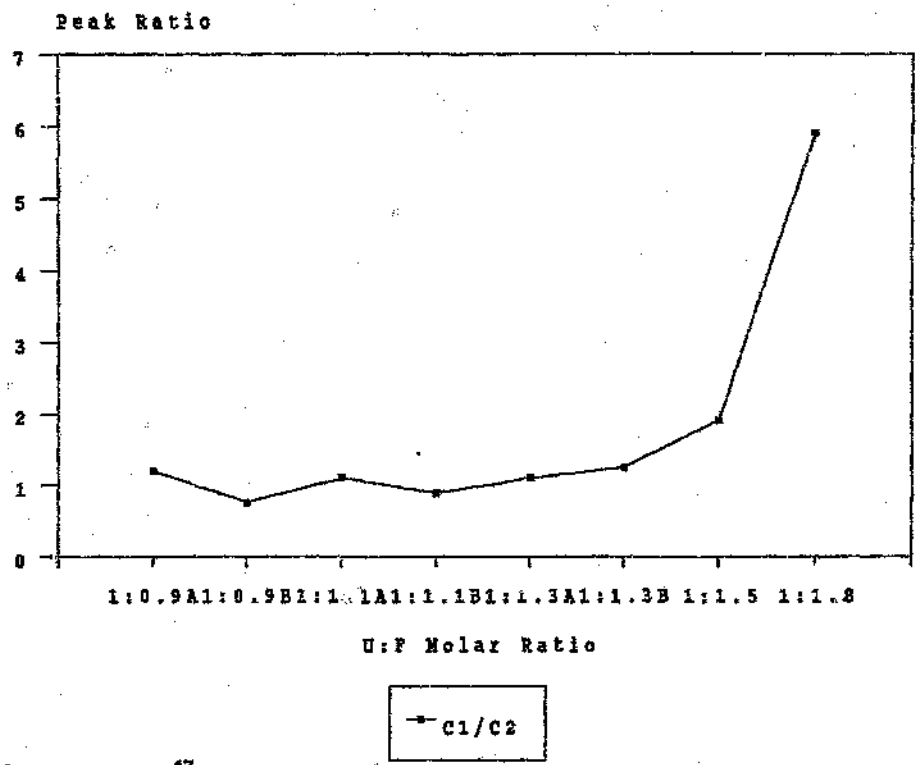

Figure 15 ^{13}C NMR peak ratio for the carbonyl groups (C1/C2).

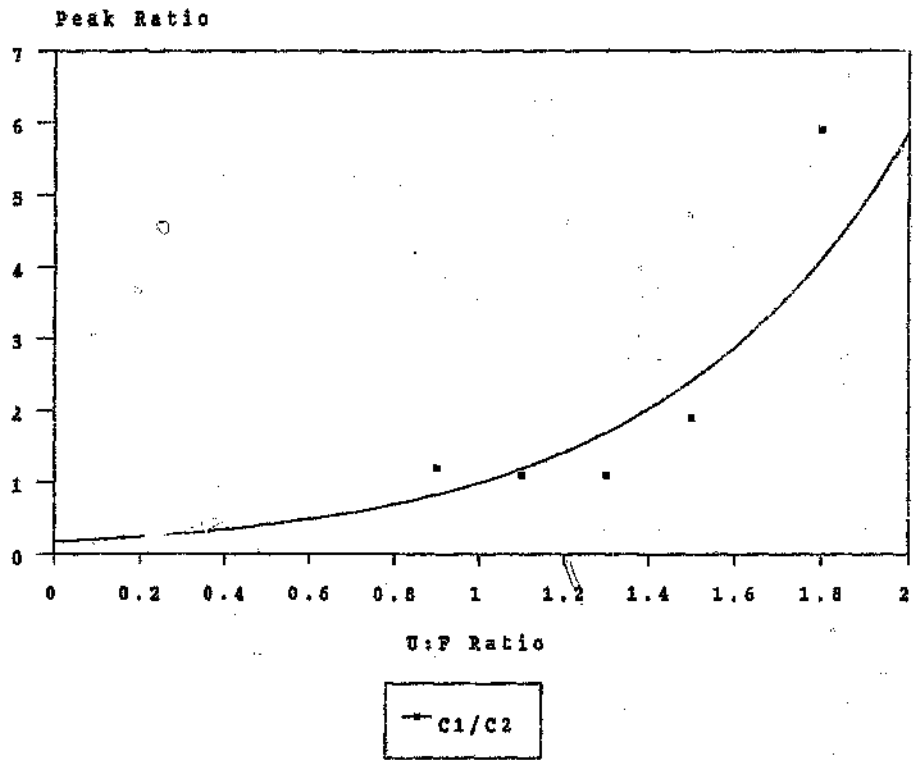

Figure 15a. ^{13}C NMR peak ratio of the carbonyl groups (C1/C2) for the A series resins.

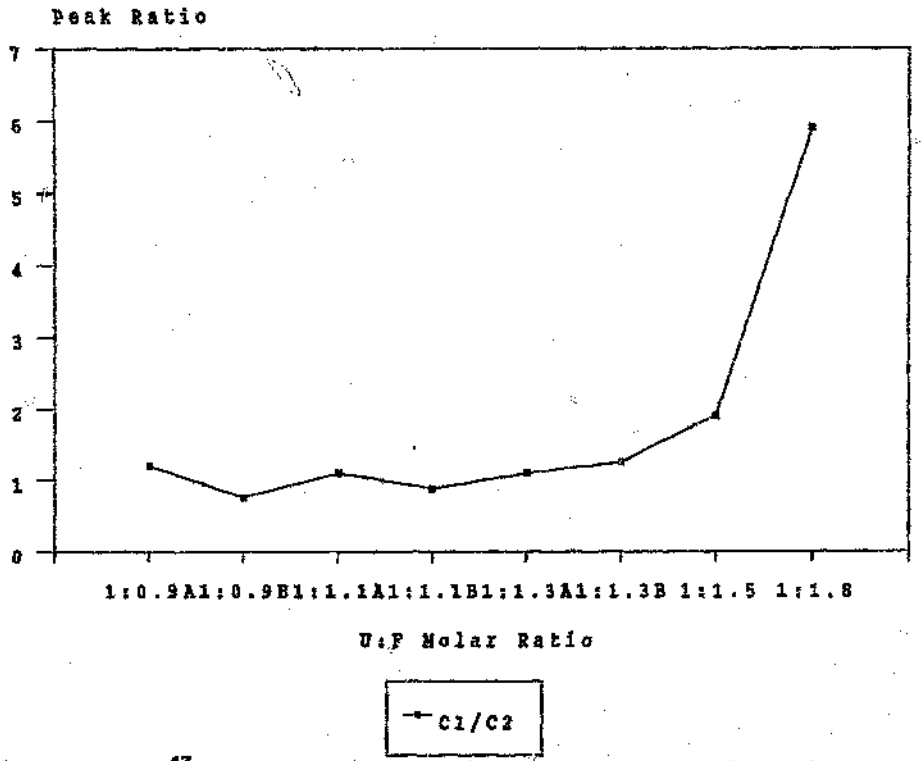

Figure 15 ^{13}C NMR peak ratio for the carbonyl groups (C1/C2).

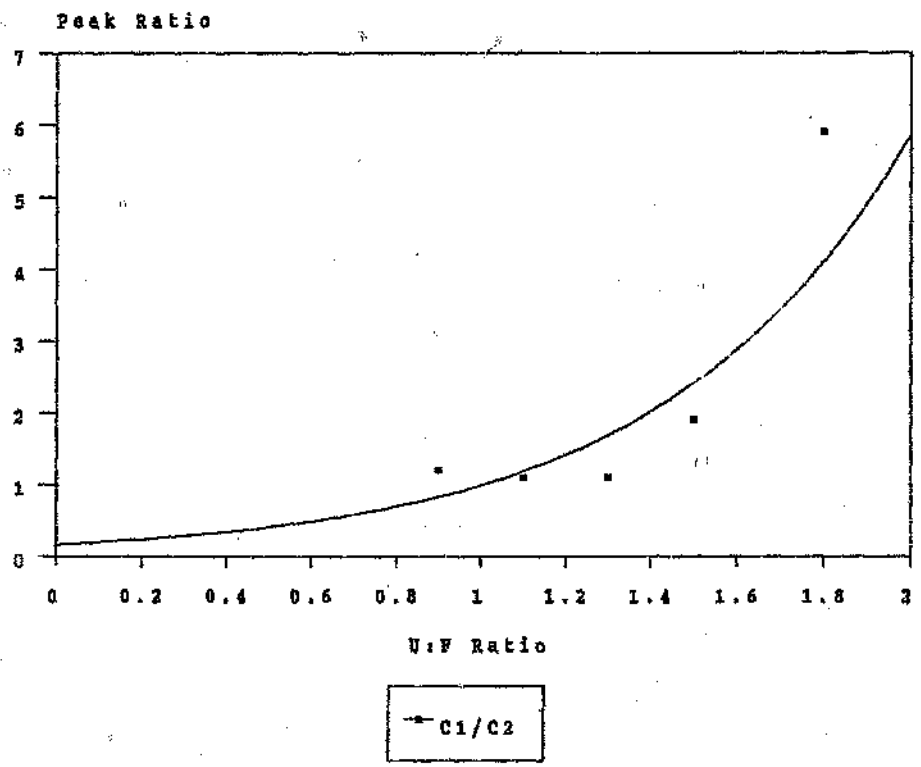

Figure 15a. ^{13}C NMR peak ratio of the carbonyl groups (C1/C2) for the A series resins.

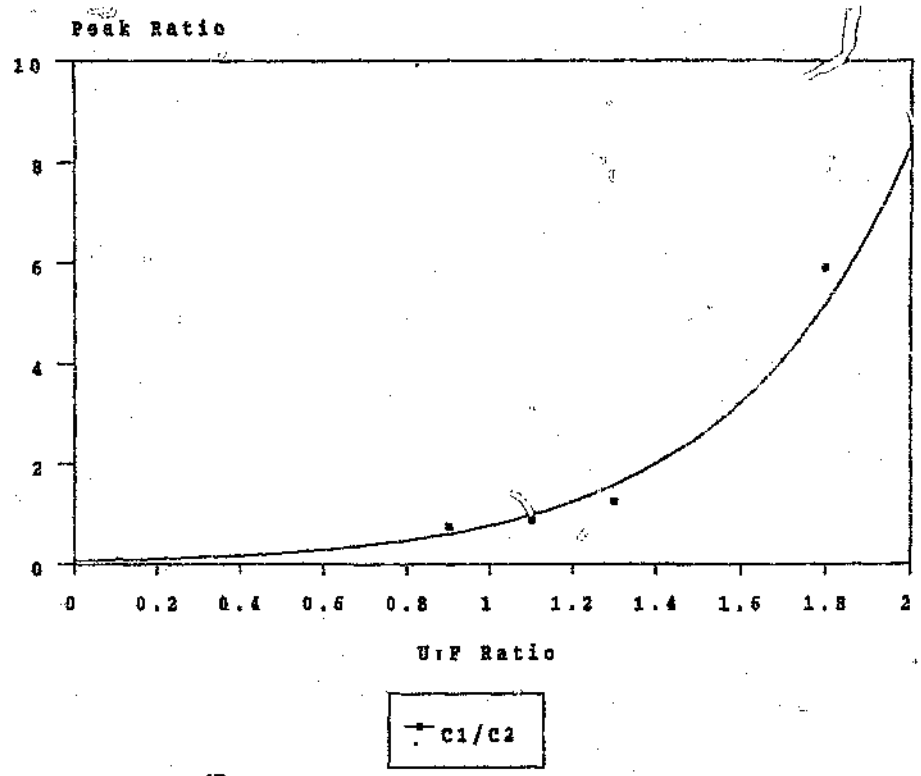

Figure 15b. ^{13}C NMR peak ratio of the carbonyl groups (C1/C2) for the B series resins.

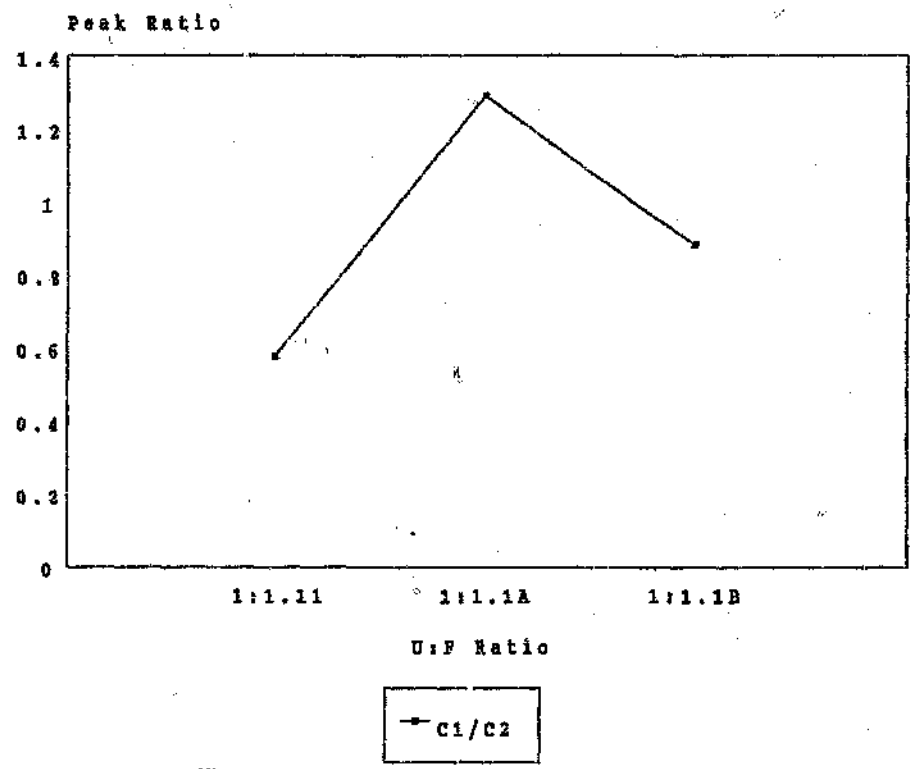

Figure 15c. ^{13}C NMR peak ratio for the carbonyl groups (C1/C2).

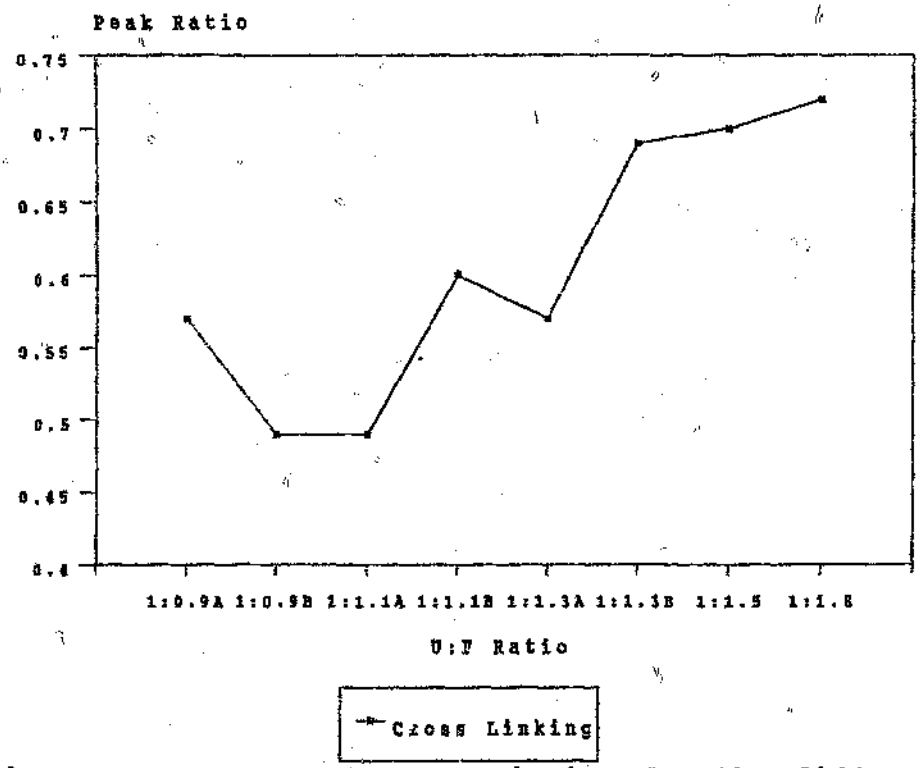

Figure 16. Degree of cross-linking for the different modified resins from B. Tomita and S. Hatono's equation.

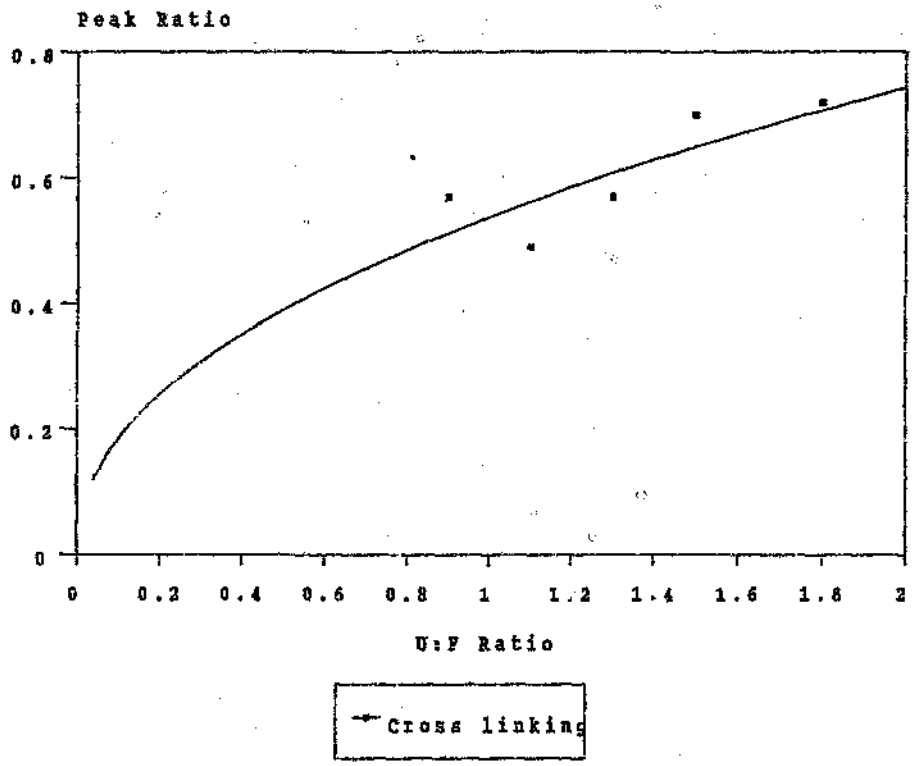

Figure 16a. Degree of cross-linking for the A series modified resins according to B. Tomita and S. Hatono's equation.

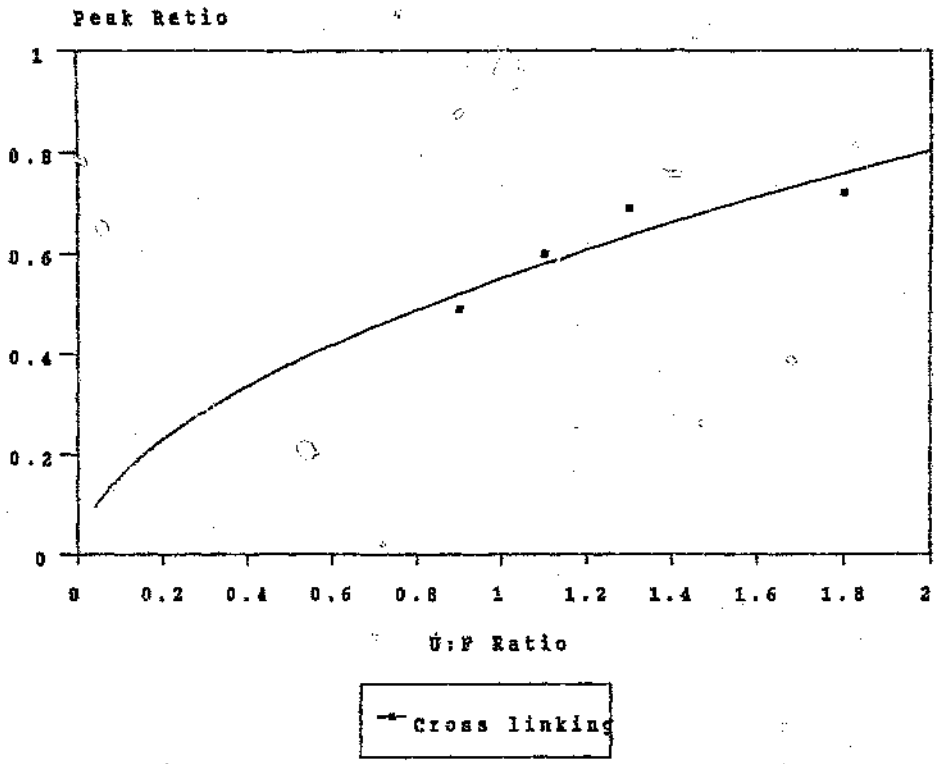

Figure 16b. Degree of cross-linking for the B series modified resins according to B. Tomita and S. Hatono's equation.

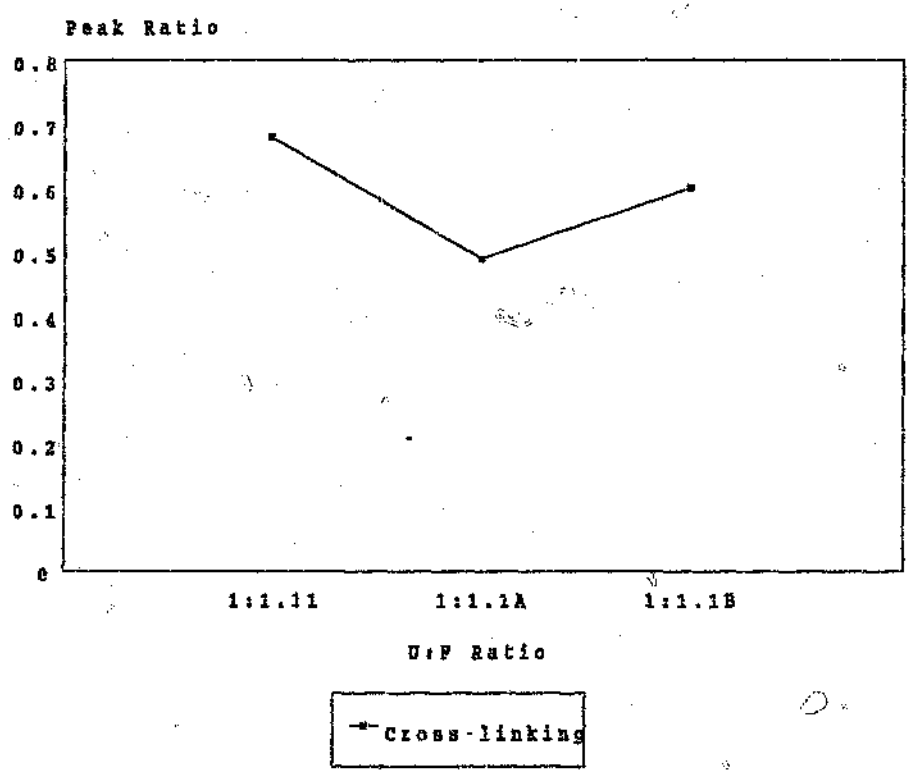

Figure 16c. Degree of cross-linking for the different resins according to B. Tomita and S. Hatono's equations.

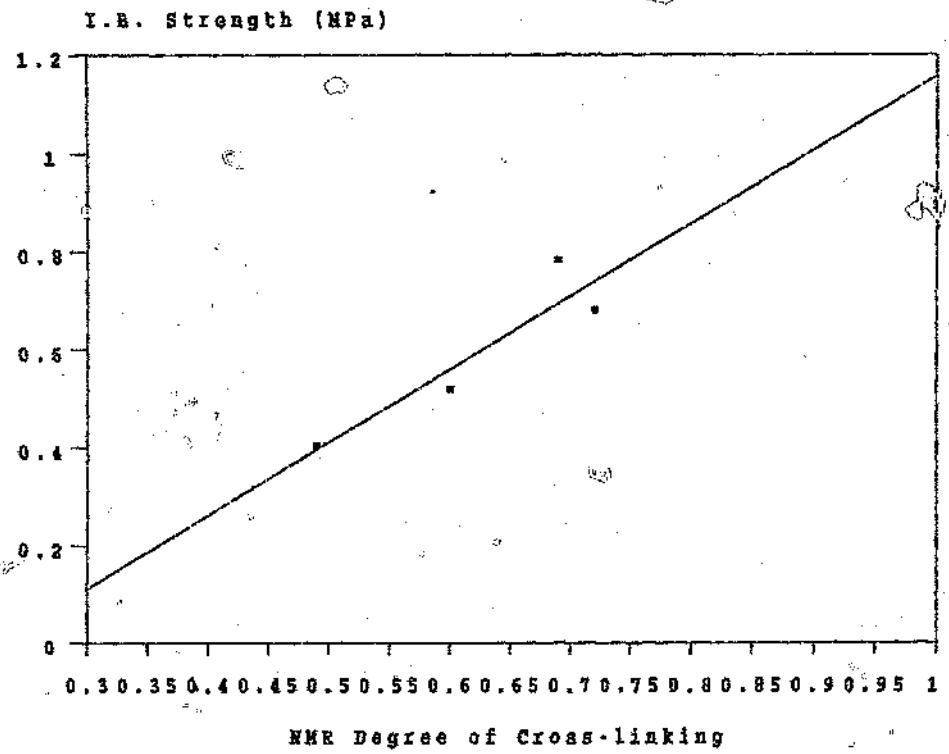

Figure 16d. Relating the degree of cross-linking to the I.B. Strength of the B series modified resins.

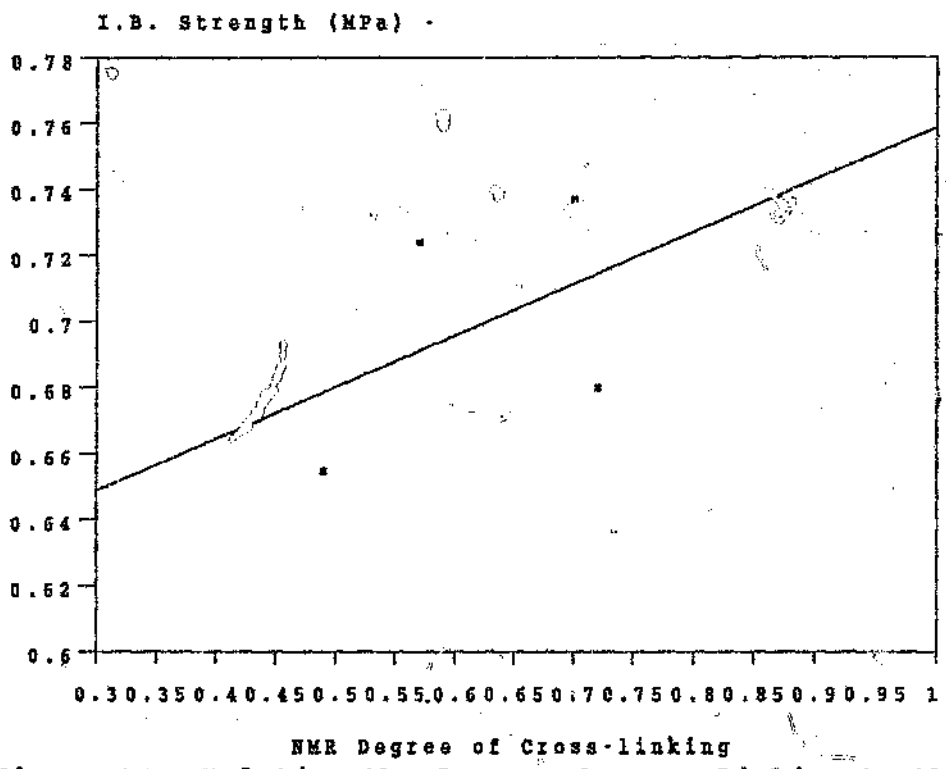

Figure 16e. Relating the degree of cross-linking to the I.B. strength of the boards for the A series resins.

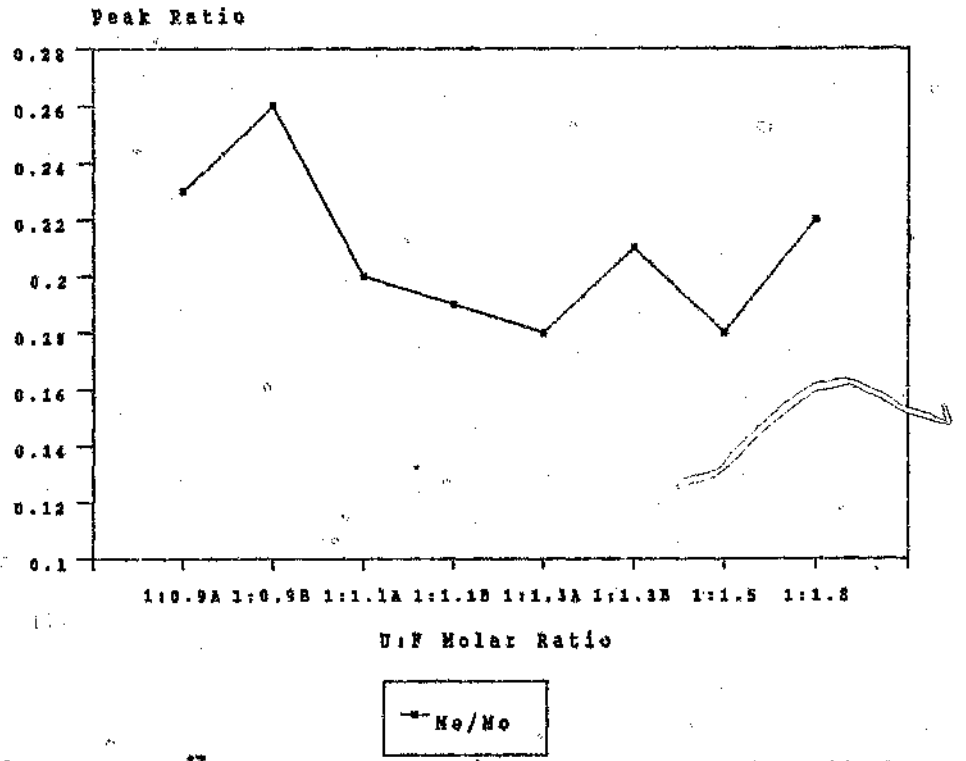

Figure 17. ^{13}C NMR peak ratio for the total methylene species to the total methylol species in the resins.

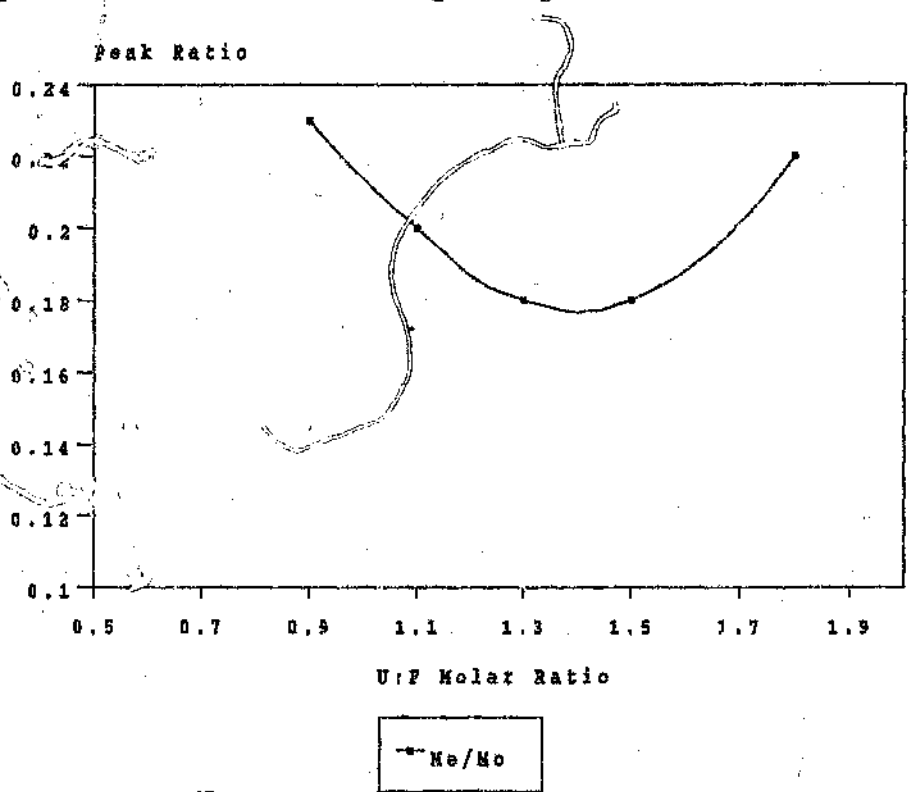

Figure 17a. ^{13}C NMR peak ratio for the total methylene species to the total methylol species in the A series resins.

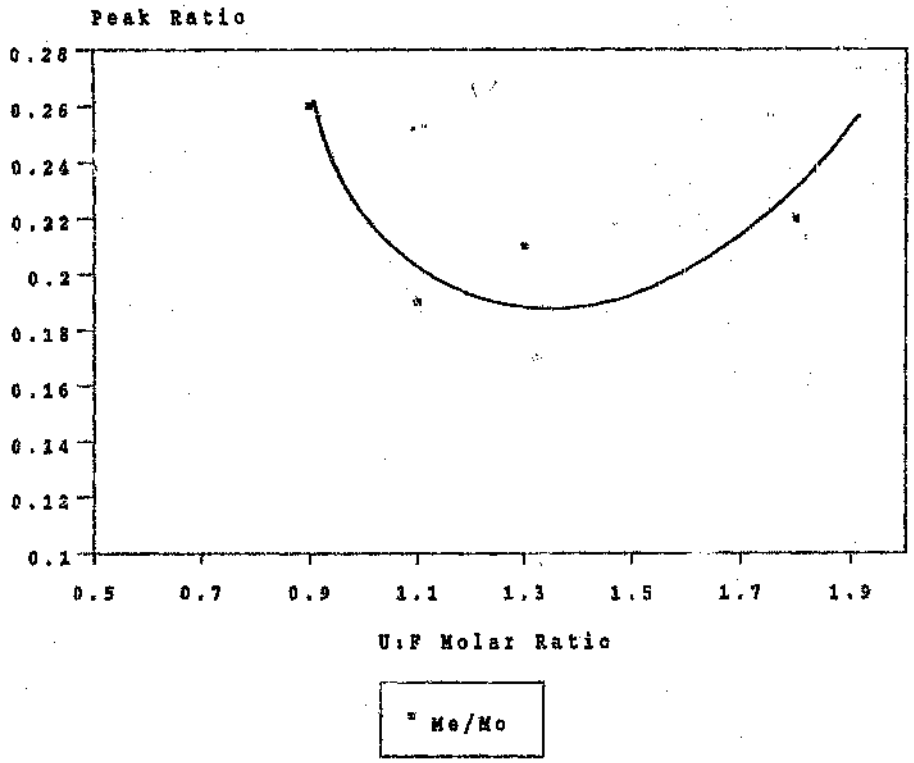

Figure 17b. 13C NMR peak ratio for the total methylene species to the total methylol species in the B series resins.

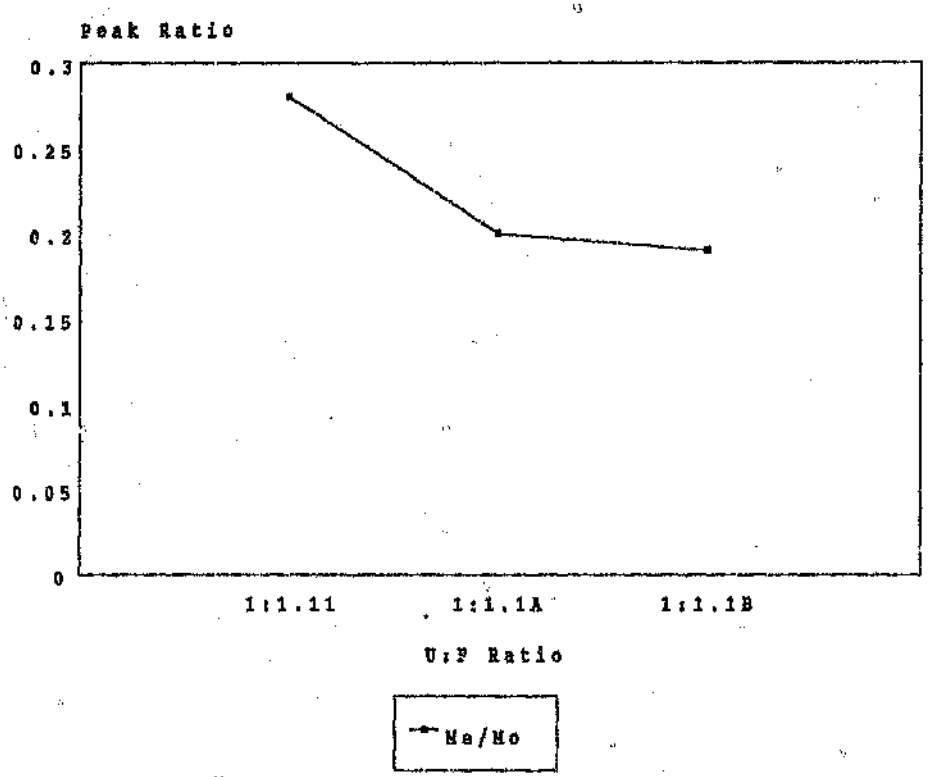

Figure 17c. ^{13}C NMR peak ratio for the total methylene species to the total methylol species in some resins.

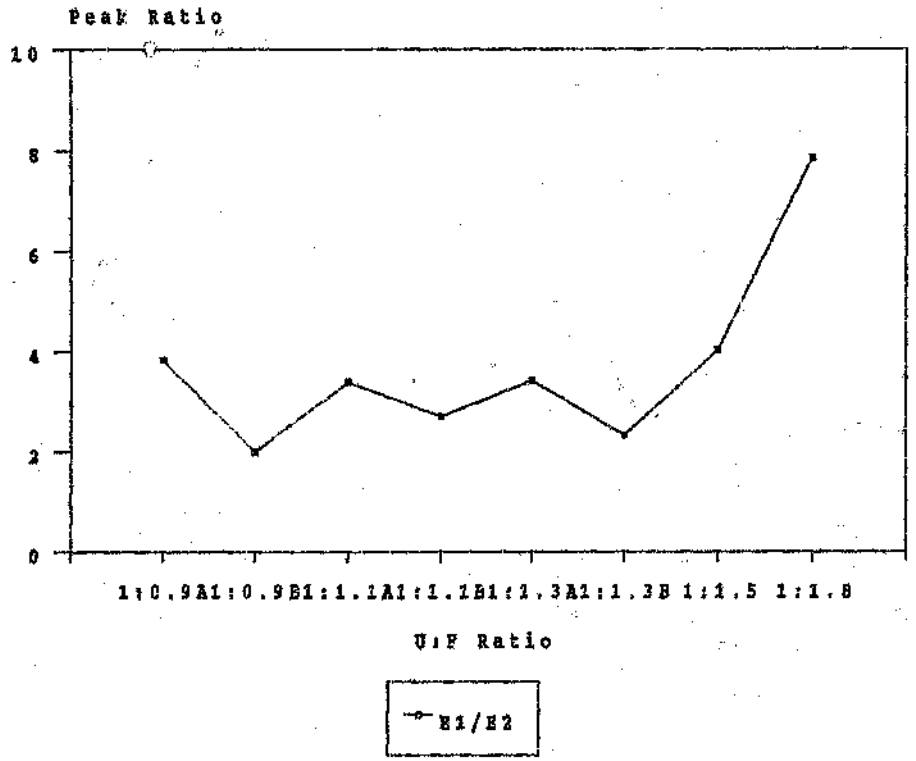

Figure 18. ^{13}C NMR peak ratio for the methylene ether species (E1/E2).

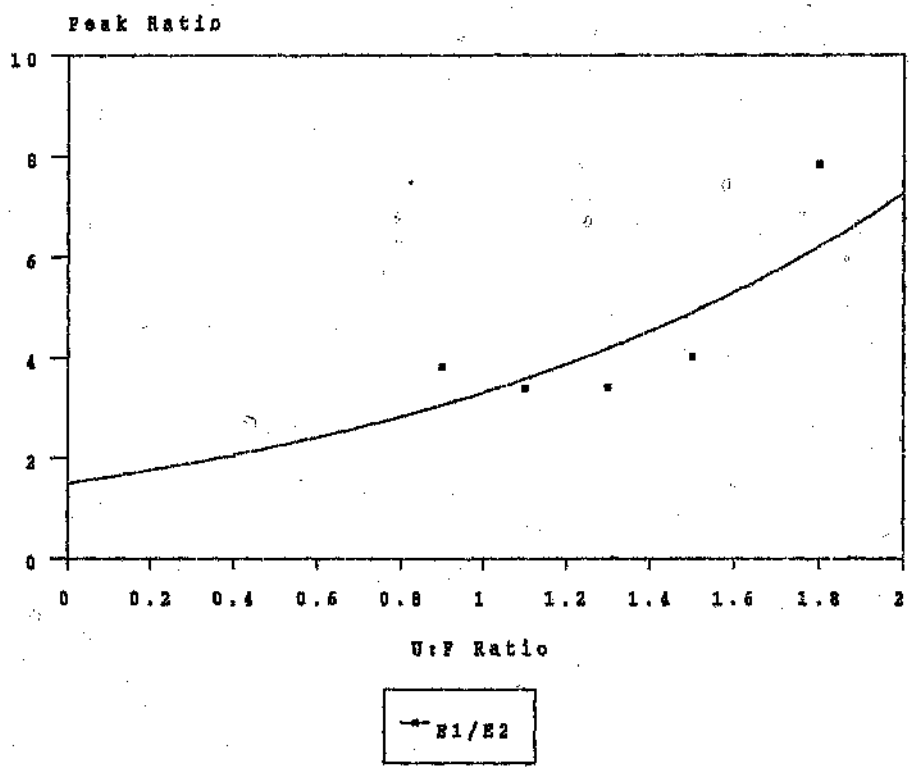

Figure 18a. NMR peak ratio for the methylene ether species (E1/E2) of the A series resins.

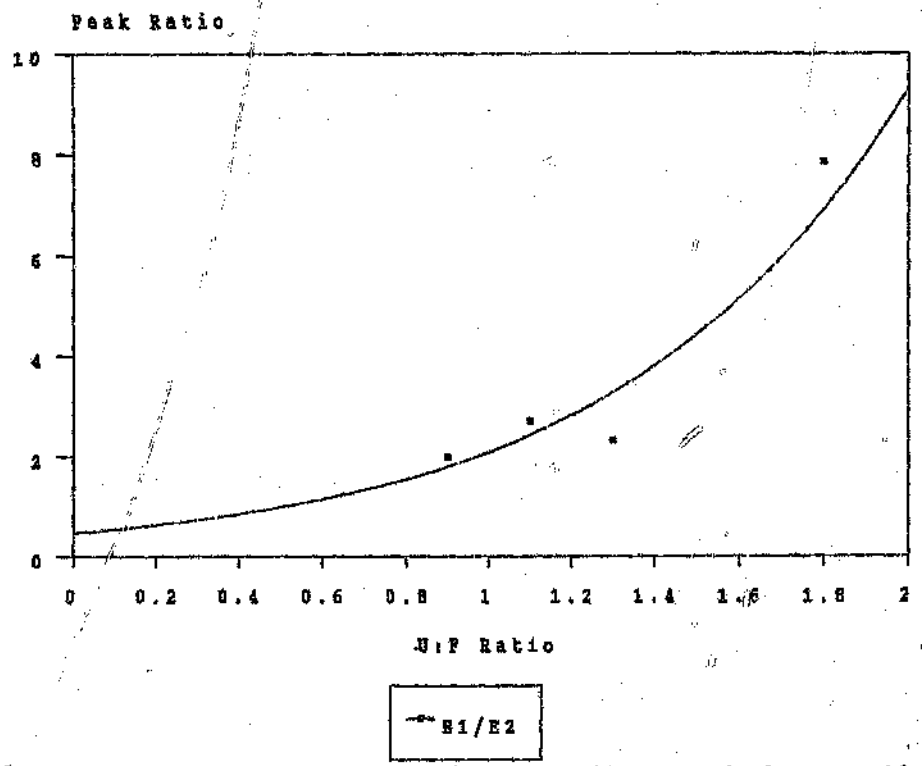

Figure 18b. NMR peak ratio for the methylene ether species (E1/E2) for the B series resins.

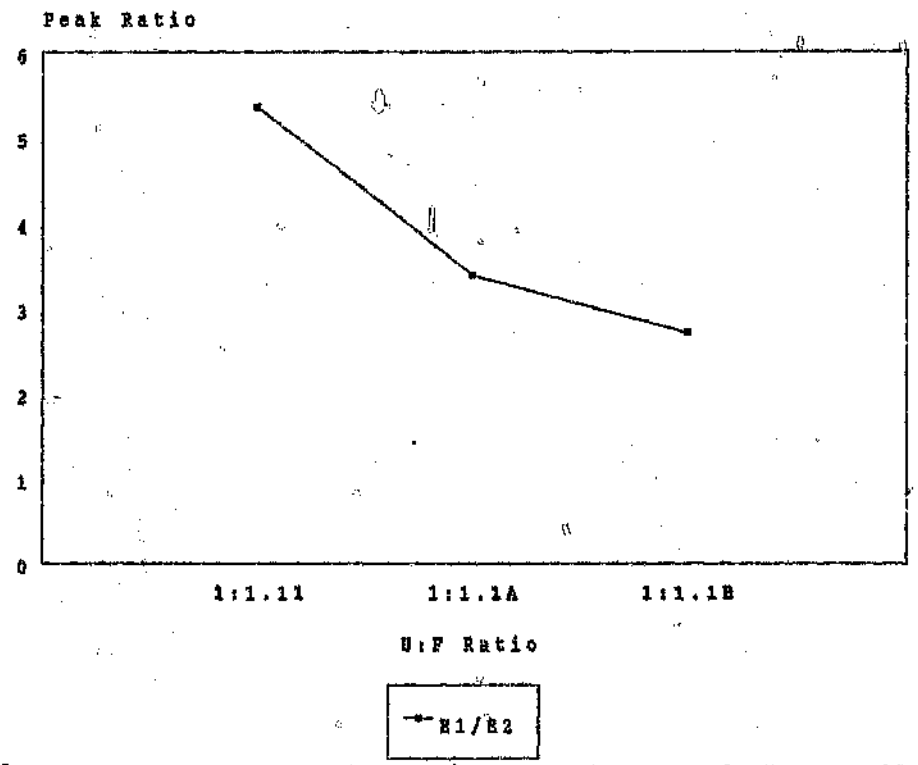

Figure 18c. NMR peak ratio for the methylene ether species (E1/E2).

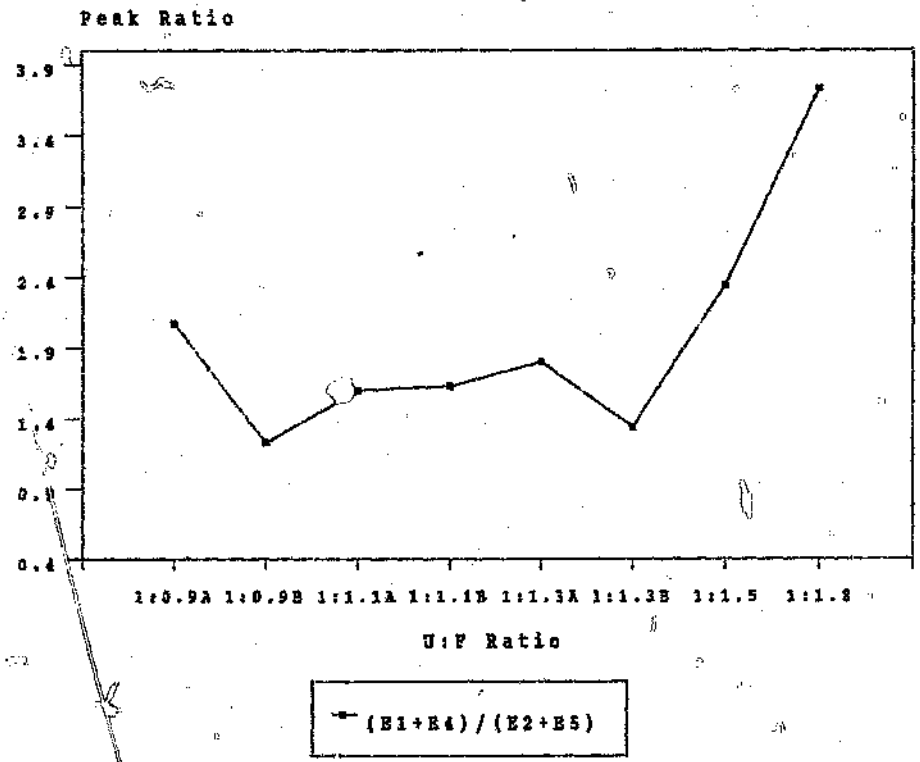

Figure 19. NMR peak ratio for some different ether species

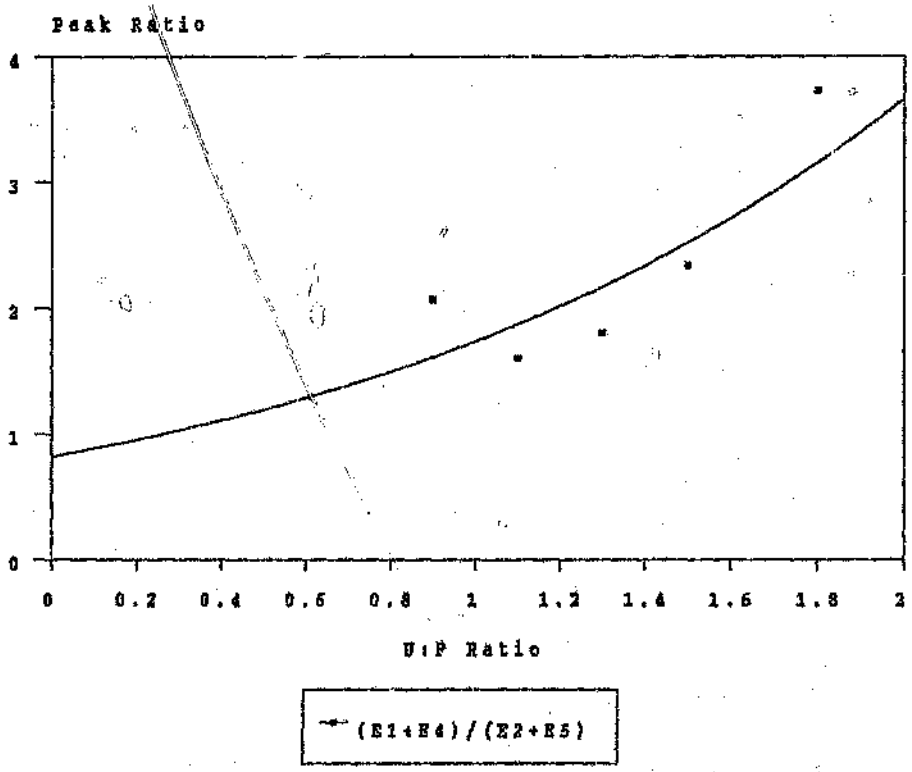

Figure 19a. NMR peak ratio for the different ether species for the A type resins.

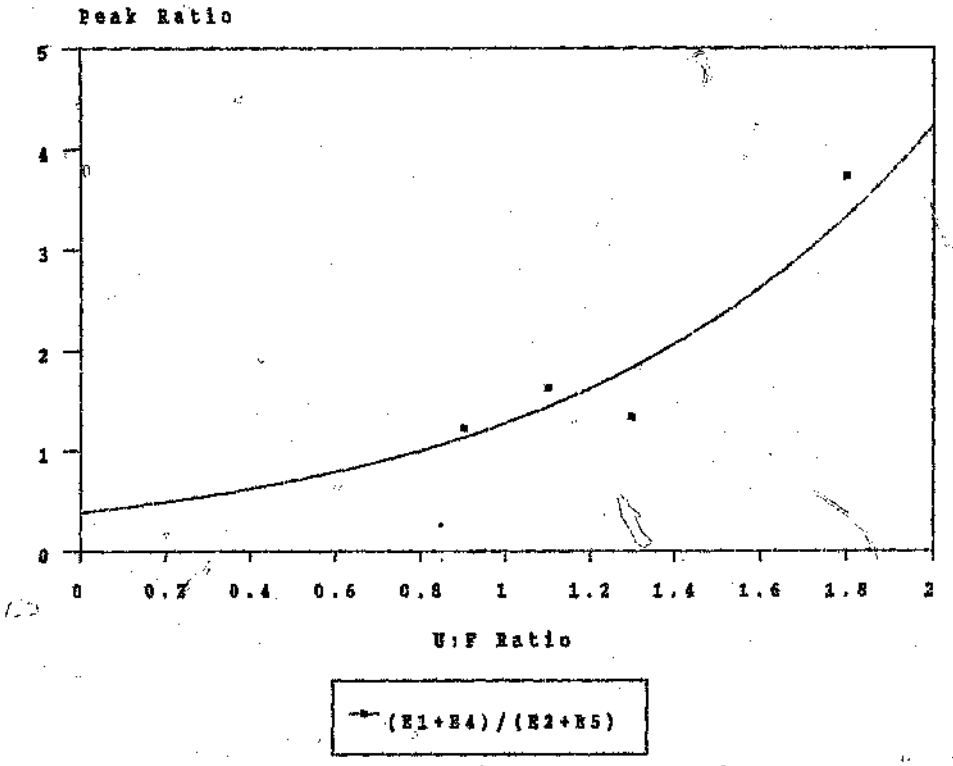

Figure 19b. NMR peak ratio for the different ether species for the B series resins.

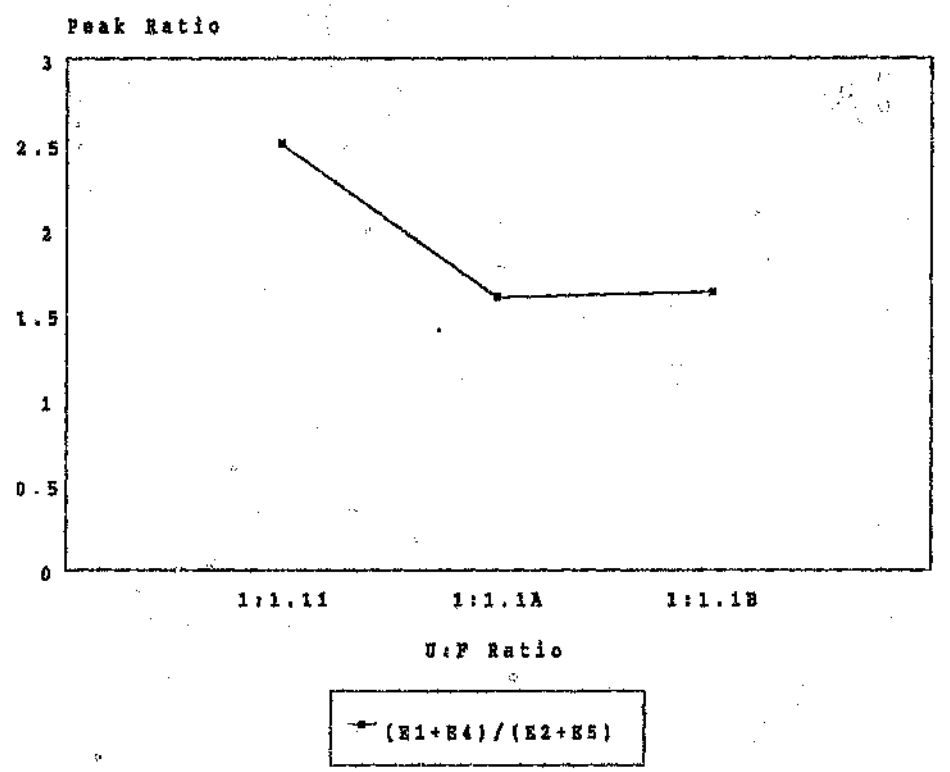

Figure 19c. NMR peak ratio for some different ether species.

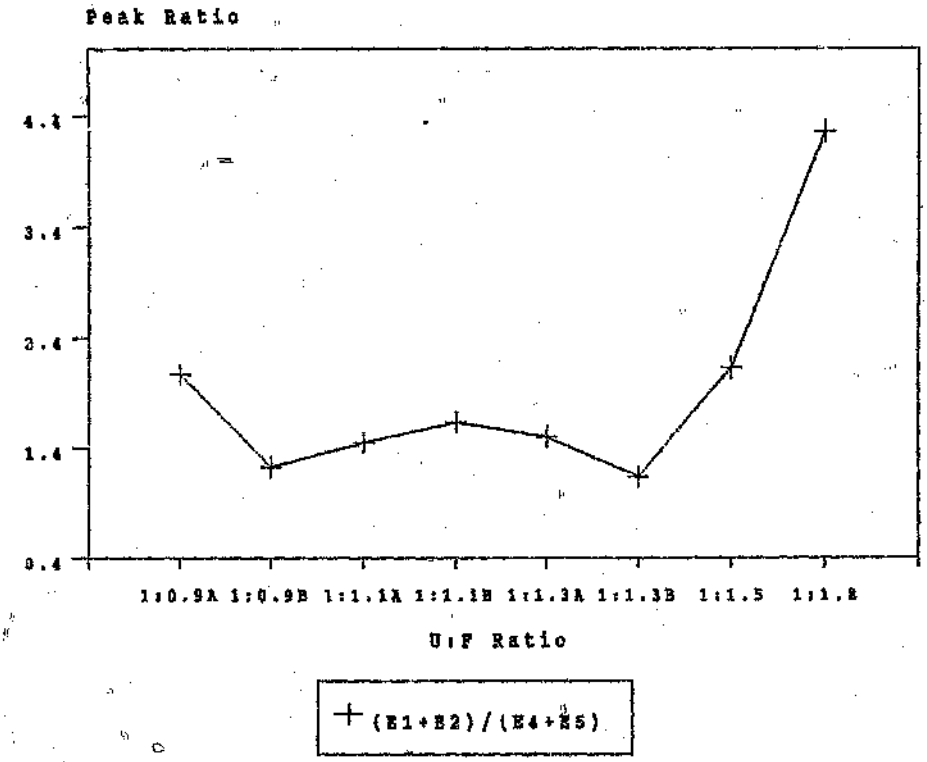

Figure 20. NMR peak ratio of different ether species

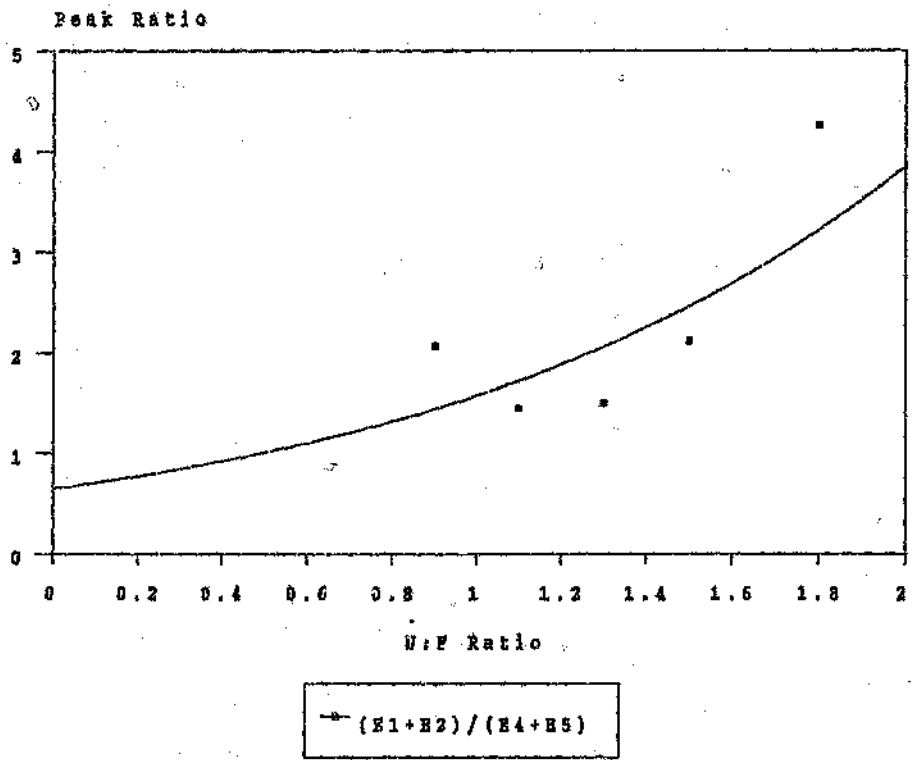

Figure 20a. NMR peak ratio for ether species for the A type resins.

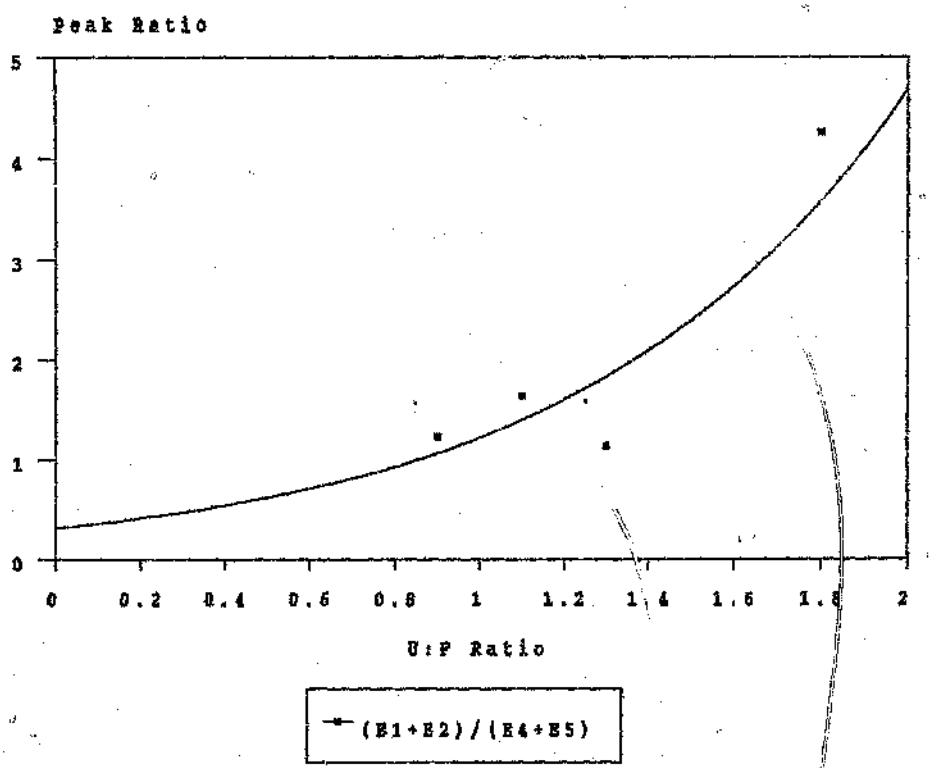

Figure 20b. NMR peak ratio for ether species for the B type resins.

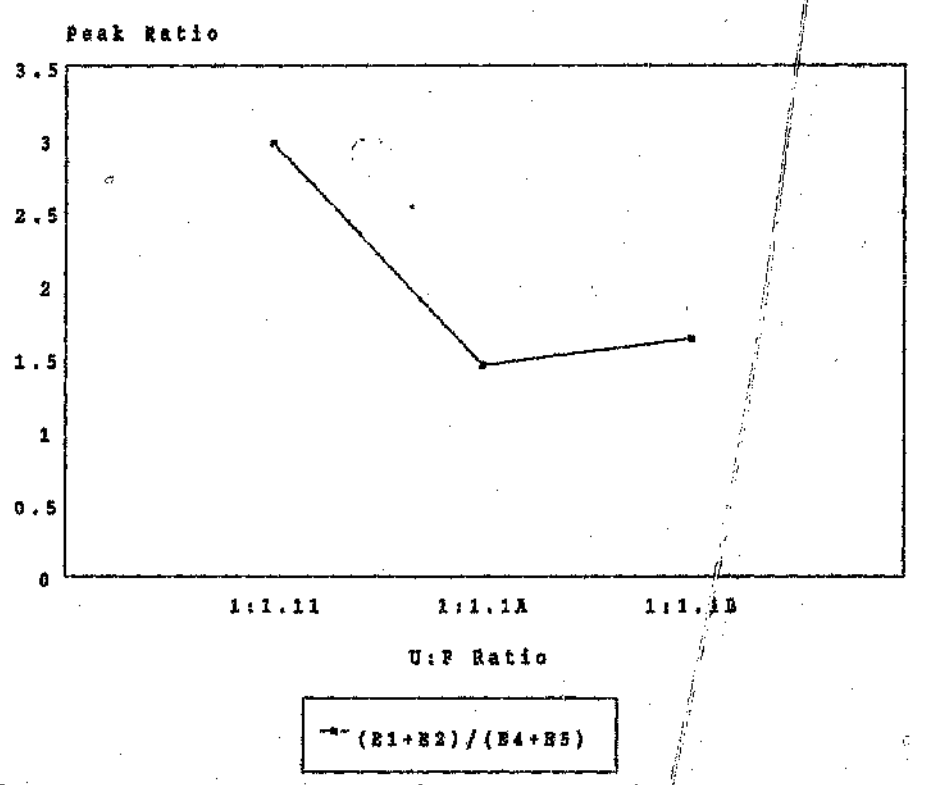

Figure 20c. NMR peak ratio for the different ethers.

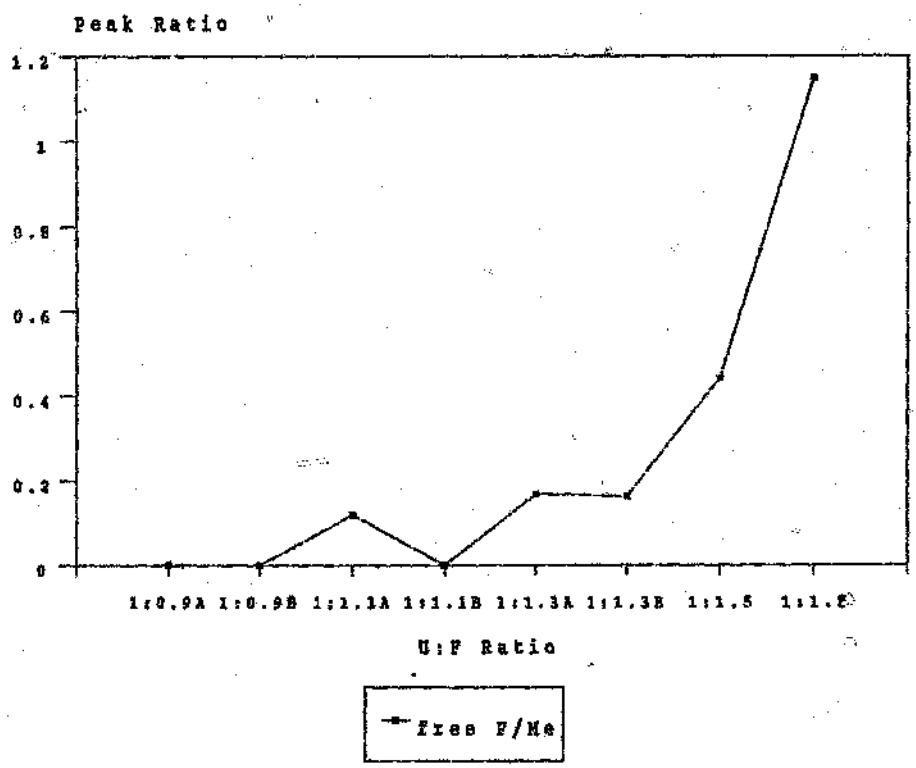

Figure 21. NMR peak ratio of free formaldehyde to the total methylene species for the modified resins.

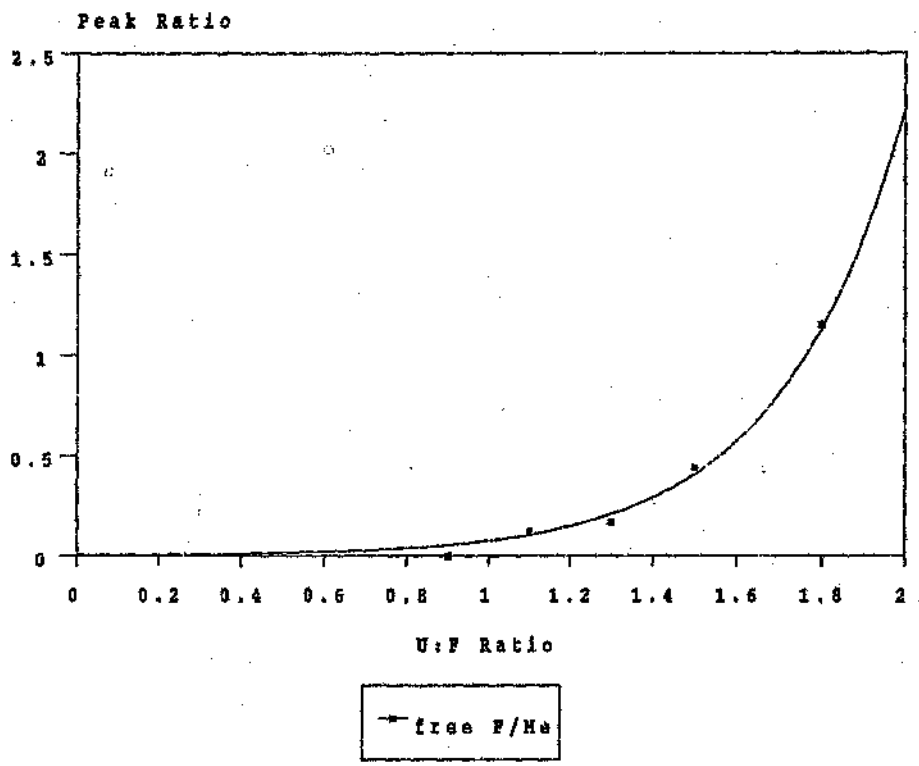

Figure 21a. NMR peak ratio of free formaldehyde to the totla methylene species for the A series resins.

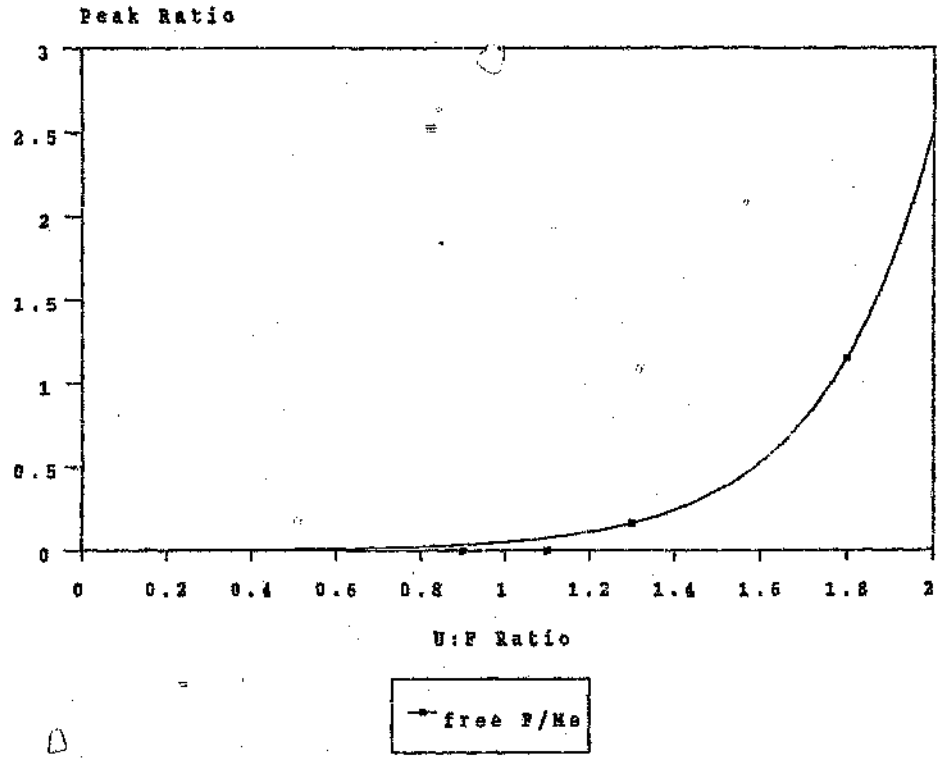

Figure 21b. NMR peak ratio of free formaldehyde to the total methylene species for the B series resins.

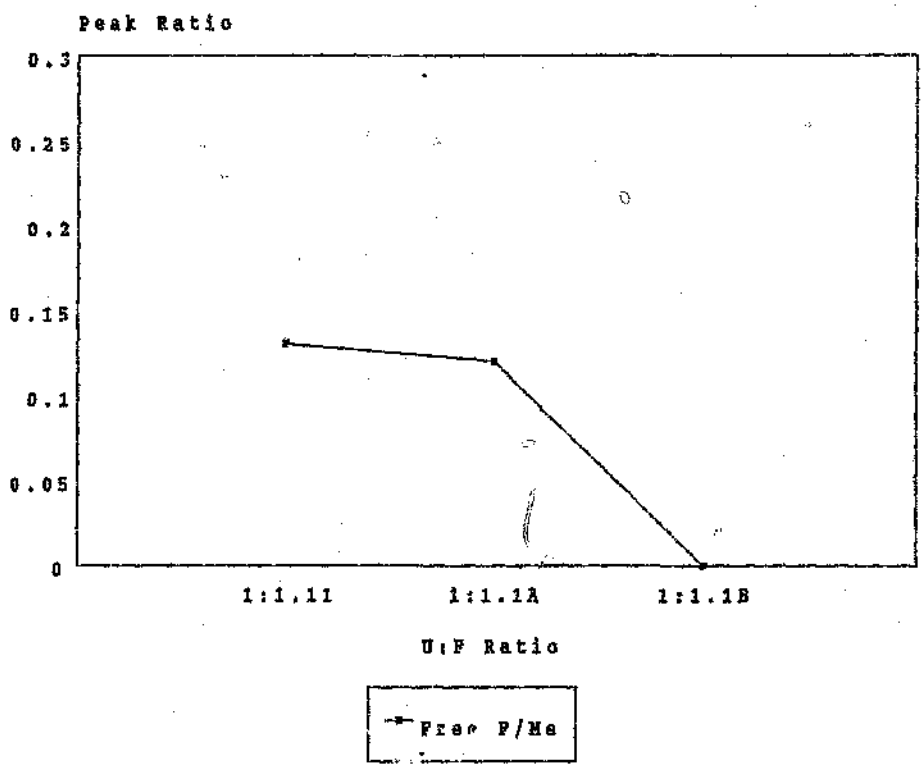

Figure 21c. NMR peak ratio of free formaldehyde to the total methylene species for some of the modified resins.

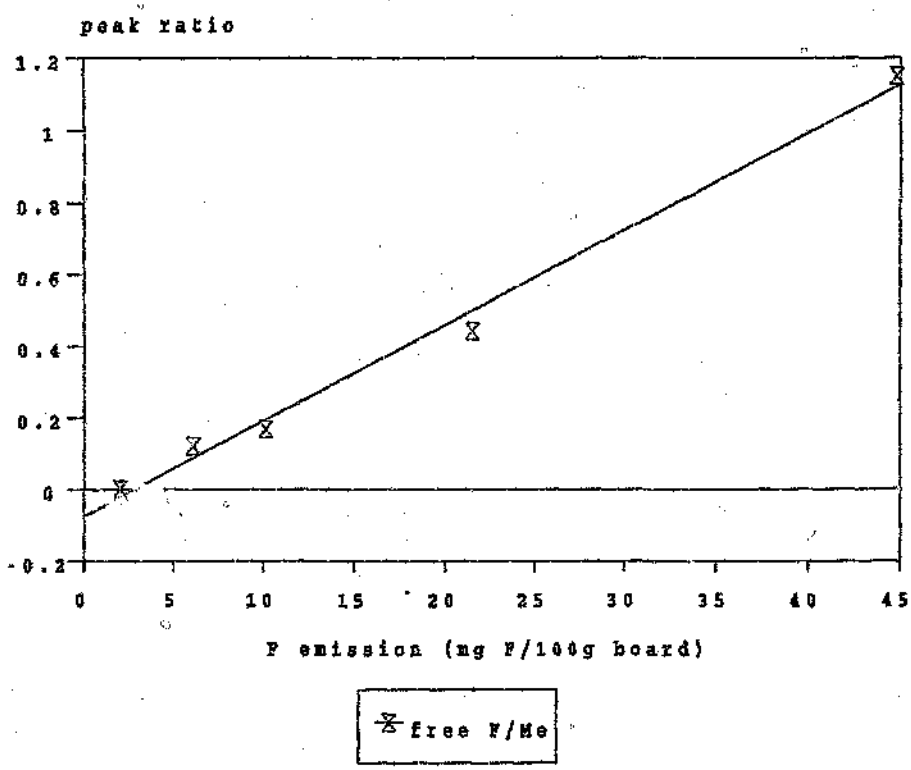

Figure 22. Relating the NMR species ratio of free F/Me to the formaldehyde emission from boards made with the A series resins.

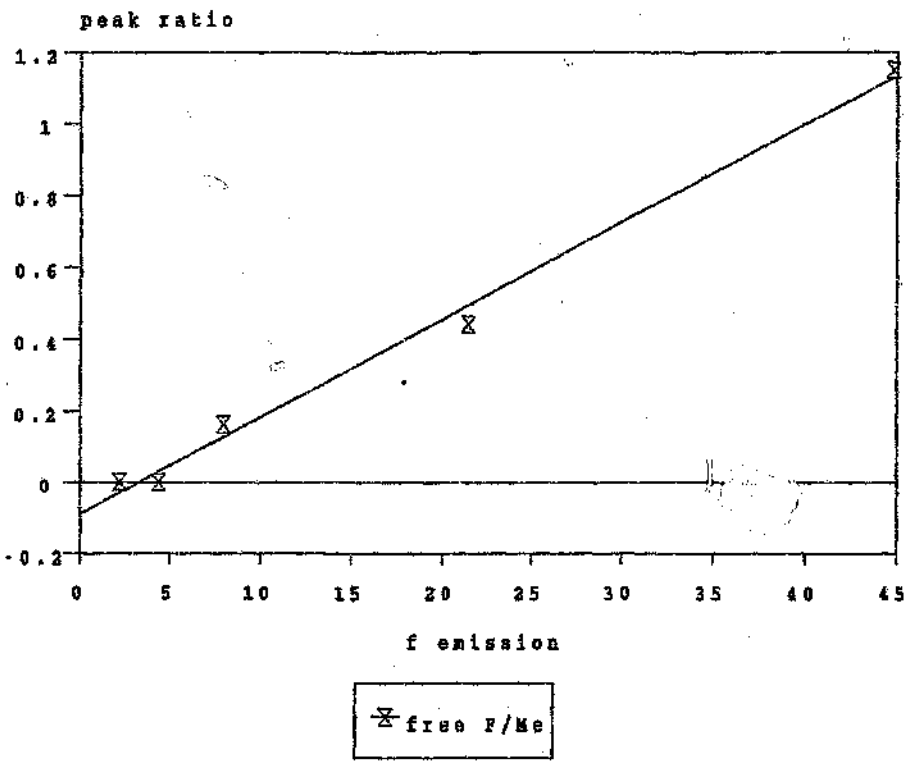

Figure 23. Relating the NMR species ratio of free F/Me to the formaldehyde emission from boards made with the B series resins.

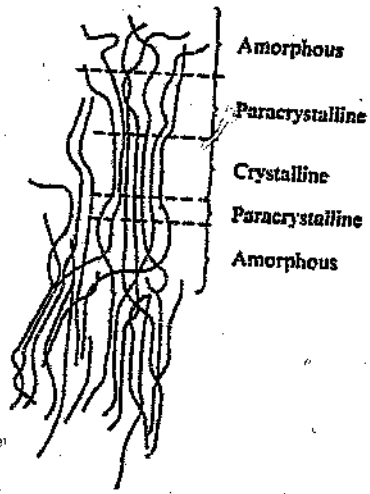

Figure 24. Semi-crystalline region part of the amorphous bulk.

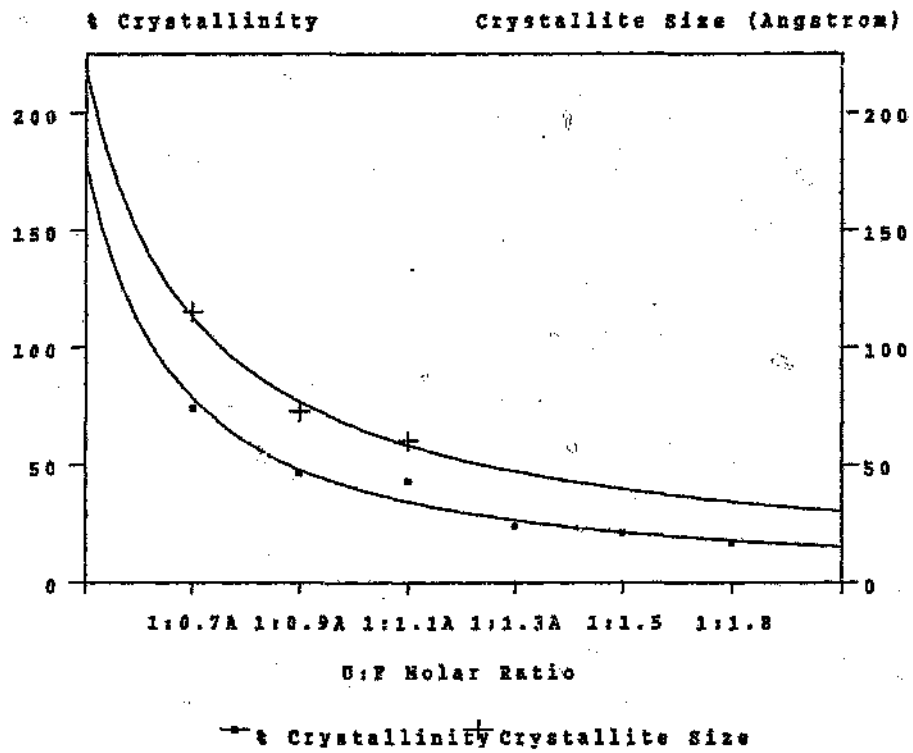

Figure 25a. % crystallinity and crystallite size for some of the resins cured with 3% NH_4Cl.

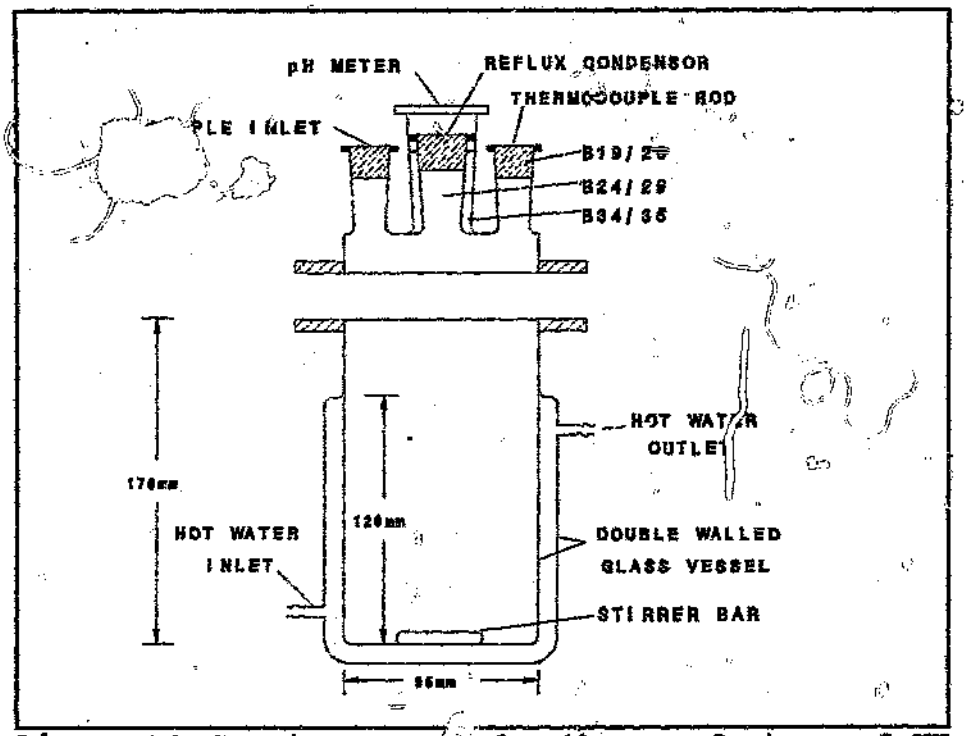

Figure 26. Reactor vessel for the manufacture of UF resins.

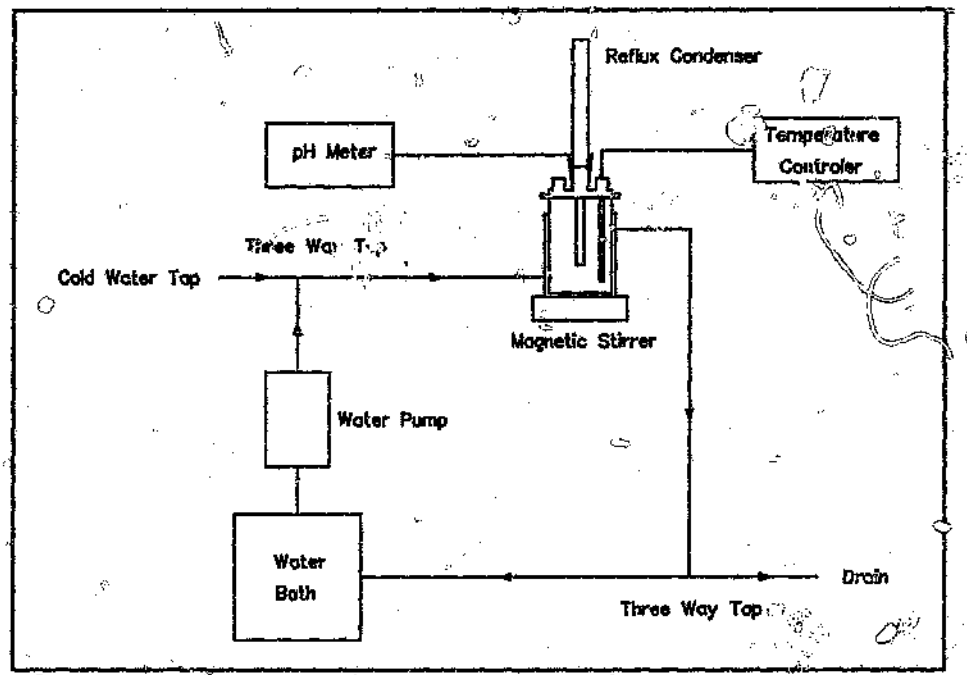

Figure 27. Schematic representation of the reactor setup.

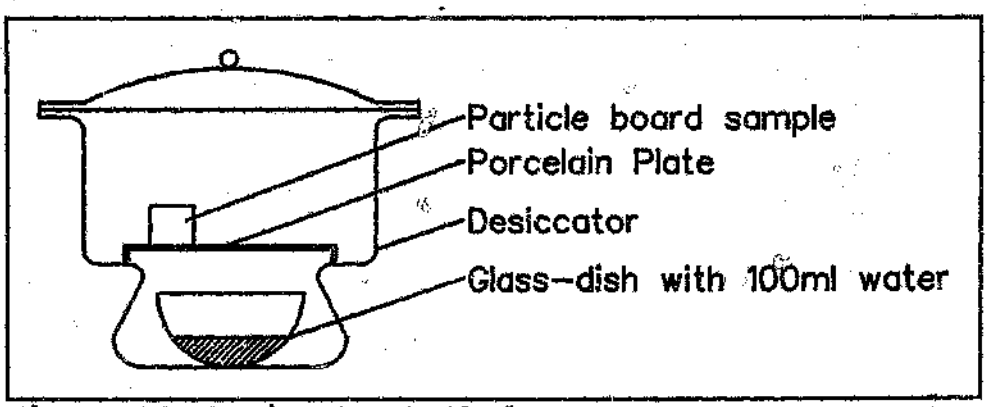

Figure 28. Desiccator Method.

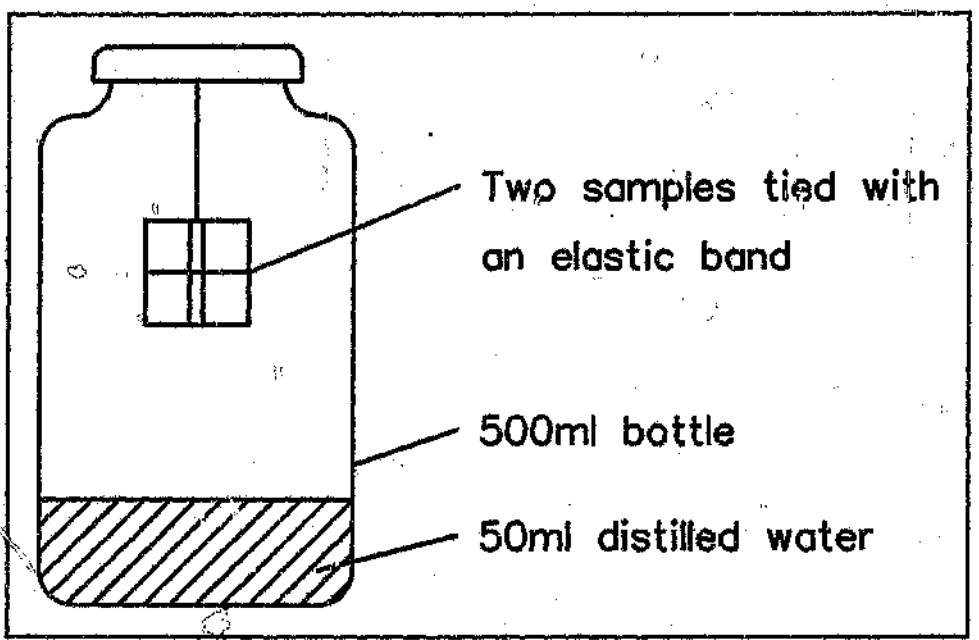

Figure 29. WKI method according to Roffael [55]

Spectra. Spectra of liquid and cured UF resins.

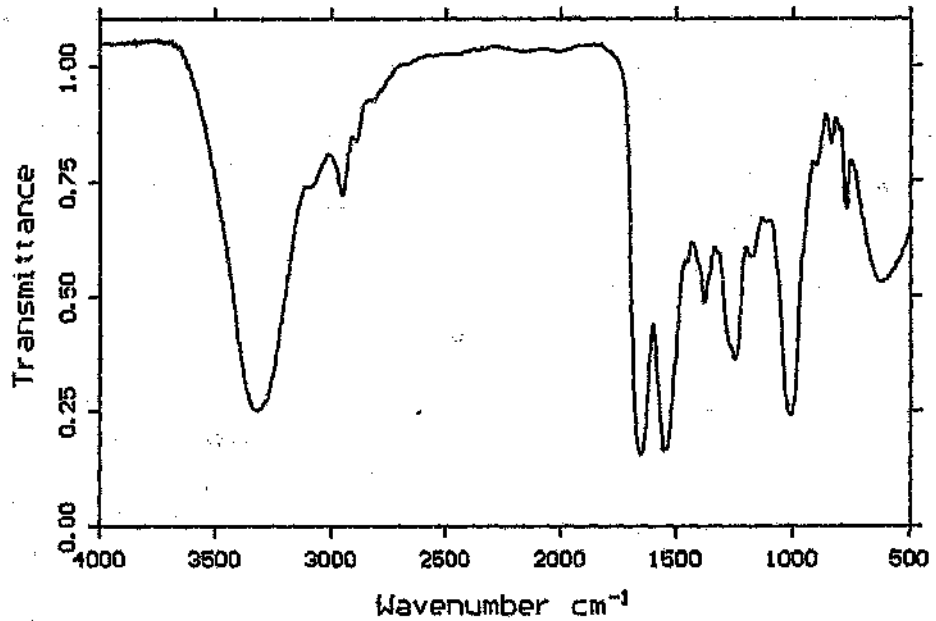

Spectrum 1. 1:1.8 UF Resin

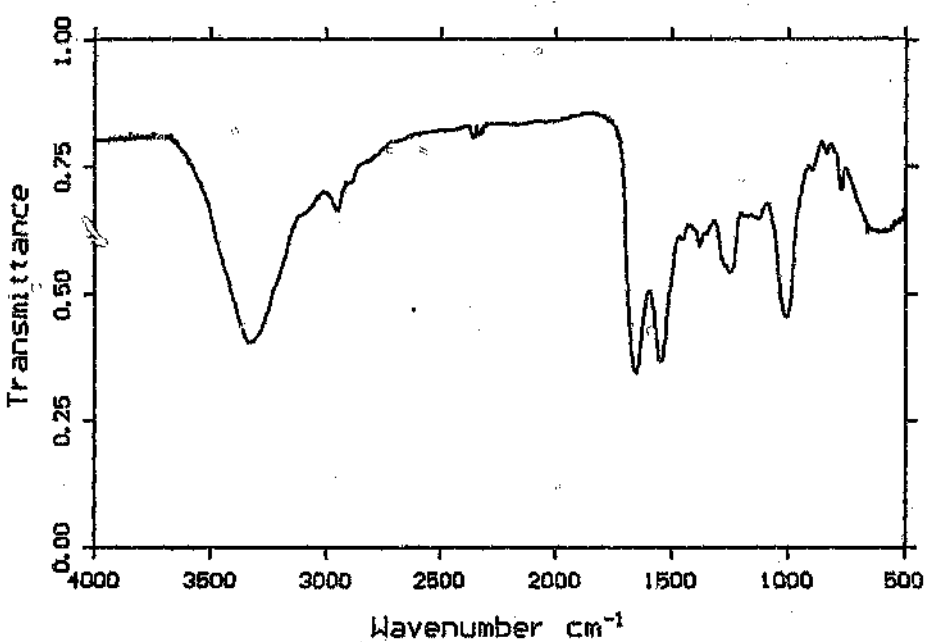

Spectrum 2. 1:1.5 UF Resin

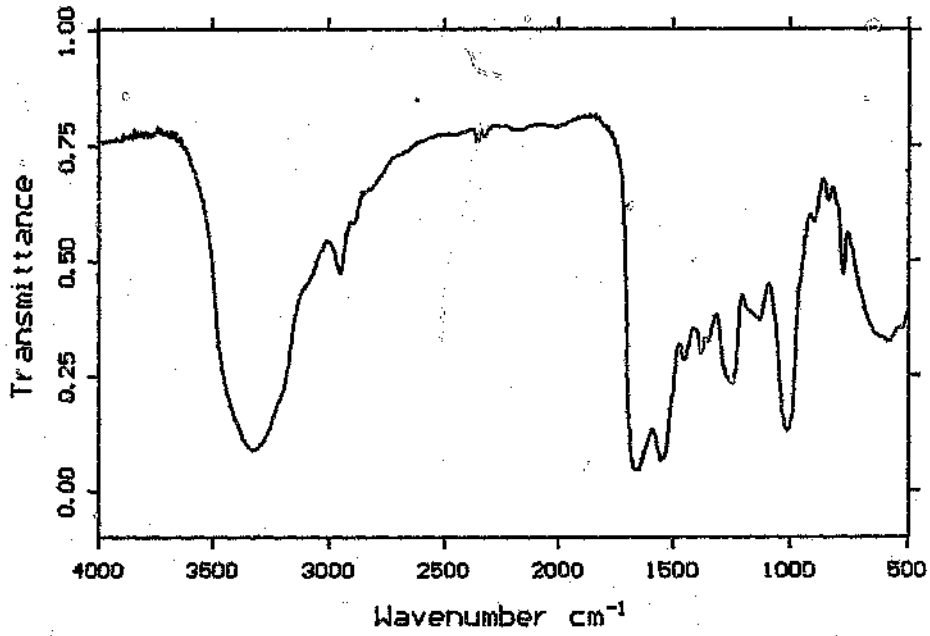

Spectrum 3. 1:1.3A UF Resin

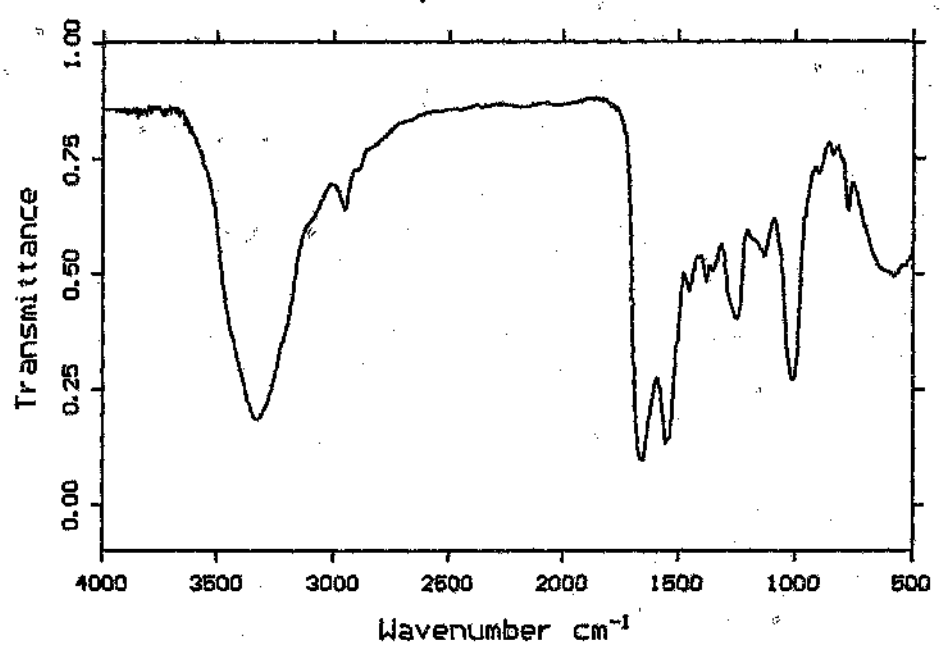

Spectrum 4. 1:1.3B UF Resin

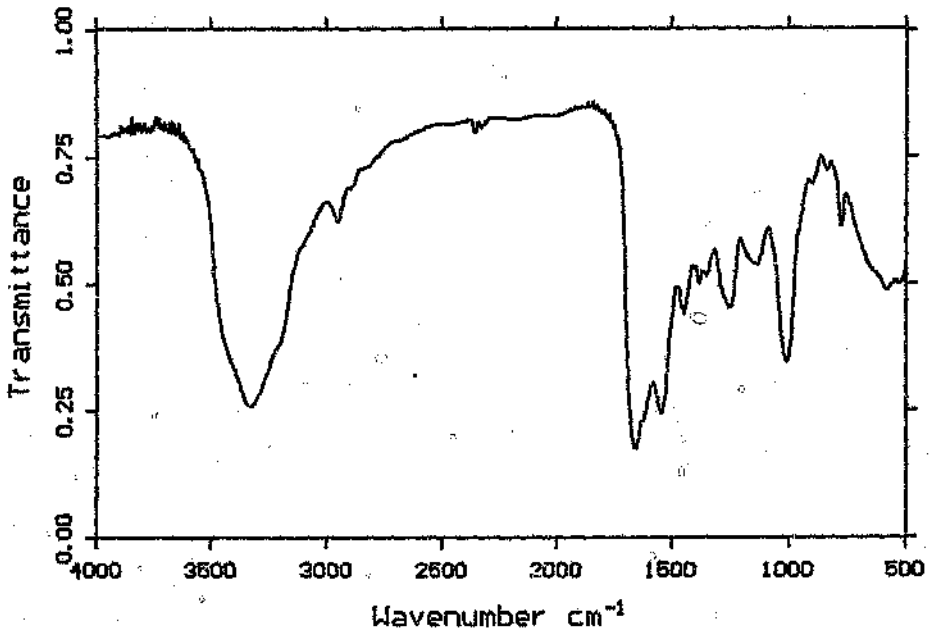

Spectrum 5. 1:1.1A UF Resin

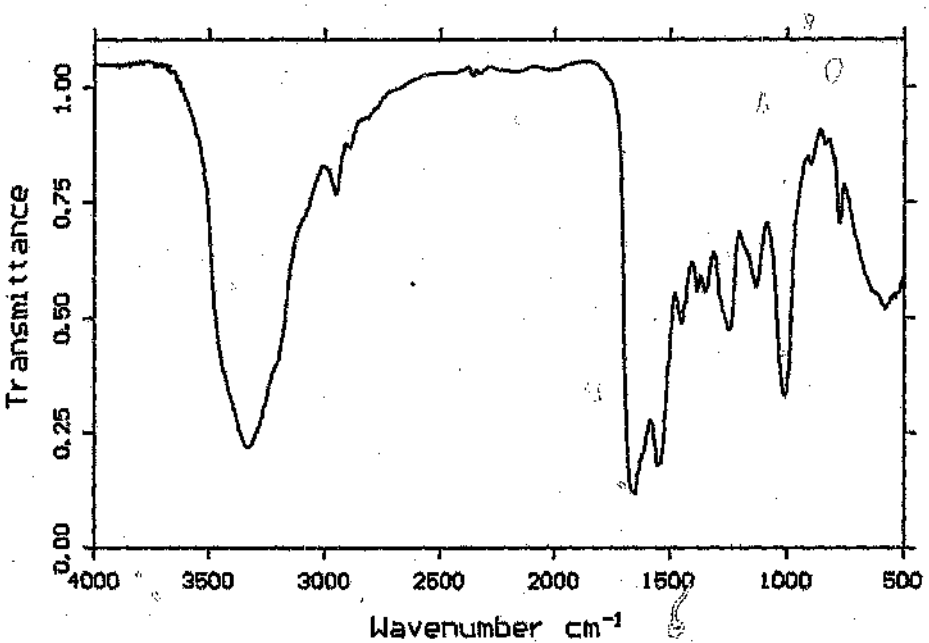

Spectrum 6. 1:1.1B UF Resin

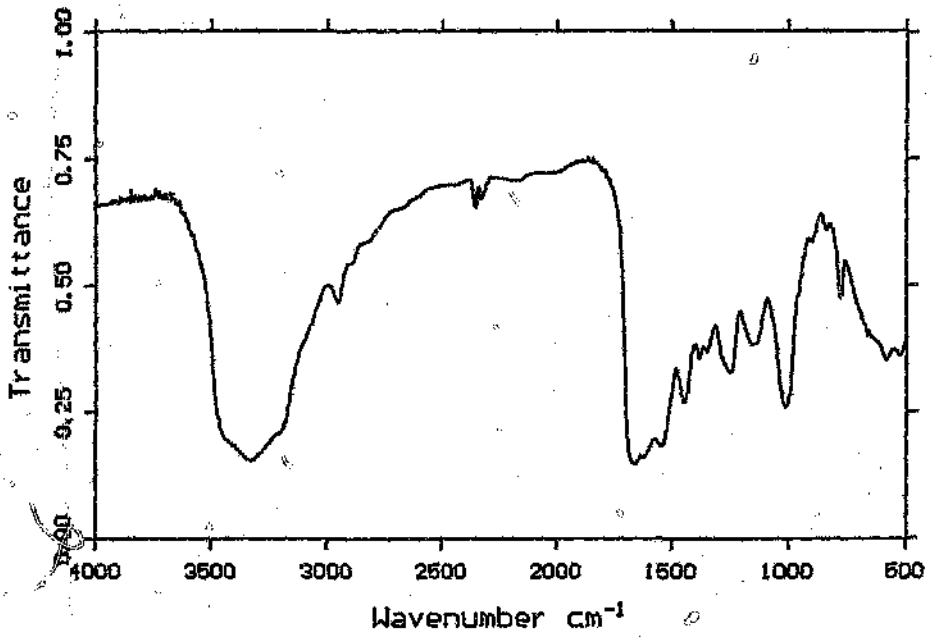

Spectrum 7. 1:0.9A UF Resin

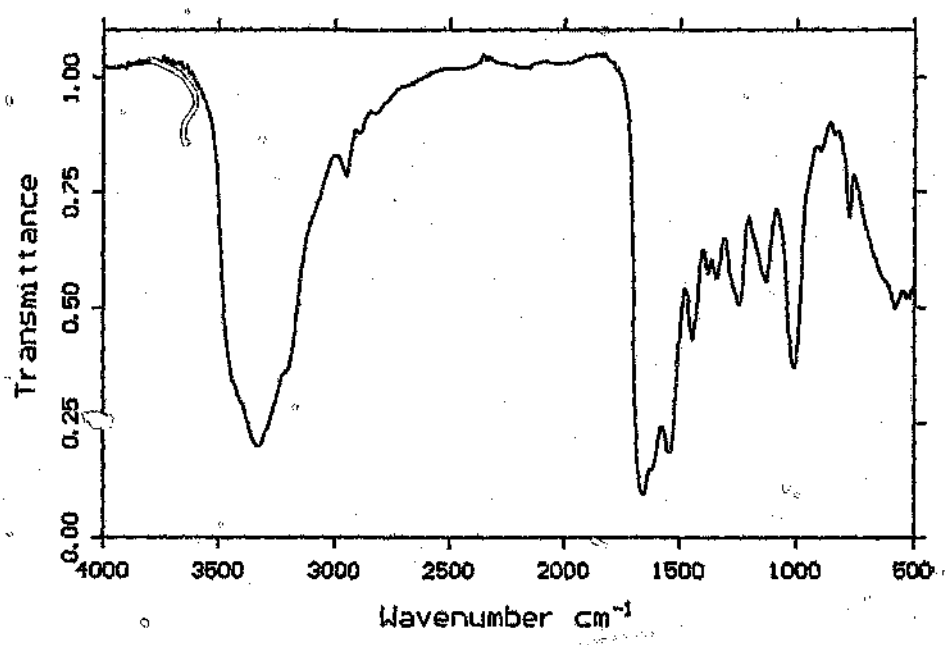

Spectrum 8. 1:0.9B UF Resin

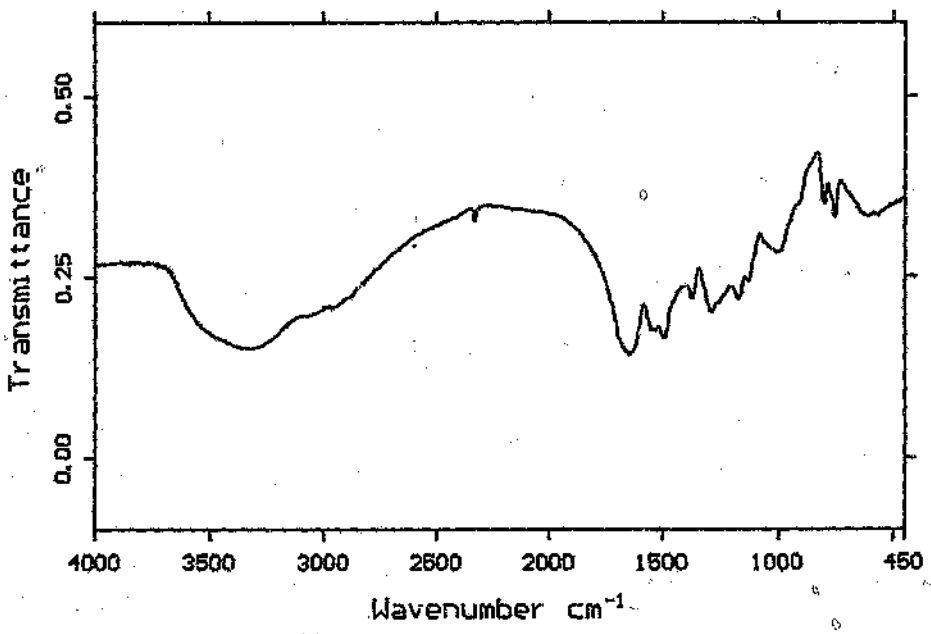

Spectrum 9. 1:1.8 UF Resin cured with 3% NH_4Cl

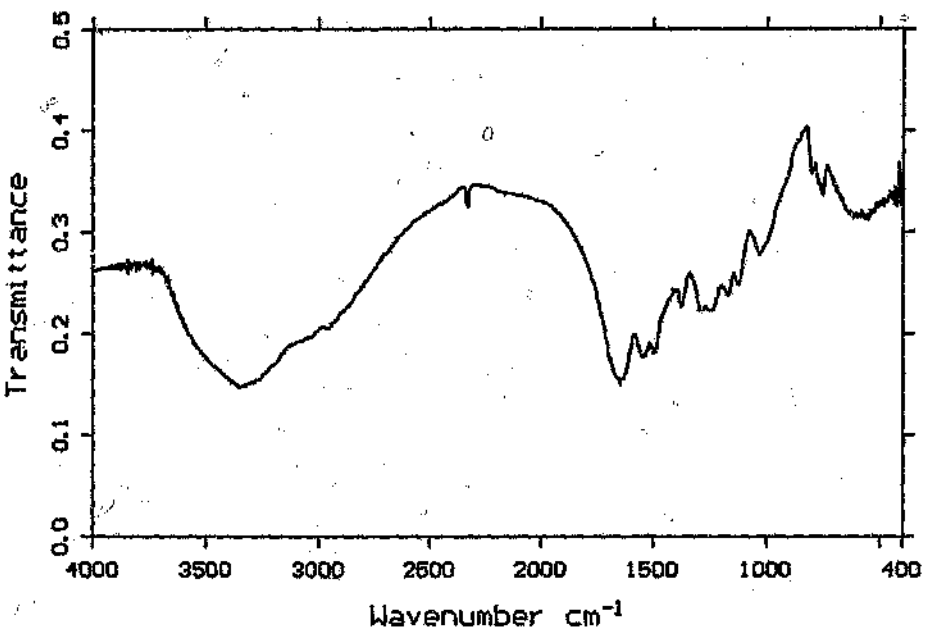

Spectrum 10. 1:1.5 UF Resin cured with 3% NH_4Cl

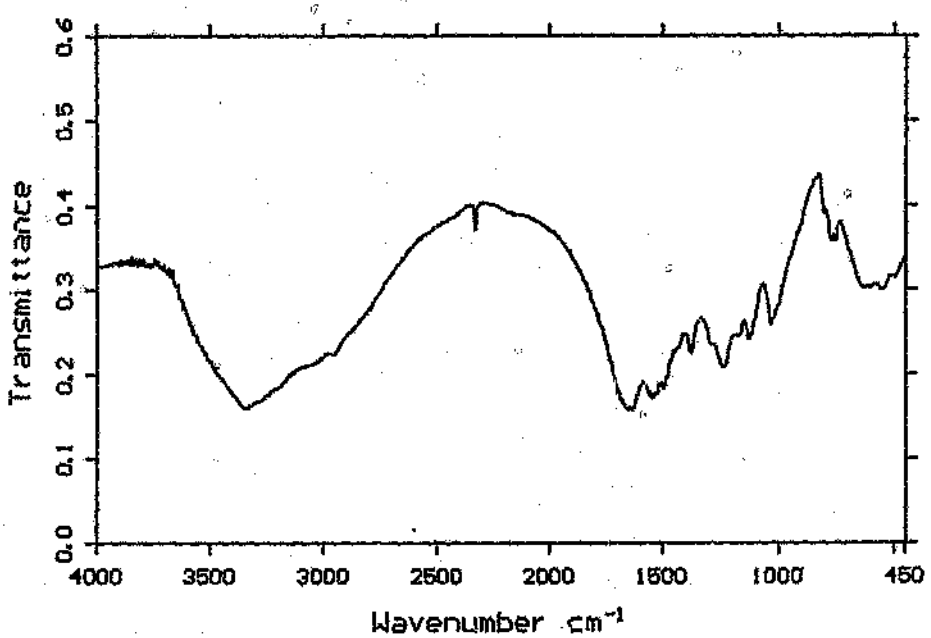

Spectrum 11. 1:1.3A UF Resin cured with 3% NH_4Cl

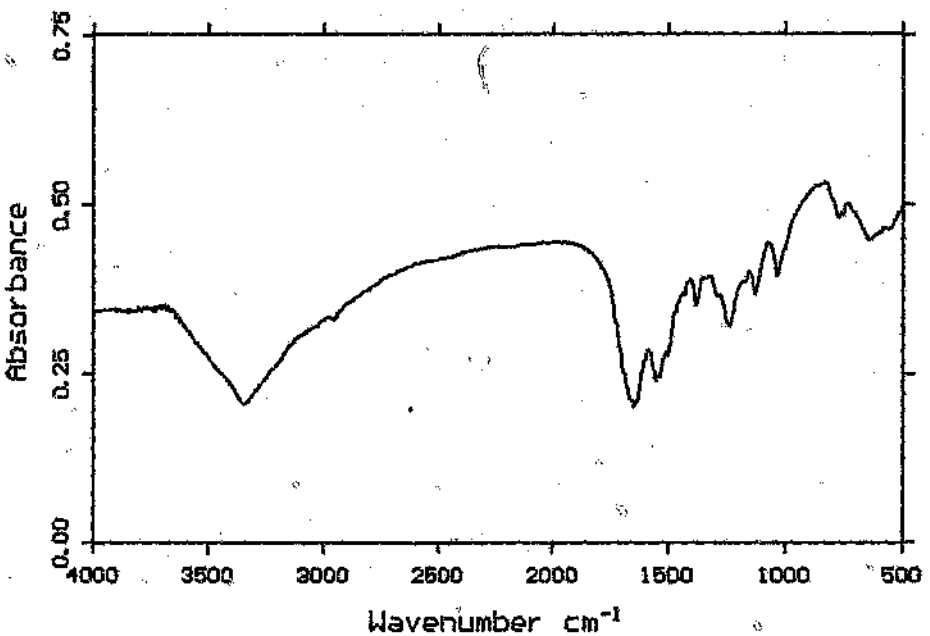

Spectrum 12. 1:1.3B UF Resin cured with 3% NH_4Cl

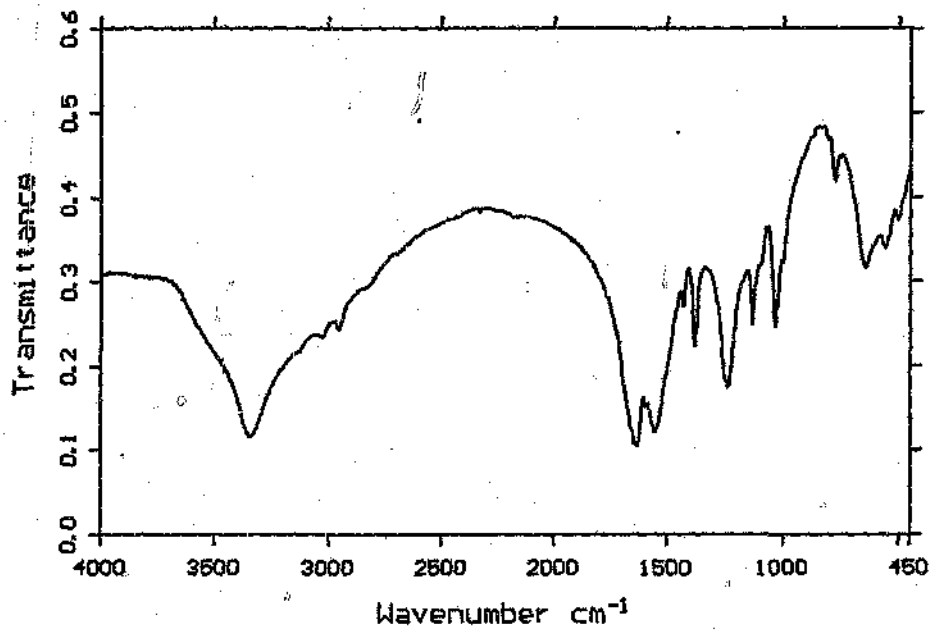

Spectrum 13. 1:1.1A UF Resin cured with 3% NH_4Cl

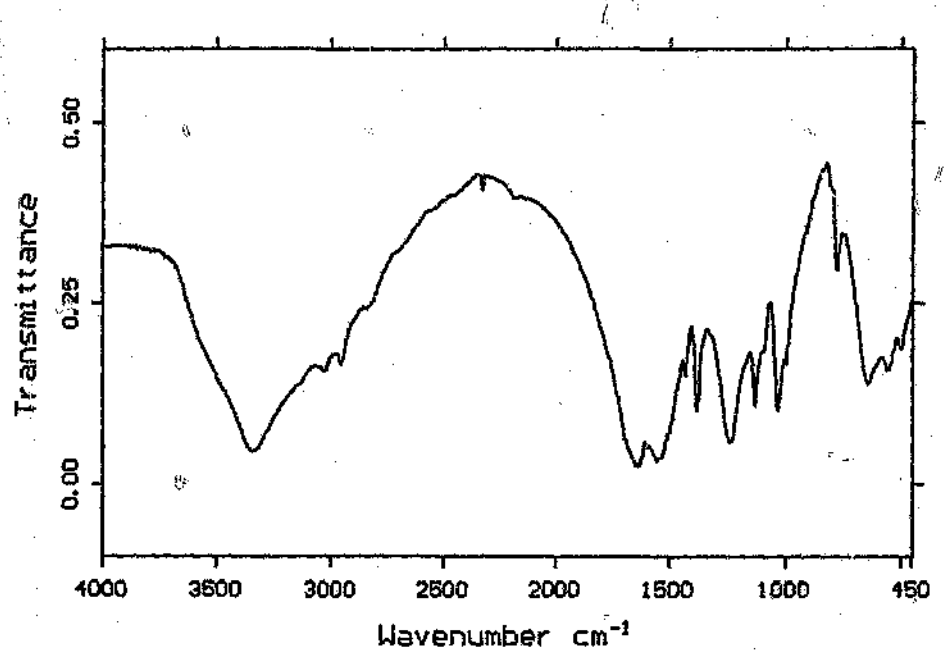

Spectrum 14. 1:1.1B UF Resin cured with 3% NH_4Cl

^{13}C NMI

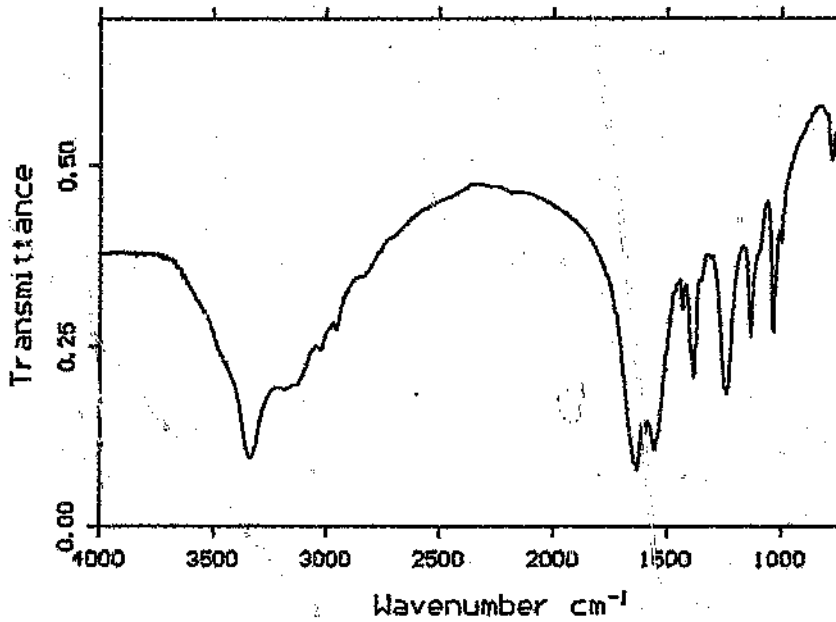

Spectrum 15. 1:0.9A UF Resin cured with 3% NH_4Cl

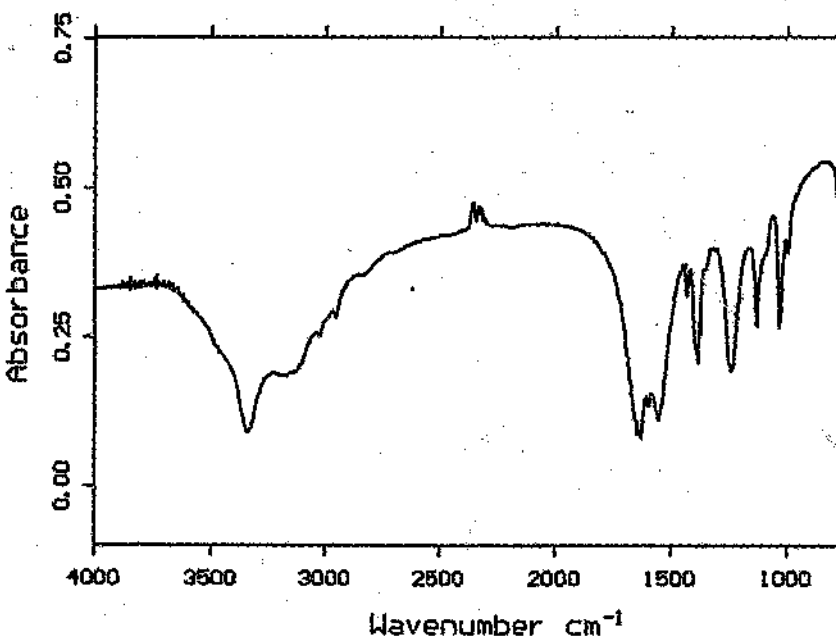

Spectrum 16. 1:0.9B UF Resin cured with 3% NH_4Cl

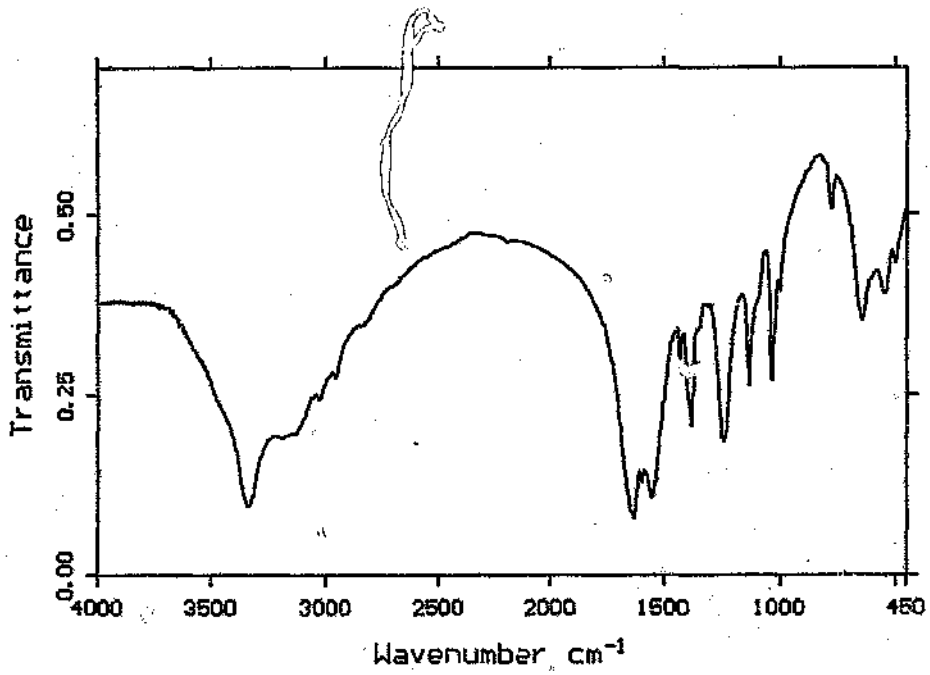

Spectrum 15. 1:0.9A UF Resin cured with 3% NH_4Cl

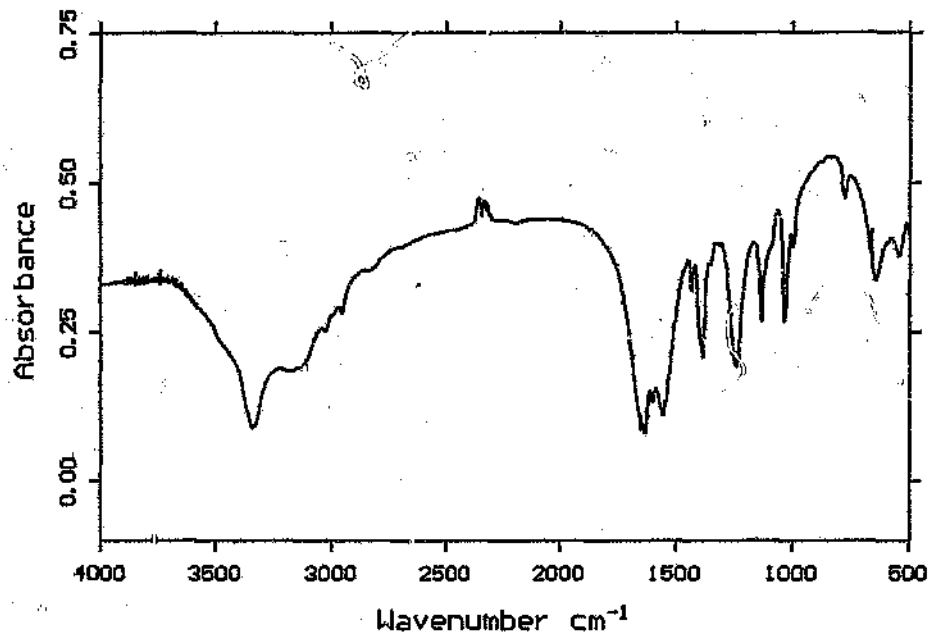

Spectrum 16. 1:0.9B UF Resin cured with 3% NH_4Cl

^{13}C NMR spectra of the liquid resins.

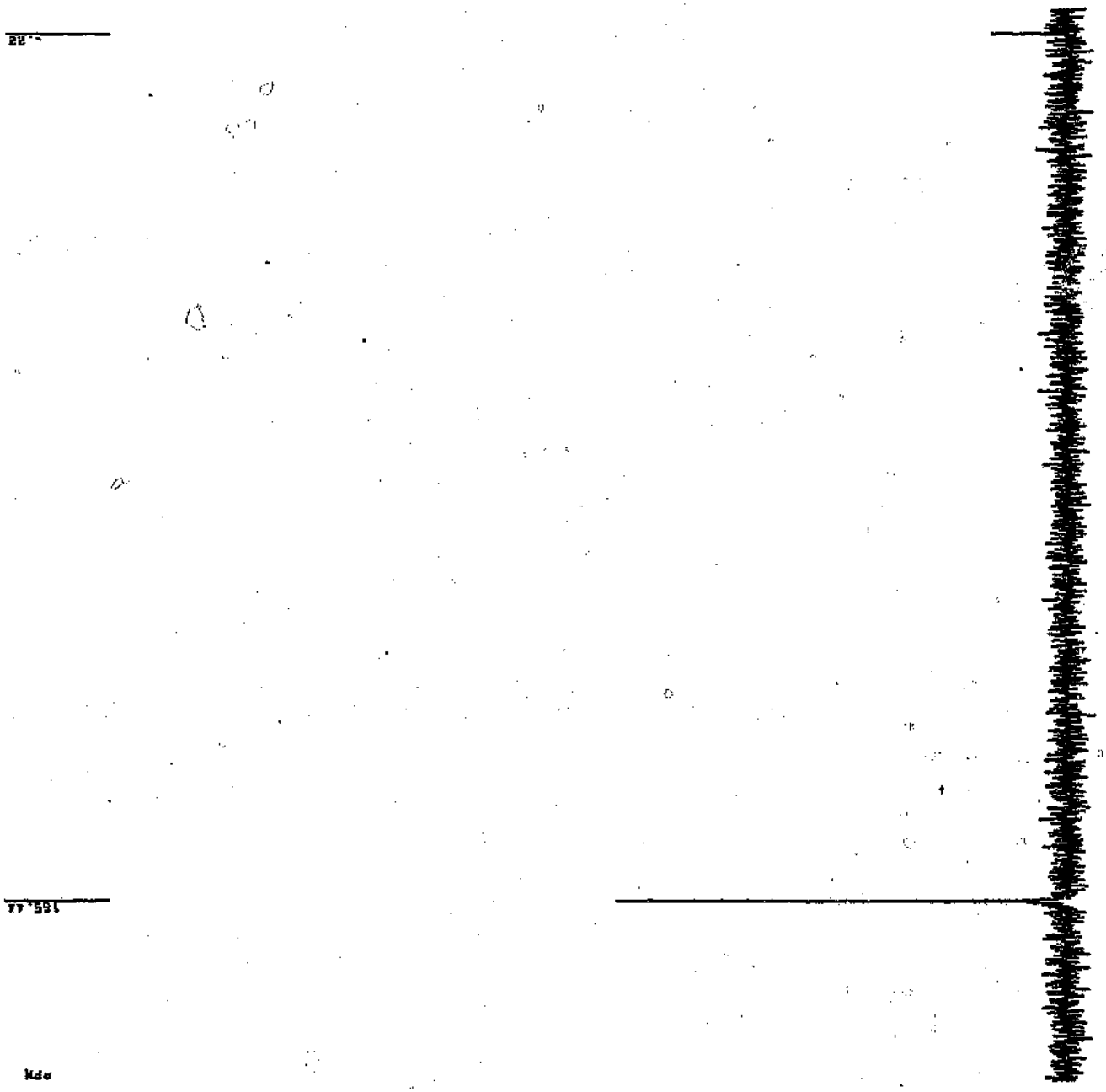

Spectra 17. Urea

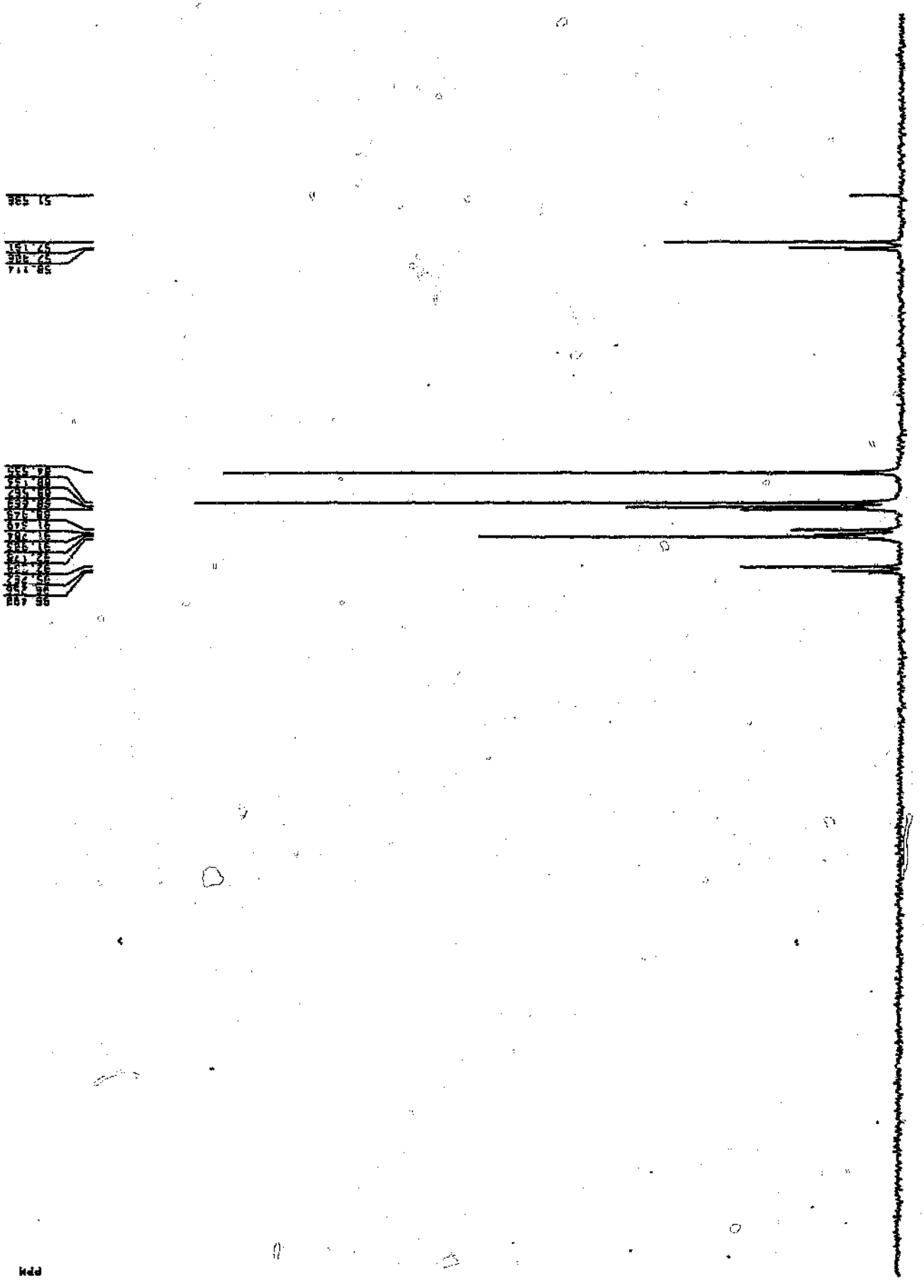

Spectra 18. Liquid Formaldehyde (formalir

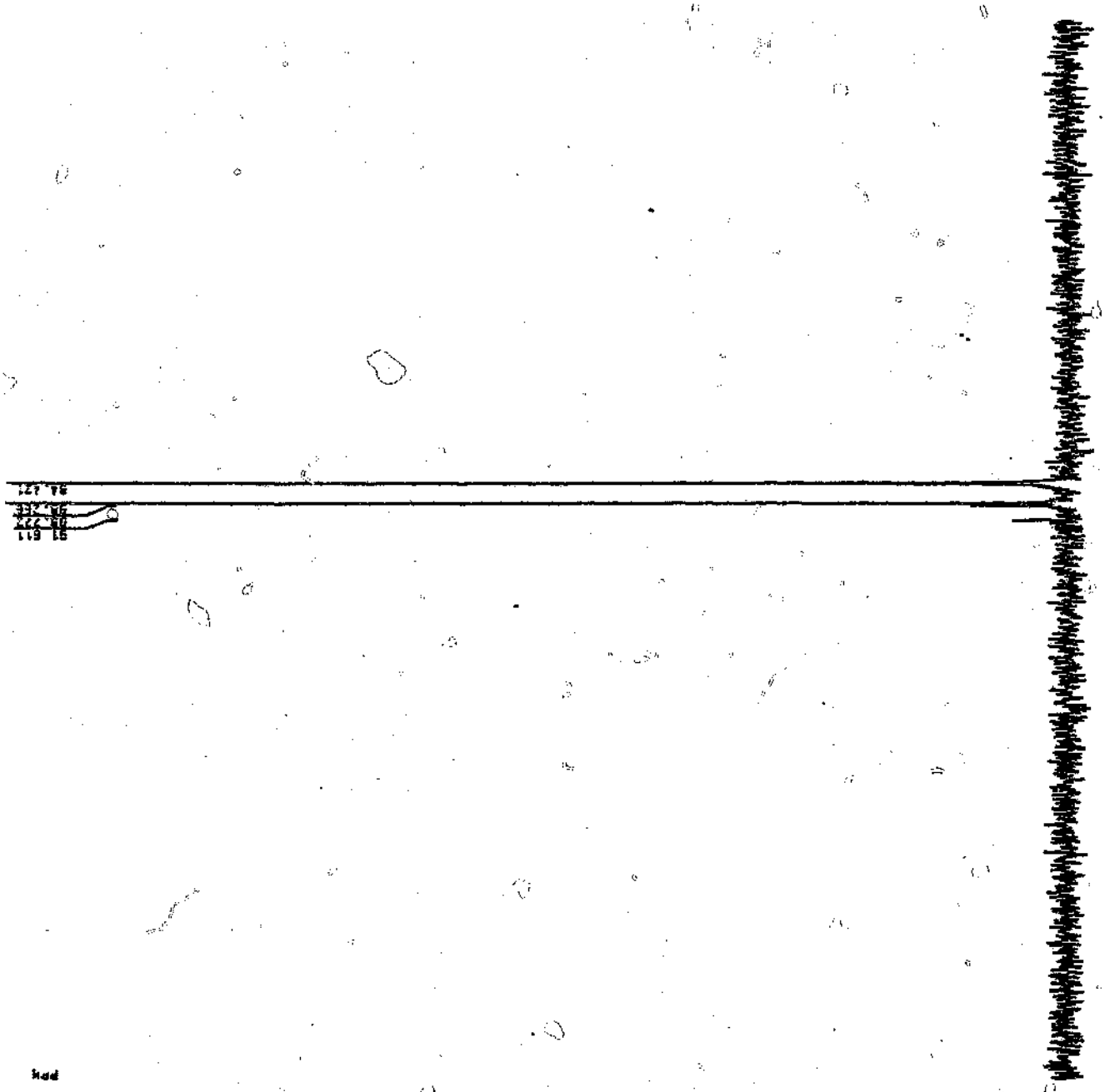

Spectra 19. Paraformaldehyde

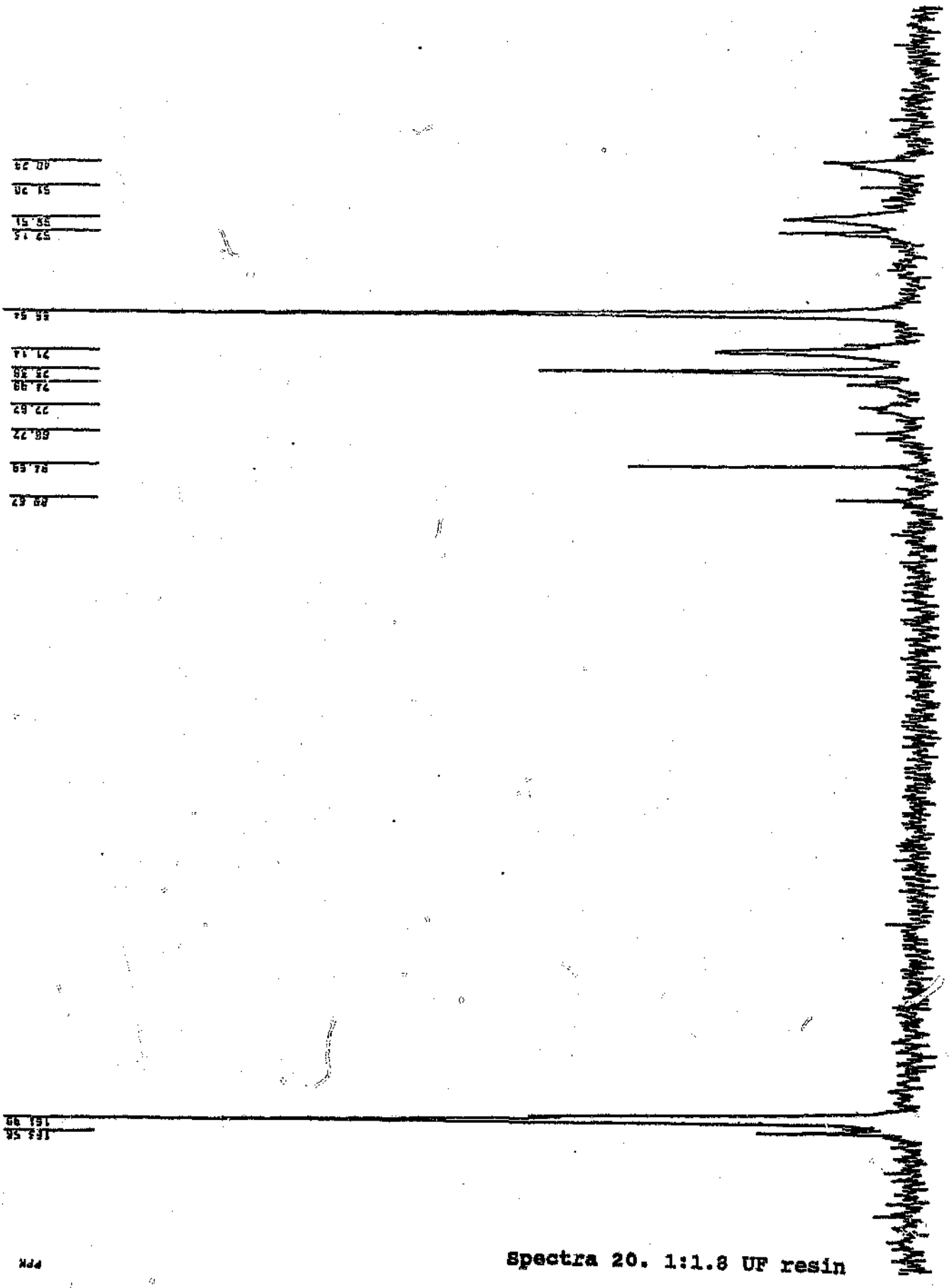

Spectra 20. 1:1.8 UF resin

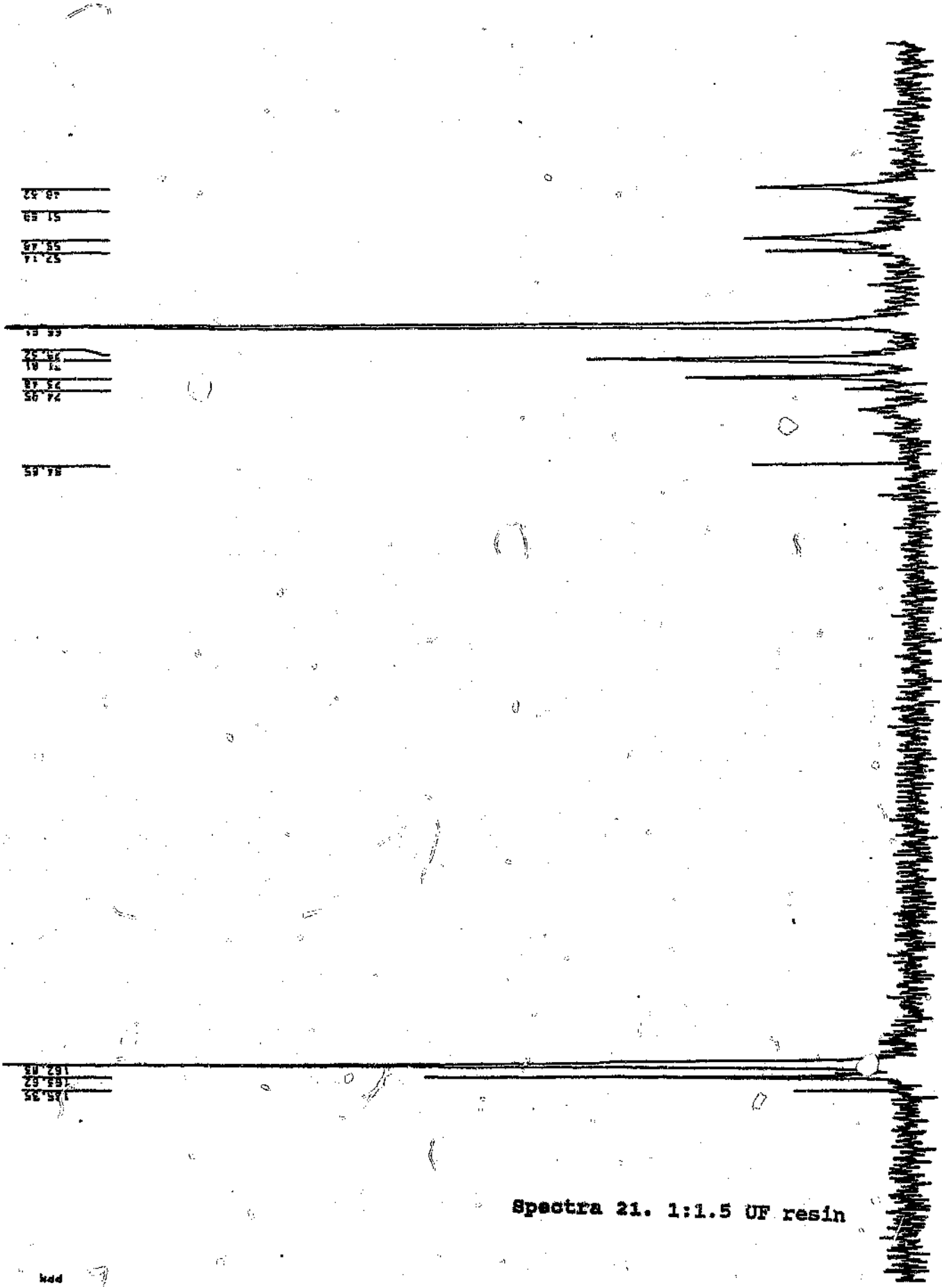

Spectra 21. 1:1.5 UF resin

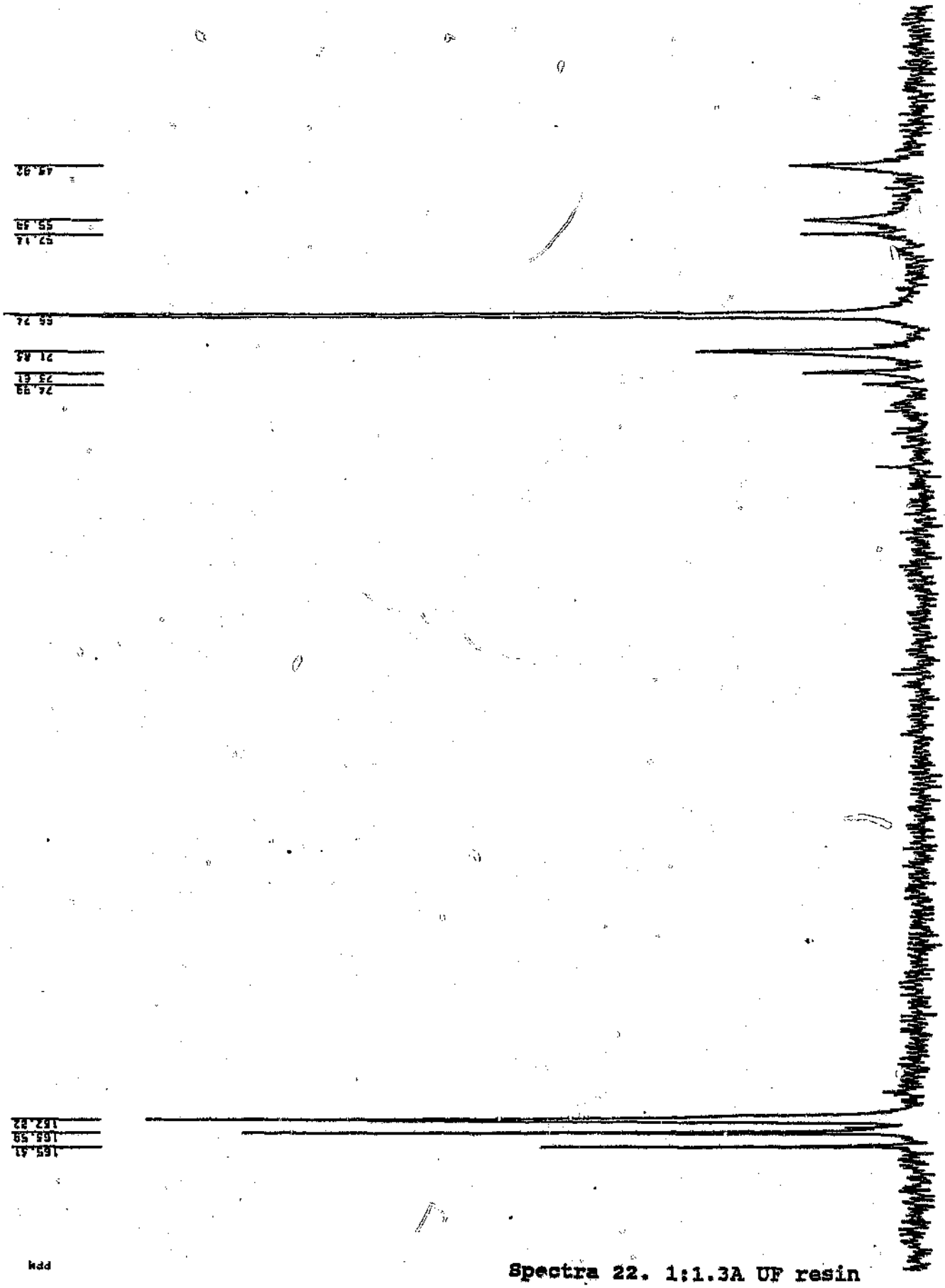

Spectra 22. 1:1.3A UF resin

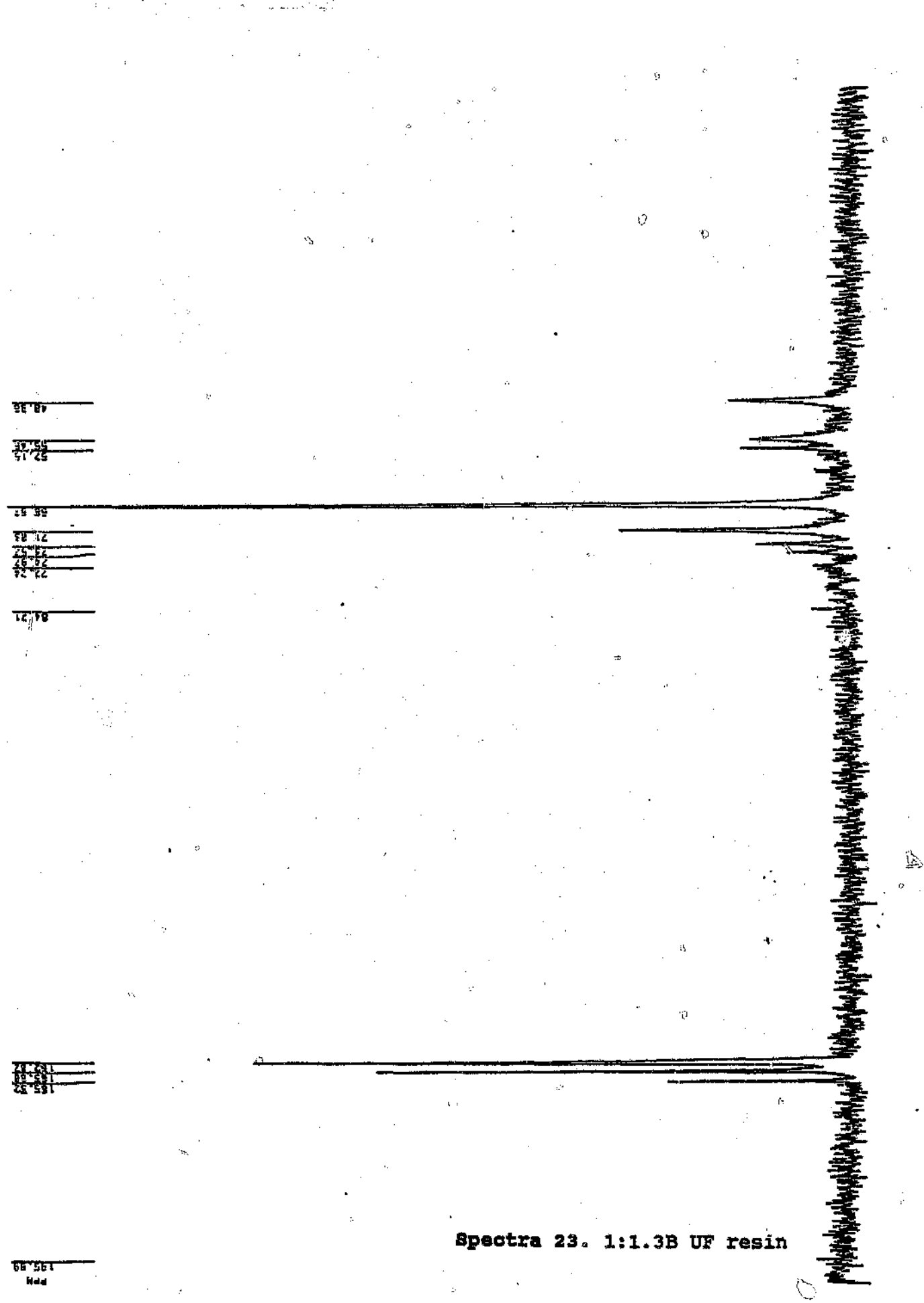

Spectra 23. 1:1.3B UF resin

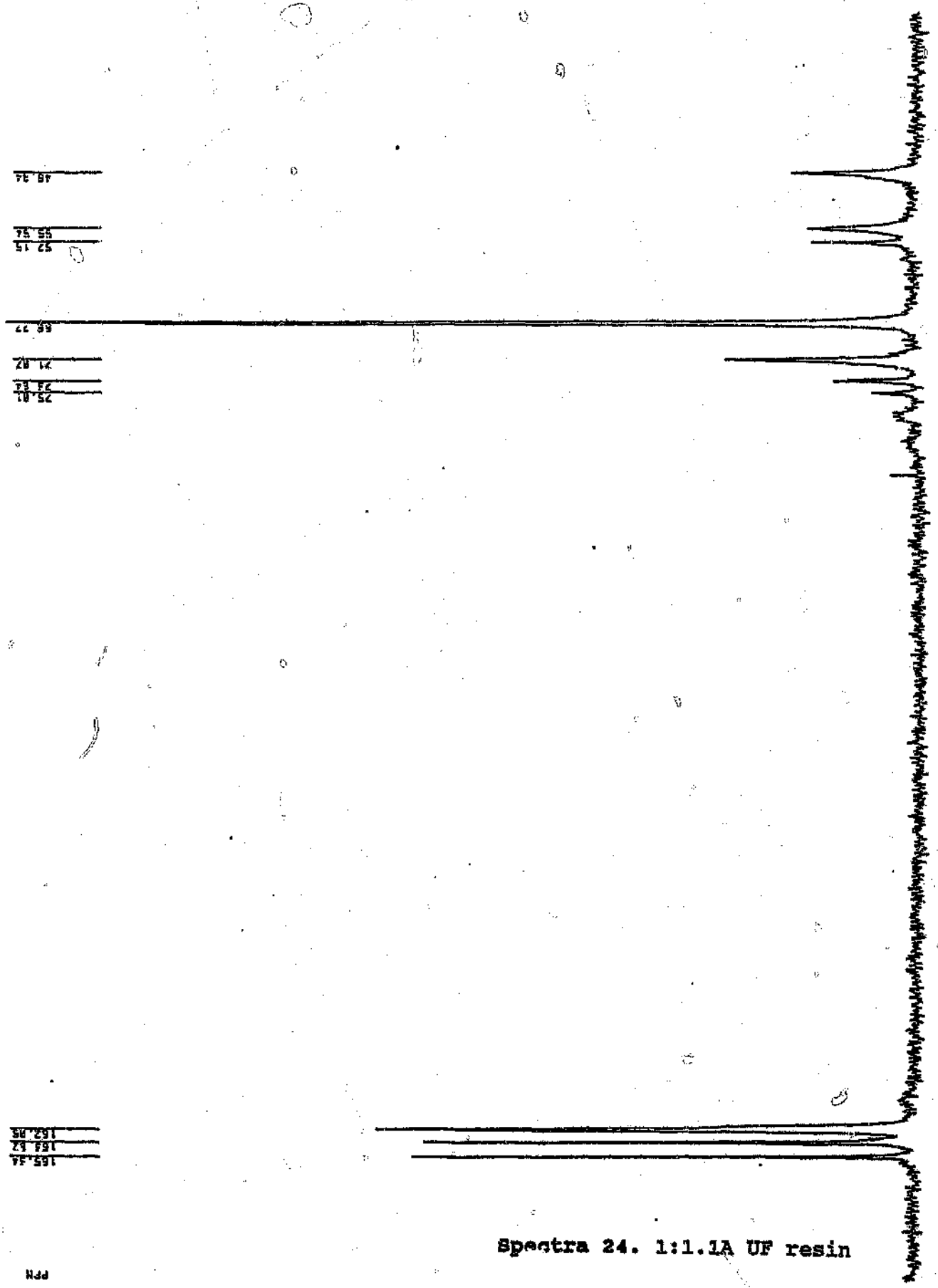

Spectra 24. 1:1.1A UF resin

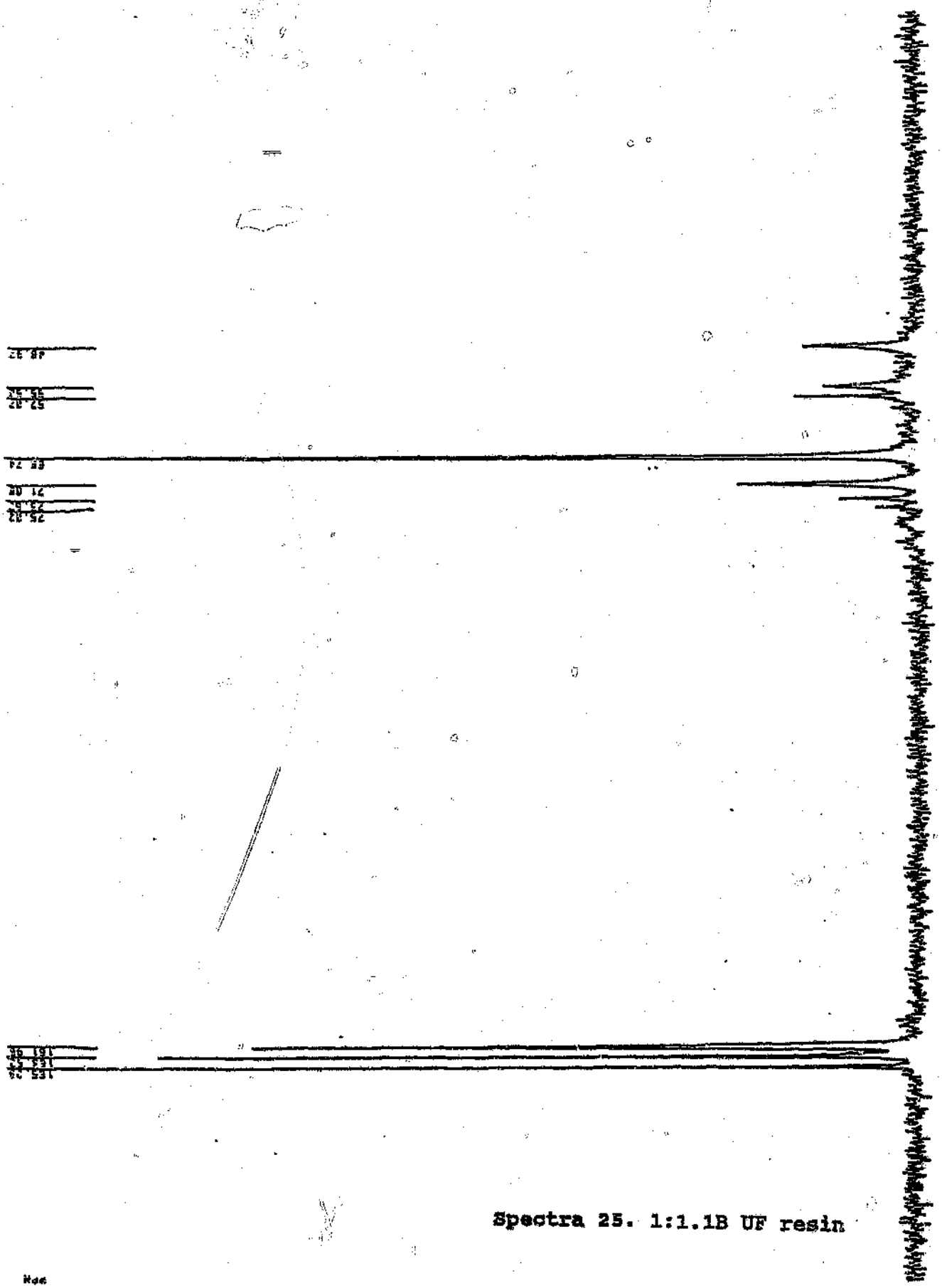

Spectra 25. 1:1.1B UF resin

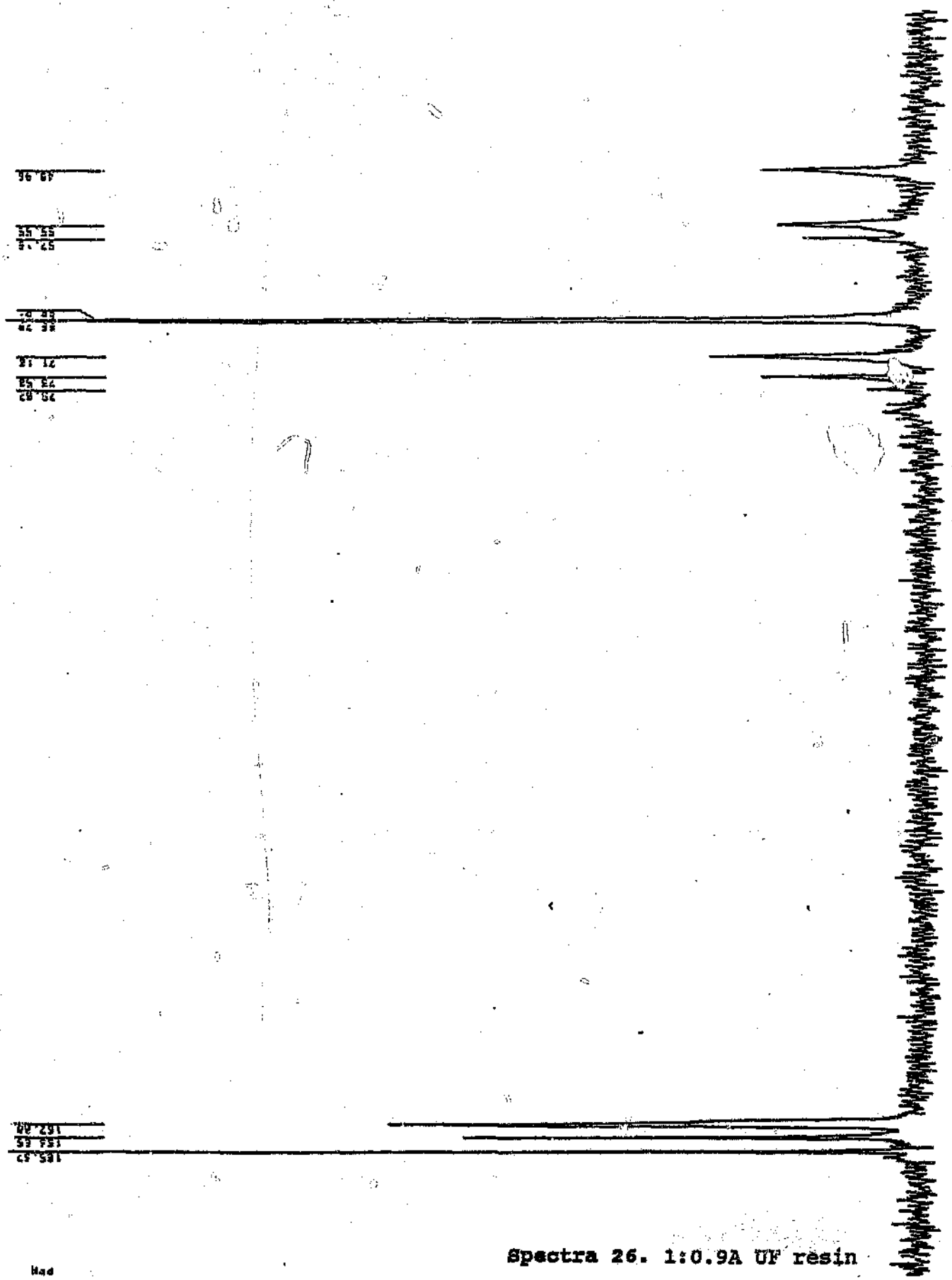

Spectra 26. 1:0.9A UF resin

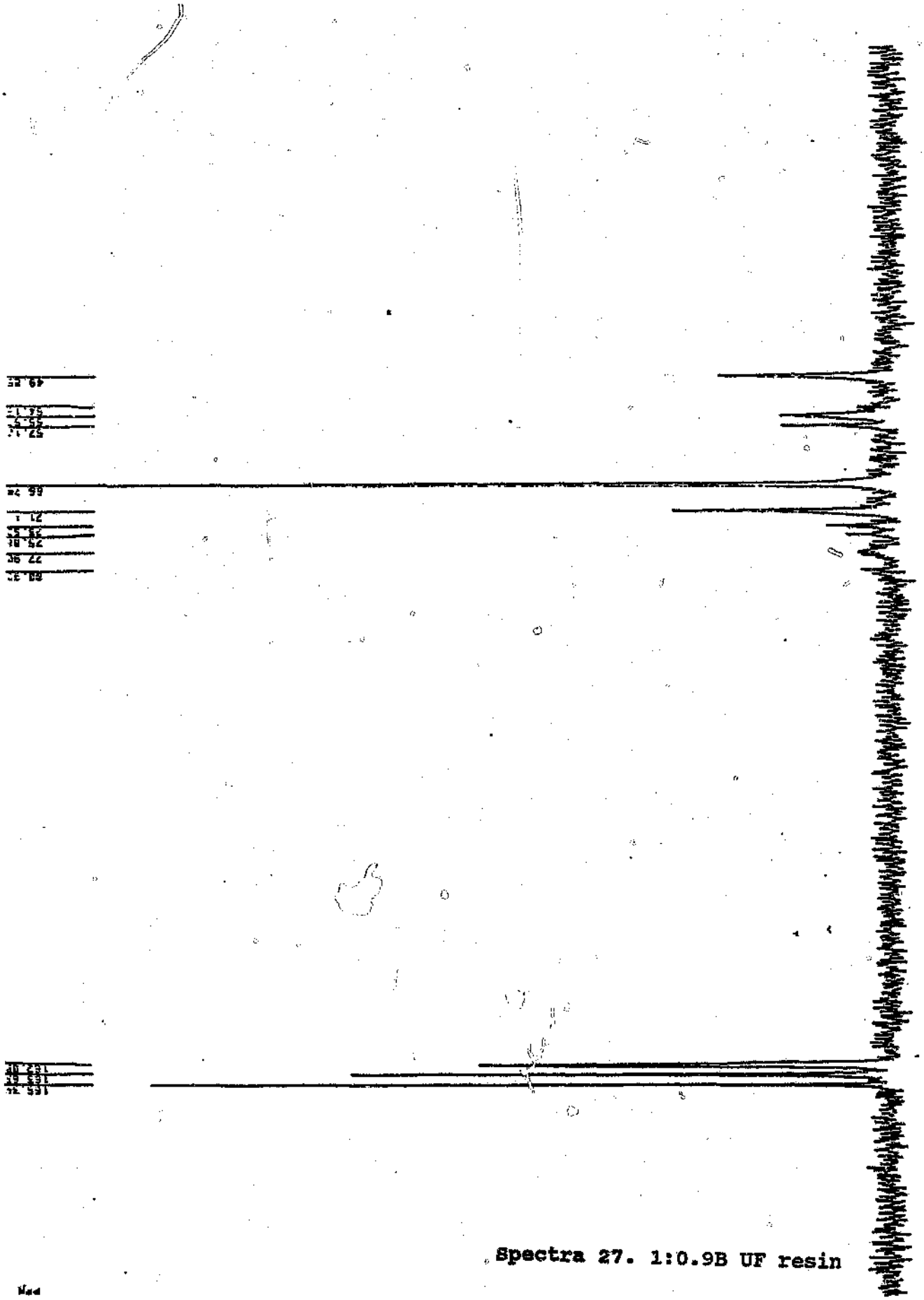

Spectra 27. 1:0.9B UF resin

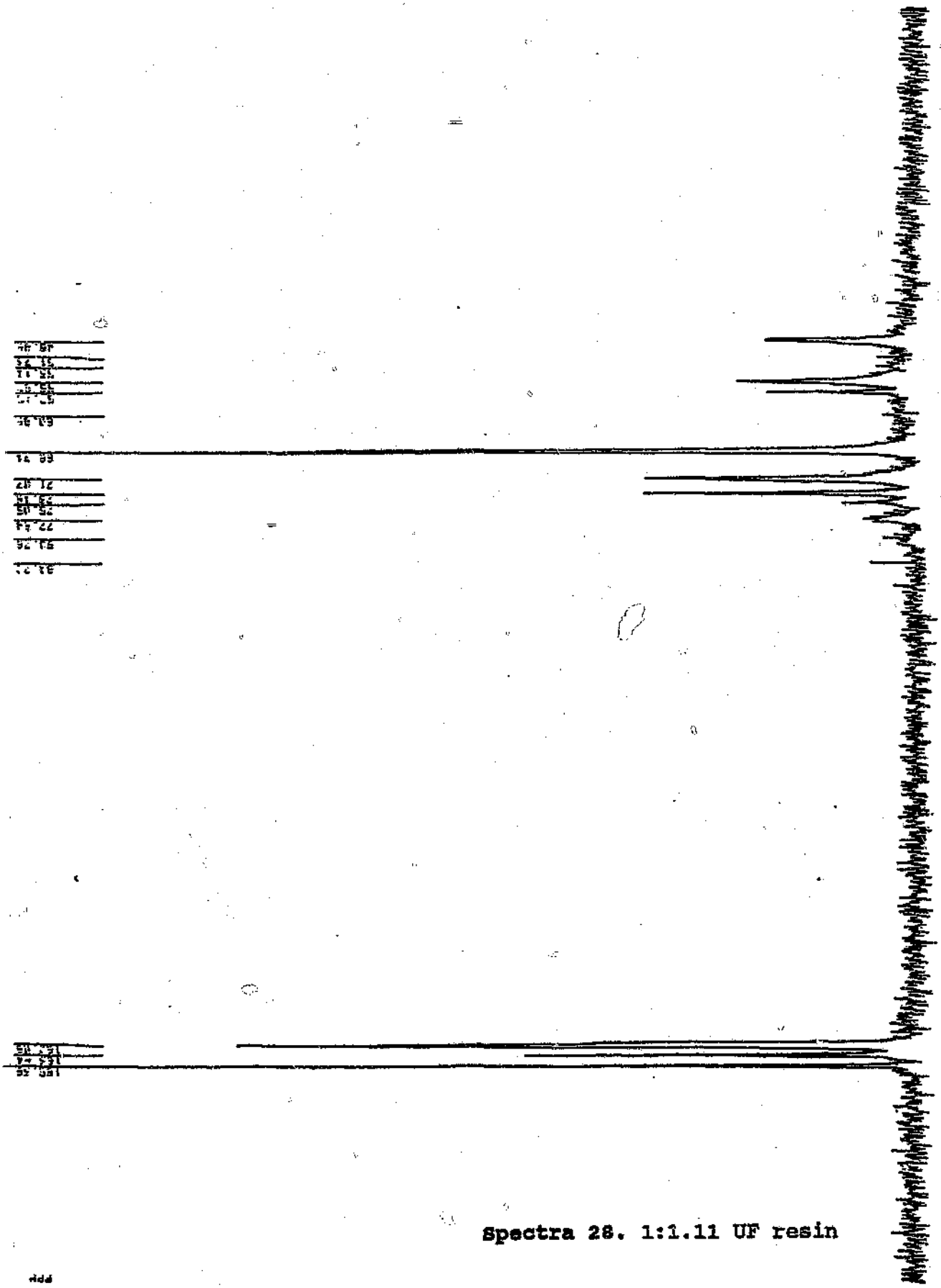

Spectra 28. 1:1.11 UF resin

Traces. X-ray Diffraction Traces of Cured Resins And Standards.

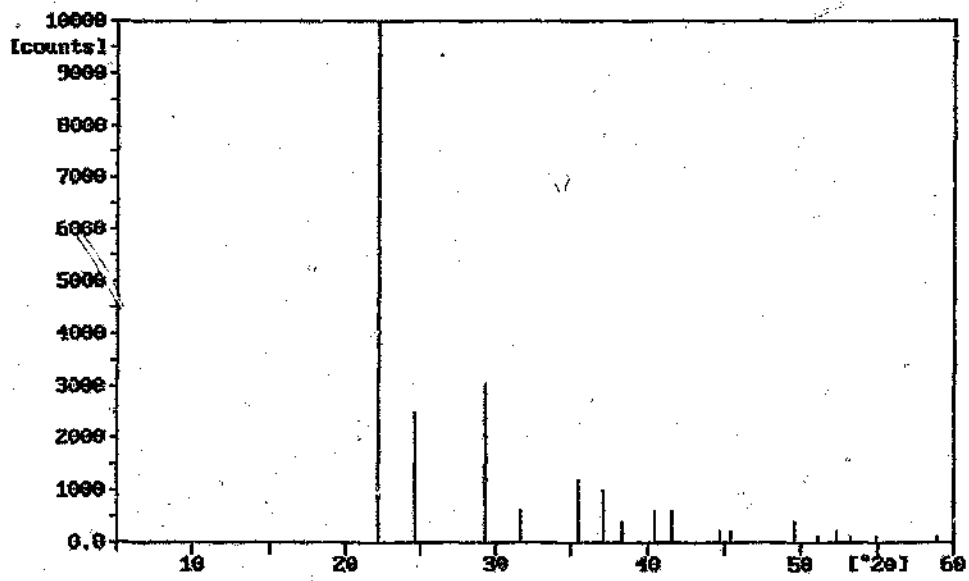

Trace 1. Urea [41]

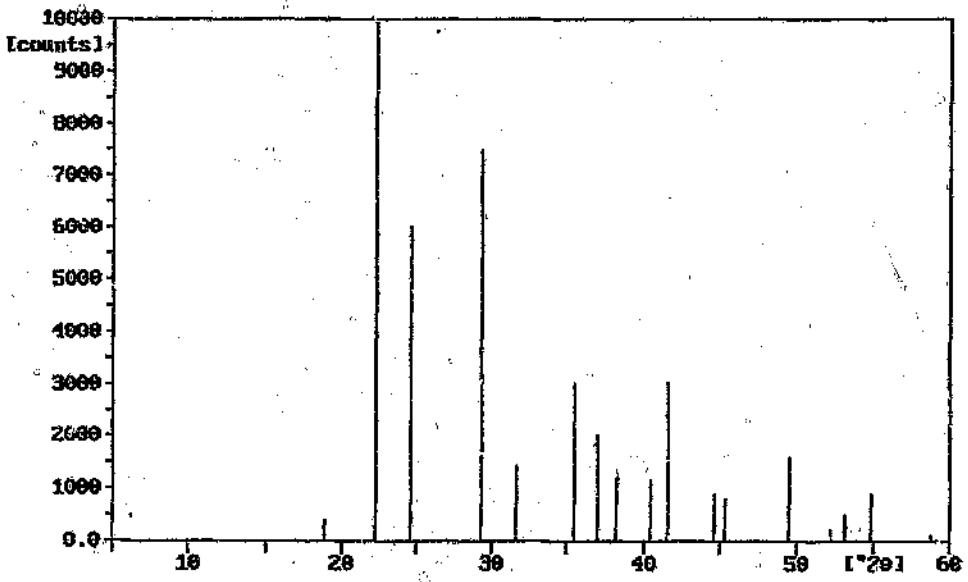

Trace 2. Urea [41]

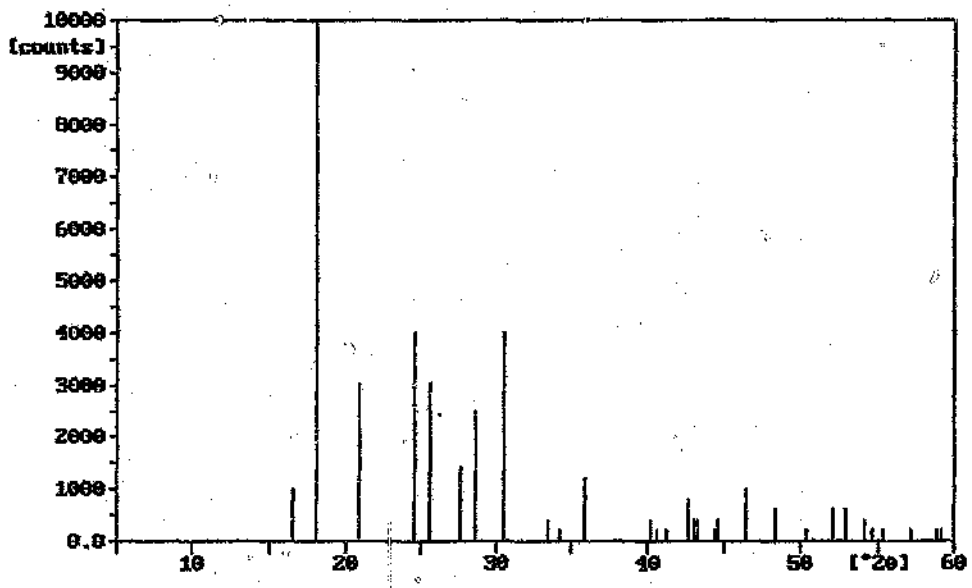

Trace 3. Methylurea [41]

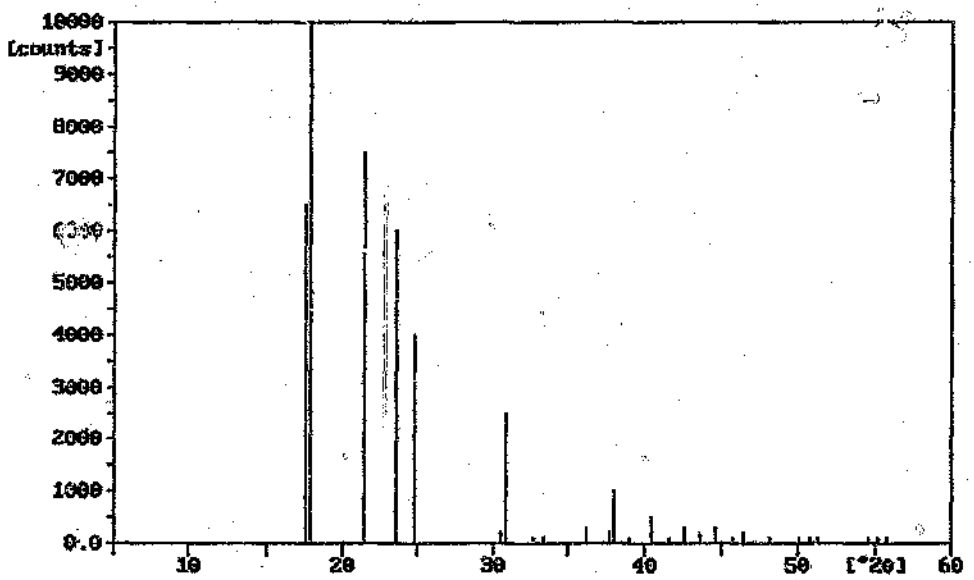

Trace 4. Dimethylurea [41]

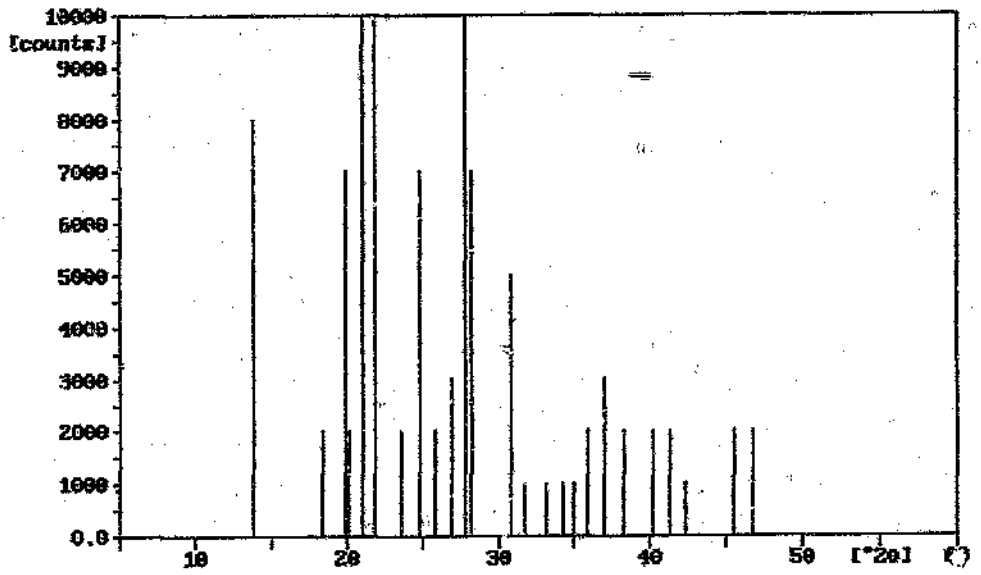

Trace 5. Methylenediurea [41]

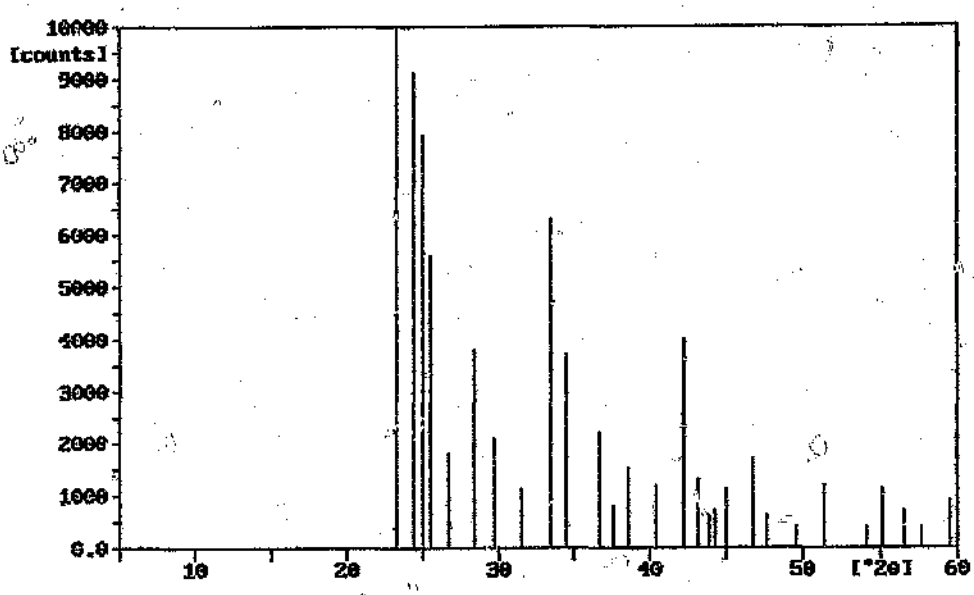

Trace 6. Methylenediurea [38]

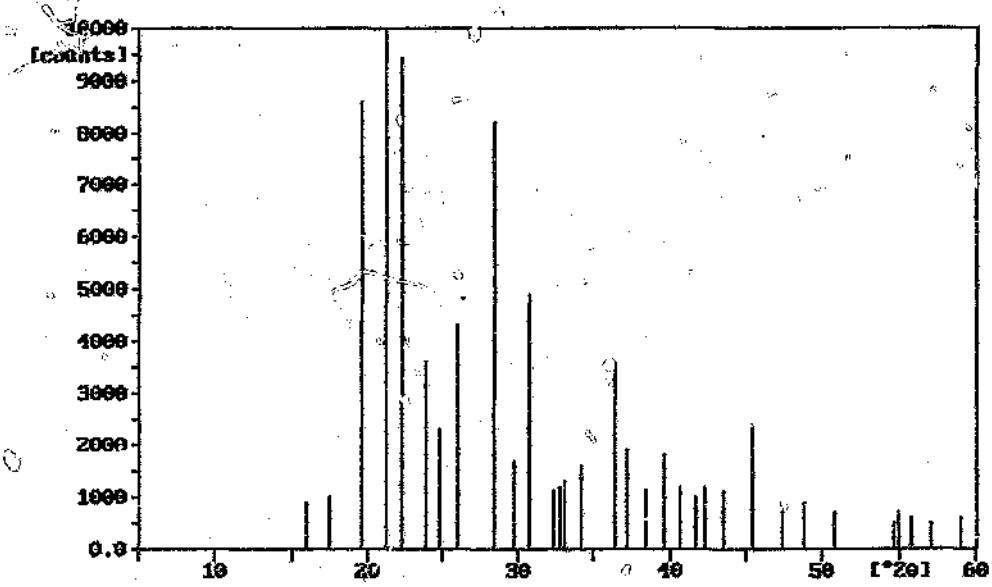

Trace 7. Dimethylenetriurea [38]

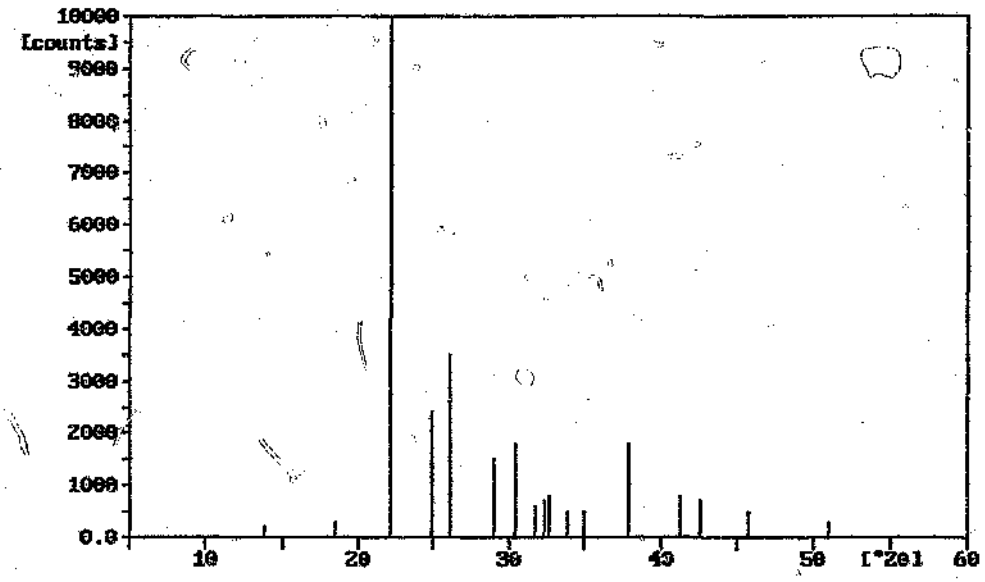

Trace 8. Trimethylenetetraurea [38]

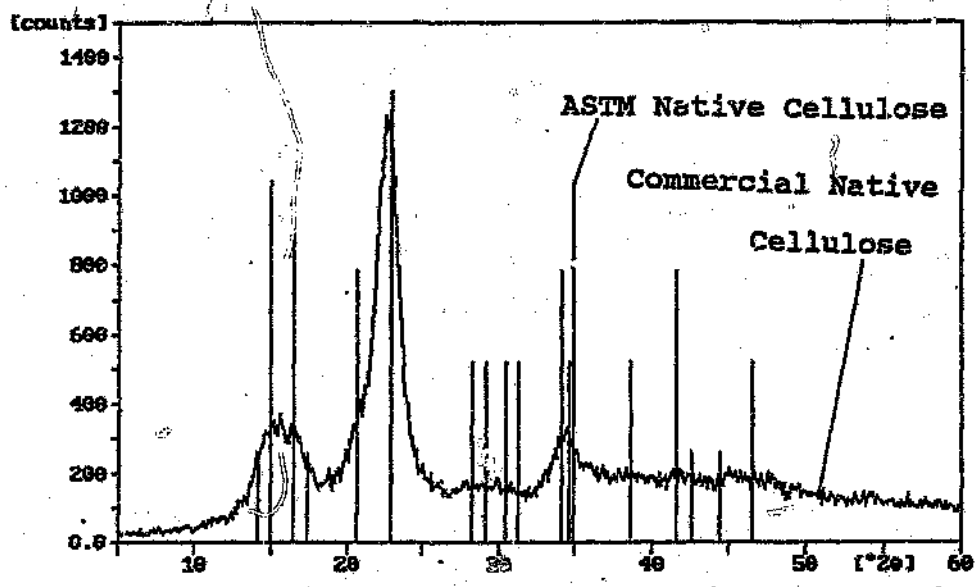

Trace 9. Commercial Native Cellulose with ASTM Native Cellulose Standard.

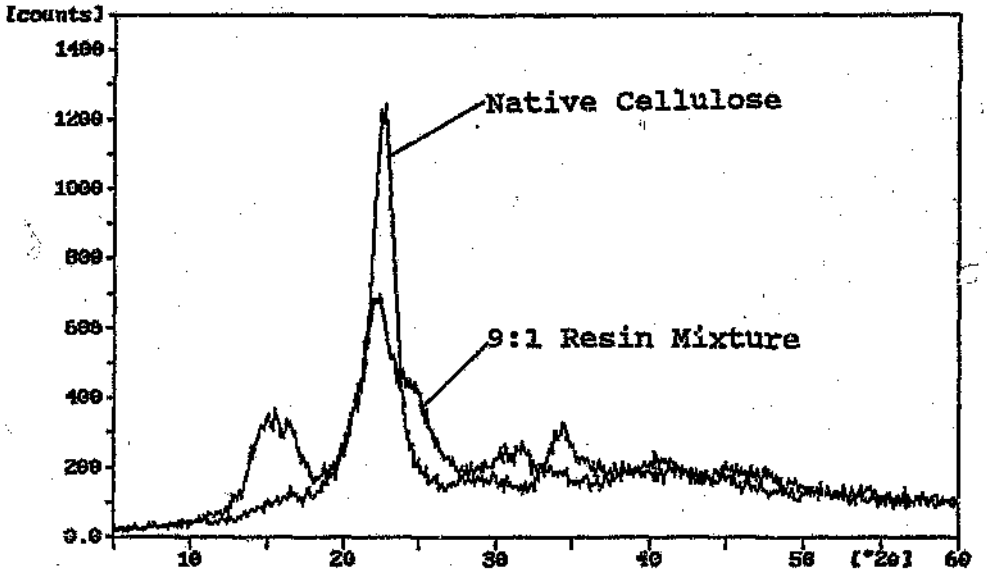

Trace 10. Native Cellulose with a resin:cellulose Mixture of 9:1.

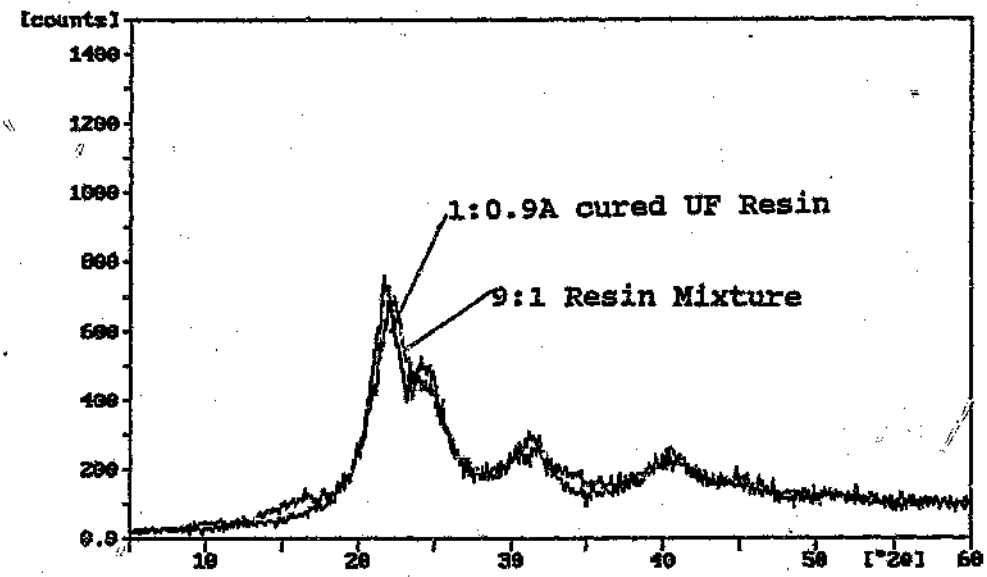

Trace 11. Resin:Cellulose mixture of 9:1 with 1:0.9A cured UF resin.

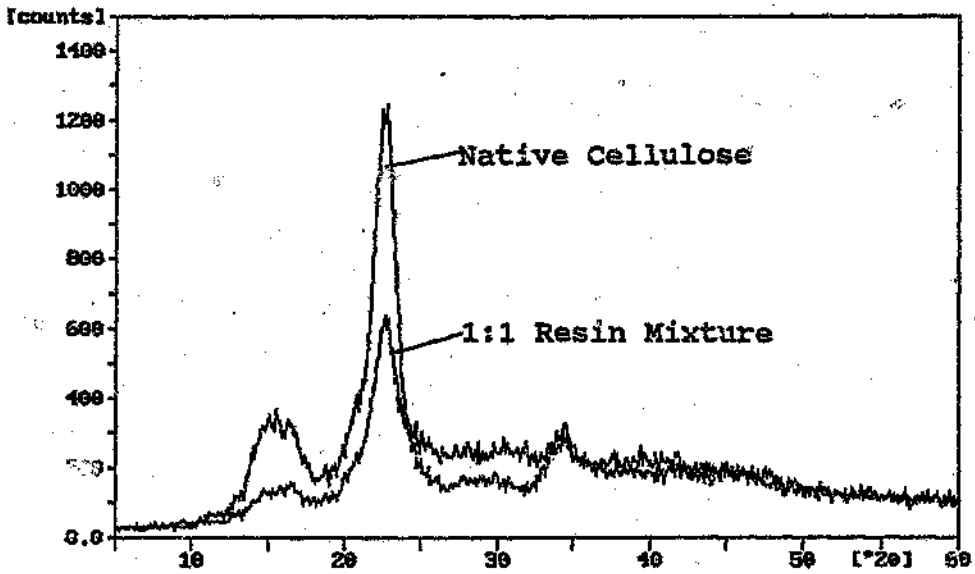

Trace 12. Native Cellulose with a Resin:Cellulose Mixture of 1:1.

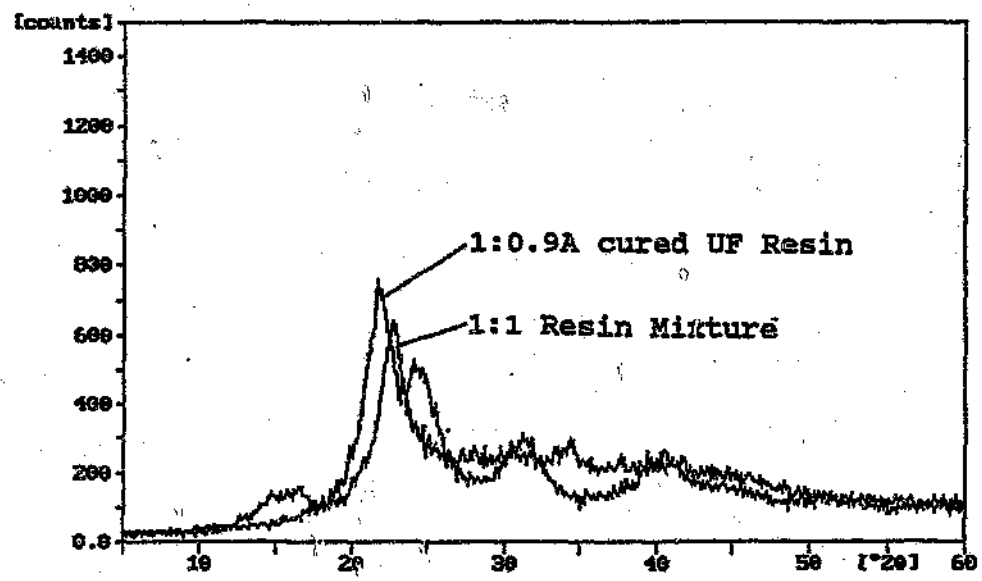

Trace 13. Resin:Cellulose Mixture of 1:1 with cured Modified Resin 1:0.9A.

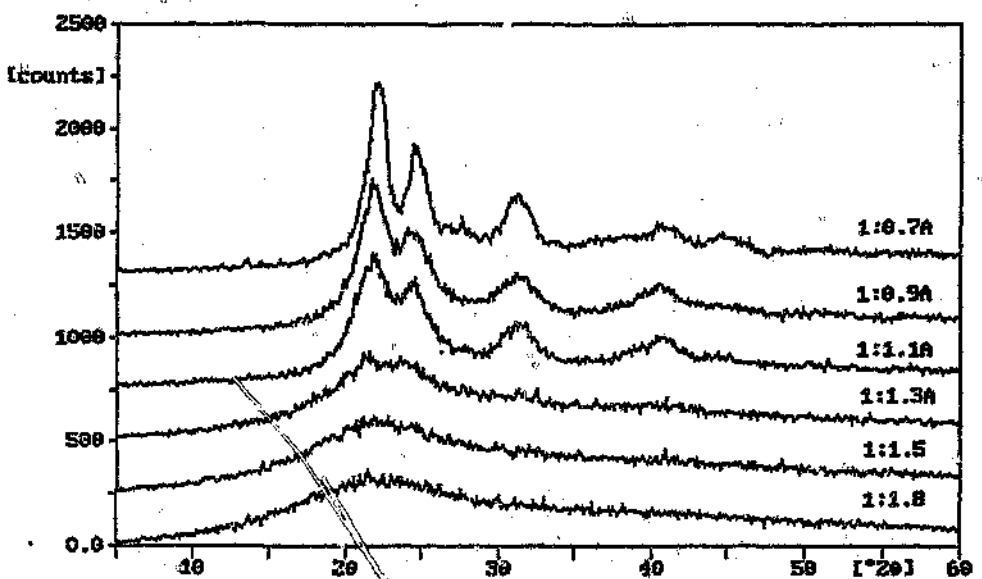

Trace 14. X-ray Diffraction Traces of the Different UF Modified Resins cured with 3% NH_4Cl.

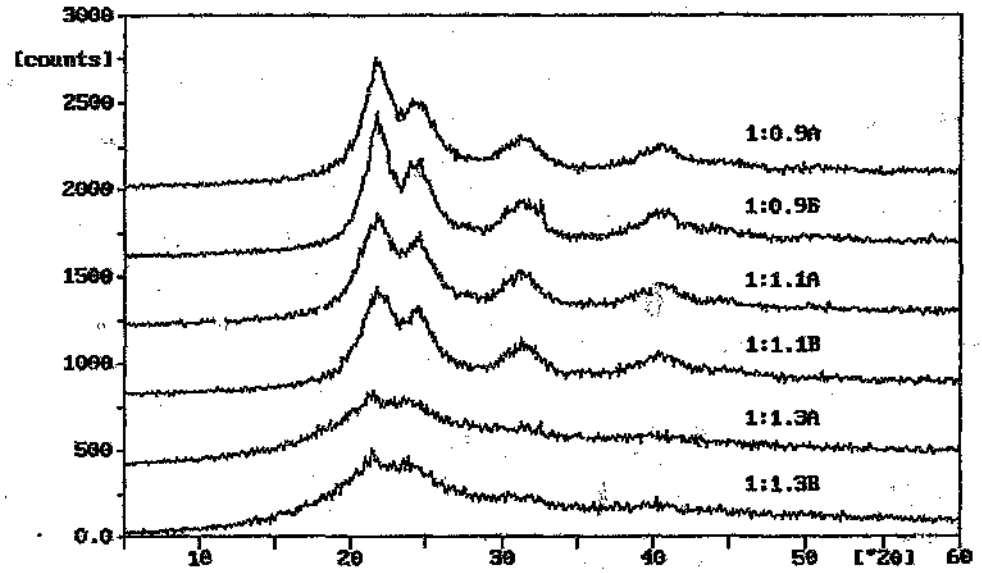

Trace 15. X-ray Diffraction Traces of the UF Modified Resins cured with 3% NH_4Cl.

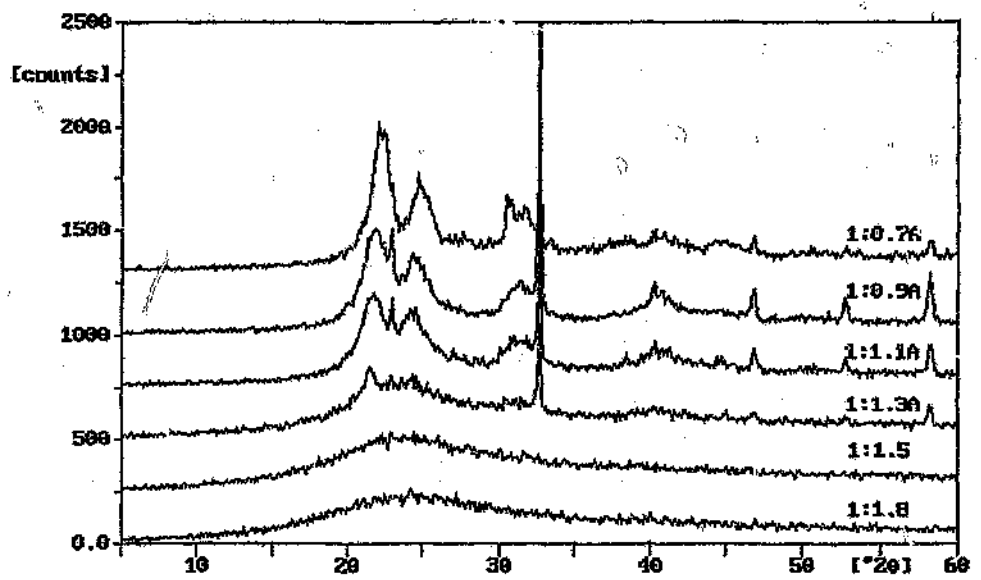

Trace 16. X-ray Diffraction Traces of the diffferent UF Modified Resins cured with 9% NH_4Cl (the strong peak are those of NH_4Cl).

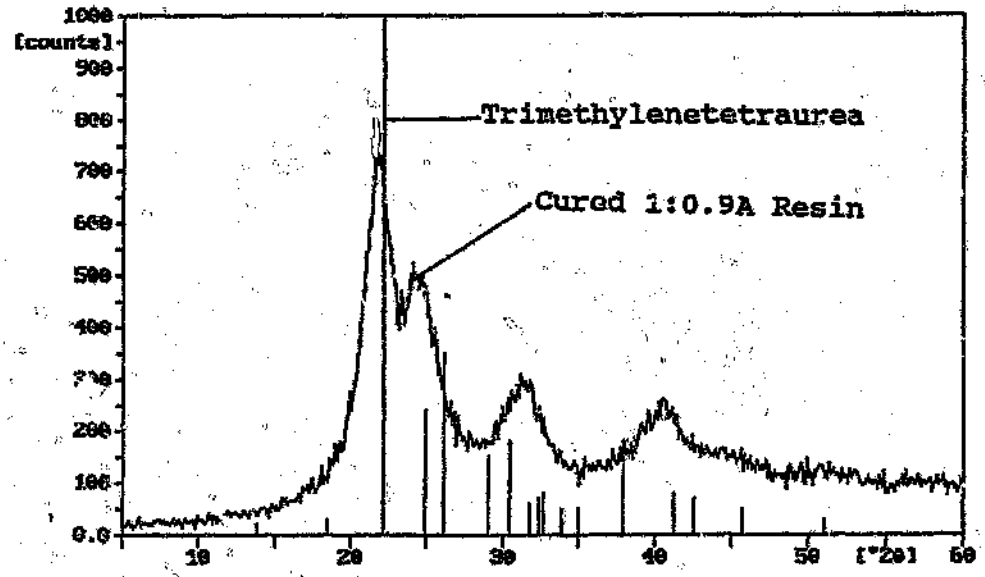

Trace 17. X-ray Diffraction Traces of Cured 1:0.9A resin superimposed with trimethylenetetraurea [38]

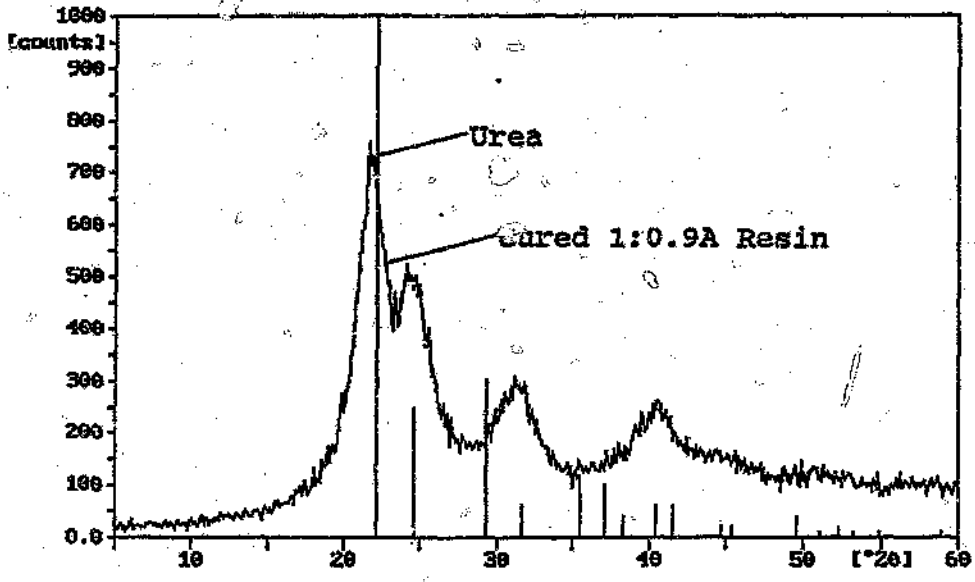

Trace 18. X-ray Diffraction Trace of cured 1:0.9A resin superimposed with urea.

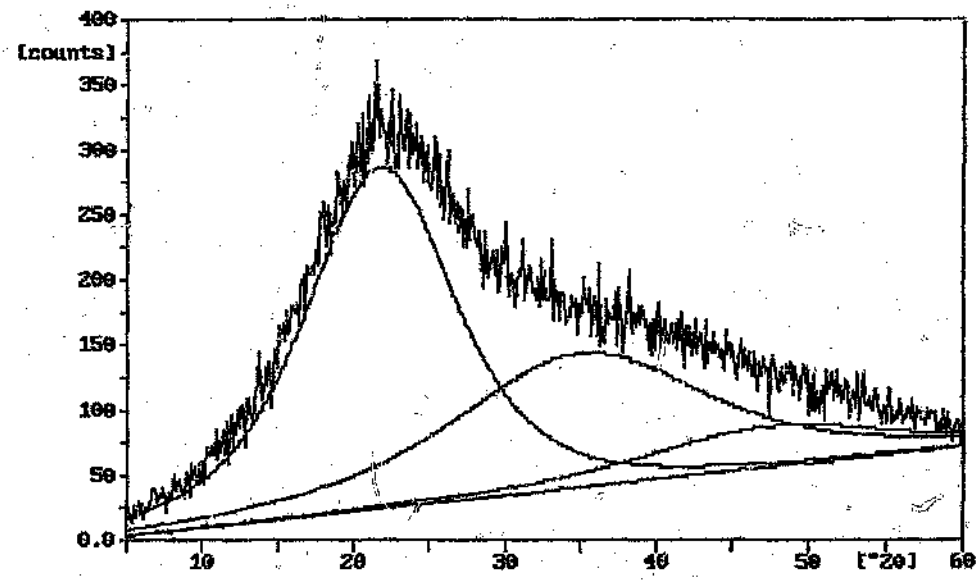

Trace 19. X-ray Diffraction Pattern of cured UF resin 1:1.8 with best Curve Fit.

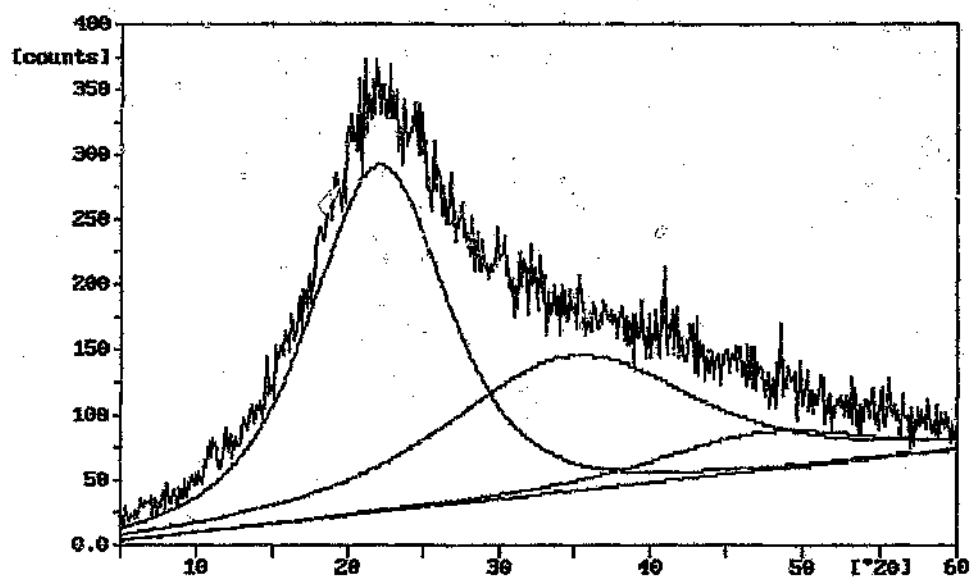

Trace 20. X-ray Diffraction Trace of Cured UF Resin 1:1.5 with best Curve Fit.

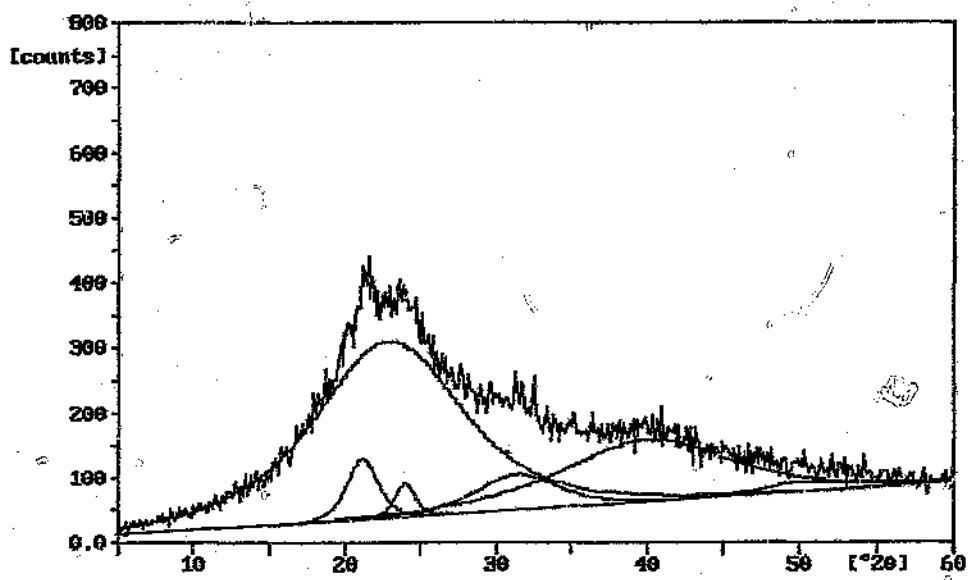

Trace 21. X-ray Diffraction Trace of cured UF resin 1:1.3A with best Curve Fit.

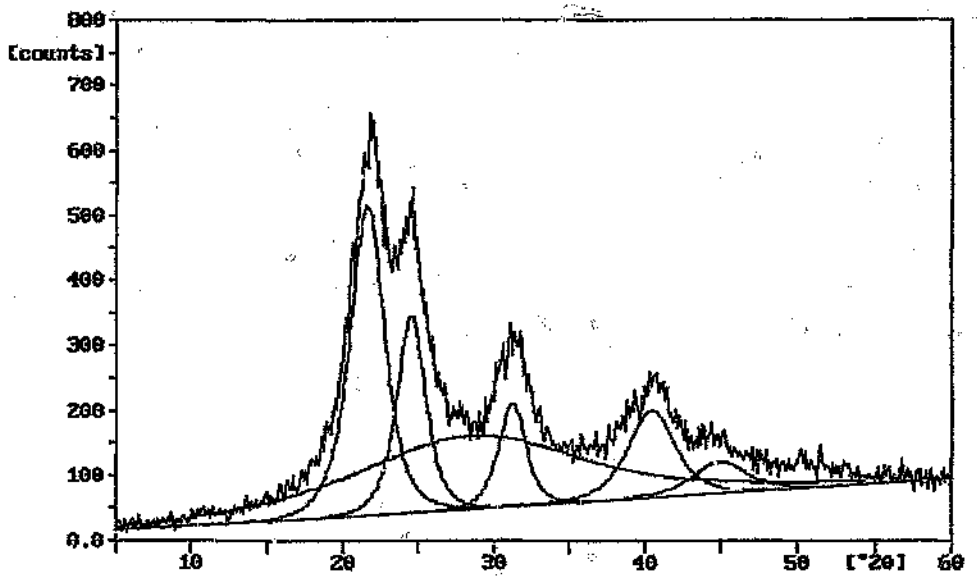

Trace 22. X-ray Diffraction Trace of cured UF Resin 1:1.1A with best Curve Fit.

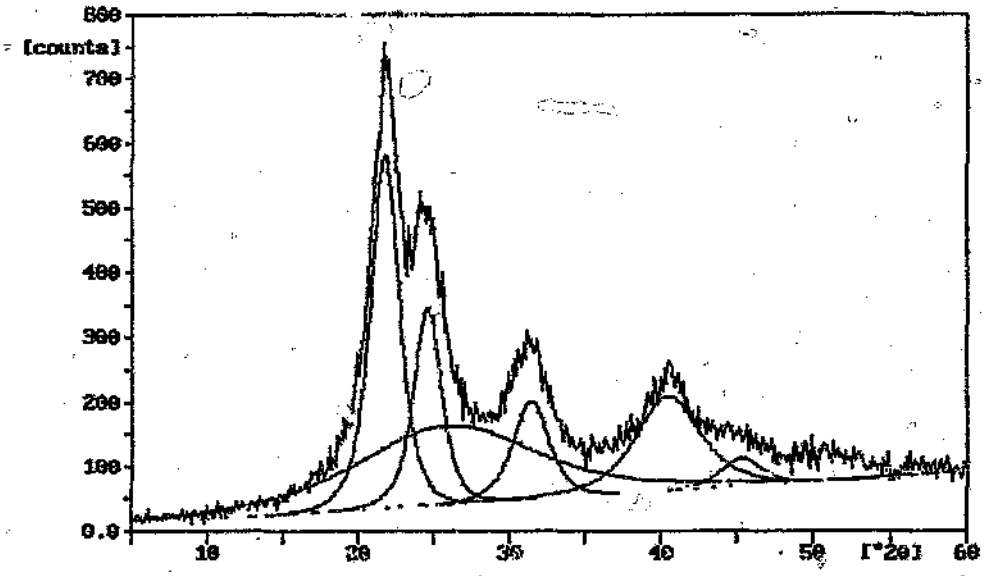

Trace 23. X-ray Diffraction Trace of Cured UF Resin 1:0.9A with best Curve Fit.

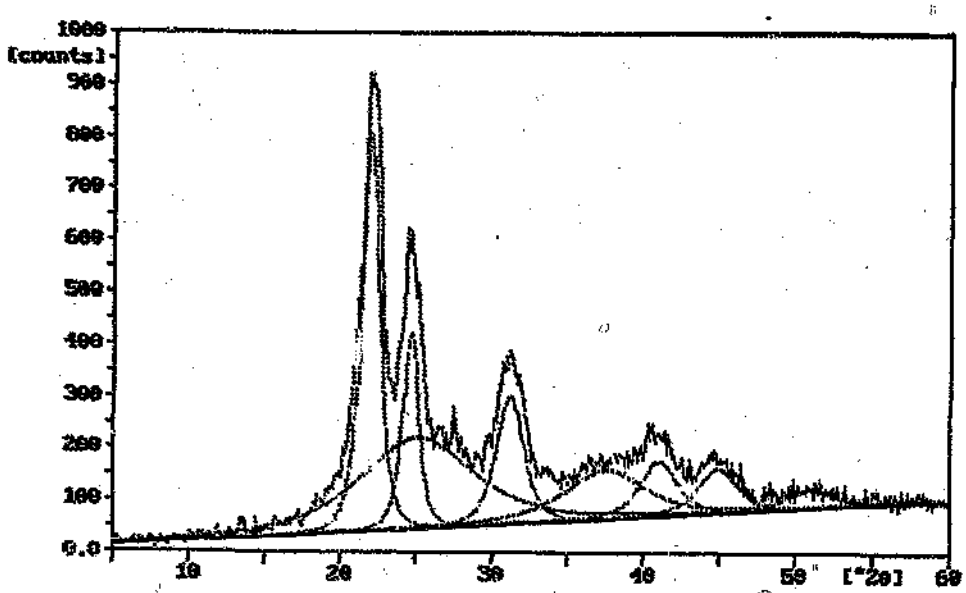

Trace 24. X-ray diffraction trace of cured UF resin 1:0.7A with best curve fits.

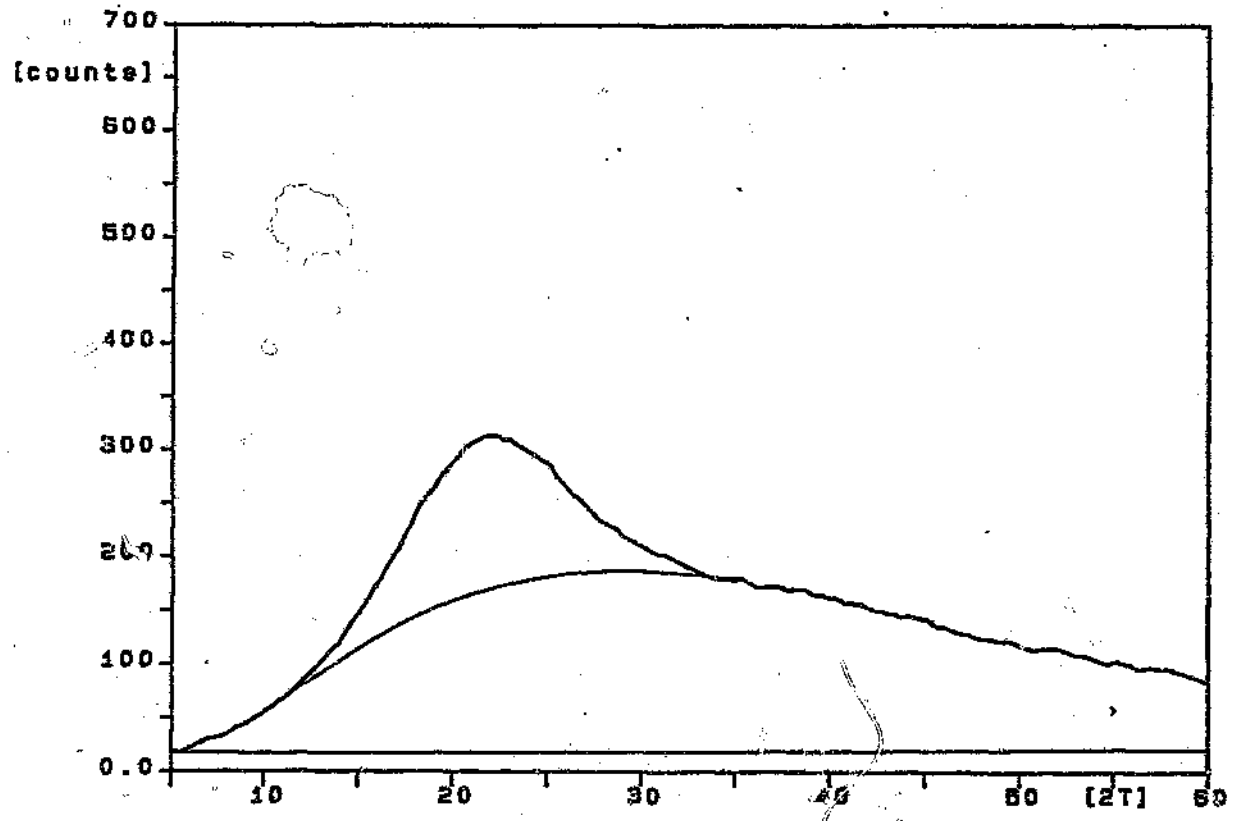

Trace 25. Smoothed X-ray diffraction trace of cured UF resin 1:1.8 representing the amorphous and crystalline regions respectively.

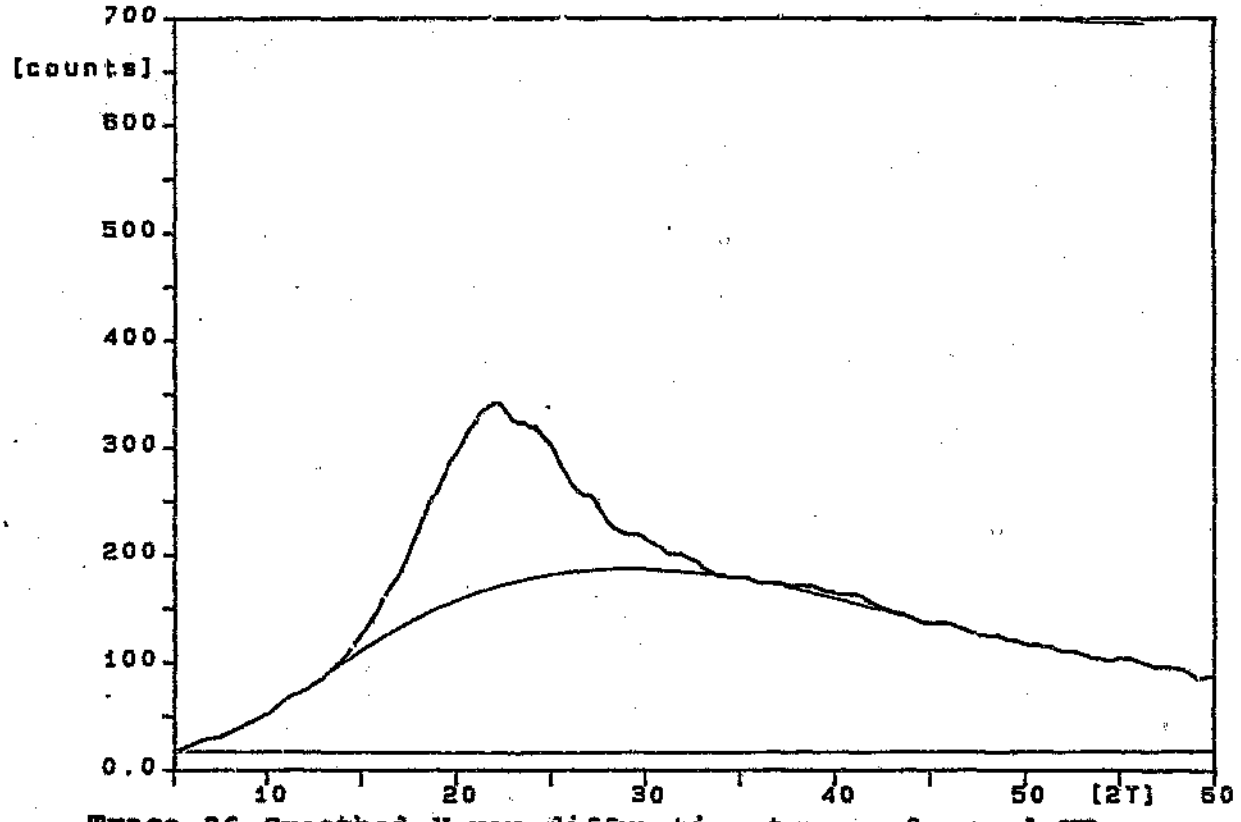

Trace 26. Smoothed X-ray diffraction trace of cured UF resin 1:1.5 representing the amorphous and crystalline regions respectively.

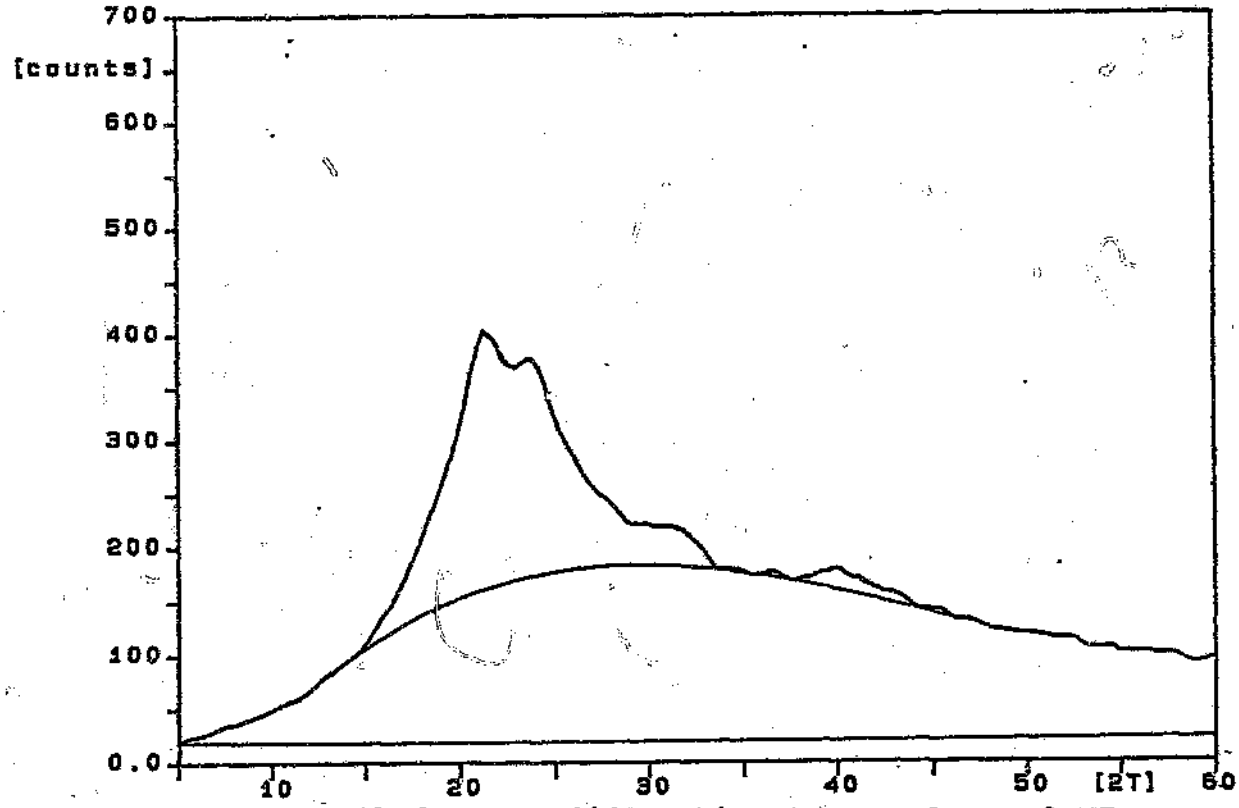

Trace 27. Smoothed X-ray diffraction trace of cured UF resin 1:1.3A representing the amorphous and crystalline regions respectively.

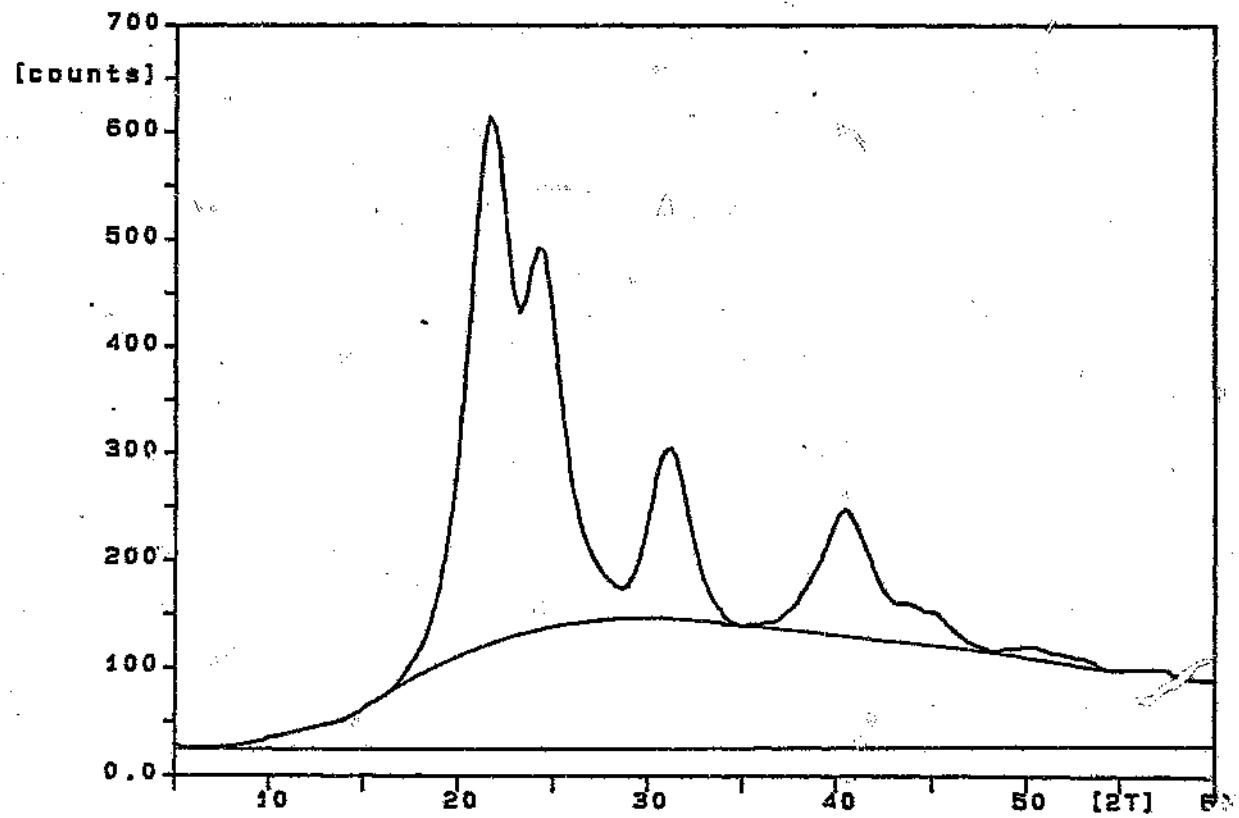

Trace 28. Smoothed X-ray diffraction trace of cured UF resin 1:1.1A representing the amorphous and crystalline regions respectively.

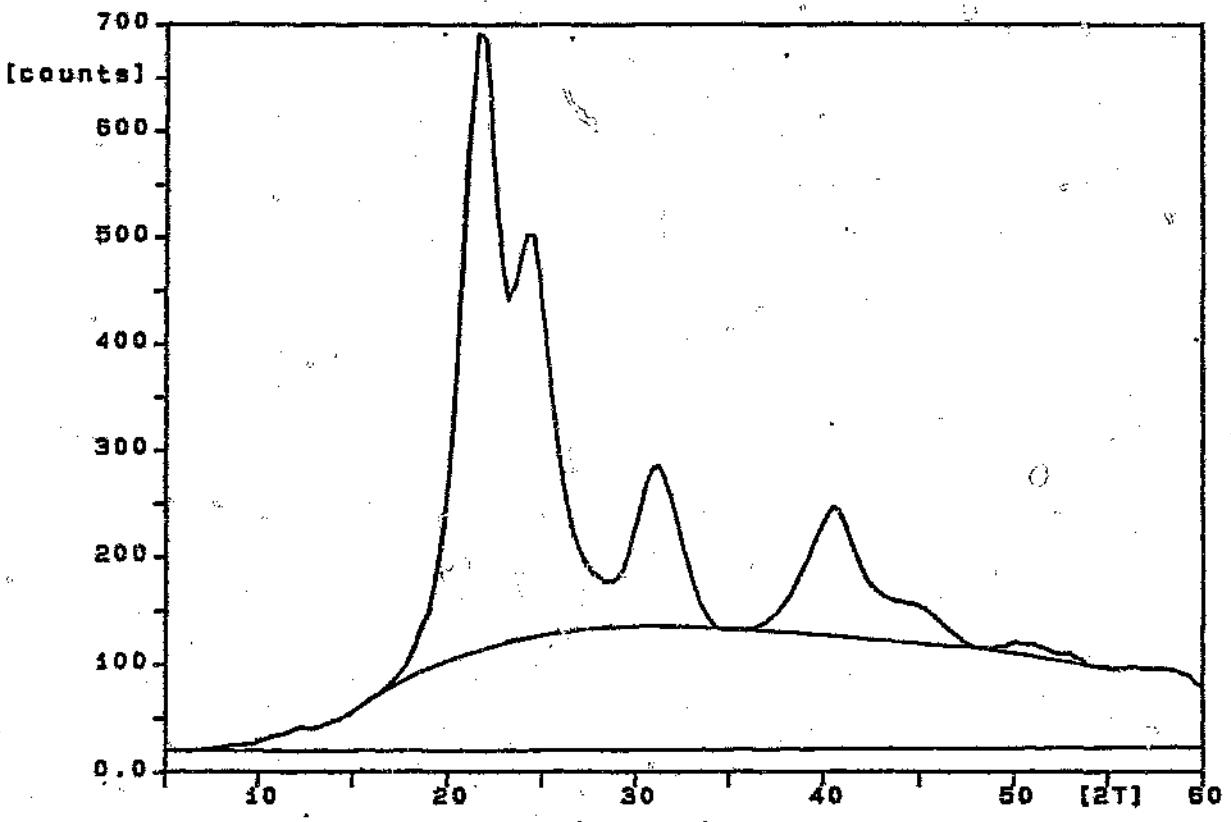

Trace 29. Smoothed X-ray diffraction trace of cured UF resin 1:0.9A representing the amorphous and crystalline regions respectively.

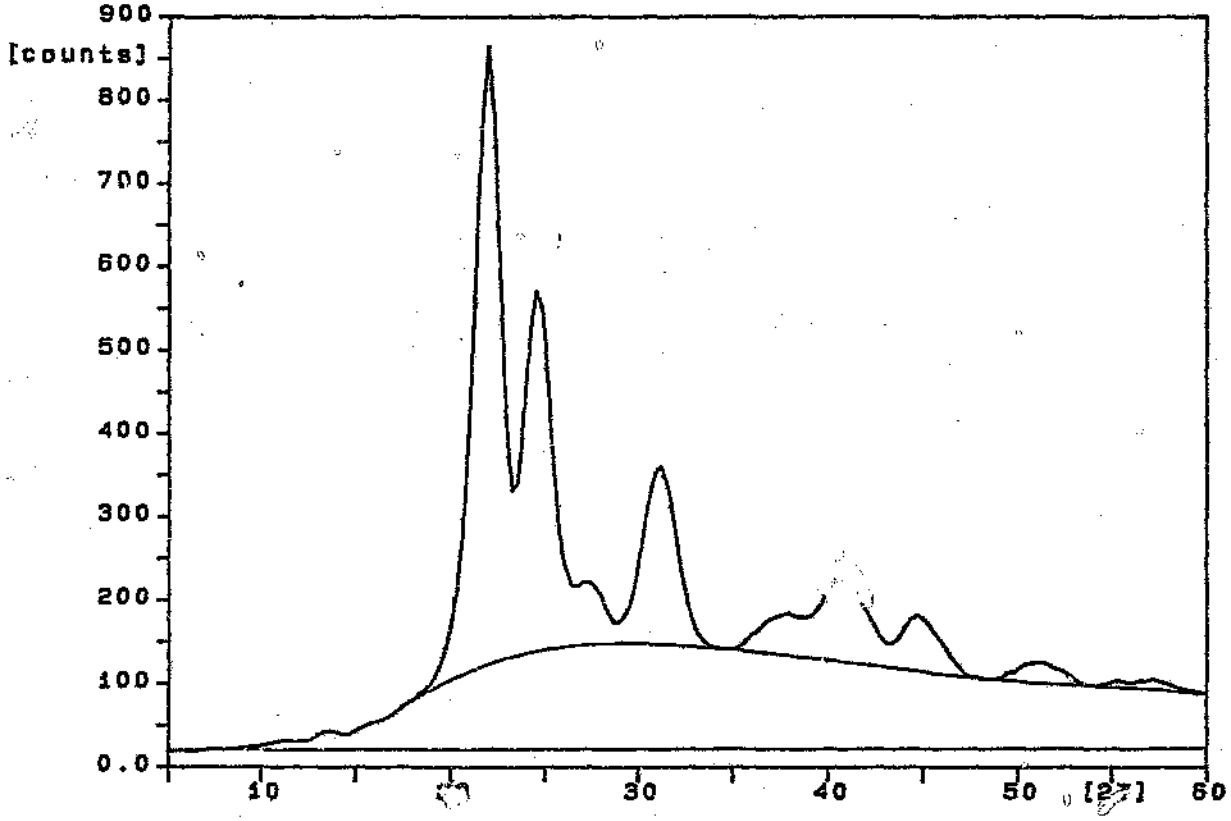

Trace 30. Smoothed X-ray diffraction trace of cured UF resin 1:0.9A representing the amorphous and crystalline regions respectively.